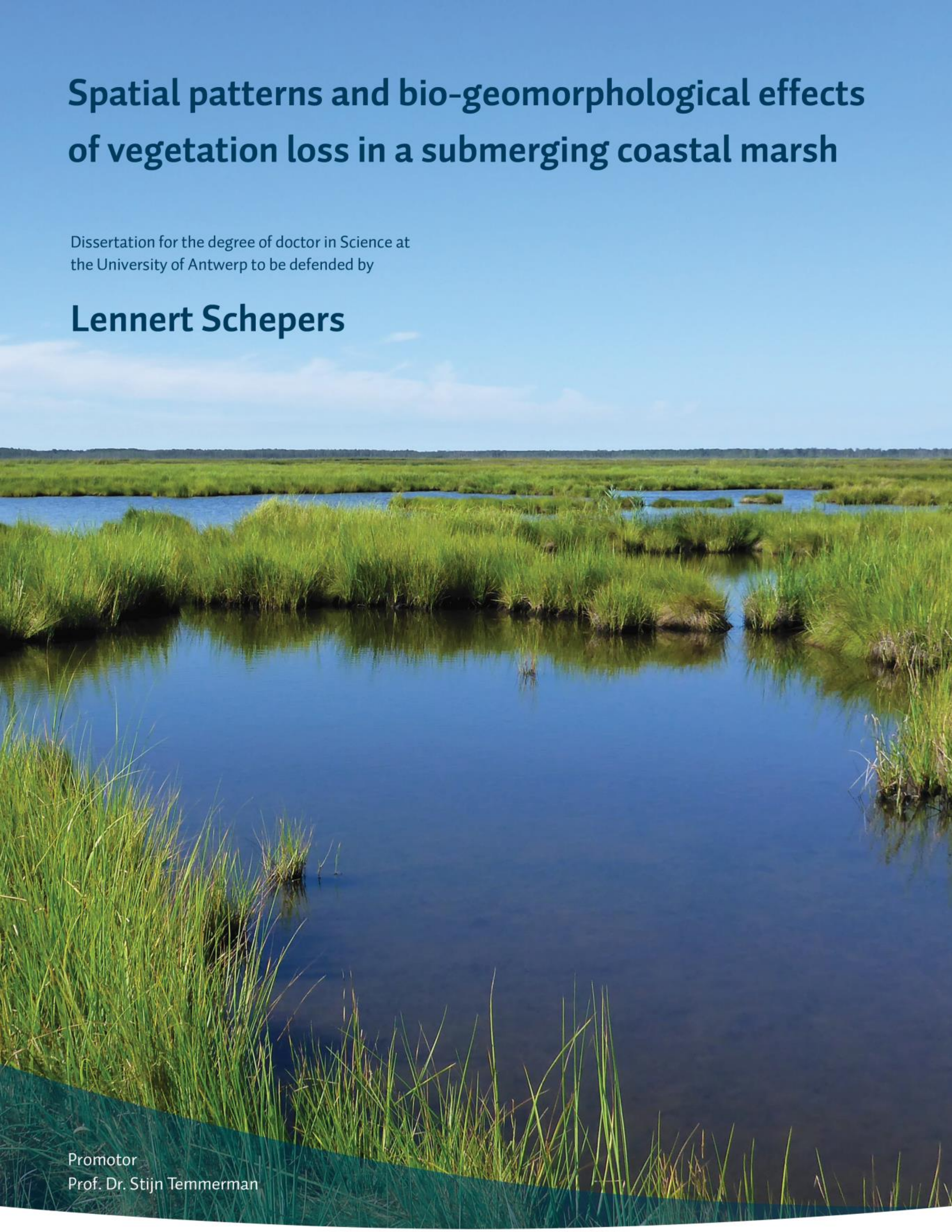

Spatial patterns and bio-geomorphological effects of vegetation loss in a submerging coastal marsh

Dissertation for the degree of doctor in Science at
the University of Antwerp to be defended by

Lennert Schepers

Promotor
Prof. Dr. Stijn Temmerman

Faculty of Science
Department of Biology
Antwerp 2017

Universiteit
Antwerpen

Spatial patterns and bio-geomorphological effects of vegetation loss in a submerging coastal marsh

Ruimtelijke patronen en biogeomorfologische effecten van het verdwijnen van vegetatie in een degraderend schorregebied

Dissertation for the degree of doctor in Science
at the University of Antwerp to be defended by

Lennert Schepers

Promotor:
Prof. Dr. Stijn Temmerman

Faculty of Science
Department of Biology
Antwerp 2017

Universiteit
Antwerpen

Cover design: Anita Muys, Nieuwe Media Dienst, University of Antwerp
Original photograph of the Blackwater Marshes (USA) by Lennert Schepers
Lay-out adapted from Alexandra Silinski

“Mean sea level is a moving target,
and tidal marshes are constantly adjusting
toward a new equilibrium.”
Morris *et al*., 2002

Acknowledgements

This adventure started more than 5 years ago, when Sander Veraverbeke, one of the supervisors of my Master thesis, forwarded a short email to me. It was a PhD vacancy about tidal marshes and he was wondering if this could be something for me. Now, more than 5 years later, I'm still very grateful to Sander for sending me that email. Along this long journey I have met a lot of people who helped me to aim at and to finally reach my moving target: this booklet, which you are now holding in your hands.

To start with, I would like to acknowledge my funders, the University of Antwerp and the Research Foundation Flanders (FWO) for funding my research and me.

I would like to thank my supervisor, Stijn Temmerman, for giving me freedom to explore the vast field of research on my own while providing necessary guidance to keep me on the winding path that leads to a PhD. Thank you for coaching me step by step the hard work of scientific research and writing scientific publications. Your enthusiasm for seemingly unimportant results is contagious.

Thank you Matthew Kirwan (Virginia Institute of Marine Science) and Glenn Guntenspergen (USGS), to enable our field work in the USA. I couldn't have imagined better support. Your trust gave me the opportunity to set out for a second field campaign in the Blackwater Marshes, which resulted in the last chapter of this thesis. Thank you for inviting me into your research groups, for the interesting discussions and for the experience of doing field work in completely different marsh systems than those along the Scheldt Estuary.

I would also like to thank the jury members: Patrick Meire (also as head of our research group), Ivan Janssens, Steven Bouillon, Johan Van de Koppel and Giulio Mariotti, thank you for your positive and insightful feedback, which helped to improve this thesis in the last stage of the process.

A big thank you to Patrick Brennand for your effort in trying to get the best measurements out of every field day, even if this involved dragging a canoe for miles across degraded marshes. Thank you David Walters and Liza McFarland for your helping hands during fieldwork. Patrick and David, thanks for giving me insights into the American way of life and beer culture. I will never forget those moments. Thank you Tom de Dobbelaer for the valuable field support in 't Kijkverdriet, during day and night, rain or shine. These field memories kept me going during long days of soil sample preparation in the lab, months of data analysis and writing of papers…

Thank you to all my former office mates for demonstrating how to pronounce difficult macrophyte names (try: *Potamogeton natans*), making whale and pirate sounds, teaching me how to make craft coffee or tea in numerous ways, for all the nearby and distant field trips. But most of all thank you for your friendship, laughs and support when one of us had a hard time, a writers' block or was stuck somewhere in the middle of a way too long R-script. Thank you Peter our secretary, Tom and Anne in the lab, technicians Dimitri and Jens for helping me with administrative, lab-related or technical advice. Thank you, all ECOBE-colleagues, for the great coffee and lunch breaks, sport sessions, dinners, parties and after-parties during which frustrations could be relieved.

Thank you adventure squad (Dienst Avontuurlijke Activiteiten) from Chirojeugd Vlaanderen, and since last year Gentle Ultimate Frisbee Team for providing the much needed distraction. To my friends from my hometown DMD and my geography classmates, sorry for not having been present at dinners, game nights or parties these last busy months, I will make it up to you.

Thank you to my family for unconditional support, even if you didn't see me for weeks. Most of all, thank you Evelien, for joining me on memorable trips to high mountain peaks, for taking care of me when I was working late, for your unfailing patience and support during this apparently endless work.

Finally it seems that this work has been completed. Let's get this party started.

Summary

Coastal marshes are situated at the interface between land and sea. They consist of a vegetated marsh platform and a channel system, and are regularly flooded by the tides. Their ecological value is of great importance as they provide important ecosystem services. For example, they provide protection against storm surges and water quality regulation. They also provide important habitat for specialized organisms and nursing grounds for fishery species. Furthermore, marshes are one of the most efficient ecosystems for carbon storage. However, when marshes cannot keep up with increasing rates of sea level rise, they will subsequently drown and eventually disappear. This results in large-scale marsh loss, which severely affects their valuable ecosystem functions.

Currently, little is known about how marshes disappear from intact marshes to large open water areas. Also, little is known about the effect of these spatial patterns on tidal flow and sediment dynamics, which is crucial for the recovery of marsh vegetation.

In this thesis we determined the spatial patterns of marsh loss and we studied the bio-geomorphological effect of these losses on flow and sedimentation dynamics. We also investigated how the geomorphology, species composition, soil strength and belowground biomass change with increasing marsh loss. These points were investigated by a combination of methods, covering aerial image analysis, a large-scale mowing experiment (the Scheldt estuary, Belgium), and a wide range of field measurements in the Blackwater Marshes (MD, USA). The Blackwater Marshes are a large micro-tidal marsh system exhibiting a spatial gradient from fairly intact marshes to vast open water where all marshes have been lost.

Our findings show that mashes disappear in particular patterns, starting from small bare patches far from the tidal channels that evolve to large ponds which will eventually be connected to the tidal channel system. Initially, the inner bare patches have little effect on flow and sediment dynamics. However, once ponds deepen below the firm marsh root mat, the underlying material is very soft and prone to erosion, which probably amplifies marsh edge loss and pond deepening. Furthermore, flow velocities might increase once ponds have been connected to the tidal channels, which might lead to export of the loose pond sediments. This results in steep and abrupt elevation changes between marshes and permanently submerged ponds which impede recovery of marsh vegetation in ponds.

These feedbacks highlight the importance of identifying marsh vulnerability as soon as possible to foresee pending shifts from the vegetated marsh state to the pond state. Our research demonstrated that two new indicators, the skewness of the marsh elevation distribution and the co-occurrence of species in mixtures, can be used to assess marsh vulnerability to sea level rise. However, the indices failed to correctly assess the most degraded marsh site by neglecting lateral erosion of the marshes that can lead to a runaway process of permanent marsh loss.

Our findings imply that management of vulnerable marshes should primarily focus on retaining existing marshes rather than trying to restore ponds. Such strategies should pay particular attention to the sediment budget of the whole marsh complex in order to enable remaining marshes to keep up with sea level rise.

While this thesis identifies important bio-geomorphological feedbacks in areas that experience marsh loss, further research is needed to fully understand the processes and interactions between the complex vegetation patterns, flow and sediment dynamics in tidal wetlands.

Samenvatting

Schorren bevinden zich op de scheiding tussen het land en de zee. Schorren bestaan uit een begroeid platform en een geulensysteem en worden regelmatig overstroomd door de getijden. Schorren zijn ecologisch zeer waardevol, ze leveren belangrijke ecosysteemdiensten zoals bescherming tegen stormvloeden en golven, en ze regelen de waterkwaliteit. Daarnaast bieden ze ook belangrijke leefgebieden voor gespecialiseerde organismen en zijn ze paaigebieden voor verschillende vissoorten. Schorren zijn bovendien een van de meest efficiënte ecosystemen voor de opslag van koolstof. Wanneer schorren zich minder snel ophogen dan de zeespiegelstijging, verdwijnen de schorren en dit heeft een grote invloed op hun waardevolle ecosysteemdiensten.

Momenteel is er zeer weinig geweten over hoe schorren ruimtelijk verdwijnen. Deze ruimtelijke patronen hebben mogelijks ook een belangrijk effect op getijdestromingen en het afzetten van slib, twee factoren die mee het herstel van deze gebieden bepalen.

In deze thesis bestudeerden we in welke ruimtelijke patronen schorren verdwijnen en het effect hiervan op getijdestromingen en afzettingspatronen van slib. Daarnaast onderzochten we ook hoe de geomorfologie, soortensamenstelling, bodemsterkte en ondergrondse biomassa veranderen in een degraderend schorregebied. Deze aspecten werden onderzocht door een combinatie van onderzoeksmethoden: luchtfotoanalyse, een grootschalig maaiexperiment langs de Schelde (België), en een breed scala aan veldmetingen in het Blackwater estuarium (Maryland, USA). Dit is een groot microtidaal schorresysteem waarbij een volledige ruimtelijke gradiënt van vegetatie-afsterfte aanwezig is, van intacte schorren tot open water gebieden waar alle schorren verdwenen zijn.

Onze resultaten tonen aan dat schorren in bijzondere patronen verdwijnen. Deze afsterfte start met kleine, kale delen die ver van getijdegeulen gelegen zijn en evolueren tot grote poelen die verbonden zijn met het geulensysteem. Initieel hebben deze kleine kale delen geen grote invloed op de stromings- en afzettingspatronen. Wanneer de eerste ondiepe poelen zich echter verdiepen tot aan de losse lagen onder de stevige wortelzone, wordt de verdieping en vergroting van de poelen waarschijnlijk versneld door erosie. De stroomsnelheid verhoogt bovendien wanneer poelen verbonden zijn met het geulensysteem, waardoor zachte poelsedimenten kunnen wegspoelen. Dit resulteert in steile en grote hoogteverschillen tussen de schorren en permanent overstroomde poelen, wat het herstel van vegetatie in deze poelen verhindert.

Deze interacties benadrukken de kwetsbaarheid van schorren en het belang om kwetsbare schorren zo snel mogelijk te identificeren zodat hierop geanticipeerd kan worden. Ons onderzoek toonde aan dat we twee nieuwe indicatoren, de scheefheid van de hoogteverdeling en de soortensamenstelling van planten, gebruikt kunnen worden om de kwetsbaarheid van schorren bij zeespiegelstijging vast te stellen. Hierbij vermelden we wel dat de indices geen goede inschatting maakten van het gebied met het meeste afsterfte, omdat deze indices geen rekening houden met laterale erosie, wat uiteindelijk kan leiden tot het permanent verdwijnen van schorregebieden.

Ons onderzoek impliceert dat beheer van deze kwetsbare schorren allereerst gericht moet zijn op het behoud van bestaande schorren in plaats van bestaande poelen te proberen herstellen.

Deze strategie moet in het bijzonder rekening houden met het sedimentbudget van het gehele schorresysteem om de bestaande schorren de kans te geven zich verticaal op te hogen met zeespiegelstijging.

Hoewel in deze thesis belangrijke bio-geomorphologische interacties geïdentificeerd werden in gebieden waar schorren verdwijnen, is meer onderzoek nodig om de processen en interacties tussen de complexe vegetatiepatronen, stroming en sedimentdynamieken volledig te begrijpen.

Table of contents

1

Introduction

1.1 Introduction to coastal marshes

Coastal marshes are situated at the interface between land and sea. They are situated around the high water line of tidally influenced coastal areas and are regularly flooded and drained. Coastal marshes are typically dissected by networks of channels (Fig. 1.1) that are the pathways of water, sediments and nutrients. Together the marshes and channels form an ecosystem with valuable ecosystem functions and services.

Figure 1.1: Aerial image of Saeftinghe marsh along the Scheldt River (NL), with a typical geomorphology of channel networks dissecting the marsh platform. The harbor and the city of Antwerp are visible in the background. (Rijkswaterstaat / Joop van Houdt, https://beeldbank.rws.nl).

Coastal marshes provide an important control on the hydrodynamics of coastal areas. They serve as a buffer against storm waves (Möller, 2006; Gedan et al., 2011; Möller et al., 2014) and storm surges (Smolders et al., 2015; Stark et al., 2015). Due to the friction induced by marsh vegetation and the marsh platform, marshes can reduce wave heights by 80% over 160 m of marsh (Möller and Spencer, 2002) or reduce peak water level of storm surges by 7 cm within 100 m of marsh (Stark et al., 2015). In this way, they also reduce erosion and protect dikes (Widdows and Brinsley, 2002; Neumeier and Ciavola, 2004; Neumeier and Amos, 2006; van der Wal et al., 2008; Möller et al., 2014).

Coastal marshes have an important filter function for the coastal zone. They remove sediments (Temmerman et al., 2004), excess nutrients (e.g. nitrogen) (Gribsholt et al., 2005; Van Damme et al., 2009) and pollutants (Du Laing et al., 2007; Teuchies et al., 2013) from the incoming water and and buffer the available silica in the water column, which is an essential important element for the primary producers of the marine food web (Struyf et al., 2005; Müller et al., 2013; Carey and Fulweiler, 2014).

Besides a protective function and a filter function, coastal marshes also provide important habitats for specialized and salt-tolerant fauna and flora (Friess et al., 2012). Their nature value is acknowledged by international directives (e.g. the EU habitat and bird directives, the RAMSAR convention). Coastal marshes provide nursing habitats for ecologically and economically important fishery species, such as shrimps, oysters, clams and fishes (Boesch and Turner, 1984; Baltz et al., 1993; Laffaille et al., 2000; Beck et al., 2001; MacKenzie and Dionne, 2008; Barbier et al., 2011). In the sheltered environment of the marshes, fishes and invertebrates can grow and survive. For example, salt marshes account for 66% of the shrimp and 25 % of the blue crab production in the Gulf of Mexico (Zimmerman et al., 2000), highlighting their importance for the economy of coastal areas.

Coastal marshes are one of the most productive ecosystems in the world, and when they are flooded, they also trap suspended organic particles from the water column. Part of this organic material is sequestered for a long time, on average 218 g carbon per m^2 per year, although burial rates might differ between systems (McLeod et al., 2011; Duarte et al., 2013). Soil oxygen is limited in these systems, which favors conservation of organic material for thousands of years, making coastal wetlands one of the most efficient systems for long-term carbon storage (McLeod et al., 2011; Duarte et al., 2013). However, the buried carbon deposits can be released again by lateral wave erosion or by decomposition after vegetation die-off (DeLaune et al., 1994; van Huissteden and van de Plassche, 1998; Day et al., 2011).

The above-mentioned list of ecosystem functions is not exhaustive and gives only a small overview on the many benefits of coastal marshes. Recently, several studies have tried to estimate the total value of the ecosystem functions and services that marshes provide. In these studies, the value of marshes is estimated between US $10,000 to $200,000 per ha of marsh per year (Barbier et al., 2011; Costanza et al., 2014), making it one of the most valuable ecosystems worldwide.

1.2 Feedbacks between inundation, biomass production and marsh accretion

1.2.1 Usually, marshes keep up with sea level rise…

Within marshes, the plants and the sediment have remarkable eco-geomorphic interactions: through feedback-loops of plant growth and sedimentation, these tidal wetlands actively engineer their environment and manage to maintain their position within the intertidal frame. This enhances ecosystem persistence even during modest sea level rise (Kirwan and Megonigal, 2013).

Marshes build up in two ways. First, the above- and belowground biomass production of marshes contributes directly to the build-up by organic material (Nyman et al., 2006; Kirwan and Guntenspergen, 2012). Secondly, the dense vegetation canopies capture sediment with their stems and leaves (Mudd et al., 2004; Li and Yang, 2009), and they also reduce flow velocities and thereby indirectly promote sediment deposition on the marsh surface (Leonard and Croft, 2006; Neumeier and Amos, 2006; Baustian et al., 2012; Moskalski and Sommerfield, 2012).

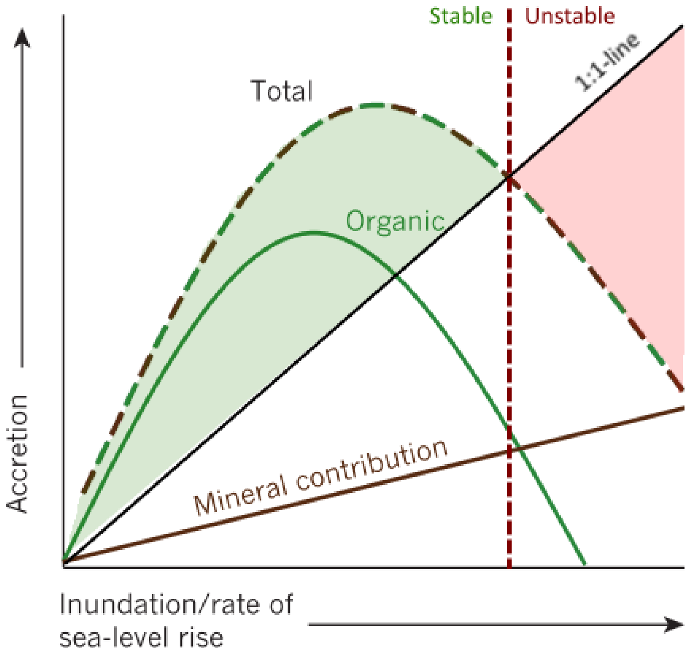

Figure 1.2: organic and inorganic contributions to sediment accretion (elevation gain) in sediment-poor systems. Increases in the inundation increase the mineral deposition (brown solid line), and also organic productivity to a certain extent (green hump-shaped curve). When total accretion (dashed green and brown line) is lower than the relative sea level rise (1:1-line), the inundation increases until marsh vegetation dies off. Modified from (Kirwan and Megonigal, 2013).

When marshes are positioned high in the tidal frame and are infrequently inundated, evaporation can increase salt stress, leading to decreased productivity (left limit of green line in Fig. 1.2) (Morris et al., 2002; Langley et al., 2013; Kirwan and Guntenspergen, 2015). Infrequent inundations also limit mineral sediment deposition (brown line in Fig. 1.2). These feedbacks prevent marshes to build up higher than high water level.

On the other hand, a number of feedbacks allow marshes to keep this high elevation even with increased sea level rise. When high elevated marshes are increasingly inundated (for example by increased sea level rise rates), above- and belowground productivity will increase so that the marshes will build up faster. More aboveground biomass leads to higher amounts of sediment being directly captured by the stems and leaves, and more flow reduction leading to more deposition of suspended sediment. Increased flooding frequencies also directly result in more suspended sediment supply to the marshes (Fig. 1.2 solid brown line) (Stoddart et al., 1989; Cahoon and Reed, 1995; Temmerman et al., 2003b). This feedback between increased flooding and increased sediment accretion is consistent with a recent meta-analysis suggesting that accretion rates could more than double during the transition from infrequently inundated, high elevation marshes to frequently inundated, low elevation marshes (Kirwan et al. 2016).

Through these feedback mechanisms, coastal marshes have been able to develop and persist over thousands of years under Holocene sea level rise rates ranging from 1 to several tens of millimeters per year (Li et al., 2012; Kirwan and Megonigal, 2013; Kirwan et al., 2016).

1.2.2 …but sometimes they drown.

However, marshes can only keep up with sea level rise to a certain extent. In some areas, low suspended sediment concentrations in the water limit mineral build-up of marshes when flooded. Micro-tidal marshes seem to be particularly vulnerable to low sediment inputs, since their flow velocities during flooding are usually too low to import substantial mineral sediment into the marsh interiors (Kearney and Turner, 2016). Therefore these marshes rely on the build-up of organic material. For plant species which have an optimal inundation level (see above), organic build-up might compensate sea level rise. However, when inundation exceeds this optimal point, plant productivity decreases (green line in Fig. 1.2)(Morris et al., 2002; Kirwan et al., 2010; Kirwan and Guntenspergen, 2015) and the marsh drowns. Furthermore, some marsh species such as *Spartina patens* and *Distichlis spicata do* not show such a parabolic relationship between inundation and plant productivity (Bertness, 1991; Langley et al., 2013; Kirwan and Guntenspergen, 2015). Instead, they show a gradual decline in biomass with more inundation. Marsh plants might also be restricted to suboptimal elevations by competitive displacement (Bertness, 1991), and as such they might not increase their productivity with increasing sea level rise. Decreasing plant biomass may even provoke a feedback effect that leads to worsening conditions for plant growth: less dense marsh canopies result in less organic matter deposition, less sediment capture by the plants and reduced sedimentation rates. When the total accretion rate (organic and mineral) is lower than the rate of sea level rise, there is an elevation deficit (red shaded area in Fig. 1.2), and marshes will keep lagging behind sea level. Marshes are more extensively flooded, until marsh vegetation eventually dies off.

1.3 Marsh vegetation loss

1.3.1 Causes of vegetation loss in coastal marshes

Several factors might cause marsh plants to die-off or to disappear, which might lead to large-scale marsh loss (see Fig. 1.3). First of all, when marsh accretion rates are exceeded by sea level rise (see above), increased flooding creates waterlogging effects such as anoxic conditions and sulphide toxicity that exceeds the tolerance limits of vegetation, and plants will die (Mendelssohn and McKee, 1988; Nyman et al., 1993; Morris et al., 2002). The other extreme, drought, can also lead to initial plant die-off when evaporation increases salt stress (Delaune and Pezeshki, 1994; Silliman et al., 2005; Baustian et al., 2012). Several studies highlight the importance of herbivory in marsh vegetation loss. Rodents such as muskrats (*Ondatra zibethicus*) and nutria (*Myocastor coypus*) feed on the roots of marsh plants and use the plants for building beds (Stevenson et al., 1985; Kendrot, 2011). Crabs (Perillo and Iribarne, 2003; Holdredge et al., 2009; Hughes et al., 2009), snails (Stevenson et al., 1985; Silliman et al., 2005; Kirwan et al., 2008) or geese (Esselink et al., 1997; Handa et al., 2002; Jefferies et al., 2006; Kotanen and Abraham, 2013; Elschot et al., 2017) all feed on marsh plants or roots and as such they can create bare patches, or even, in the case of snails, traveling 'consumer fronts' that consume all aboveground biomass (Silliman et al., 2005). Initial die-off can also start as physical disturbance by tidal deposition of litter or ice rafting (Pethick, 1974; Boston, 1983; Ewanchuk and Bertness, 2003). These are all local, small disturbances to which marshes are generally tolerant and typically, multiple stressors are needed to have long-term effects (Silliman et al., 2005). Often, these small die-off areas might recover and become recolonized after disturbance (Redfield, 1972; Perillo et al., 1996; Millette et al., 2010; Wilson et al., 2010, 2014; Elschot et al., 2017).

Figure 1.3: Aerial image of the Blackwater marshes (Maryland, USA) that experiences extensive vegetation loss. (IAN Image Library/ Jane Thomas, http://ian.umces.edu/imagelibrary/)

1.3.2 Deepening and enlargement of bare areas to ponds

The loss of vegetation can create an elevation deficit compared to the surrounding marsh areas where marsh vegetation still captures sediment and promotes deposition of suspended sediment by reducing flow velocities (Baustian et al., 2012; Temmerman et al., 2012b). Several studies point to the collapse of the root structure and gradual decomposition or disintegration of the soil organic matter by sulfate-reducing bacteria as mechanism for further deepening and pond formation (DeLaune et al., 1994; van Huissteden and van de Plassche, 1998; Day et al., 2011). The exact location of these bare patches has not been studied before, but some studies describe these ponds as 'interior ponds' (Redfield, 1972; Stevenson et al., 1985) with the larger ones located relatively remote from the drainage creeks (Redfield 1972).

It has been suggested that ponds can enlarge by surficial flooding of the adjacent marsh surface and consequent vegetation die-off (Wilson et al., 2009), or by decomposition and decay of the surrounding marsh edges (Redfield, 1972; van Huissteden and van de Plassche, 1998). Rotational slumping (Stevenson et al., 1985), failure of unstable marsh scarps (Day et al., 2011) and soil creep (Mariotti et al., 2016) are processes that describe the downslope transport of marsh sediment to the pond bottom, which might expand ponds. The marsh edge might also retreat with deepening ponds as passive adjustment to an equilibrium bed slope (Mariotti, 2016).

Neighboring ponds may merge to form larger ponds (Yapp et al., 1917; Redfield, 1972; Kearney et al., 1988; Wilson et al., 2009). This process likely starts by subsurface connections between adjacent ponds (van Huissteden and van de Plassche, 1998; Wilson et al., 2009). When ponds are large enough, wind-generated wave erosion may further expand the ponds (Stevenson et al., 1985; Perillo et al., 1996; Morton et al., 2003; Mariotti and Fagherazzi, 2013). Larger waves in larger ponds can also deepen the ponds when wave shear stresses exceed the critical erosion threshold of the pond bottom. This feedback is however limited, since the wave shear stresses decrease deeper in the water column. So at a certain depth, the decreasing wave shear stresses will equal the critical erosion threshold, which limits erosion of the underlying pond bottom (Fagherazzi et al., 2006; Defina et al., 2007; Wilson and Allison, 2008).

1.3.3 Recovery or permanent marsh loss?

Several studies report the recovery of ponds after they have connected to the tidal channel network, for example in several New England (USA) saltmarshes (Redfield, 1972; van Huissteden and van de Plassche, 1998; Wilson et al., 2009, 2010, 2014; Millette et al., 2010), while in other areas such as the Chesapeake Bay, the marshes are permanently lost (Stevenson et al., 1985; Kearney et al., 1988; Wray et al., 1995). Recovery of marsh vegetation in ponds seems to be possible when (i) there is a connection to the tidal channel network, (ii) there is sufficient sediment import and (iii) ponds are smaller than a critical size for wind-induced wave erosion.

A connection to the tidal channel might be necessary to halt decomposition of organic material and to restore the water chemistry conducive for plant growth in ponds (Mariotti, 2016). Furthermore, the connection of the channel might drain the ponds and deliver sediments to the ponds (Redfield, 1972; van Huissteden and van de Plassche, 1998; Wilson et al., 2009, 2010, 2014; Millette et al., 2010).

The input of sediment is crucial for marsh recovery, as this is needed to accrete ponds faster than sea level rise rates. In unvegetated ponds there is no organic contribution to building up the ponds, thus pond accretion depends fully on external sediment supply. This has been confirmed by modeling studies that highlight the importance of sediment supply for marsh recovery after disturbance or pond formation (Kirwan et al., 2008; Kirwan and Guntenspergen, 2010; Mariotti and Carr, 2014; Mariotti, 2016). Also a field experiment with experimental disturbances of the marsh vegetation demonstrated that the rate of recovery is directly related to sediment availability (Slocum and Mendelssohn, 2008).

When ponds or open water areas reach a critical threshold size, they become susceptible to wind-induced wave erosion, which accelerates marsh loss (Mariotti and Fagherazzi, 2013; Mariotti, 2016; Ortiz et al., 2017) and limits marsh recovery. Importantly, this loss accelerates non-linearly with increasing pond size and hence may lead to complete marsh collapse (Fagherazzi et al., 2013; Ortiz et al., 2017). This has been observed in the Blackwater estuary (Maryland, USA) (Stevenson et al., 1985; Ganju et al., 2013), in several marsh basins along the US Atlantic coast (Mariotti and Fagherazzi, 2013; Leonardi and Fagherazzi, 2014) and in the Mississippi delta (Ortiz et al., 2017).

1.3.4 Effect of marsh vegetation die-off on water flow and sedimentation patterns

Pond formation and expansion is considered as one of the major drivers of coastal marsh loss in micro-tidal areas, where sediment supply and tidal range are very low (Kearney et al., 1988; Penland et al., 2000; Morton et al., 2003; Mariotti and Fagherazzi, 2013; Kearney and Turner, 2016; Mariotti, 2016). Despite this acknowledgement, very little is known about the spatial development of marsh loss through pond formation and the effect of these patterns on flow and sedimentation patterns. Previous studies describe the pattern of marsh loss (see above) without quantitative analysis, or they focus on a large scale (>1km) irrelevant for geomorphic and hydrodynamic processes (Day et al., 2000; Penland et al., 2000). As a result, existing models simulate vegetation loss as a stochastic process (Kirwan et al., 2008), by complete vegetation removal (Temmerman et al., 2012b) or by only considering one single pond or marsh basin (Mariotti and Fagherazzi, 2013; Mariotti and Carr, 2014; Mariotti, 2016). To our knowledge, only (Temmerman et al., 2012a)) used simulated spatial patterns of vegetation die-off with respect to the tidal channel system for simulating coastal flood attenuation. However, also these die-off patterns are not simulated based on quantitative observations.

Furthermore, the bio-geomorphic interactions between patterns of vegetation loss, tidal flow and sediment dynamics are poorly understood. It is known that complete removal of the vegetation shows higher flow velocities and changing flow directions (Temmerman et al., 2012b), and generally lower surface accretion rates (Baustian et al., 2012). When ponds become larger than ~100 m, wind-induced waves can erode the pond edges (see above). These are clear examples demonstrating that vegetation loss is changing the known flow or sediment dynamics. However, research so far has only focused on the last stages of marsh loss where ponds are large, or no vegetation is left. At these stages, marsh restoration is unlikely due to the feedbacks between pond size and wave erosion. Thus research focusing on the full spectrum of marsh vegetation loss is needed to detect marsh vulnerability and prevent marsh loss in the first place, and to take adequate restoration measures when marsh loss has been observed.

1.4 Objectives for this thesis

In this thesis we pursued the general aim of determining spatial patterns of vegetation loss and the processes that are linked to marsh loss and to study their bio-geomorphological effect on flow and sedimentation dynamics. We studied the full spectrum of marsh loss, from intact marshes to large-scale marsh loss (Fig. 1.4). First we determined the spatial and temporal patterns of marsh vegetation loss (**Chapter 2**). We then looked into short-term effects on tidal flow and sedimentation patterns (**Chapter 3**), and into the long-term effects by studying elevation of marshes and ponds (**Chapter 4**). Furthermore, we focus also on marsh properties that are linked with marsh loss and sea level rise. We tested if two marsh metrics can be used to assess marsh vulnerability to sea level rise and thus foresee marsh loss (**Chapter 5**). Finally, we tested if marsh soil properties enhance erosion (**Chapter 6**).

More specifically, we addressed following aspects:

In **Chapter 2**, we quantified the spatial and temporal patterns of vegetation loss. Where do initial bare patches and ponds occur? How do these evolve? Do they always become larger? In order to address these questions, we analyzed time series of aerial images of the Blackwater marshes, a brackish marsh system along the Chesapeake Bay (Maryland, USA). This system was chosen because it represents a spatial gradient from intact marshes at the coast to degraded marshes inland that have completely been converted to shallow water. They are a poster example on how marshes will evolve with continued sea level rise in a micro-tidal system. We test if changes in vegetation loss patterns through time are similar to the patterns occurring along the spatial gradient and hypothesize that the distance from tidal channels is a key determining factor explaining the spatial pattern of pool initiation and development.

In the next step, we determined the effect of the spatial and temporal patterns of vegetation loss on a short and a long time frame. In Chapter 3, we investigated the short-term effects of the spatio-temporal patterns of vegetation die-off on flow and sedimentation patterns. This was studied by simulating the vegetation loss patterns with a mowing experiment and by measuring the flow and sediment dynamics during tidal inundations. Different mowing patterns were applied that resemble the typical spatio-temporal stages of marsh vegetation loss as observed in the second chapter. This was done in a tidal marsh along the Scheldt River in Belgium. In Chapter 4, we quantified the long-term effects of the vegetation die-off on elevation changes by measuring topographic elevations in the Blackwater marshes, as an integrated measure of long-term sedimentation or erosion. These measurements reveal insights into the processes leading to changes in vertical elevation of marshes and interior ponds along the spatial gradient from intact marshes to completely degraded marshes.

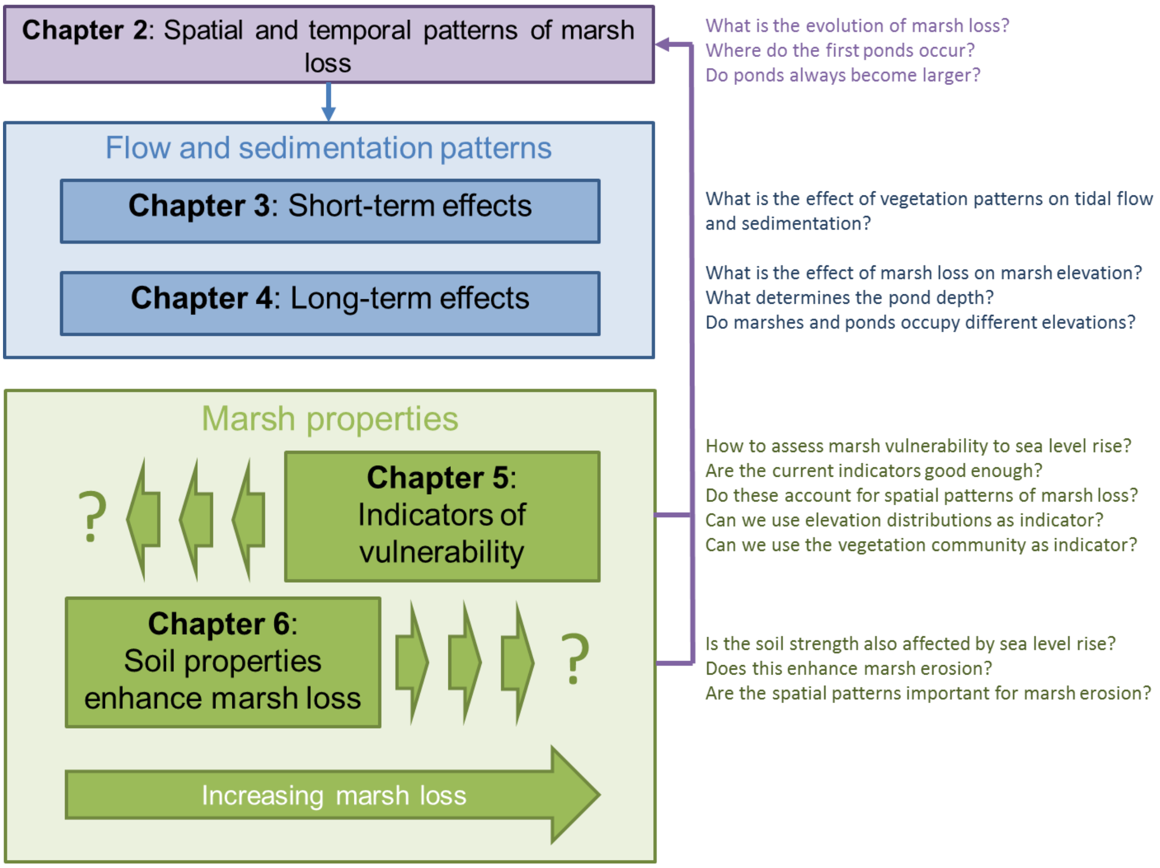

What is the evolution of marsh loss?
Where do the first ponds occur?
Do ponds always become larger?

What is the effect of vegetation patterns on tidal flow and sedimentation?

What is the effect of marsh loss on marsh elevation?
What determines the pond depth?
Do marshes and ponds occupy different elevations?

How to assess marsh vulnerability to sea level rise?
Are the current indicators good enough?
Do these account for spatial patterns of marsh loss?
Can we use elevation distributions as indicator?
Can we use the vegetation community as indicator?

Is the soil strength also affected by sea level rise?
Does this enhance marsh erosion?
Are the spatial patterns important for marsh erosion?

Figure 1.4: Schematic overview of the thesis chapters and key questions addressed in each of the chapters.

We studied different marsh properties to gain more insights into the processes of marsh loss. In **Chapter 5**, we tested if we can predict or detect imminent vegetation loss along the marsh die-off gradient of the Blackwater marshes, by two indicators of vegetation loss vulnerability that have never been tested in the field: the skewness of the elevation distribution and the species composition. We compared our results with newly created indices specifically developed to assess vulnerability to sea level rise. We formulated some suggestions for improvements of these indices, especially regarding the observed spatio-temporal marsh loss patterns and their effects. In **Chapter 6**, we quantified the soil strength and associated soil properties along the gradient of marsh die-off in the Blackwater marshes, because this determines how easily marshes are eroded. We investigated the differences between marsh areas with a different degree of vegetation loss, different ponds and between different soil depths. This will help us to understand if soil properties enhance vegetation loss in submerging marshes.

We end our thesis with a general conclusion of our findings, management advice and an outlook for potential research in the synthesis chapter (**Chapter 7**).

1.5 Overview of field sites

Most of the research in this thesis was focused on the Blackwater marshes along the Chesapeake Bay, USA (**Chapter 2, 4, 5, 6**). In **Chapter 3** we conducted a field experiment at a small marsh (Kijkverdriet) along the Scheldt estuary, Belgium.

1.5.1 Blackwater marshes, Maryland, USA

The Blackwater marshes (38°24' N, 76°40' W, Fig. 1.5) are located in Dorchester County, Maryland, on the Eastern Shore of the Chesapeake Bay. The marshes are situated along the Blackwater River that discharges into the Fishing Bay, which is a tributary embayment of the larger Chesapeake Bay. Nearly all of the marshes are currently protected as part of the Blackwater National Wildlife Refuge (upstream areas) or the Fishing Bay Wildlife Management Area (downstream marshes).

During the last glacial maximum (30 ka BP), the Chesapeake Bay region was uplifted at the forebulge of the Laurentide ice sheet and the Blackwater river incised a large valley of about 10 m depth (Dejong et al., 2015). This forebulge subsided during the Holocene, and from about 5000 years ago the Blackwater River valley was inundated which started the deposition of a 4-5 m thick layer of silt (Dejong et al., 2015). Widespread marshes established in the course of the last millennium and accreted another 4-5 m of dense organic peat, keeping pace with sea-level rise. Subsidence by glacial isostatic adjustment still accounts for about 1mm/yr at the Chesapeake Bay (Engelhart et al., 2009). Sea level rise accelerated during the twentieth century, and especially during the last decades with sea level rise rates that are 3-4 times higher than the global average (Engelhart et al., 2009; Sallenger et al., 2012). This increase (compared to the global average) is probably due to local ocean circulations and variations in temperature and salinity (Sallenger et al., 2012). Currently, relative sea level rise is 3.7 mm/yr nearby in Cambridge, MD, (NOAA station 8571892, http://tidesandcurrents.noaa.gov/sltrends, 10/10/2017).

Historical accretion rates (on average 1.7-3.6 mm yr^{-1} (Stevenson et al., 1985)) were insufficient to follow this accelerated sea level rise, which lead to inundation and erosion of the marshes. Since the 1930s, more than 2000 ha or 51 % of the upstream marshes have been lost and converted to open water (Stevenson et al., 1985; Scott et al., 2009; Cahoon et al., 2010). The historical marsh loss is focused in the most upstream areas, which resulted in an apparent gradient from fairly intact marshes closest to the Fishing Bay (SE in Fig. 1.5) up to the vast open shallow water Lake Blackwater (NW in Fig. 1.5) that was still partly vegetated until the 1930s.

Marsh loss at the Blackwater marshes has, besides submergence by sea level rise, also been attributed to vegetation disturbance by rodents (muskrats (*Ondatra zibethicus*) and invasive nutria (*Myocastor coypus*), subsequent open-water expansion (Stevenson et al., 1985; Kendrot, 2011) and wave erosion at Lake Blackwater (Ganju et al., 2013). Recent measurements close to the Blackwater River revealed that root zone subsidence or collapse is significant as it contributes up to 6 mm/yr in addition to sea level rise. However, the measurements also demonstrate that current accretion rates (up to 10 mm/yr) are sufficient to offset shallow subsidence and sea level rise (Cahoon et al. 2010, Guntenspergen 2017, unpublished data). This is due to unexpectedly high suspended sediment concentrations (50 mg/L)(Ganju et al., 2013), likely originating from internal wetland collapse and marsh retreat along Lake Blackwater

(Stevenson et al., 1985; Cahoon et al., 2010; Ganju et al., 2013). Moreover, while some of the internally generated sediment accretes the nearby marshes, a considerable amount is exported out of the marsh complex during northeasterly wind events (Ganju et al., 2013, 2015). At the Blackwater National Wildlife Refuge, managers try to restore the marshes by prescribed burning of selected marsh areas during winter, which promotes biomass production the next season (Cahoon et al., 2010; Geatz et al., 2013), by sediment infilling at local restoration sites, and by designing corridors for the landward migration of the tidal marshes.

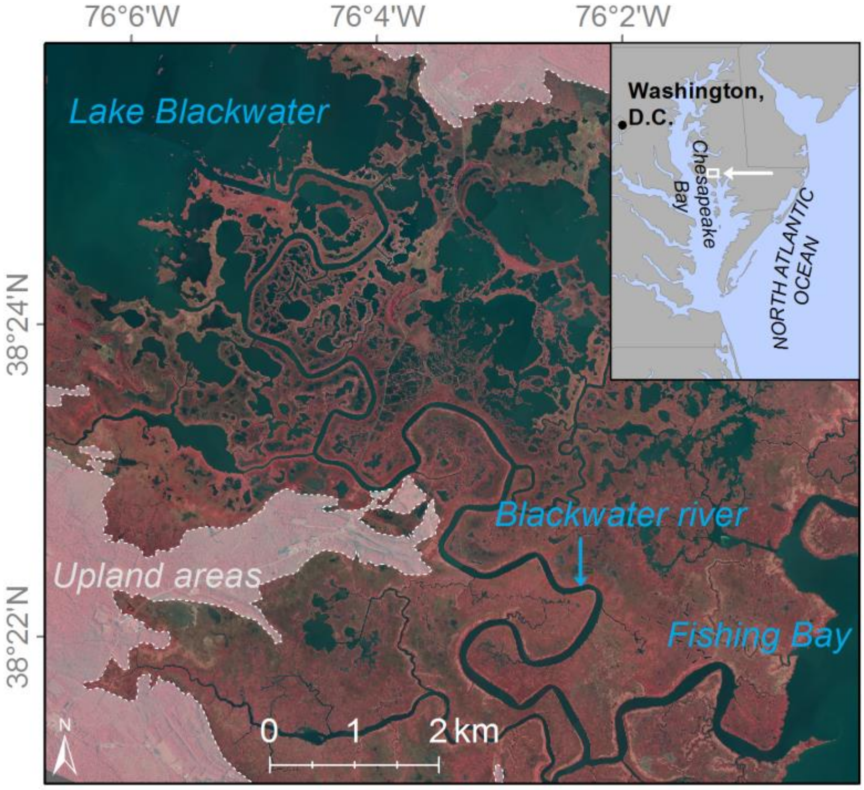

Figure 1.5: False color aerial image of the Blackwater Marshes in 2010. From SE to NW in the image (i.e. in upstream direction along the Blackwater River) marshes are evolving from high marsh vegetation cover (reddish color) close to the Fishing Bay (SE) to increasingly degraded marshes and open water areas (dark color) in upstream direction, and ultimately to Lake Blackwater (NW). White shaded areas with dashed outlines are no marshes but upland areas. Inset: Location of the Blackwater marshes along the Chesapeake Bay (white rectangle).

Short-term measurements showed that salinity varies little (<2 ppt) between the most downstream site of the Blackwater marshes near Fishing Bay and the upstream marshes at Lake Blackwater. The semi-diurnal micro-tidal estuary has a spring tidal range varying from over 1.0 m at the Fishing Bay to less than 0.2 m at Lake Blackwater (Ganju et al., 2013). However, storm tides may exceed 1.0 m at the Chesapeake Bay (Wang and Elliott, 1978; Stevenson et al., 1985). The marshes are characterized by mesohaline marsh vegetation: *Spartina cynosuroides* is dominant on a small band next to the river and the bigger tidal channels. *Spartina alterniflora* and *Schoenoplectus americanus* are most abundant in the other areas, often in assemblages with *Spartina patens* and *Distichlis spicata*.

Freshwater inflow to the Blackwater marshes comes primarily from the Little Blackwater River and varies seasonally, with peaks at 6 m^3/s during winter months but negative discharges (more water flowing upstream) during the summer months (Fleming et al., 2011). Similarly, salinity levels at this point varies seasonally from <1 to 12 ppt in winter and summer, respectively (Fleming et al., 2011). The watershed of the Little Blackwater river is small (ca. 110 km^2) and mainly consists out of agricultural land and forest (Fleming et al., 2011). Visual inspection of 1938 aerial imagery and recent aerial imagery showed little land-use changes in this period. Sediment supply from the Little Blackwater River to the marshes are low (<10 mg/L) (Ganju et al., 2013).

1.5.2 Kijkverdriet, Scheldt estuary, Belgium

The estuary of the River Scheldt extends from the mouth at the North Sea near Vlissingen (the Netherlands) to Ghent (Belgium), at 160 km from the estuary mouth where sluices impede further inland propagation of the tidal wave (Meire et al., 2005) (Fig. 1.6). Along this stretch, the salinity gradually decreases in landward direction, and therefore the intertidal marshes can be differentiated into salt, brackish and freshwater marshes (Fig. 1.6, see Meire et al. (2005) for more information). Historical land reclamation and industrial and urban developments have decreased the tidal area of the Scheldt estuary (Meire et al., 2005), while historical shortening, straightening and dredging have increased the tidal wave propagation into the estuary (Van Braeckel et al., 2006). Today the semi-diurnal tidal range increases from the North Sea (4 m) towards our study site Kijkverdriet (6 m) from where it decreases again towards Ghent (2 m) (data 2001-2010, http://www.waterinfo.be). At the location of the Kijkverdriet, the Scheldt river is about 400 m wide and peak ebb and flood velocities in the river channel are higher than 1m/s (Plancke et al., 2009). Wind-induced waves are negligible. Salinities range between 0.4 and 2.1 ppt (data http://www.scheldemonitor.be/ 25/11/2017).

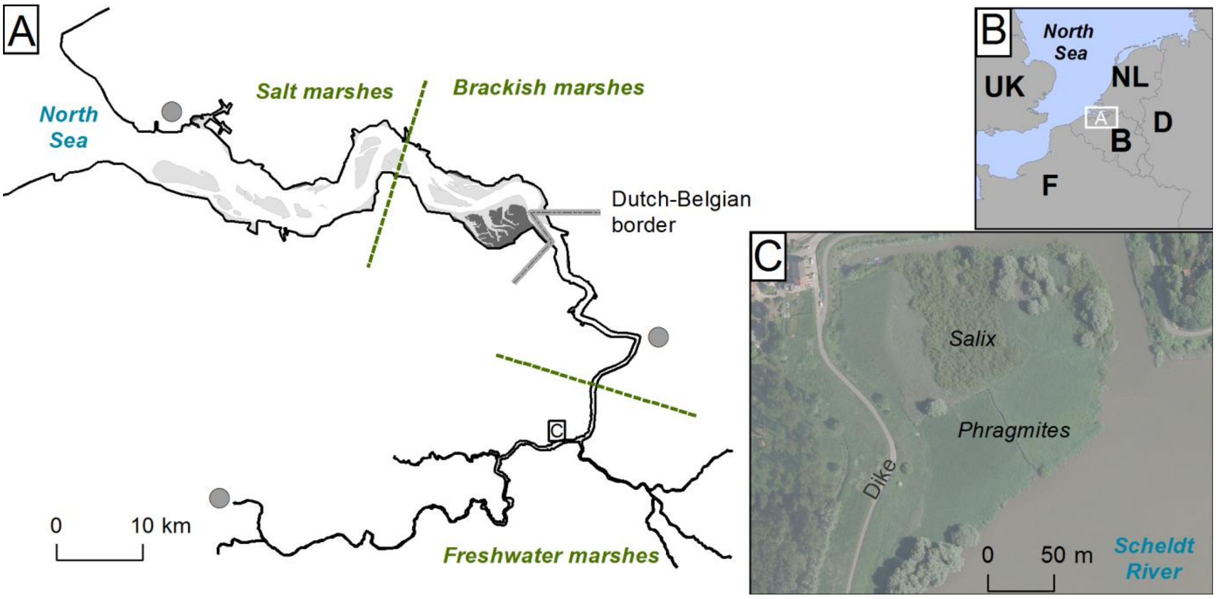

Figure 1.6: A: Overview of the Scheldt estuary. B: Location of the Scheldt estuary within Belgium and the Netherlands. C: Aerial image of Kijkverdriet marsh.

Our study area, Kijkverdriet (51.1213° N, 4.2641° E), is a small freshwater marsh that was embanked around the year 1850 to be used as grassland. After 1950, the embankment was no longer sustained and was exposed to tidal influence again. Since 1980, the managers of the area mow the marsh once per year in order to preserve the native *Phragmites australis* (common reed) vegetation and to prevent succession to *Salix* (willow) shrubs, which are already present in some parts. The human history is still visible in the geomorphology of the marsh, which consists of a generally flat marsh platform around mean high water level dissected by a single unvegetated tidal creek (Temmerman et al., 2012b) (Fig. 1.6). Local suspended sediment concentrations in the adjacent estuarine channel range between < 5 and 300 mg/L, with highest concentrations during spring tides in winter (Temmerman et al., 2003a).

1.6 References

Baltz, D.M., Rakocinski, C., Fleeger, J.W., 1993. Microhabitat use by marsh-edge fishes in a Louisiana estuary. Environ. Biol. Fishes 36, 109–126. doi:10.1007/BF00002790

Barbier, E.B., Hacker, S.D., Kennedy, C., Koch, E.W., Stier, A.C., Silliman, B.R., 2011. The value of estuarine and coastal ecosystem services. Ecol. Monogr. 81, 169–193. doi:10.1890/10-1510.1

Baustian, J.J., Mendelssohn, I.A., Hester, M.W., 2012. Vegetation's importance in regulating surface elevation in a coastal salt marsh facing elevated rates of sea level rise. Glob. Chang. Biol. 18, 3377–3382. doi:10.1111/j.1365-2486.2012.02792.x

Beck, M.W., Heck, K.L., Able, K.W., Childers, D.L., Eggleston, D.B., Gillanders, B.M., Halpern, B., Hays, C.G., Hoshino, K., Minello, T.J., Orth, R.J., Sheridan, P.F., Weinstein, M.P., 2001. The Identification, Conservation, and Management of Estuarine and Marine Nurseries for Fish and Invertebrates. Bioscience 51, 633. doi:10.1641/0006-3568(2001)051[0633:TICAMO]2.0.CO;2

Bertness, M.D., 1991. Interspecific Interactions among High Marsh Perennials in a New England Salt Marsh. Ecology 72, 125–137. doi:10.2307/1938908

Boesch, D.F., Turner, R.E., 1984. Dependence of Fishery Species on Salt Marshes: The Role of Food and Refuge. Estuaries 7, 460–468. doi:10.2307/1351627

Boston, K.G., 1983. The development of salt pans on tidal marshes, with particular reference to south-eastern Australia. J. Biogeogr. 10, 1–10.

Cahoon, D.R., Guntenspergen, G.R., Baird, S., 2010. Do Annual Prescribed Fires Enhance or Slow the Loss of Coastal Marsh Habitat at Blackwater National Wildlife Refuge? Final Report to Joint Fire Science Program Project Number 06-2-1-35.

Cahoon, D.R., Reed, D.J., 1995. Relationships among Marsh Surface Topography, Hydroperiod, and Soil Accretion in a Deteriorating Louisiana Salt Marsh. J. Coast. Res. 11, 357–369. doi:10.2307/4298345

Carey, J.C., Fulweiler, R.W., 2014. Salt marsh tidal exchange increases residence time of silica in estuaries. Limnol. Oceanogr. 59, 1203–1212. doi:10.4319/lo.2014.59.4.1203

Costanza, R., de Groot, R., Sutton, P., van der Ploeg, S., Anderson, S.J., Kubiszewski, I., Farber, S., Turner, R.K., 2014. Changes in the global value of ecosystem services. Glob. Environ. Chang. 26, 152–158. doi:10.1016/j.gloenvcha.2014.04.002

Day, J.W., Britsch, L.D., Hawes, S.R., Shaffer, G.P., Reed, D.J., Cahoon, D.R., 2000. Pattern and Process of Land Loss in the Mississippi Delta: A Spatial and Temporal Analysis of Wetland Habitat Change. Estuaries 23, 425–438. doi:10.2307/1353136

Day, J.W., Kemp, G.P., Reed, D.J., Cahoon, D.R., Boumans, R.M., Suhayda, J.M., Gambrell, R., 2011. Vegetation death and rapid loss of surface elevation in two contrasting Mississippi delta salt marshes: The role of sedimentation, autocompaction and sea-level rise. Ecol. Eng. 37, 229–240. doi:10.1016/j.ecoleng.2010.11.021

Defina, A., Carniello, L., Fagherazzi, S., D'Alpaos, L., 2007. Self-organization of shallow basins in tidal flats and salt marshes. J. Geophys. Res. Earth Surf. 112, 1–11. doi:10.1029/2006JF000550

Dejong, B.D., Bierman, P.R., Newell, W.L., Rittenour, T.M., Mahan, S.A., Balco, G., Rood, D.H., 2015. Pleistocene relative sea levels in the Chesapeake Bay region and their implications for the next century. GSA Today 25, 4–10. doi:10.1130/GSATG223A.1.4

DeLaune, R.D., Nyman, J.A., Patrick, W.H., 1994. Peat collapse, ponding and wetland loss in a rapidly submerging coastal marsh. J. Coast. Res. 10, 1021–1030.

Delaune, R.D.D., Pezeshki, S.R.R., 1994. The Influence of Subsidence and Saltwater Intrusion on Coastal Marsh Stability:Louisiana Gulf Coast, U.S.A. J. Coast. Res. Sp.Issue 1, 77–89.

Du Laing, G., Vandecasteele, B., De Grauwe, P., Moors, W., Lesage, E., Meers, E., Tack, F.M.G., Verloo, M.G., 2007. Factors affecting metal concentrations in the upper sediment layer of intertidal reedbeds along the river Scheldt. J. Environ. Monit. 9, 449–455. doi:10.1039/b618772b

Duarte, C.M., Losada, I.J., Hendriks, I.E., Mazarrasa, I., Marbà, N., 2013. The role of coastal plant communities for climate change mitigation and adaptation. Nat. Clim. Chang. 3, 961–968. doi:10.1038/nclimate1970

Elschot, K., Vermeulen, A., Vandenbruwaene, W., Bakker, J.P., Bouma, T.J., Stahl, J., Castelijns, H., Temmerman, S., 2017. Top-down vs. bottom-up control on vegetation composition in a tidal marsh depends on scale. PLoS One 12, e0169960. doi:10.1371/journal.pone.0169960

Engelhart, S.E., Horton, B.P., Douglas, B.C., Peltier, W.R., Törnqvist, T.E., 2009. Spatial variability of late Holocene and 20th century sea-level rise along the Atlantic coast of the United States. Geology 37, 1115–1118. doi:10.1130/G30360A.1

Esselink, P., Helder, G.J.F., Aerts, B.A., Gerdes, K., 1997. The impact of grubbing by Greylag Geese (Anser anser) on the vegetation dynamics of a tidal marsh. Aquat. Bot. 55, 261–279.

Ewanchuk, P.J., Bertness, M.D., 2003. Recovery of a northern New England salt marsh plant community from winter icing. Oecologia 136, 616–626. doi:10.1007/s00442-003-1303-7

Fagherazzi, S., Carniello, L., D'Alpaos, L., Defina, A., 2006. Critical bifurcation of shallow microtidal landforms in tidal flats and salt marshes. Proc. Natl. Acad. Sci. U. S. A. 103, 8337–8341. doi:10.1073/pnas.0508379103

Fagherazzi, S., Mariotti, G., Wiberg, P., McGlathery, K., 2013. Marsh Collapse Does Not Require Sea Level Rise. Oceanography 26, 70–77. doi:10.5670/oceanog.2013.47

Fleming, B.J., DeJong, B.D., Phelan, D.J., 2011. Geology, hydrology, and water quality of the Little Blackwater River watershed, Dorchester County, Maryland, 2006–09: U.S. Geological Survey Scientific Investigations Report 2011–5054. http://pubs.usgs.gov/sir/2011/5054/.

Friess, D.A., Krauss, K.W., Horstman, E.M., Balke, T., Bouma, T.J., Galli, D., Webb, E.L., 2012. Are all intertidal wetlands naturally created equal? Bottlenecks, thresholds and knowledge gaps to mangrove and saltmarsh ecosystems. Biol. Rev. 87, 346–366. doi:10.1111/j.1469-185X.2011.00198.x

Ganju, N.K., Kirwan, M.L., Dickhudt, P.J., Guntenspergen, G.R., Cahoon, D.R., Kroeger, K.D., 2015. Sediment transport-based metrics of wetland stability. Geophys. Res. Lett. 42, 7992–8000. doi:10.1002/2015GL065980

Ganju, N.K., Nidzieko, N.J., Kirwan, M.L., 2013. Inferring tidal wetland stability from channel sediment fluxes: Observations and a conceptual model. J. Geophys. Res. Earth Surf. 118, 2045–2058. doi:10.1002/jgrf.20143

Geatz, G.W., Needelman, B.A., Weil, R.R., Megonigal, J.P., 2013. Nutrient Availability and Soil Organic Matter Decomposition Response to Prescribed Burns in Mid-Atlantic Brackish Tidal Marshes. Soil Sci. Soc. Am. J. 77, 1852–1864. doi:10.2136/sssaj2012.0272

Gedan, K.B., Kirwan, M.L., Wolanski, E., Barbier, E.B., Silliman, B.R., 2011. The present and future role of coastal wetland vegetation in protecting shorelines: Answering recent challenges to the paradigm. Clim. Change 106, 7–29. doi:10.1007/s10584-010-0003-7

Gribsholt, B., T., H., Boschker, S., Struyf, E., Andersson, M., Tramper, A., De Brabandere, L., van Damme, S., Brion, N., Meire, P., Dehairs, F., Middelburg, J.J., Heip, C.H.R., 2005. Nitrogen processing in a tidal freshwater marsh: A whole-ecosystem 15 N labeling study. Limnol. Oceanogr. 50, 1945–1959. doi:10.4319/lo.2005.50.6.1945

Handa, I.T., Harmsen, R., Jefferies, R.L., 2002. Patterns of vegetation change and the recovery potential of degraded areas in a coastal marsh system of the hudson bay lowlands. J. Ecol. 90, 86–99. doi:10.1046/j.0022-0477.2001.00635.x

Holdredge, C., Bertness, M.D., Altieri, A.H., 2009. Role of Crab Herbivory in Die-Off of New England Salt Marshes. Conserv. Biol. 23, 672–679. doi:10.1111/j.1523-1739.2008.01137.x

Hughes, Z.J., FitzGerald, D.M., Wilson, C.A., Pennings, S.C., Wiçski, K., Mahadevan, A., 2009. Rapid headward erosion of marsh creeks in response to relative sea level rise. Geophys. Res. Lett. 36, 1–5. doi:10.1029/2008GL036000

Jefferies, R.L., Jano, A.P., Abraham, K.F., 2006. A biotic agent promotes large-scale catastrophic change in the coastal marshes of Hudson Bay. J. Ecol. 94, 234–242. doi:10.1111/j.1365-

2745.2005.01086.x

Kearney, M.S., Grace, R.E., Stevenson, J.C., 1988. Marsh Loss in Nanticoke Estuary, Chesapeake Bay. Geogr. Rev. 78, 205–220. doi:10.2307/214178

Kearney, M.S., Turner, R.E., 2016. Microtidal Marshes: Can These Widespread and Fragile Marshes Survive Increasing Climate–Sea Level Variability and Human Action? J. Coast. Res. 319, 686–699. doi:10.2112/JCOASTRES-D-15-00069.1

Kendrot, S.R., 2011. Restoration through eradication : protecting Chesapeake Bay marshlands from invasive nutria (Myocastor coypus), in: Veitch, C.R., Clout, M.N., Towns, D.R. (Eds.), Island Invasives: Eradication and Management. Proceedings of the International Conference on Island Invasives. Gland, Switzerland: IUCN and Auckland, New Zealand: CBB, pp. 313–319.

Kirwan, M.L., Guntenspergen, G.R., 2015. Response of Plant Productivity to Experimental Flooding in a Stable and a Submerging Marsh. Ecosystems 18, 903–913. doi:10.1007/s10021-015-9870-0

Kirwan, M.L., Guntenspergen, G.R., 2012. Feedbacks between inundation, root production, and shoot growth in a rapidly submerging brackish marsh. J. Ecol. 100, 764–770. doi:10.1111/j.1365-2745.2012.01957.x

Kirwan, M.L., Guntenspergen, G.R., 2010. Influence of tidal range on the stability of coastal marshland. J. Geophys. Res. 115, F02009. doi:10.1029/2009JF001400

Kirwan, M.L., Guntenspergen, G.R., D'Alpaos, A., Morris, J.T., Mudd, S.M., Temmerman, S., 2010. Limits on the adaptability of coastal marshes to rising sea level. Geophys. Res. Lett. 37, L23401. doi:10.1029/2010GL045489

Kirwan, M.L., Megonigal, J.P., 2013. Tidal wetland stability in the face of human impacts and sea-level rise. Nature 504, 53–60. doi:10.1038/nature12856

Kirwan, M.L., Murray, A.B., Boyd, W.S., 2008. Temporary vegetation disturbance as an explanation for permanent loss of tidal wetlands. Geophys. Res. Lett. 35, L05403. doi:10.1029/2007GL032681

Kirwan, M.L., Temmerman, S., Skeehan, E.E., Guntenspergen, G.R., Fagherazzi, S., 2016. Overestimation of marsh vulnerability to sea level rise. Nat. Clim. Chang. 6, 253–260. doi:10.1038/nclimate2909

Kotanen, P.M., Abraham, K.F., 2013. Decadal changes in vegetation of a subarctic salt marsh used by lesser snow and Canada geese. Plant Ecol. 214, 409–422. doi:10.1007/s11258-013-0178-x

Laffaille, P., Feunteun, E., Lefeuvre, J.-C., 2000. Composition of Fish Communities in a European Macrotidal Salt Marsh (the Mont Saint-Michel Bay, France). Estuar. Coast. Shelf Sci. 51, 429–438. doi:10.1006/ecss.2000.0675

Langley, J.A., Mozdzer, T.J., Shepard, K.A., Hagerty, S.B., Megonigal, J.P., 2013. Tidal marsh plant responses to elevated CO2, nitrogen fertilization, and sea level rise. Glob. Chang. Biol. 19, 1495–1503. doi:10.1111/gcb.12147

Leonard, L.A., Croft, A.L., 2006. The effect of standing biomass on flow velocity and turbulence in Spartina alterniflora canopies. Estuar. Coast. Shelf Sci. 69, 325–336. doi:10.1016/j.ecss.2006.05.004

Leonardi, N., Fagherazzi, S., 2014. How waves shape salt marshes. Geology 42, 887–890. doi:10.1130/G35751.1

Li, H., Yang, S.L., 2009. Trapping Effect of Tidal Marsh Vegetation on Suspended Sediment, Yangtze Delta. J. Coast. Res. 254, 915–924. doi:10.2112/08-1010.1

Li, Y.-X., Törnqvist, T.E., Nevitt, J.M., Kohl, B., 2012. Synchronizing a sea-level jump, final Lake Agassiz drainage, and abrupt cooling 8200 years ago. Earth Planet. Sci. Lett. 315–316, 41–50. doi:10.1016/j.epsl.2011.05.034

MacKenzie, R.A., Dionne, M., 2008. Habitat heterogeneity: Importance of salt marsh pools and high marsh surfaces to fish production in two Gulf of Maine salt marshes. Mar. Ecol. Prog. Ser. 368, 217–230. doi:10.3354/meps07560

Mariotti, G., 2016. Revisiting salt marsh resilience to sea level rise: Are ponds responsible for permanent land loss? J. Geophys. Res. Earth Surf. 121, 1391–1407. doi:10.1002/2016JF003900

Mariotti, G., Carr, J., 2014. Dual role of salt marsh retreat: Long-term loss and short-term resilience. Water Resour. Res. 50, 2963–2974. doi:10.1002/2013WR014676

Mariotti, G., Fagherazzi, S., 2013. Critical width of tidal flats triggers marsh collapse in the absence of sea-level rise. Proc. Natl. Acad. Sci. U. S. A. 110, 5353–5356. doi:10.1073/pnas.1219600110

Mariotti, G., Kearney, W.S., Fagherazzi, S., 2016. Soil creep in salt marshes. Geology 44, 459–462. doi:10.1130/G37708.1

McLeod, E., Chmura, G.L., Bouillon, S., Salm, R., Björk, M., Duarte, C.M., Lovelock, C.E., Schlesinger, W.H., Silliman, B.R., 2011. A blueprint for blue carbon: Toward an improved understanding of the role of vegetated coastal habitats in sequestering CO2. Front. Ecol. Environ. 9, 552–560. doi:10.1890/110004

Meire, P., Ysebaert, T., Van Damme, S., Van Den Bergh, E., Maris, T., Struyf, E., 2005. The Scheldt estuary: A description of a changing ecosystem. Hydrobiologia 540, 1–11. doi:10.1007/s10750-005-0896-8

Mendelssohn, I.A., McKee, K.L., 1988. Spartina Alterniflora Die-Back in Louisiana: Time-Course Investigation of Soil Waterlogging Effects. J. Ecol. 76, 509–521. doi:10.2307/2260609

Millette, T.L., Argow, B.A., Marcano, E., Hayward, C., Hopkinson, C.S., Valentine, V., 2010. Integration of Multitemporal Multispectral Remote Sensing with LIDAR and GIS. J. Coast. Res. 265, 809–816. doi:10.2112/JCOASTRES-D-09-00101.1

Möller, I., 2006. Quantifying saltmarsh vegetation and its effect on wave height dissipation: Results from a UK East coast saltmarsh. Estuar. Coast. Shelf Sci. 69, 337–351. doi:10.1016/j.ecss.2006.05.003

Möller, I., Kudella, M., Rupprecht, F., Spencer, T., Paul, M., van Wesenbeeck, B.K., Wolters, G., Jensen, K., Bouma, T.J., Miranda-Lange, M., Schimmels, S., 2014. Wave attenuation over coastal salt marshes under storm surge conditions. Nat. Geosci. 7, 727–731. doi:10.1038/ngeo2251

Möller, I., Spencer, T., 2002. Wave dissipation over macro-tidal saltmarshes: Effects of marsh edge typology and vegetation change. J. Coast. Res. 521, 506–521. doi:ISSN:0749-0208

Morris, J.T., Sundareshwar, P. V., Nietch, C.T., Kjerfve, B., Cahoon, D.R., 2002. Responses of Coastal Wetlands to Rising Sea Level. Ecology 83, 2869–2877. doi:10.1890/0012-9658(2002)083[2869:ROCWTR]2.0.CO;2

Morton, R.A., Tiling, G., Ferina, N.F., 2003. Causes of hot-spot wetland loss in the Mississippi delta plain. Environ. Geosci. 10, 71–80. doi:10.1306/eg100202007

Moskalski, S.M., Sommerfield, C.K., 2012. Suspended sediment deposition and trapping efficiency in a Delaware salt marsh. Geomorphology 139–140, 195–204. doi:10.1016/j.geomorph.2011.10.018

Mudd, S.M., Fagherazzi, S., Morris, J.T., Furbish, D.J., 2004. Flow, Sedimentation, and Biomass Production on a Vegetated Salt Marsh in South Carolina: Toward a Predictive Model of Marsh Morphologic and Ecologic Evolution, in: The Ecogeomorphology of Tidal Marshes. American Geophysical Union, pp. 165–188. doi:10.1029/CE059p0165

Müller, F., Struyf, E., Hartmann, J., Wanner, A., Jensen, K., 2013. A Comprehensive Study of Silica Pools and Fluxes in Wadden Sea Salt Marshes. Estuaries and Coasts 36, 1150–1164. doi:10.1007/s12237-013-9621-4

Neumeier, U., Amos, C.L., 2006. The influence of vegetation on turbulence and flow velocities in European salt-marshes. Sedimentology 53, 259–277. doi:10.1111/j.1365-3091.2006.00772.x

Neumeier, U., Ciavola, P., 2004. Flow Resistance and Associated Sedimentary Processes in a Spartina maritima Salt-Marsh. J. Coast. Res. 202, 435–447. doi:10.2112/1551-5036(2004)020[0435:FRAASP]2.0.CO;2

Nyman, J.A., DeLaune, R.D., Roberts, H.H., Patrick, W.H., 1993. Relationship between vegetation and soil formation in a rapidly submerging coastal marsh. Mar. Ecol. Prog. Ser. 96, 269–279. doi:10.3354/meps096269

Nyman, J.A., Walters, R.J., DeLaune, R.D., Patrick, W.H., 2006. Marsh vertical accretion via vegetative growth. Estuar. Coast. Shelf Sci. 69, 370–380. doi:10.1016/j.ecss.2006.05.041

Ortiz, A.C., Roy, S., Edmonds, D.A., 2017. Land loss by pond expansion on the Mississippi River Delta Plain. Geophys. Res. Lett. 44, 3635–3642. doi:10.1002/2017GL073079

Penland, S., Wayne, L., Britsch, D., Williams, S.J., Beall, A.D., Butterworth, V., 2000. Geomorphic Classification of Coastal Land Loss between 1932 and 1990 in the Mississippi River Delta Plain, Southeastern Louisiana. USGS Open File Report 00-417. https://pubs.usgs.gov/of/2000/of00-417/.

Perillo, G.M.E., Iribarne, O.O., 2003. New mechanisms studied for creek formation in tidal flats: From crabs to tidal channels. Eos, Trans. Am. Geophys. Union 84, 1–12. doi:10.1029/2003EO010001

Perillo, G.M.E., Ripley, M.D., Piccolo, M.C., Dyer, K.R., 1996. The Formation of Tidal Creeks in a Salt Marsh : New Evidence from the Loyola Bay Salt Marsh, Rio Gallegos Estuary, Argentina. Mangroves Salt Marshes 1, 37–46. doi:10.1023/A:1025942111382

Pethick, J.S., 1974. The Distribution of Salt Pans on Tidal Salt Marshes. J. Biogeogr. 1, 57–62.

Plancke, Y., Ides, S., Mostaert, F., 2009. Vervolgstudie Inventarisatie en historische analyse van slikken en schorren langs de Zeeschelde: Verkennende vlottermetingen Ballooi en Notelaer. Versie 2_0. WL Rapport.

Redfield, A.C., 1972. Development of a New England Salt Marsh. Ecol. Monogr. 42, 201–237. doi:10.2307/1942263

Sallenger, A.H., Doran, K.S., Howd, P.A., 2012. Hotspot of accelerated sea-level rise on the Atlantic coast of North America. Nat. Clim. Chang. 2, 884–888. doi:10.1038/nclimate1597

Scott, M., McDermott, L., Silva, E., Watson, E., 2009. Project report: Digital Spatial Data Capture of Marsh Extent in Blackwater National Wildlife Refuge, 1938 and 2006. Eastern Shore Regional GIS Cooperative, Salisbury University.

Silliman, B.R., van de Koppel, J., Bertness, M.D., Stanton, L.E., Mendelssohn, I.A., 2005. Drought, Snails, and Large-Scale Die-Off of Southern U.S. Salt Marshes. Science 310, 1803–1806. doi:10.1126/science.1118229

Slocum, M.G., Mendelssohn, I.A., 2008. Use of experimental disturbances to assess resilience along a known stress gradient. Ecol. Indic. 8, 181–190. doi:10.1016/j.ecolind.2007.01.011

Smolders, S., Plancke, Y., Ides, S., Meire, P., Temmerman, S., 2015. Role of intertidal wetlands for tidal and storm tide attenuation along a confined estuary: a model study. Nat. Hazards Earth Syst. Sci. 15, 1659–1675. doi:10.5194/nhess-15-1659-2015

Stark, J., Van Oyen, T., Meire, P., Temmerman, S., 2015. Observations of tidal and storm surge attenuation in a large tidal marsh. Limnol. Oceanogr. 60, 1371–1381. doi:10.1002/lno.10104

Stevenson, J.C., Kearney, M.S., Pendleton, E.C., 1985. Sedimentation and erosion in a Chesapeake Bay brackish marsh system. Mar. Geol. 67, 213–235. doi:10.1016/0025-3227(85)90093-3

Stoddart, D.R., Reed, D.J., French, J.R., 1989. Understanding Salt-Marsh Accretion, Scolt Head Island, Norfolk, England. Estuaries 12, 228–236. doi:10.2307/1351902

Struyf, E., Van Damme, S., Gribsholt, B., Meire, P., 2005. Freshwater marshes as dissolved silica recyclers in an estuarine environment (Schelde estuary, Belgium). Hydrobiologia 540, 69–77. doi:10.1007/s10750-004-7104-0

Temmerman, S., De Vries, M.B., Bouma, T.J., 2012a. Coastal marsh die-off and reduced attenuation of coastal floods: A model analysis. Glob. Planet. Change 92–93, 267–274. doi:10.1016/j.gloplacha.2012.06.001

Temmerman, S., Govers, G., Meire, P., Wartel, S., 2003a. Modelling long-term tidal marsh growth under changing tidal conditions and suspended sediment concentrations, Scheldt estuary, Belgium. Mar. Geol. 193, 151–169. doi:10.1016/S0025-3227(02)00642-4

Temmerman, S., Govers, G., Wartel, S., Meire, P., 2004. Modelling estuarine variations in tidal marsh sedimentation: Response to changing sea level and suspended sediment concentrations. Mar. Geol. 212, 1–19. doi:10.1016/j.margeo.2004.10.021

Temmerman, S., Govers, G., Wartel, S., Meire, P., 2003b. Spatial and temporal factors controlling short-term sedimentation in a salt and freshwater tidal marsh, Scheldt estuary, Belgium, SW Netherlands. Earth Surf. Process. Landforms 28, 739–755. doi:10.1002/esp.495

Temmerman, S., Moonen, P., Schoelynck, J., Govers, G., Bouma, T.J., 2012b. Impact of vegetation die-off on spatial flow patterns over a tidal marsh. Geophys. Res. Lett. 39, 1–5. doi:10.1029/2011GL050502

Teuchies, J., Vandenbruwaene, W., Carpentier, R., Bervoets, L., Temmerman, S., Wang, C., Maris, T., Cox, T.J.S., Van Braeckel, A., Meire, P., 2013. Estuaries as Filters: The Role of Tidal Marshes in Trace Metal Removal. PLoS One 8, e70381. doi:10.1371/journal.pone.0070381

Van Braeckel, A., Piesschaert, F., Van den Bergh, E., 2006. Historische analyse van de Zeeschelde en haar getijgebonden zijrivieren. 19e eeuw tot heden. Report of the Research Institute for Nature and Forest (INBO.R.2006.29). Brussel.

Van Damme, S., Frank, D., Micky, T., Olivier, B., Eric, S., Britta, G., Oswald, V.C., Patrick, M., 2009. Tidal exchange between a freshwater tidal marsh and an impacted estuary: the Scheldt estuary, Belgium. Estuar. Coast. Shelf Sci. 85, 197–207. doi:10.1016/j.ecss.2009.08.005

van der Wal, D., Wielemaker-Van den Dool, A., Herman, P.M.J., 2008. Spatial patterns, rates and mechanisms of saltmarsh cycles (Westerschelde, The Netherlands). Estuar. Coast. Shelf Sci. 76, 357–368. doi:10.1016/j.ecss.2007.07.017

van Huissteden, J., van de Plassche, O., 1998. Sulphate reduction as a geomorphological agent in tidal marshes (“Great Marshes” at Barnstable, Cape Cod, USA). Earth Surf. Process. Landforms 23, 223–236. doi:10.1002/(SICI)1096-9837(199803)23:3<223::AID-ESP843>3.0.CO;2-I

Wang, D.-P., Elliott, A.J., 1978. Non-Tidal Variability in the Chesapeake Bay and Potomac River: Evidence for Non-Local Forcing. J. Phys. Oceanogr. 8, 225–232. doi:10.1175/1520-0485(1978)008<0225:NTVITC>2.0.CO;2

Widdows, J., Brinsley, M., 2002. Impact of biotic and abiotic processes on sediment dynamics and the consequences to the structure and functioning of the intertidal zone. J. Sea Res. 48, 143–156. doi:10.1016/S1385-1101(02)00148-X

Wilson, C.A., Allison, M.A., 2008. An equilibrium profile model for retreating marsh shorelines in southeast Louisiana. Estuar. Coast. Shelf Sci. 80, 483–494. doi:10.1016/j.ecss.2008.09.004

Wilson, C.A., Hughes, Z.J., FitzGerald, D.M., Hopkinson, C.S., Valentine, V., Kolker, A.S., 2014. Saltmarsh pool and tidal creek morphodynamics: Dynamic equilibrium of northern latitude saltmarshes? Geomorphology 213, 99–115. doi:10.1016/j.geomorph.2014.01.002

Wilson, K.R., Kelley, J.T., Croitoru, A., Dionne, M., Belknap, D.F., Steneck, R., 2009. Stratigraphic and ecophysical characterizations of salt pools: Dynamic landforms of the Webhannet Salt Marsh, Wells, ME, USA. Estuaries and Coasts 32, 855–870. doi:10.1007/s12237-009-9203-7

Wilson, K.R., Kelley, J.T., Tanner, B.R., Belknap, D.F., 2010. Probing the Origins and Stratigraphic Signature of Salt Pools from North-Temperate Marshes in Maine, U.S.A. J. Coast. Res. 26, 1007–1026. doi:10.2112/JCOASTRES-D-10-00007.1

Wray, R.D., Leatherman, S.P., Nicholls, R.J., 1995. Historic and Future Land Loss for Upland and Marsh Islands in the Chesapeake Bay, Maryland, U.S.A. J. Coast. Res. 11, 1195–1203.

Yapp, R.H., Johns, D., Jones, O.T., 1917. The Salt Marshes of the Dovey Estuary. J. Ecol. 5, 65–103. doi:10.2307/2255644

Zimmerman, R.J., Minello, T.J., Rozas, L.P., 2000. Salt Marsh Linkages to Productivity of Penaeid Shrimps and Blue Crabs in the Northern Gulf of Mexico, in: Concepts and Controversies in Tidal Marsh Ecology. Kluwer Academic Publishers, Dordrecht, pp. 293–314. doi:10.1007/0-306-47534-0_14

2

Spatio-temporal development of vegetation die-off in a submerging coastal marsh

Lennert Schepers, Matthew Kirwan, Glenn Guntenspergen, Stijn Temmerman

Schepers, L., M. Kirwan, G. Guntenspergen, and S. Temmerman. 2017. Spatio-temporal development of vegetation die-off in a submerging coastal marsh. Limnol. Oceanogr. 62: 137–150. doi:10.1002/lno.10381

2.1 Abstract

In several places around the world, coastal marsh vegetation is converting to open water through the formation of pools. This is concerning, as vegetation die-off is expected to reduce the marshes' capacity to adapt to sea level rise by vegetation-induced sediment accretion. Quantitative analyses of the spatial and temporal development of marsh vegetation die-off are scarce, although these are needed in order to understand the bio-geomorphic feedback effects of vegetation die-off on flow, erosion, and sedimentation. In this study, we quantified the spatial and temporal development of marsh vegetation die-off with aerial images from 1938 to 2010 in a submerging micro-tidal, organic-rich coastal marsh along the Blackwater River (Maryland, USA). Our results indicate that die-off begins with conversion of marsh vegetation into bare open water pools that are relatively far (> 75 m) from tidal channels. As vegetation die-off continues, pools expand, and new pools emerge at shorter and shorter distances from channels. Consequently larger pools are found at larger distances from the channels. Our results suggest that the size of the pools and possibly the connection of pools with the tidal channel system have important bio-geomorphic implications and aggravate marsh deterioration. Moreover, we found that the temporal development of vegetation die-off in moderately degraded marshes is similar as the spatial die-off development along a present-day gradient, which indicates that the contemporary die-off gradient might be considered a chronosequence that offers a unique opportunity to study vegetation die-off processes.

2.2 Introduction

Coastal marshes are wetlands with important ecosystem functions such as coastal protection (Temmerman et al., 2013; Möller et al., 2014; Temmerman and Kirwan, 2015), improving water quality and recreation (Barbier et al., 2011), with estimated total monetary values ranging from 2,000 – 215,000 $\$ha^{-1}yr^{-1}$ (Russi et al., 2013). These functions may disappear when coastal marsh vegetation dies off and marshes convert to bare intertidal flats, pools, or open water, as is observed in different places around the world (Boston, 1983; Day et al., 2000; Kearney et al., 2002; Perillo and Iribarne, 2003; Kirwan and Megonigal, 2013). Vegetation die-off and pool formation have been proposed as an early indicator of a marsh that is failing to survive sea level rise (e.g., Kearney et al., 1988; Nyman et al., 1993) and pool enlargement is a primary component of wetland loss in submerging marshes typical, for example, of the Mississippi Delta, Chesapeake Bay and Venice lagoon (Stevenson et al., 1985; Wells and Coleman, 1987; Kearney et al., 1988; Nyman et al., 1993; Penland et al., 2000; Carniello et al., 2009).

Marshes are known to have two contrasting ecosystem states (Fagherazzi et al., 2006; Marani et al., 2010; Wang and Temmerman, 2013): (i) an elevated, vegetated marsh state and (ii) a low, unvegetated tidal flat or shallow open water (pool) state. In the vegetated marsh state, several bio-geomorphic feedback mechanisms allow the marsh platform elevation to keep up with sea level rise. As marsh vegetation is flooded for longer periods of time and more frequently, the vegetation will trap and accumulate more suspended sediment, resulting in the build-up of the marsh surface that may be in balance with sea level rise (Pethick, 1981; Allen, 1990; French, 1993; Vandenbruwaene et al., 2011a). Aboveground and belowground plant production increases elevation by (i) reduction of tidal flow and enhanced suspended sediment deposition (Mudd et al., 2010; Baustian et al., 2012; Temmerman et al., 2012b) and (ii) organic matter accumulation that directly contributes to elevation increase (Nyman et al., 2006; Kirwan and Guntenspergen, 2012). For some marsh species such as *Spartina alterniflora* and *Schoenoplectus americanus* maximum productivity occurs at intermediate or low elevations within the intertidal zone, so that increased flooding of high marshes will enhance productivity and accretion (Morris et al., 2002; Kirwan and Guntenspergen, 2015). Consistent with these observations, a recent meta-analysis suggests that accretion rates could more than double during the transition from infrequently flooded, high elevation marshes to frequently flooded, low elevation marshes (Kirwan et al., 2016). These bio-geomorphic feedbacks between tidal inundation, vegetation productivity, and surface elevation change provide vegetated marshes a certain ability to keep up with rising sea level (Kirwan et al., 2010; Fagherazzi et al., 2012; Mariotti and Carr, 2014).

However, marshes can only keep up with sea level rise to a certain extent. When excessive flooding becomes harmful to plant growth, plant productivity and vegetation-induced accretion processes decline (Nyman et al., 1993; Morris et al., 2002; Leonard and Croft, 2006). When reduced accretion rates get lower than the rate of sea level rise, this results in an increasing inundation stress, which may ultimately lead to vegetation die-off and the formation of shallow water pools without vegetation. Plant mortality may be accompanied by loss of elevation due to collapse of root structure or decomposition and disintegration of soil organic matter, resulting in die-off areas that are too low for vegetation to re-establish (Delaune and Pezeshki, 1994; van Huissteden and van de Plassche, 1998; Day et al., 2011).

The origin, causes, and evolution of tidal marsh die-off have been an important area of study. Initial vegetation die-off usually starts as isolated areas in the interior marsh (DeLaune et al., 1994; Morton et al., 2003) by excessive flooding and waterlogging (Boston, 1983; Mendelssohn and McKee, 1988; Nyman et al., 1993; DeLaune et al., 1994; Day et al., 2011), salt stress (Delaune and Pezeshki, 1994), herbivory (Stevenson et al., 1985; Silliman et al., 2005; Kirwan et al., 2008; Holdredge et al., 2009; Smith, 2009), deposition of tidal litter (Pethick, 1974; Boston, 1983), physical disturbances or other reasons that may not be always clear (see e.g. Alber et al. (2008) for an overview of rapid die-off mechanisms). The loss of vegetation may decrease the physical deposition of suspended sediments or even provoke erosion (Baustian et al., 2012; Temmerman et al., 2012b), leading to the formation of depressions or pools with weak soil strength that may inhibit the re-establishment of vegetation (Day et al., 2011). The enlargement of pools is a poorly understood phenomena, but might be caused by rotational slumping (Stevenson et al., 1985), failure of unstable marsh scarps (Day et al., 2011), surficial flooding of the adjacent marsh surface and consequent vegetation die-off (Wilson et al., 2009), or by decomposition and decay of the upper soil layer, leading to pool enlargement (Redfield, 1972; van Huissteden and van de Plassche, 1998). Also wind-generated wave erosion may expand the pools (Stevenson et al., 1985; Perillo et al., 1996; Morton et al., 2003; Mariotti and Fagherazzi, 2013). Neighboring pools may merge to form larger pools (Yapp et al., 1917; Redfield, 1972; Kearney et al., 1988; Wilson et al., 2009). This process can start by subsurface connections between adjacent pools (van Huissteden and van de Plassche, 1998; Wilson et al., 2009). Pools can also get connected to the tidal channel network by headward erosion of channels into pools (Redfield, 1972; Kearney et al., 1988; Perillo et al., 1996). The pools can become subsequently drained, which may induce (partial) revegetation of the pools and rapid sediment accretion (Redfield, 1972; Perillo et al., 1996; van Huissteden and van de Plassche, 1998; Wilson et al., 2009, 2010, 2014; Millette et al., 2010). In this way, pools can also become smaller in size, break apart or completely disappear (Redfield, 1972; Wilson et al., 2009, 2014). Wilson et al. (2009) observed several pools and their development over time in the Webhannet Salt Marsh (Maine, USA), concluding that pools are highly dynamic, with simultaneous contraction and expansion of pools and most of the pools decreasing in size during the time period studied (1962-2003). However, in other marsh areas such as in the Nanticoke and Blackwater estuaries (Maryland, USA) and the Mississippi delta (Louisiana, USA) pools enlarge until they are big enough for wind-generated wave erosion of the pool bottom and edges (Stevenson et al., 1985; Kearney et al., 1988; Mariotti and Fagherazzi, 2013) and die-off gradually continues over time to mostly open water areas with a few remnant islands of marsh that eventually disappear (Morton et al., 2003).

Detailed quantitative studies of spatio-temporal die-off patterns at a geomorphic relevant scale (< 1 km) are largely lacking, and this hinders the quantitative study of the feedbacks of vegetation die-off patterns on flow and sedimentation (D'Alpaos et al., 2007; Kirwan and Murray, 2007; Temmerman et al., 2012a, 2012b). In this study, we quantify the spatio-temporal development of vegetation die-off in a submerging marsh area of the Chesapeake Bay (Blackwater marshes, Maryland, USA) by analyzing aerial images from 1938 to 2010. We test if changes in die-off patterns through time are similar to die-off patterns occurring along an apparent present-day spatial gradient and hypothesize that the distance from tidal channels is a key determining factor explaining the spatial pattern of pool initiation and development. More specifically, we test if initial pool formation and consequent enlargement occurs randomly relative to the tidal channels, or preferentially at certain distances from channels. Finally, we formulate possible implications of the observed die-off patterns for bio-geomorphic feedback mechanisms.

2.3 Methods

2.3.1 Study area

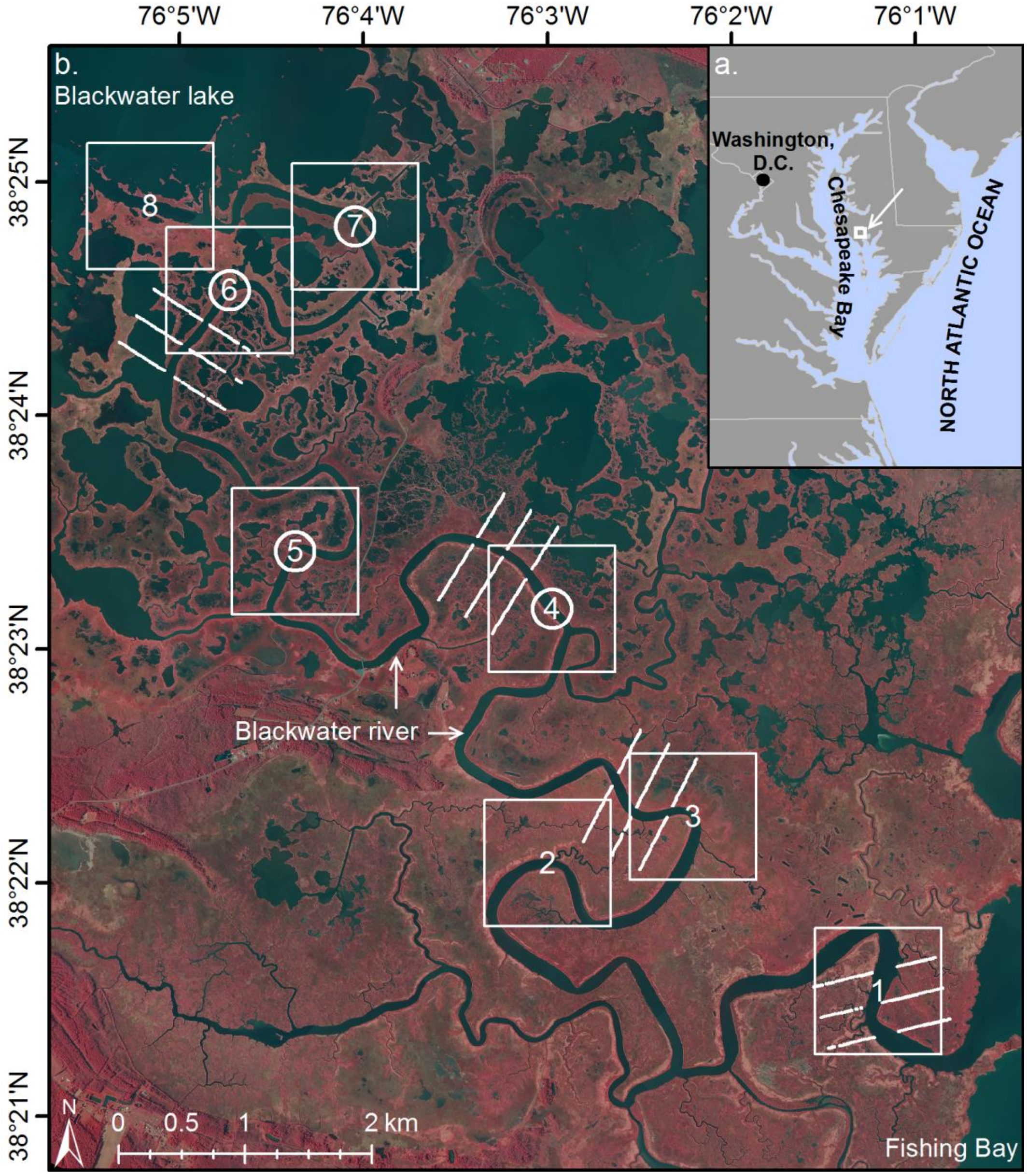

Figure 2.1: a. Position of the Blackwater marshes (white arrow) along the Chesapeake Bay, Maryland, USA. b. Black-white (False color image online: Near Infrared, Red and Green band) of the Blackwater marshes in 2010. Dark areas are water areas, brighter (online: reddish) colors are vegetation. The numbered squares (1-8) represent the areas used in the spatial image analyses. Squares with encircled numbers (4-7) are also used in the temporal image analyses. White lines consist of ground validation points for the 2010 image classification.

The study area is located along the Blackwater River (Maryland, USA) that discharges into the Fishing Bay (38°24’ N, 76°40’ W, Fig. 2.1), which is a tributary embayment of the larger Chesapeake Bay. The upstream marshes are part of the Blackwater National Wildlife Refuge, the downstream marshes are situated in the Fishing Bay Wildlife Management Area. The estuary is micro-tidal with the spring tidal range varying from over 1.0 m at the Fishing Bay (in the southeast corner of Fig. 2.1b) to less than 0.2 m at the open water area (indicated as “Blackwater lake” in the northwest corner of Fig. 2.1b) (Ganju et al., 2013). However, episodic meteorological tides may exceed 1.0 m at the Chesapeake Bay (Wang and Elliott, 1978; Stevenson et al., 1985). The marshes are characterized by mesohaline marsh vegetation: *Spartina cynosuroides* is dominant on natural levees next to the river and the bigger tidal channels. Intermediate elevations are dominated by different mixtures of *Spartina alterniflora*, *Spartina patens* and *Distichlis spicata*, and the lowest areas are dominated by *Schoenoplectus americanus*.

Since the 1930s, more than 2,000 ha of marshland or 51 % of the Blackwater National Wildlife Refuge marshes have been lost and converted to open water (Stevenson et al., 1985; Scott et al., 2009; Cahoon et al., 2010), resulting in an upstream gradient of increasing vegetation die-off from fairly intact marshes closest to the Fishing Bay up to the vast open shallow water Lake Blackwater that was still partly vegetated until the 1930s. As marsh vegetation died, it was replaced by subtidal pools that are clearly distinguishable from aerial pictures (Fig. 2.1b). The historical marsh accretion rate (on average 1.7-3.6 mm yr^{-1} (Stevenson et al., 1985)) is lower than the local relative sea level rise (currently 3.72 mm yr^{-1} nearby in Cambridge, MD, (NOAA station 8571892, http://tidesandcurrents.noaa.gov/sltrends, 2/23/2016). Marsh loss at the Blackwater marshes has, besides submergence by sea level rise, also been attributed to vegetation disturbance by rodents (muskrats (*Ondatra zibethicus*) and invasive nutria (*Myocastor coypus*)) and subsequent open-water expansion (Stevenson et al., 1985; Kendrot, 2011).

2.3.2 Aerial images

Aerial photographs were acquired for the historical analyses for 1938, 1981 and 2010 (Table 2.1) and were converted into maps delineating marsh vegetation, pools and tidal channels. We obtained 1938 imagery (black and white) that was scanned and georeferenced (Scott et al., 2009). Scott et al. (2009) also digitized the extent of the wetland vegetation and water areas within the Blackwater National Wildlife Refuge area, that is, the more upstream marshes. We checked and adjusted this layer and extended it to the wetlands of the whole study area (Fig. 2.1). Upland areas and anthropogenic areas (roads, houses, wharfs) were excluded from the analysis. The 1981 image (infrared) was georeferenced (RMS: 5.4 m). A supervised classification of the 1981 image was unsuccessful in discriminating vegetation and water areas, but we could clearly differentiate these two classes visually so we digitized the 1981 image manually. All manual digitization was done at a scale of 1:2,500 using a conservative interpretation of die-off areas: only larger (> 50 m^2) areas that were very likely ponds/water were characterized as such. Therefore, marsh die-off by pool formation might be slightly underestimated.

Table 2.1: overview of used imagery

Date	Type	Resolution (m)	Source	Digitization
1938	Black and white	0.86	(Scott et al., 2009)	Manual
1981	Color Infrared	1.55	USGS Earthexplorer	Manual
2010	Visible + near infrared (4 bands)	0.30	Blackwater NWR	Classification

The 2010 imagery (visible light and near infrared) was classified with a supervised maximum likelihood classification to distinguish between vegetation and water areas. In the summer of 2014, ground validation points (n = 1022, see Fig. 2.1b) were collected every 10 m along transects crossing the Blackwater River and were used to validate the classification. The accuracy of the classification was very high (0.97), meaning that 97 % of our ground control points were classified correctly. If we account for the chance of randomly assigning a value to a class, 91% of our points were classified correctly (Kappa: 0.91), still a very good result. All images were resampled to the coarsest resolution of 1.55 m with majority resampling in ArcGIS. To make the 2010 classification comparable to the manual delineations on the 1981 and 1937 images (where only pools or vegetated patches where mapped when they were > 50 m^2), individual areas smaller than 50 m^2 were removed and replaced by its surrounding class. In this step, we used the 4-connected neighborhood to evaluate connectivity between cells to delineate individual areas. As a final step, the Blackwater River and the main tidal channels were classified separately from the pools. The tidal channels are defined as elongated water stretches (length at least two times larger than width) that are directly connected to the river.

2.3.3 Spatial and temporal analysis

Within the study area we selected discrete working areas to facilitate comparisons across the die-off gradient. We created a point every 2000 m along the centerline of the Blackwater RiverBlackwater River, from its mouth in the Fishing Bay in the SE up to the open water area in the NW, that is, 13 points in total. Two points were excluded because they were situated within 500 m of upland areas. The size of the square working areas was selected based on two aspects: (i) the change in proportion of water of the working area as the window size (i.e., size of the square working areas) increases and (ii) the overlap of working areas. The proportion of water was defined as the ratio of water pixels to the total amount of pixels within a working area. We centered our working areas around the 11 retained points. As we expand the window size beyond the river banks, the proportion of water drops as we encounter more vegetated marshes. When the window size reaches 1 km^2, the proportion of water has stabilized for most working areas. For larger window sizes the chance of overlap between adjacent working areas becomes high. Hence an appropriate window size for our analysis was chosen at 1 km^2 (Fig. 2.2).

Three points were excluded at this stage since they had very similar vegetation cover (see Fig. 2.2) and significant overlap. Historical aerial imagery for all time steps was available for area 4 to area 7 (see Fig. 2.1, Table 2.1), and hence these areas were used for the temporal analyses.

Die-off proportion

As a first measure to see if the temporal evolution and apparent spatial gradient of vegetation die-off are similar, we defined the proportion of vegetation die-off (pools) as the ratio of pool pixels to the total of pool and vegetated marsh pixels for each working area. River pixels and tidal channel pixels are excluded since these are natural features of a marsh system and are not formed by vegetation die-off, while pools are considered the result of marsh vegetation die-off.

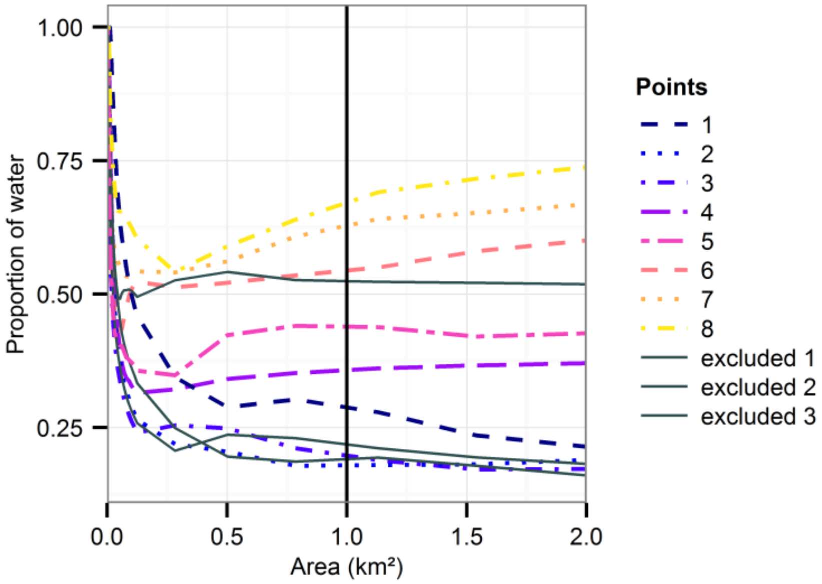

Figure 2.2: Proportions of marsh occupied by water (Y-axis) as a function of increasing size of the working areas (X-axis). Dashed lines correspond to areas in Fig. 2.1. Solid lines indicate the three excluded areas. The vertical line marks the size of the working areas used in this study (1 km^2).

Relations between die-off percentage and distance from channels

We determined the distance of each pixel to the Blackwater RiverBlackwater River by Euclidean distance calculation. We divided the distances in 5 m bins and calculated within each distance bin the proportion of pools (the same method as above). Distances were visualized until a bin represents less than 0.5 % of the total amount of pixels in the working area (pool + marsh pixels). By doing so, larger distances that represent only a very small percentage of the total area were left out of the analyses.

Relations between pool size and distance from channels

An important measure regarding pool enlargement is the size of the pools and how the size evolves in time. As pools are often connected by channel-like patterns which do not allow for individual pool delineation and the marsh landscape is inherently intersected by tidal channels, conventional spatial pattern analyses based on identification of individual patches (McGarigal et al., 2012; Kéfi et al., 2014) are not possible. Therefore we used fetch length as a proxy for pool size. The fetch or fetch length of a pool is defined as the length of a line that covers a continuous water surface, from one side of the pool to the other. For each pool pixel, we determined the fetch length oriented along the cardinal and intercardinal directions s (N-S, E-W, NW-SE; NE-SW). The mean fetch was calculated from these four fetch lengths. We analyzed the fetch length for different distance classes to the river (bins), identically as the method used above.

All analyses were performed with ArcGIS (ArcGIS 10.3, ESRI) and R (R Core Team, 2017).

2.4 Results

2.4.1 Evolution of die-off proportion

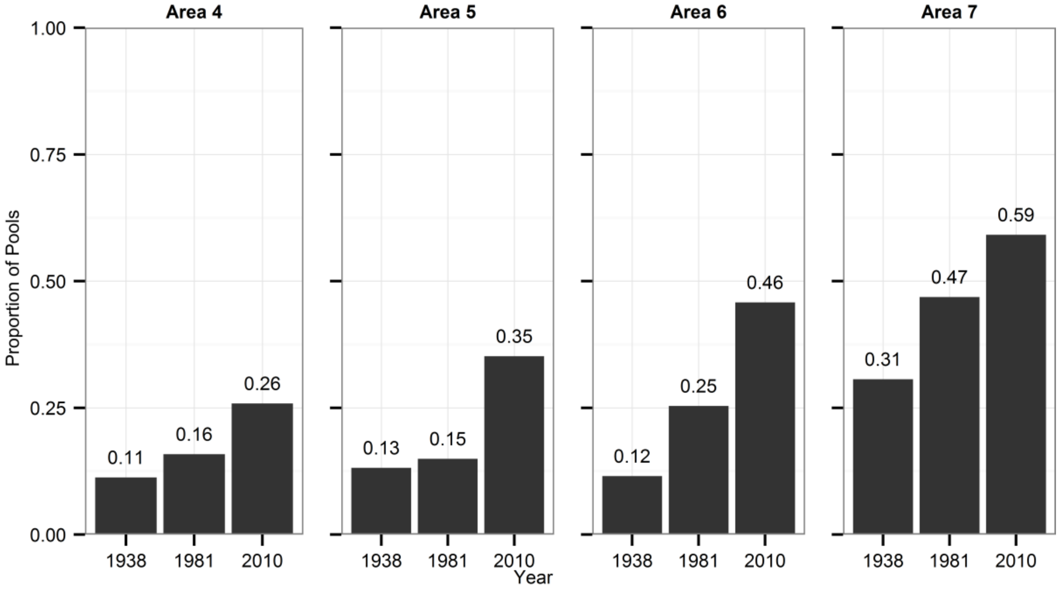

Figure 2.3: Fraction of each working area occupied by unvegetated pools in 1938, 1981, and 2010. Pools represent areas of vegetation die-off and do not include tidal channels. Working areas 4-7 correspond to increasing distances up the Blackwater River towards Lake Blackwater.

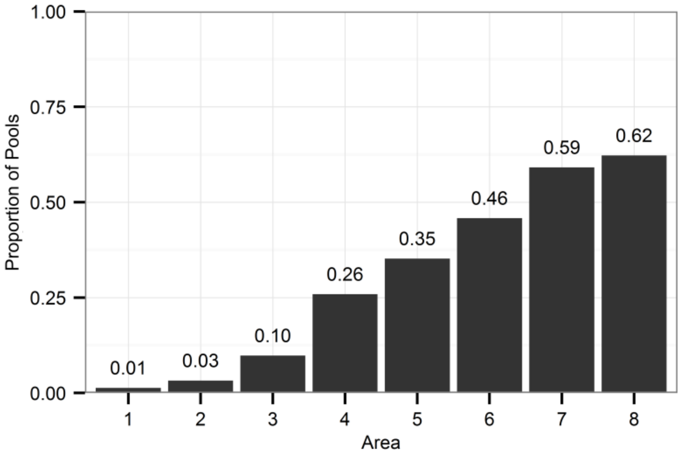

Figure 2.4: Fraction of each working area occupied by unvegetated pools in 2010 (values above bar). Pools represent vegetation die-off and do not include tidal channels. Working areas 1-8 correspond to increasing distances up the Blackwater River towards Lake Blackwater.

Figures 2.3 and 2.4 represent the proportion of pools compared to the total amount of pool and marsh pixels, excluding tidal channels and the river channel, for the time steps and all spatial areas, respectively. We observe an increase in pool cover for all time steps and all the areas in the temporal analysis, with up to 21 % of marsh converted to pools in 29 years (Fig. 2.3: area 6, 1981 to 2010). This indicates that the die-off is an ongoing, active process. The spatial analysis shows the same trend as the temporal change: a very small percentage of pool cover at area 1 increases gradually along the Blackwater River, up to 62 % of pools close to Lake Blackwater in area 8 (Fig. 2.4). It should be noted, however that there are no intact marshes (<10 % vegetation die-off) in the temporal analysis.

2.4.2 Relations between die-off percentage and distance from channels

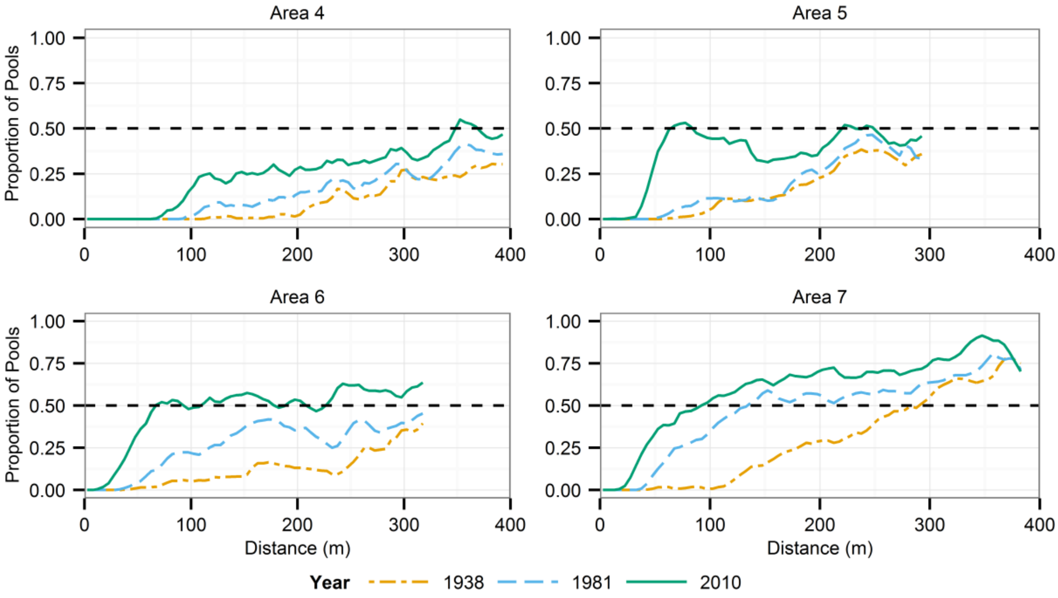

Figure 2.5: Proportion of pool pixels with increasing distance to the Blackwater River for the different areas and time steps. The horizontal dashed line indicates 50%.

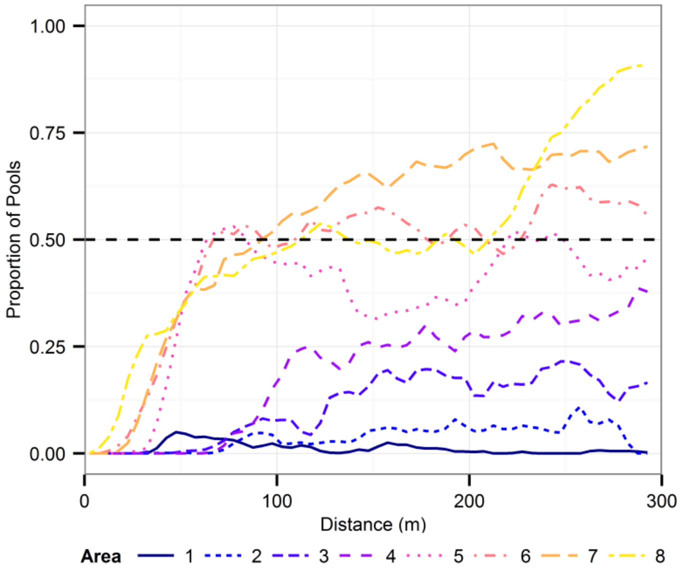

Figure 2.6: Proportion of pool pixels with increasing distance to the Blackwater River for the different areas in 2010. The black horizontal dashed line indicates 50%.

The proportion of pools for different distances to the Blackwater River are presented in Fig. 2.5 for different time steps and for all the areas in 2010 in Fig. 2.6. In 1938, the pool proportions were limited and there were almost no pools within 100 m from the river (see Fig. 2.5, yellow dash dot lines). Increasing numbers of pool pixels were situated with increasing distances above 100 m from the river. At later time steps (1981 and 2010 represented in Fig. 2.5 as blue dashed and green solid lines, respectively), more pools start to form closer to the river as the amount of pool pixels keeps increasing. In the most intact marshes along the spatial die-off gradient in 2010 (Fig. 2.6, working area 1) almost no detectable pool pixels are present, and if any, there is no apparent spatial pattern. As we move upstream the river, pools appear first at distances further than 75 m from the river and continue to increase in number and toward the river, so that from area 3 onward (the dashed line in Fig. 2.6), similar patterns and developments arise as observed in the temporal analysis: in areas that are little affected by vegetation die-off, the pool percentage increases almost linearly with distance from the river, with the distance of first die-off decreasing at higher die-off percentages (e.g., from Fig. 2.5 area 4, the distance to the river decreases). In the more degraded areas, however, there is a sharp increase in vegetation die-off with increasing distance from the river until ca. 50 % is reached, and at higher distances it seems to fluctuate around the 50 % line. At the highest die-off percentages (area 7 and 8), the percentage of pools continues to rise with increasing distance from the river. At all areas and time steps, there are no pools at distances < 30 m from the river.

2.4.2 Relations between pool size and distance from channels

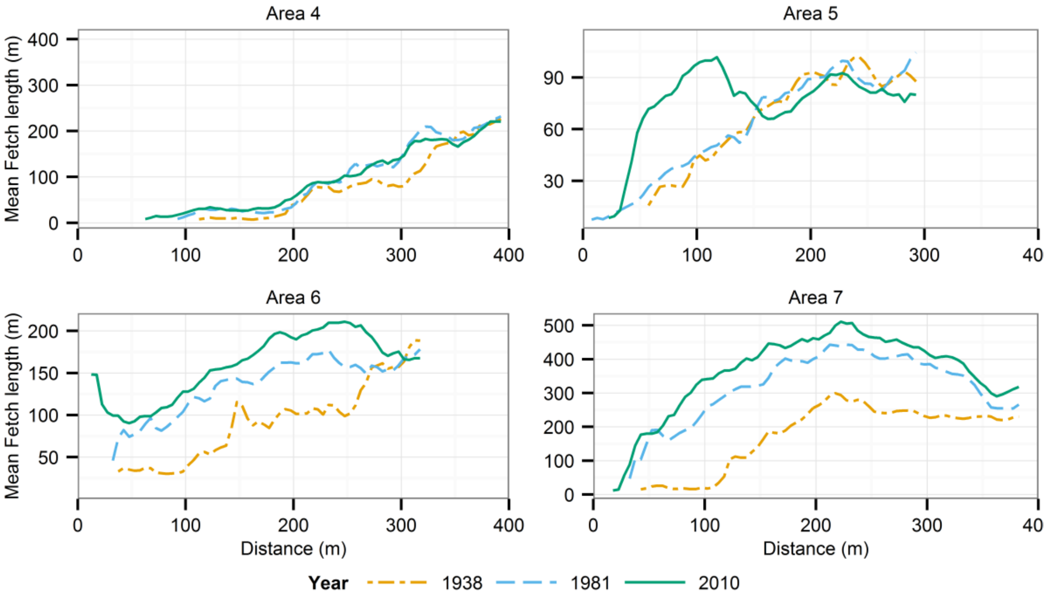

Figure 2.7: Temporal evolution of mean fetch length (m), the average distance across pools measured along four line orientations, as a function of distance to the river for different study sites. Note that the Y-axes have different scales.

The mean fetch length, a proxy for the size of the pools calculated as the average distance across pools along four line orientations, is visualized at different distances from the river in Fig. 2.7 and 2.8. The fetches increase with distance from the river, meaning that bigger pools or open water areas occur with increasing distance from the river. No pools are visible very close to the river (< 30 m), except for area 6 where a big pool expanded very close to the river in 2010, visible as high fetch length values at short distances (green solid line in Fig. 2.7, area 6). In time, there is a gradual increase in fetch length over the distance section (Fig. 2.7). In area 4 there is not a big difference between the time steps, but more upstream (areas 5-7) the changes are remarkable. The results along the spatial die-off gradient (Fig. 2.8) are consistent with the results for the temporal die-off development (Fig. 2.7).

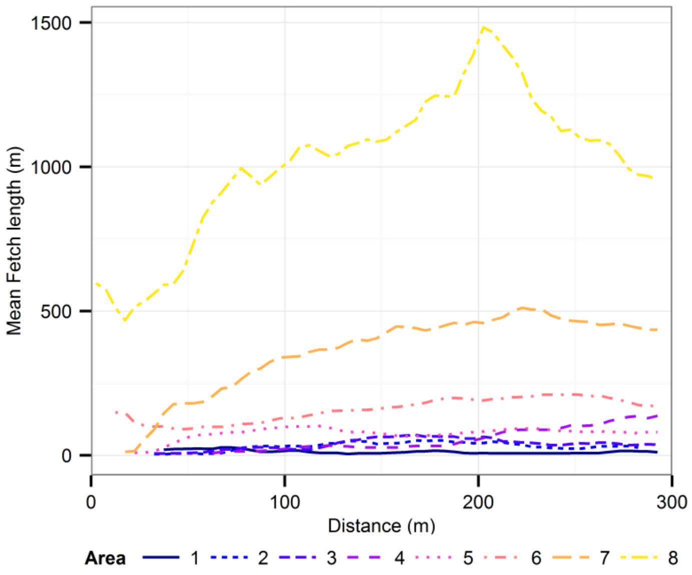

Figure 2.8: Mean fetch length (m), the average distance across pools measured along four line orientations, as function of distance to the river for the different study sites along the spatial die-off gradient in 2010.

2.5 Discussion

2.5.1 Observed spatial and temporal patterns of vegetation die-off

Vegetation die-off is a key process influencing the loss of tidal marshes, and quantitative descriptions of its spatio-temporal development are needed to help understand the eco-geomorphic feedbacks driving wetland submergence. To our knowledge, this is the first time that the spatio-temporal development of a complete gradient of vegetation die-off from small isolated pools to a totally degraded marsh has been quantified. Our observations reveal two key insights: (i) The extent of die-off increases with distance upriver and through time. ii) Die-off is not randomly distributed across the marsh surface but begins as small pools far from the river. At these locations pools grow, while new small pools gradually emerge closer to the river. The most stable areas that are unaffected by vegetation die-off are mainly located close to the river.

Our results document an increase in the extent of unvegetated pools with distance up the Blackwater River, where pools represent approximately 1% of marsh area at Area 1 (Fishing Bay) and 62% of marsh area in area 8 (close to Lake Blackwater). Gradients in sediment availability and tidal range may explain this spatial gradient in die-off extent. In our study area, both Ganju et al. (2013) and Stevenson et al. (1985) postulate two processes explaining a gradient in sediment availability: (i) at the upstream end, there is no external source of sediment. The long distance from the nearest downstream source, Fishing Bay, may result in a decreasing sediment supply to places with an increasing upstream distance from the sediment source. So the further upstream, the less likely suspended sediment will reach these sites. (ii) Wind-generated wave erosion and resuspension at Lake Blackwater leads locally to high sediment concentrations during northwestern storms, but the same northwestern winds drive a meteorological ebb tide, transporting a lot of the material toward Fishing Bay through the river. The internal generated sediment is exported out of the system and leads to an unstable system in the upstream parts of the river (Ganju et al., 2013, 2015). A significant amount of the transported sediment from Lake Blackwater, however, might be deposited at the marsh surface close to the river banks (Ganju et al., 2013). A third (iii) possible explanation for the die-off gradient in our study area is the decrease of (spring) tidal amplitude at upstream sites along the Blackwater River, from over 1.0 m at the Fishing Bay to less than 0.2 m at the Blackwater lake (Ganju et al., 2013). As tidal amplitude decreases, we may expect that the elevation range at which marsh plants can grow squeezes (e.g. McKee and Patrick, 1988). It is expected that marshes with a larger tidal range and hence a larger elevation range suitable for marsh vegetation have a higher capacity to keep up with sea level rise (Kirwan and Guntenspergen, 2010; Kirwan et al., 2010; D'Alpaos et al., 2011). However, these responses to different tidal ranges have not been shown within a single estuary, and field measurements (e.g. elevation measurements compared to the local tidal frame) need to confirm this hypothesis.

The main tidal channel is an important factor determining vegetation die-off. We observed that the marsh loss starts as small die-off areas in the inner marsh, at a distance of at least 75 m from the main tidal creek, and increases with distance from the Blackwater RiverBlackwater River (Figures 2.4 and 2.5). At shorter distances, the marshes appear to be stable. This is also qualitatively described in other study areas: in coastal Louisiana, interior die-off 'hot spots' start as isolated patches (Morton et al., 2003), and previous studies in the Blackwater marshes (Stevenson et al., 1985) and in a New England Marsh (Redfield, 1972) describe the occurrence of interior ponds, the larger ones located relatively remote from the drainage creeks (Redfield, 1972). Our observations might be explained by several mechanisms. First, the majority of suspended sediment is deposited close to main tidal channels so that interior marshes typically receive less sediment input (Reed et al., 1999; Leonard and Reed, 2002; Temmerman et al., 2003; Moskalski and Sommerfield, 2012). This might explain the higher stability of marsh zones close to tidal channels. Indeed, the average sediment deposition rates close to the river edges is 6 mm yr^{-1} (Ganju et al., 2013), offsetting local relative sea level rise of 3.72 mm yr^{-1} (NOAA, 2016). These differences can have profound effects on biological feedback mechanisms. Higher elevations at the channel levees compared to the interior marshes supports higher aboveground (Nyman et al., 2006; Langley et al., 2013) and belowground biomass (Kirwan and Guntenspergen, 2012; Langley et al., 2013). Also productivity (Morris et al., 2002) and growth rate (Mudd et al., 2009) may be enhanced by the recent sea level rise in high elevated marsh portions. As a consequence, we may expect more accretion by aboveground and belowground organic matter production and more soil-stabilizing roots close to the river, stabilizing these areas. The accretion deficit (i.e. accretion rates being lower than rate of relative sea level rise) at the interior marsh, on the other hand, might lead to elevations where biomass production is reduced (Morris et al., 2002; Nyman et al., 2006; Kirwan et al., 2010; Langley et al., 2013) and hence both organic matter accumulation and vegetation-induced suspended sediment deposition will decrease. This may result in an enhanced lowering within the tidal frame, up to the point where vegetation will die-off. The vegetation die-off far from the river might also be initiated by insufficient subsurface drainage of the wetland soil, since vegetation die-off was found to start far from tidal channels that act as drainage channels for soil subsurface flow and consequent soil aeration (Ursino et al., 2004). It is known that insufficient drainage can cause waterlogging and salinity stress that kill vegetation (Redfield, 1972; Wilson et al., 2009).

2.5.2 Possible implications for bio-geomorphic response of marshes

The pattern of development of marsh die-off is expected to have important implications for the bio-geomorphic response of marshes, as spatial vegetation patterns are known to be important in determining the spatial distribution of hydrodynamic and erosional forces (Temmerman et al., 2007; Vandenbruwaene et al., 2011b; Bouma et al., 2013). At initial vegetation die-off, small and medium sized pools far from the tidal channels are expected to have limited hydrodynamic feedback effects, since tidal flows are slowed down by friction of the surrounding vegetation, and fetches are too small to create significant waves (Mariotti and Fagherazzi, 2013). This is shown in our analysis, where the pools start small, far from the main tidal channels and gradually expand.

As pools further expand, it can be expected that they become more vulnerable to wave erosion (Ganju et al., 2013; Stevenson et al., 1985). Once a critical threshold fetch length is passed, irreversible wave-induced marsh erosion will likely take place (Mariotti and Fagherazzi, 2013). This has already been started in Blackwater Lake, where erosion of the lake shoreline takes place (Ganju et al., 2013).

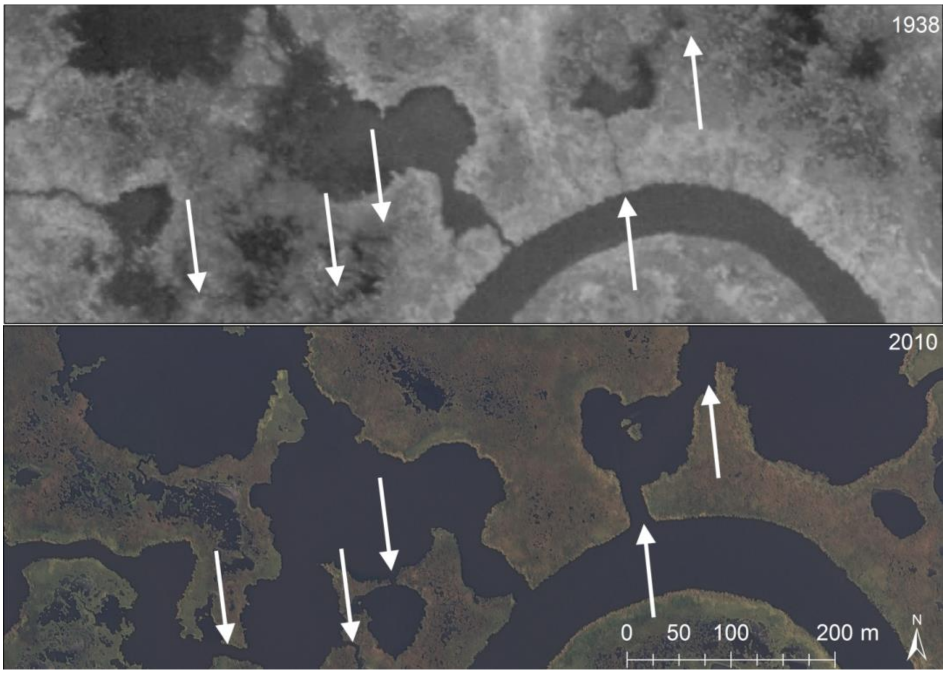

Figure 2.9: Examples of increased connectivity between pools and the tidal channel network (white arrows) in 2010 (bottom) compared to 1938 (top) (location: working area 6, see Figure 2.1b). Dark areas represent channels or pools.

At some locations, there might be another physical feedback mechanism that enhances erosion. When pools expand, they connect to the tidal creek network. This is observed in our study area (see Fig. 2.9) and is also observed in other marsh areas by a.o. Kearney et al. (1988), Perillo and Iribarne (2003), Van Huissteden and Van De Plassche (1998), Wilson et al. (2009, 2014). When the pools are hydraulically connected to the tidal channel system, the flow velocities in the pools during tidal flooding and drainage are expected to become higher and the pool bottom might become more susceptible to erosion, because pool substrates are generally loose muddy sediments with a high water content (Stevenson et al., 1985; van Huissteden and van de

Plassche, 1998; Wilson et al., 2010). Also (Day et al., 2011) noted that the degraded, liquefied soil material in inner-marsh pools might be exported by low energy waves and currents. It should be noted that the erosional effect of tidal connections applies to the studied low-energy micro-tidal river system. In other areas with higher tidal range or energy, a new tidal connection might be a source of sediment and can lead to high rates of sediment accretion and pool infilling, especially after revegetation (Redfield, 1972; Perillo et al., 1996; Millette et al., 2010; Wilson et al., 2010, 2014).The above-discussed feedback mechanism between vegetation die-off and erosion may imply that there might be a vegetation die-off threshold after which irreversible erosion by waves and possibly by tidal currents will take place.

2.5.3 Evidence for a chronosequence along the main tidal channel

We observed a similar spatial development of vegetation die-off from moderately to highly degraded marshes over a time series from 1938 to 2010 and along a contemporary spatial gradient along the Blackwater RiverBlackwater River. Both developments show a steady increase in pool cover (Fig. 2.3 and 2.4) and, in particular, the distances at which pools form (Fig. 2.5 and 2.6) and enlarge (Fig. 2.7 and 2.8) are very similar along the temporal and spatial gradient. This finding suggest that the present-day spatial gradient might be used as a chronosequence, a space-for-time substitution often used by ecologists and geomorphologists to study long-term temporal evolution and development of landscapes (Conn and Day, 1997; Olff et al., 1997; van de Koppel et al., 2005). In other words, the spatial gradient of vegetation die-off along the Blackwater RiverBlackwater River offers a unique opportunity to study the processes that lead to progressive marsh die-off, such as the effect of spatial patterns and feedbacks of vegetation die-off over time. The chronosequence also implies that, if marsh vegetation die-off continues, we may expect the same temporal development as observed along the present-day spatial gradient.

2.6 Conclusion

We found that the spatial distribution of vegetation die-off (the location of pools) in our study area is not a random process. Initial vegetation die-off starts at a distance of more than 75 m from tidal channels. As vegetation die-off continues, pools expand and new pools emerge closer and closer to the tidal channels. As a result, the larger pools will be situated at distant locations from the tidal channels and pools are smaller closer to the channels. These developments are observed in time, as well as on a spatial gradient, indicating that the present-day spatial gradient can be considered a chronosequence. Potential processes explaining our observed patterns are differential sedimentation and soil drainage between marsh locations at different distances from the tidal channels, with marshes adjacent to channels having higher sedimentation rates, better soil drainage and hence better plant growth conditions and stronger soils than inner marsh locations farther away from channels.

Based on our observations, we expect that for a certain degree of vegetation die-off, bio-geomorphic feedback mechanisms will enhance marsh soil erosion, resulting in even more marsh loss. Hence our study highlights the importance of studying the spatial development of vegetation die-off and the effect on bio-geomorphic feedback mechanisms. However, further studies are necessary to gain more knowledge about a possible shift in sedimentation and erosion rates with increasing vegetation die-off in order to prevent further marsh loss on a large scale.

Acknowledgements

This project was financed by an UA-BOF DOCPRO grant (to L.S. and S.T.), the Research Foundation Flanders (FWO, PhD grant L.S., 11S9614N, travel grants L.S. V428214N and S.T. K217414N), by the U.S. Geological Survey, Climate and Land-Use Research and Development Program (G.G.), by NSF GLD 1529245, NSF SEES 1426981, NSF LTER 1237733 (M.K.).

We would like to thank the managers and biologists of the Blackwater National Wildlife Refuge for their assistance and valuable comments; and P. Brennand (USGS) for indispensable field assistance. Any use of trade, product, or firm names is for descriptive purposes only and does not imply endorsement by the US Government.

2.8 References

Alber, M., Swenson, E.M., Adamowicz, S.C., Mendelssohn, I.A., 2008. Salt Marsh Dieback: An overview of recent events in the US. Estuar. Coast. Shelf Sci. 80, 1–11. doi:10.1016/j.ecss.2008.08.009

Allen, J.R.L., 1990. Salt-marsh growth and stratification: A numerical model with special reference to the Severn Estuary, southwest Britain. Mar. Geol. 95, 77–96. doi:10.1016/0025-3227(90)90042-I

Barbier, E.B., Hacker, S.D., Kennedy, C., Koch, E.W., Stier, A.C., Silliman, B.R., 2011. The value of estuarine and coastal ecosystem services. Ecol. Monogr. 81, 169–193. doi:10.1890/10-1510.1

Baustian, J.J., Mendelssohn, I.A., Hester, M.W., 2012. Vegetation's importance in regulating surface elevation in a coastal salt marsh facing elevated rates of sea level rise. Glob. Chang. Biol. 18, 3377–3382. doi:10.1111/j.1365-2486.2012.02792.x

Boston, K.G., 1983. The development of salt pans on tidal marshes, with particular reference to south-eastern Australia. J. Biogeogr. 10, 1–10.

Bouma, T.J., Temmerman, S., van Duren, L.A., Martini, E., Vandenbruwaene, W., Callaghan, D.P., Balke, T., Biermans, G., Klaassen, P.C., van Steeg, P., Dekker, F., van de Koppel, J., de Vries, M.B., Herman, P.M.J., 2013. Organism traits determine the strength of scale-dependent bio-geomorphic feedbacks: A flume study on three intertidal plant species. Geomorphology 180–181, 57–65. doi:10.1016/j.geomorph.2012.09.005

Cahoon, D.R., Guntenspergen, G.R., Baird, S., 2010. Do Annual Prescribed Fires Enhance or Slow the Loss of Coastal Marsh Habitat at Blackwater National Wildlife Refuge? Final Report to Joint Fire Science Program Project Number 06-2-1-35.

Carniello, L., Defina, A., D'Alpaos, L., 2009. Morphological evolution of the Venice lagoon: Evidence from the past and trend for the future. J. Geophys. Res. Earth Surf. 114, 1–10. doi:10.1029/2008JF001157

Conn, C.E., Day, F.P., 1997. Root decomposition across a barrier island chronosequence: Litter quality and environmental controls. Plant Soil 195, 351–364. doi:10.1023/A:1004214216889

D'Alpaos, A., Lanzoni, S., Marani, M., Rinaldo, A., 2007. Landscape evolution in tidal embayments: Modeling the interplay of erosion, sedimentation, and vegetation dynamics. J. Geophys. Res. Earth Surf. 112, 1–17. doi:10.1029/2006JF000537

D'Alpaos, A., Mudd, S.M., Carniello, L., 2011. Dynamic response of marshes to perturbations in suspended sediment concentrations and rates of relative sea level rise. J. Geophys. Res. Earth Surf. 116, 1–13. doi:10.1029/2011JF002093

Day, J.W., Britsch, L.D., Hawes, S.R., Shaffer, G.P., Reed, D.J., Cahoon, D.R., 2000. Pattern and Process of Land Loss in the Mississippi Delta: A Spatial and Temporal Analysis of Wetland Habitat Change. Estuaries 23, 425–438. doi:10.2307/1353136

Day, J.W., Kemp, G.P., Reed, D.J., Cahoon, D.R., Boumans, R.M., Suhayda, J.M., Gambrell, R., 2011. Vegetation death and rapid loss of surface elevation in two contrasting Mississippi delta salt marshes: The role of sedimentation, autocompaction and sea-level rise. Ecol. Eng. 37, 229–240. doi:10.1016/j.ecoleng.2010.11.021

DeLaune, R.D., Nyman, J.A., Patrick, W.H., 1994. Peat collapse, ponding and wetland loss in a rapidly submerging coastal marsh. J. Coast. Res. 10, 1021–1030.

Delaune, R.D.D., Pezeshki, S.R.R., 1994. The Influence of Subsidence and Saltwater Intrusion on Coastal Marsh Stability:Louisiana Gulf Coast, U.S.A. J. Coast. Res. Sp.Issue 1, 77–89.

Fagherazzi, S., Carniello, L., D'Alpaos, L., Defina, A., 2006. Critical bifurcation of shallow microtidal landforms in tidal flats and salt marshes. Proc. Natl. Acad. Sci. U. S. A. 103, 8337–8341. doi:10.1073/pnas.0508379103

Fagherazzi, S., Kirwan, M.L., Mudd, S.M., Guntenspergen, G.R., Temmerman, S., D'Alpaos, A., van de Koppel, J., Rybczyk, J.M., Reyes, E., Craft, C., Clough, J., 2012. Numerical models of salt marsh evolution: Ecological, geomorphic, and climatic factors. Rev. Geophys. 50, RG1002. doi:10.1029/2011RG000359

French, J.R., 1993. Numerical simulation of vertical marsh growth and adjustment to accelerated sea-level rise, North Norfolk, U.K. Earth Surf. Process. Landforms 18, 63–81. doi:10.1002/esp.3290180105

Ganju, N.K., Kirwan, M.L., Dickhudt, P.J., Guntenspergen, G.R., Cahoon, D.R., Kroeger, K.D., 2015. Sediment transport-based metrics of wetland stability. Geophys. Res. Lett. 42, 7992–8000. doi:10.1002/2015GL065980

Ganju, N.K., Nidzieko, N.J., Kirwan, M.L., 2013. Inferring tidal wetland stability from channel sediment fluxes: Observations and a conceptual model. J. Geophys. Res. Earth Surf. 118, 2045–2058. doi:10.1002/jgrf.20143

Holdredge, C., Bertness, M.D., Altieri, A.H., 2009. Role of Crab Herbivory in Die-Off of New England Salt Marshes. Conserv. Biol. 23, 672–679. doi:10.1111/j.1523-1739.2008.01137.x

Kearney, M.S., Grace, R.E., Stevenson, J.C., 1988. Marsh Loss in Nanticoke Estuary, Chesapeake Bay. Geogr. Rev. 78, 205–220. doi:10.2307/214178

Kearney, M.S., Rogers, A.S., Townshend, J.R.G., Rizzo, E., Stutzer, D., Stevenson, J.C., Sundborg, K., 2002. Landsat imagery shows decline of coastal marshes in Chesapeake and Delaware Bays. Eos, Trans. Am. Geophys. Union 83, 173–178. doi:10.1029/2002EO000112

Kéfi, S., Guttal, V., Brock, W. a, Carpenter, S.R., Ellison, A.M., Livina, V.N., Seekell, D. a, Scheffer, M., Nes, E.H. Van, Dakos, V., 2014. Early Warning Signals of Ecological Transitions : Methods for Spatial Patterns. PLoS One 9, 10–13. doi:10.1371/journal.pone.0092097

Kendrot, S.R., 2011. Restoration through eradication : protecting Chesapeake Bay marshlands from invasive nutria (Myocastor coypus), in: Veitch, C.R., Clout, M.N., Towns, D.R. (Eds.), Island Invasives: Eradication and Management. Proceedings of the International Conference on Island Invasives. Gland, Switzerland: IUCN and Auckland, New Zealand: CBB, pp. 313–319.

Kirwan, M.L., Guntenspergen, G.R., 2015. Response of Plant Productivity to Experimental Flooding in a Stable and a Submerging Marsh. Ecosystems 18, 903–913. doi:10.1007/s10021-015-9870-0

Kirwan, M.L., Guntenspergen, G.R., 2012. Feedbacks between inundation, root production, and shoot growth in a rapidly submerging brackish marsh. J. Ecol. 100, 764–770. doi:10.1111/j.1365-2745.2012.01957.x

Kirwan, M.L., Guntenspergen, G.R., 2010. Influence of tidal range on the stability of coastal marshland. J. Geophys. Res. 115, F02009. doi:10.1029/2009JF001400

Kirwan, M.L., Guntenspergen, G.R., D'Alpaos, A., Morris, J.T., Mudd, S.M., Temmerman, S., 2010. Limits on the adaptability of coastal marshes to rising sea level. Geophys. Res. Lett. 37, L23401. doi:10.1029/2010GL045489

Kirwan, M.L., Megonigal, J.P., 2013. Tidal wetland stability in the face of human impacts and sea-level rise. Nature 504, 53–60. doi:10.1038/nature12856

Kirwan, M.L., Murray, A.B., 2007. A coupled geomorphic and ecological model of tidal marsh evolution. Proc. Natl. Acad. Sci. U. S. A. 104, 6118–6122. doi:10.1073/pnas.0700958104

Kirwan, M.L., Murray, A.B., Boyd, W.S., 2008. Temporary vegetation disturbance as an explanation for permanent loss of tidal wetlands. Geophys. Res. Lett. 35, L05403. doi:10.1029/2007GL032681

Kirwan, M.L., Temmerman, S., Skeehan, E.E., Guntenspergen, G.R., Fagherazzi, S., 2016. Overestimation of marsh vulnerability to sea level rise. Nat. Clim. Chang. 6, 253–260. doi:10.1038/nclimate2909

Langley, J.A., Mozdzer, T.J., Shepard, K.A., Hagerty, S.B., Megonigal, J.P., 2013. Tidal marsh plant responses to elevated CO2, nitrogen fertilization, and sea level rise. Glob. Chang. Biol. 19, 1495–1503. doi:10.1111/gcb.12147

Leonard, L.A., Croft, A.L., 2006. The effect of standing biomass on flow velocity and turbulence in Spartina alterniflora canopies. Estuar. Coast. Shelf Sci. 69, 325–336. doi:10.1016/j.ecss.2006.05.004

Leonard, L.A., Reed, D.J., 2002. Hydrodynamics and sediment transport through tidal marsh canopies. J. Coast. Res. 36, 459–469.

Marani, M., D'Alpaos, A., Lanzoni, S., Carniello, L., Rinaldo, A., 2010. The importance of being coupled: Stable states and catastrophic shifts in tidal biomorphodynamics. J. Geophys. Res. Earth Surf. 115, 1–15. doi:10.1029/2009JF001600

Mariotti, G., Carr, J., 2014. Dual role of salt marsh retreat: Long-term loss and short-term resilience. Water Resour. Res. 50, 2963–2974. doi:10.1002/2013WR014676

Mariotti, G., Fagherazzi, S., 2013. Critical width of tidal flats triggers marsh collapse in the absence of sea-level rise. Proc. Natl. Acad. Sci. U. S. A. 110, 5353–5356. doi:10.1073/pnas.1219600110

McGarigal, K., Cushman, S.A., Ene, E., 2012. FRAGSTATS v4: Spatial Pattern Analysis Program for Categorical and Continuous Maps. Computer software program produced by the authors at the University of Massachusetts, Amherst. Available at http://www.umass.edu/landeco/research/fragstats/fragstats.html.

McKee, K.L., Patrick, W.H., 1988. The Relationship of Smooth Cordgrass (Spartina alterniflora) to Tidal Datums: A Review. Estuaries 11, 143–151. doi:10.2307/1351966

Mendelssohn, I.A., McKee, K.L., 1988. Spartina Alterniflora Die-Back in Louisiana: Time-Course Investigation of Soil Waterlogging Effects. J. Ecol. 76, 509–521. doi:10.2307/2260609

Millette, T.L., Argow, B.A., Marcano, E., Hayward, C., Hopkinson, C.S., Valentine, V., 2010. Integration of Multitemporal Multispectral Remote Sensing with LIDAR and GIS. J. Coast. Res. 265, 809–816. doi:10.2112/JCOASTRES-D-09-00101.1

Möller, I., Kudella, M., Rupprecht, F., Spencer, T., Paul, M., van Wesenbeeck, B.K., Wolters, G., Jensen, K., Bouma, T.J., Miranda-Lange, M., Schimmels, S., 2014. Wave attenuation over coastal salt marshes under storm surge conditions. Nat. Geosci. 7, 727–731. doi:10.1038/ngeo2251

Morris, J.T., Sundareshwar, P. V., Nietch, C.T., Kjerfve, B., Cahoon, D.R., 2002. Responses of Coastal Wetlands to Rising Sea Level. Ecology 83, 2869–2877. doi:10.1890/0012-9658(2002)083[2869:ROCWTR]2.0.CO;2

Morton, R.A., Tiling, G., Ferina, N.F., 2003. Causes of hot-spot wetland loss in the Mississippi delta plain. Environ. Geosci. 10, 71–80. doi:10.1306/eg100202007

Moskalski, S.M., Sommerfield, C.K., 2012. Suspended sediment deposition and trapping efficiency in a Delaware salt marsh. Geomorphology 139–140, 195–204. doi:10.1016/j.geomorph.2011.10.018

Mudd, S.M., D'Alpaos, A., Morris, J.T., 2010. How does vegetation affect sedimentation on tidal marshes? Investigating particle capture and hydrodynamic controls on biologically mediated sedimentation. J. Geophys. Res. 115, F03029. doi:10.1029/2009JF001566

Mudd, S.M., Howell, S.M., Morris, J.T., 2009. Impact of dynamic feedbacks between sedimentation, sea-level rise, and biomass production on near-surface marsh stratigraphy and carbon accumulation. Estuar. Coast. Shelf Sci. 82, 377–389. doi:10.1016/j.ecss.2009.01.028

NOAA, 2016. NOAA Sea level trends station 8571892. http://tidesandcurrents.noaa.gov/sltrends/sltrends_station.shtml?stnid=8571892 [WWW Document]. URL http://tidesandcurrents.noaa.gov/sltrends/sltrends_station.shtml?stnid=8571892 (accessed 1.15.16).

Nyman, J.A., DeLaune, R.D., Roberts, H.H., Patrick, W.H., 1993. Relationship between vegetation and soil formation in a rapidly submerging coastal marsh. Mar. Ecol. Prog. Ser. 96, 269–279. doi:10.3354/meps096269

Nyman, J.A., Walters, R.J., DeLaune, R.D., Patrick, W.H., 2006. Marsh vertical accretion via vegetative growth. Estuar. Coast. Shelf Sci. 69, 370–380. doi:10.1016/j.ecss.2006.05.041

Olff, H., De Leeuw, J., Bakker, J.P., Platerink, R.J., van Wijnen, H.J., 1997. Vegetation Succession and Herbivory in a Salt Marsh: Changes Induced by Sea Level Rise and Silt Deposition Along an Elevational Gradient. J. Ecol. 85, 799. doi:10.2307/2960603

Penland, S., Wayne, L., Britsch, D., Williams, S.J., Beall, A.D., Butterworth, V., 2000. Geomorphic Classification of Coastal Land Loss between 1932 and 1990 in the Mississippi River Delta Plain, Southeastern Louisiana. USGS Open File Report 00-417. https://pubs.usgs.gov/of/2000/of00-417/.

Perillo, G.M.E., Iribarne, O.O., 2003. Processes of tidal channel development in salt and freshwater marshes. Earth Surf. Process. Landforms 28, 1473–1482. doi:10.1002/esp.1018

Perillo, G.M.E., Ripley, M.D., Piccolo, M.C., Dyer, K.R., 1996. The Formation of Tidal Creeks in a Salt Marsh : New Evidence from the Loyola Bay Salt Marsh, Rio Gallegos Estuary, Argentina. Mangroves Salt Marshes 1, 37–46. doi:10.1023/A:1025942111382

Pethick, J.S., 1981. Long-term Accretion Rates on Tidal Salt Marshes. J. Sediment. Res. 51, 571–577. doi:10.1306/212F7CDE-2B24-11D7-8648000102C1865D

Pethick, J.S., 1974. The Distribution of Salt Pans on Tidal Salt Marshes. J. Biogeogr. 1, 57–62.

R Core Team, 2017. R: A Language and Environment for Statistical Computing, Vienna, Austria.

Redfield, A.C., 1972. Development of a New England Salt Marsh. Ecol. Monogr. 42, 201–237. doi:10.2307/1942263

Reed, D.J., Spencer, T., Murray, A.L., French, J.R., Leonard, L., 1999. Marsh surface sediment deposition and the role of tidal creeks: Implications for created and managed coastal marshes. J. Coast. Conserv. 5, 81–90. doi:10.1007/BF02802742

Russi, D., ten Brink, P., Farmer, A., Badura, T., Coates, D., Förster, J., Kumar, R., Davidson, N., 2013. The Economics of Ecosystems and Biodiversity (TEEB) for Water and Wetlands. IEEP, London and Brussels; Ramsar Secretariat, Gland.

Scott, M., McDermott, L., Silva, E., Watson, E., 2009. Project report: Digital Spatial Data Capture of Marsh Extent in Blackwater National Wildlife Refuge, 1938 and 2006. Eastern Shore Regional GIS Cooperative, Salisbury University.

Silliman, B.R., van de Koppel, J., Bertness, M.D., Stanton, L.E., Mendelssohn, I.A., 2005. Drought, Snails, and Large-Scale Die-Off of Southern U.S. Salt Marshes. Science 310, 1803–1806. doi:10.1126/science.1118229

Smith, S.M., 2009. Multi-Decadal Changes in Salt Marshes of Cape Cod, MA: Photographic Analyses of Vegetation Loss, Species Shifts, and Geomorphic Change. Northeast. Nat. 16, 183–208. doi:10.1656/045.016.0203

Stevenson, J.C., Kearney, M.S., Pendleton, E.C., 1985. Sedimentation and erosion in a Chesapeake Bay brackish marsh system. Mar. Geol. 67, 213–235. doi:10.1016/0025-3227(85)90093-3

Temmerman, S., Bouma, T.J., van de Koppel, J., van der Wal, D., De Vries, M.B., Herman, P.M.J., 2007. Vegetation causes channel erosion in a tidal landscape. Geology 35, 631–634. doi:10.1130/G23502A.1

Temmerman, S., De Vries, M.B., Bouma, T.J., 2012a. Coastal marsh die-off and reduced attenuation of coastal floods: A model analysis. Glob. Planet. Change 92–93, 267–274. doi:10.1016/j.gloplacha.2012.06.001

Temmerman, S., Govers, G., Wartel, S., Meire, P., 2003. Spatial and temporal factors controlling short-term sedimentation in a salt and freshwater tidal marsh, Scheldt estuary, Belgium, SW Netherlands. Earth Surf. Process. Landforms 28, 739–755. doi:10.1002/esp.495

Temmerman, S., Kirwan, M.L., 2015. Building land with a rising sea. Science 349, 588–589. doi:10.1126/science.aac8312

Temmerman, S., Meire, P., Bouma, T.J., Herman, P.M.J., Ysebaert, T., De Vriend, H.J., 2013. Ecosystem-based coastal defence in the face of global change. Nature 504, 79–83. doi:10.1038/nature12859

Temmerman, S., Moonen, P., Schoelynck, J., Govers, G., Bouma, T.J., 2012b. Impact of vegetation die-off on spatial flow patterns over a tidal marsh. Geophys. Res. Lett. 39, 1–5. doi:10.1029/2011GL050502

Ursino, N., Silvestri, S., Marani, M., 2004. Subsurface flow and vegetation patterns in tidal environments. Water Resour. Res. 40, W05115. doi:10.1029/2003WR002702

van de Koppel, J., van der Wal, D., Bakker, J.P., Herman, P.M.J., 2005. Self-Organization and Vegetation Collapse in Salt Marsh Ecosystems. Am. Nat. 165, E1–E12. doi:10.1086/426602

van Huissteden, J., van de Plassche, O., 1998. Sulphate reduction as a geomorphological agent in tidal marshes (“Great Marshes” at Barnstable, Cape Cod, USA). Earth Surf. Process. Landforms 23, 223–236. doi:10.1002/(SICI)1096-9837(199803)23:3<223::AID-ESP843>3.0.CO;2-I

Vandenbruwaene, W., Maris, T., Cox, T.J.S., Cahoon, D.R., Meire, P., Temmerman, S., 2011a. Sedimentation and response to sea-level rise of a restored marsh with reduced tidal exchange: Comparison with a natural tidal marsh. Geomorphology 130, 115–126. doi:10.1016/j.geomorph.2011.03.004

Vandenbruwaene, W., Temmerman, S., Bouma, T.J., Klaassen, P.C., De Vries, M.B., Callaghan, D.P., Van Steeg, P., Dekker, F., Van Duren, L.A., Martini, E., Balke, T., Biermans, G., Schoelynck, J., Meire, P., 2011b. Flow interaction with dynamic vegetation patches: Implications for biogeomorphic evolution of a tidal landscape. J. Geophys. Res. Earth Surf. 116, 1–13. doi:10.1029/2010JF001788

Wang, C., Temmerman, S., 2013. Does biogeomorphic feedback lead to abrupt shifts between alternative landscape states?: An empirical study on intertidal flats and marshes. J. Geophys. Res. Earth Surf. 118, 229–240. doi:10.1029/2012JF002474

Wang, D.-P., Elliott, A.J., 1978. Non-Tidal Variability in the Chesapeake Bay and Potomac River: Evidence for Non-Local Forcing. J. Phys. Oceanogr. 8, 225–232. doi:10.1175/1520-0485(1978)008<0225:NTVITC>2.0.CO;2

Wells, J.T., Coleman, J.M., 1987. Wetland loss and the subdelta life cycle. Estuar. Coast. Shelf Sci. 25, 111–125. doi:10.1016/0272-7714(87)90029-1

Wilson, C.A., Hughes, Z.J., FitzGerald, D.M., Hopkinson, C.S., Valentine, V., Kolker, A.S., 2014. Saltmarsh pool and tidal creek morphodynamics: Dynamic equilibrium of northern latitude saltmarshes? Geomorphology 213, 99–115. doi:10.1016/j.geomorph.2014.01.002

Wilson, K.R., Kelley, J.T., Croitoru, A., Dionne, M., Belknap, D.F., Steneck, R., 2009. Stratigraphic and ecophysical characterizations of salt pools: Dynamic landforms of the Webhannet Salt Marsh, Wells, ME, USA. Estuaries and Coasts 32, 855–870. doi:10.1007/s12237-009-9203-7

Wilson, K.R., Kelley, J.T., Tanner, B.R., Belknap, D.F., 2010. Probing the Origins and Stratigraphic Signature of Salt Pools from North-Temperate Marshes in Maine, U.S.A. J. Coast. Res. 26, 1007–1026. doi:10.2112/JCOASTRES-D-10-00007.1

Yapp, R.H., Johns, D., Jones, O.T., 1917. The Salt Marshes of the Dovey Estuary. J. Ecol. 5, 65–103. doi:10.2307/2255644

3

Vegetation loss affects spatial flow and sedimentation patterns in a tidal marsh

Lennert Schepers, Alexander Van Braeckel, Tjeerd J. Bouma, Stijn Temmerman

3.1 Abstract

Coastal marshes provide valuable ecosystem functions, but some are facing sea level rise rates higher than they can withstand, which can result in large-scale marsh vegetation loss. A key question is how tidal flow and sedimentation patterns are affected by the spatio-temporal patterns of vegetation loss, as this will govern the potential for recovery of marsh vegetation. In this study we performed a field experiment in a uniform macro-tidal minerogenic reed marsh where typical spatio-temporal patterns of vegetation loss were simulated by consecutive spatial mowing patterns. For each mowing pattern, the resulting spatial patterns of flow velocities and sediment deposition were recorded. Our results indicate that initial vegetation loss in inner marshes at a distance of 15-50 m from the tidal channels has limited effect on tidal flows, but creating vegetation-less corridors between the bare inner marsh and channels results in higher flow velocities over unvegetated surfaces. Flow velocities in remaining vegetation patches experience relative little effect from surrounding vegetation removal. When all vegetation is removed, flow velocities further increase and sheet flow occurs over the complete marsh platform instead of concentrated channel flow. Effects on spatial sedimentation patterns are complex, but our experiments clearly showed that complete vegetation removal does not simply lead to reduced sedimentation rates everywhere on the marsh platform. Instead vegetation removal results in redistributed sedimentation patterns, with locally reduced sedimentation rates at short distances (<15 m) from channels and increased sediment supply and increased sedimentation rates in inner marshes at farther distance (15-50 m) from channels. Our results highlight that feedbacks between spatial patterns of vegetation loss, tidal sediment transport and deposition are key to understanding and mitigating the mechanisms of marsh loss.

3.2 Introduction

Sea level rise is challenging the persistence of coastal mashes and their valuable ecosystem services, including carbon sequestration (McLeod et al., 2011; Duarte et al., 2013), attenuation of storm surges (Smolders et al., 2015; Stark et al., 2015) and storm waves (Möller, 2006; Gedan et al., 2011; Möller et al., 2014). Marsh vegetation plays an important role in the provision of these services and in the survival of coastal marshes with sea level rise, as the vegetation reduces waves and flow velocities and promotes sediment deposition on the marsh surface (Bouma et al., 2005a, 2005b, 2010; Leonard and Croft, 2006; Neumeier and Amos, 2006; Baustian et al., 2012), enabling many marsh areas to keep up with increasing sea level rise (Kirwan et al., 2016). However, if sediment deposition is not sufficient, sea level rise may provoke increasing marsh flooding until it exceeds the marsh plant's tolerance for inundation, ultimately leading to a loss of marsh vegetation (Kirwan et al., 2010, 2013). A key question is then how marsh loss affects flow and sedimentation patterns, as this may induce detrimental consequences for the ecosystem functions of marshes.

Complete removal of vegetation increases flow velocities on the marsh platform, which has been shown in a field experiment (Temmerman et al., 2012) and in a number of modeling studies (Temmerman et al., 2005; D'Alpaos et al., 2007; Kirwan and Murray, 2007; Kirwan et al., 2008; Ashall et al., 2016; Nardin et al., 2016; Wu et al., 2017). The increase in flow velocity has been attributed to reduced friction and would imply lower sedimentation rates or even erosion after marsh die-off (Temmerman et al., 2005; Silliman et al., 2012; Sheehan and Ellison, 2015). In the unvegetated channels that typically cut through marsh platforms and that supply water and sediments to and from the surrounding marsh platform, a contrasting effect has been demonstrated in a field experiment: complete removal of surrounding marsh vegetation resulted in lower channel flow velocities (Temmerman et al., 2012). Comparison with modelling showed that vegetation-induced friction on the marsh platform concentrates flood and ebb flows towards the channels; vice versa, complete vegetation removal leads to lower flow velocities (Temmerman et al., 2005; Ashall et al., 2016) and more sedimentation in the channels, which might even lead to partial channel infilling (Temmerman et al., 2005). In agreement with this vegetation effect on channel flow and sediment transport, aerial picture analyses have demonstrated that channel networks are denser (more closely spaced) in vegetated intertidal marshes as compared to non-vegetated intertidal flats (Temmerman et al., 2007; Vandenbruwaene et al., 2013; Kearney and Fagherazzi, 2016).

However, the only two experimental studies on large-scale vegetation removal we are aware of (Temmerman et al., 2012; Sheehan and Ellison, 2015), only considered complete, instantaneous vegetation removal, while marsh vegetation die-off is a gradual process with distinct spatio-temporal patterns of vegetation loss (Mariotti, 2016; Schepers et al., 2017). Initial die-off typically starts at the inner portions of marshes at a distance from channels, where surface elevation is lower and soil drainage is less developed as compared to the higher elevated natural levees directly adjacent to channels (Redfield, 1972; Kearney et al., 1988; Morton et al., 2003; Schepers et al., 2017). These areas with initial marsh die-off expand and subsequently become connected to the tidal channels network. Connections with the tidal channels can lead to sediment infilling and vegetation recovery (Redfield, 1972; Perillo et al., 1996; Millette et al., 2010; Wilson et al., 2010, 2014), while other research suggests that connections can lead to erosion of the bare inner portions of marshes (Day et al., 2011;

Schepers et al., 2017)(Chapter 4). Hence the spatio-temporal patterns of vegetation die-off are expected to have a crucial impact on the tidal flow and the spatial sedimentation pattern. Yet, no field experiments have directly quantified the effects of the different stages of vegetation loss on tidal flow and sedimentation patterns.

In this study, we performed a large-scale field experiment where the different stages of tidal marsh vegetation die-off are simulated by artificial mowing of the vegetation in a sequence of spatial patterns with reducing vegetation cover. Sediment deposition and tidal flows are measured and repeated for the consecutive mowing patterns. We hypothesize that removal of vegetation in inner parts of the marsh at a distance from the channels has initially limited impact due to the intact vegetation buffer along the channels, but that further vegetation removal in connection to the channels and finally complete vegetation removal increases flow velocities significantly and limits sediment deposition on the marsh platform.

3.3 Methods

3.3.1 Study area

The experiment was conducted in a freshwater tidal marsh (Kijkverdriet) in the Scheldt Estuary, Belgium (Fig. 3.1, 51.1213° N, 4.2641° E). The semi-diurnal tidal range is 6 m during spring tides and 4.5 m during neap tides. The geomorphology of the marsh consists of a generally flat marsh platform with a mean elevation of 0.05 m relative to mean high water level and a standard deviation of 0.17 m (Temmerman et al., 2012). The marsh platform is dissected by a single unvegetated tidal creek with a width of 2.5 m and depth of 1.4 m below the surrounding marsh platform (Temmerman et al., 2012) (Fig. 3.1). The marsh consists of a uniform *Phragmites australis* (common reed) vegetation up to 4 m high, which stays emergent even during the highest spring tides. Local suspended sediment concentrations in the adjacent estuarine channel range between < 5 and 300 mg/l (Temmerman et al., 2003a). At the location of the Kijkverdriet, the Scheldt river is about 400 m wide and peak ebb and flood velocities in the river channel are higher than 1m/s (Plancke et al., 2009). Wind-induced waves are negligible. Salinities range between 0.4 and 2.1 ppt (data http://www.scheldemonitor.be/ 25/11/2017).

3.3.2 Flow and sedimentation measurements

The vertical tide was measured using a pressure sensor recording water levels at the mudflat just in front of the main tidal creek every 30 seconds. The water levels were corrected for barometric pressure variations with a simultaneously deployed pressure sensor outside the marsh. We recorded the elevation of the sensor with a high-precision GPS (Trimble R4 RTK-GPS, vertical error <1.5 cm) to refer the water level measurements to the mean marsh platform elevation as measured by Temmerman et al. (2012).

We measured tidal flow and sedimentation patterns at different locations on the marsh surface. Tidal flows were measured in the creek (locations D and E in Fig. 3.1) and on the marsh platform (locations A, B and C in Fig. 3.1). In the creek, two high resolution acoustic Doppler velocity profilers (HR-ADCP, Nortek AS) were attached to the bottom of the creek and deployed upward-looking. On the marsh platform, three acoustic Doppler velocity meters (ADV, Nortek AS) measured three dimensional flow velocities at 12 cm above the marsh platform. One ADV was positioned near the riverside edge of the marsh, one near the edge of the main creek and one at the inner marsh platform (Fig. 3.1).

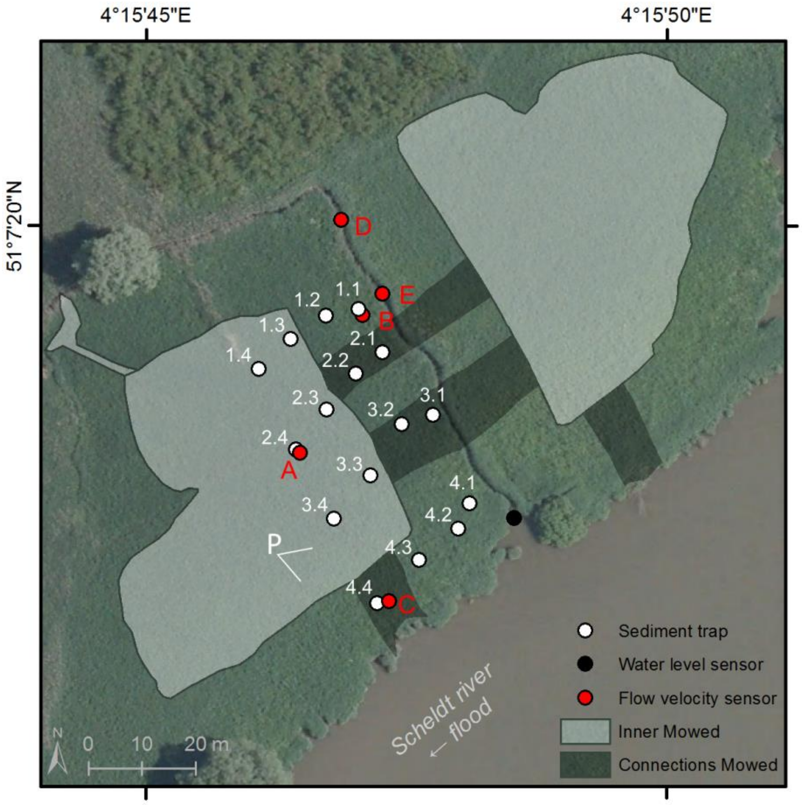

Figure 3.1: Overview of the study area with locations of flow velocity measurements (red dots labelled A-D), water level measurements (black dot), sediment traps (white dots labelled 1.1-4.4), and mowing patterns (different shades of green). P indicates the approximate location from which photo Fig. SI 3.1 was taken (see Supplementary Information).

During each tide, a sample of the flooding water was collected using a siphon sampler (1L bottle with siphon tubes which is filled when one of the tubes is submerged). The sample was taken at the creek inlet, at the average marsh elevation. The suspended sediment concentration from this flood water was determined by filtering and weighing pre-weighed filter papers.

Sediment deposition during single tides was measured on 16 spatially distributed, circular sediment traps (Fig. 3.1). The design and validation of the sediment traps is presented in detail in Schoelynck et al. (2015). In brief, they consist of PVC plates that are fixed to the sediment surface and that hold circular filter papers (diameter 0.2 m), onto which suspended sediment deposition takes place. As such, this method is a measure of sedimentation and resuspension of the deposited sediment, this method cannot measure net erosion. It is also possible that our thin (5 mm) plates disturbed the natural sedimentary environment. Nevertheless, this method is currently the best and most accurate method for determining sedimentation over single tides (Nolte et al., 2013; Schoelynck et al., 2015), and we only used the data for relative comparison between different mowing patterns (see section 3.3.4). Filter papers were pre-weighed and labelled before applying them in the field. After each high tide, the traps were collected, filter papers dried and weighted again to determine the weight of the sediment deposited on the filter papers.

3.3.3 Mowing patterns

Marsh vegetation die-off usually starts at the interior parts of marshes at a distance from channels and creeks (Stevenson et al., 1985; DeLaune et al., 1994; Morton et al., 2003; Schepers et al., 2017). These vegetation-loss areas may subsequently become larger and may connect to the tidal channel network (Redfield, 1972; Kearney et al., 1988; Schepers et al., 2017). In our experiment we simulated the effect of such subsequent stages of marsh loss by consecutive reed mowing, after which only short stems of maximum 0.1 m high remained. We first measured flow velocities and sedimentation rates on the fully vegetated marsh (no mowing applied) during October-November 2013. Before the measurements in December 2013, the inner marsh platform was mowed (Fig. 3.1, light green areas**)**, leaving a vegetated buffer of 15 m along both sides of the creek and along the riverside edge of the marsh. As a second stage, vegetation-free connections were mown from the river and the creek to the interior marsh (Fig. 3.1, dark green areas). Measurements with this pattern were carried out in February and March 2014 (Table SI 3.1). Since we could not finish our measurements in one season, the fully mowed stage was measured at the end of the next winter season in February 2015 (mowing occurs in winter for reed and target plant species conservation such as spring-flowering *Caltha palustris subsp. araneosa, Leucojum aestivum*). All mowing patterns were applied symmetrically at both sides of the tidal creek (Fig. 3.1).

3.3.4 Data processing and analysis

In order to compare flow measurements between similar tides, we only considered tides with similar high water levels between 0.40 and 0.75 m above the average marsh platform elevation and with very similar shapes of the hydrograph (Fig. 3.2, Table SI 3.1).

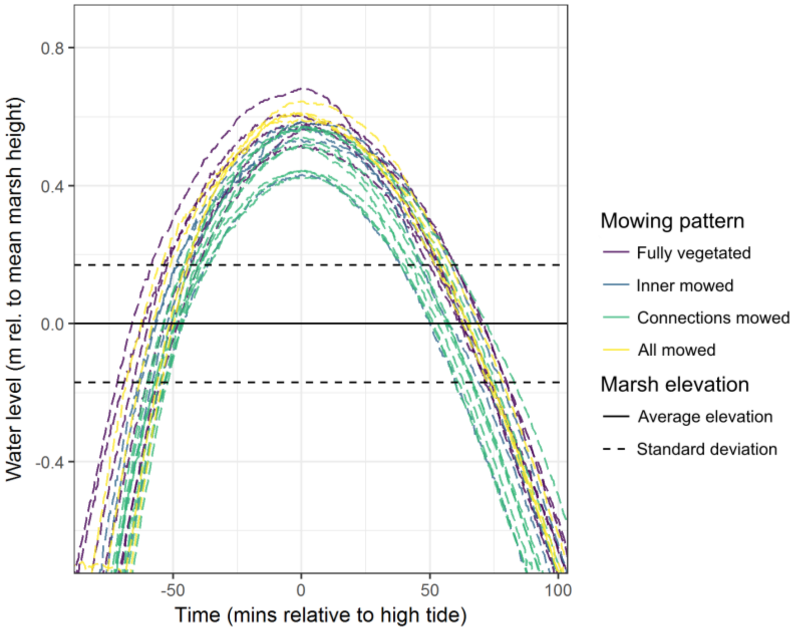

Figure 3.2: selected tides for the flow velocity measurements, with very similar shapes of the hydrographs and with high water levels between 0.40 and 0.75 m above mean marsh elevation.

Creek HR-ADCP data were filtered to retain only data with amplitudes higher than 50 counts (1 count is approximately 0.4 dB) and correlations higher than 50 %. We corrected the ADCP data for velocity folding. This happens when the recorded velocity is higher than the predefined velocity range resulting in a phase shift and incorrect velocity estimates (Franca and Lemmin, 2006). This is a known issue and can easily be corrected by adding or subtracting two times the maximum velocity (for example see Fig. SI 3.2). After correction, beam velocities of the extended velocity cell (0.6 m above the HR-ADCP's) were transformed to the resulting horizontal flow velocity vector and flow direction at one measurement cell about 50 cm below the marsh surface surrounding the creek. Marsh ADV measurements with amplitudes lower than 90 counts and correlations lower than 70 % were discarded. All HR-ADCP and ADV velocities were combined per minute and averaged by tidal stage (flood: 2h before high water, ebb: 2h after high water) and by mowing pattern. The moment of high water was determined by the water level sensor at the river. Velocity differences between the mowing patterns were tested by the non-parametric pairwise Wilcoxon rank sum test with Bonferroni correction ($\alpha=0.05$).

Due to rain splashing we could not use the sediment traps of several tides (Table SI 1). Since sediment deposition is determined by incoming suspended sediment concentration, which varies significantly even on short temporal timescales (Fettweis et al., 1998; Temmerman et al., 2003b; Butzeck et al., 2014), we quantified for each tide the relative spatial sedimentation patterns, calculated as the ratio between the local sedimentation rate measured at a point and the spatially averaged sedimentation rate of the 16 sediment traps. Hence a relative sedimentation rate of, for instance, 0.5 means that the sedimentation rate measured at that location was halve of the spatially averaged sedimentation rate for that tide. As such we could compare the spatial sedimentation patterns in between different tides.

All analysis were performed in R (R Core Team, 2017).

3.4 Results and discussion

3.4.1 Effect of mowing on flow velocities

In the first mowing stage the inner marsh vegetation is removed, with a 15 m wide buffer of tall reed vegetation still present along the creek and river (Fig. 3.1). This vegetation removal increased the average flood velocity (Fig. 3.3A, 3.3B) although the flow velocities remain however very small (<0.05 ms^{-1}) and comparable with the situation with the fully vegetated marshes. This confirms our initial hypothesis that inner marsh removal did not drastically alter the flow velocities, most likely due to the 15 m vegetation buffer surrounding the creek and the river.

Removing parts of the vegetation bordering the creek and the river significantly impacts the flow patterns on the marsh surface. The mowed connections become preferential flow routes for flood and ebb flows (Fig. 3.4), with a drastic increase in both ebb and flood velocities (Fig. 3.3B, 3.3C). The increased flow velocity can be explained by the friction induced by the remaining vegetation that channels the flow within the mowed corridor. This effect of flow routing and flow acceleration towards bare surfaces around and in between vegetated surfaces is well-known and has been shown by field, flume and modeling studies (e.g. (Temmerman et al., 2005; Vandenbruwaene et al., 2011, 2015; Bouma et al., 2013; Meire et al., 2014). Within the remaining vegetation, no significant changes in flow velocity or direction were detected (Fig. 3.3B, 3.3C, Fig. SI 3.3). This observation supports previous studies showing the strong reduction of flow velocities in marsh vegetation (Allen, 2000; Christiansen et al., 2000;

Friedrichs and Perry, 2001; Bouma et al., 2005a; Leonard and Croft, 2006; Mudd et al., 2010). (Leonard and Croft, 2006) for example found that 50% of the mean velocity and turbulent kinetic energy was dissipated within 5 m of a *Spartina alterniflora* canopy.

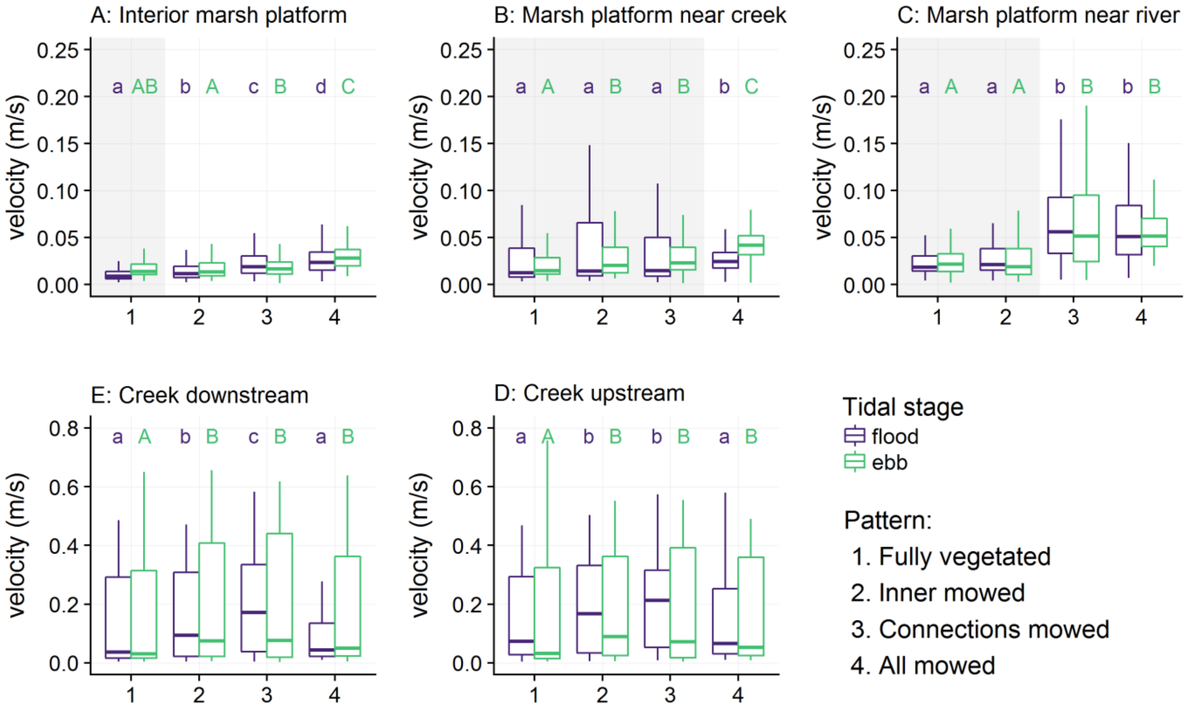

Figure 3.3: Boxplots of 1-minute averaged flow velocities for the different mowing patterns (1-4) and the different measurement locations (see Fig. 1): A : inner marsh platform, B : on the platform near the main creek, C : on the platform near the river, D : in the creek most inland, E : in the creek closest to the river. Significantly different velocities between different mowing patterns have different letters (pairwise Wilcoxon rank sum test with Bonferroni correction, α= 0.05). Light grey background means that the measuring point is within the vegetation.

Complete mowing increases the platform velocities even more (Fig. 3A), and is clearly visible in the flow direction diagrams (Fig. 4). Near the marsh edge close to the river, flood and ebb flows are no longer channeled through the narrow corridors but now the water flows over the platform edge as sheet flow, repeatedly changing its direction which results in a broad range of flow directions. At location B near the creek, the flood flow no longer originates from the nearby creek, but instead the sheet flow from the riverside marsh edge redirects the flow towards the creek in the same direction as the ebb flow (Fig. 4). A previous study at the same location with complete vegetation removal did not measure this sheet flow towards the creek (Temmerman et al., 2012), although mowing changed the flow velocity to a more parallel direction with the creek. The discrepancy between this study and our study is probably a result of different calculation methods as (Temmerman et al., 2012) only extracted a short 15 minute interval at beginning of flood and end of ebb to calculate flow directions, while here we show the flow directions over the whole duration of the tidal cycles. Our measurements provides empirical evidence for the model work by Temmerman et al. (2005); Ashall et al. (2016); Wu et al. (2017), showing that a vegetation-less marsh platform is flooded by sheet flow from the marsh edge instead of flooding via tidal creeks.

The different mowing patterns appear to have little effect on the overall flow velocity in the tidal creek. A fully vegetated platform and a fully mowed platform even result in similar creek velocities (Fig. 3.3D, 3.3E, Fig. SI 3.4D, SI 3.4E). Our creek velocities are comparable to the values reported in the earlier studies for situation with the fully vegetated platform (up to 0.6 ms^{-1}), but do not decrease with vegetation removal. This is contradictory to a previous field experiment (Temmerman et al., 2012) and modeling study (Temmerman et al., 2005) that show a reduction in creek flow velocity when marsh vegetation is removed. Ashall et al. (2016) however, found also minor influence of vegetation on creek velocities in their model study.

3.4.2 Effect of mowing on sedimentation patterns

Suspended sediment concentrations varied considerably between season and tide (ranging between 65 and 325 mg/L), so we calculated the relative spatial sedimentation, the sedimentation relative to the average of all sediment traps per tide (see Methods section).

The different mowing patterns clearly have an effect on the sedimentation patterns (Fig. 3.5, Fig. SI 3.4), but some trends are not consistent among the measurement locations. The most evident effect is the difference between the fully vegetated and the fully mowed marsh (Fig. 3.5). In the fully vegetated marsh (purple bars in Fig. 3.5), the points bordering the river and tidal creek receive more than the average sediment deposition on the marsh. The inner marsh locations clearly receive less sediment input. When the vegetation is removed, a contrasting spatial sedimentation pattern is apparent (yellow bars in Fig. 3.5): relative sedimentation rates are lower on the levee locations bordering the creek and river, which is associated with more sediment that is delivered to and deposited on the inner marsh. At first sight this may be counterintuitive, since vegetation loss is commonly expected to result in lower sediment deposition rates (Mudd et al., 2010; Baustian et al., 2012). Our flow velocity measurements can explain this remarkable result. With a fully vegetated marsh, vegetation-induced friction concentrates the tidal flow through the creek, from which it perpendicularly flows over the marsh (Fig. 3.4). Flow velocities are reduced within the first meters and most sediment is deposited or captured by the marsh vegetation (Leonard and Croft, 2006; Mudd et al., 2010). Without vegetation, the marsh is mainly flooded as sheet flow from the marsh edge and the sediment is transported further onto the marsh platform before it is deposited. Hence complete vegetation loss does not simply lead to reduced sedimentation rates all over the marsh platform, but in a spatial redistribution of the sediment, resulting in locally reduced sedimentation rates close to channels and creeks, and locally increased sedimentation rates in inner marsh areas at farther distance from channels and creeks. This is in agreement with earlier modelling (Temmerman et al., 2005) and is shown now for the first time with experimental evidence.

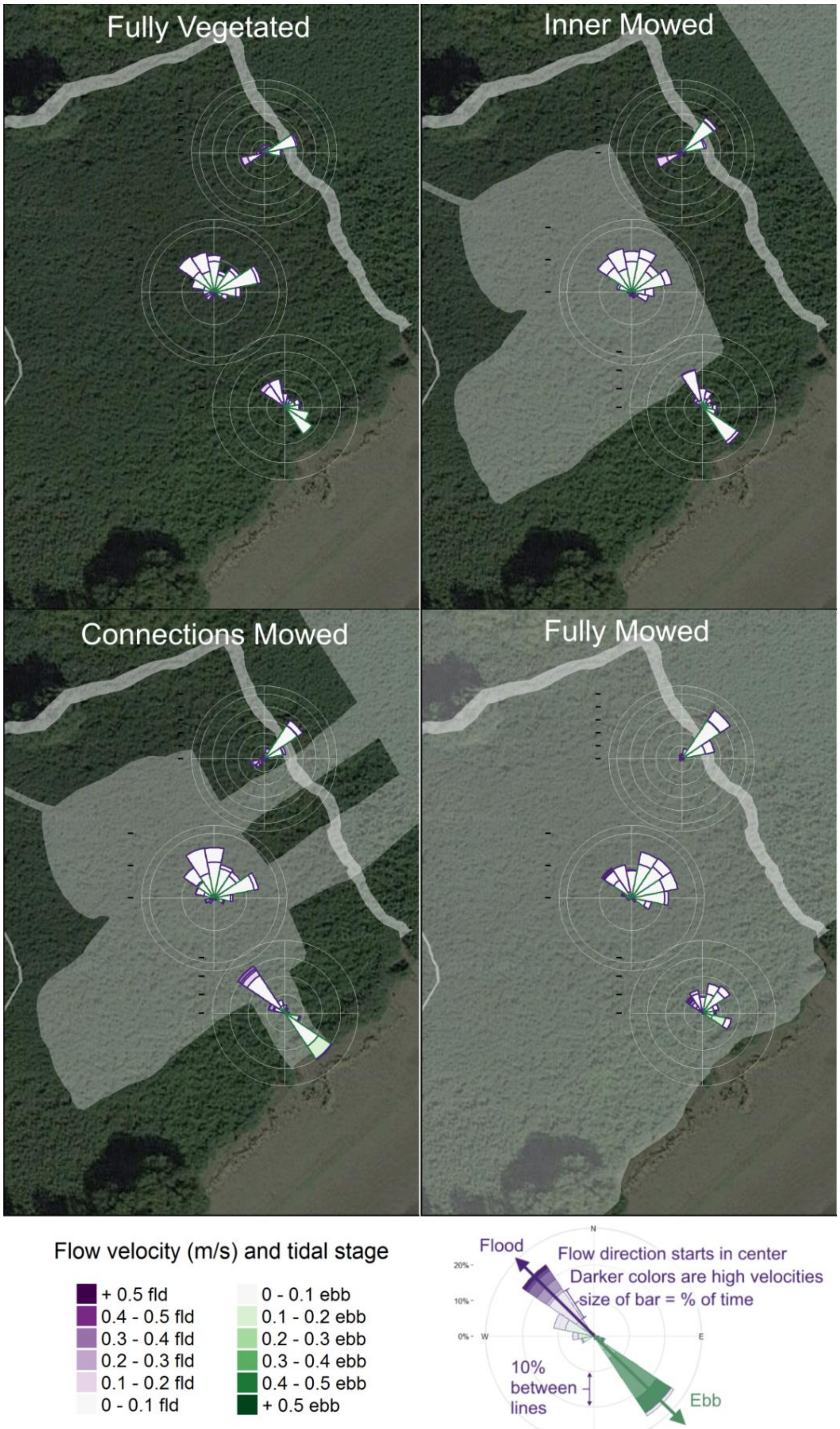

Figure 3.4: Flow velocities and directions on the marsh change with different mowing patterns. When the marsh is fully mowed, the flood direction and the ebb direction near the creek flow in the same direction, from the marsh surface towards the tidal creek. Mowing connections to the channels increases the flow in these corridors, complete removal of the vegetation changes the flow directions further. See Fig. SI 3.3 for the all the points and all the patterns.

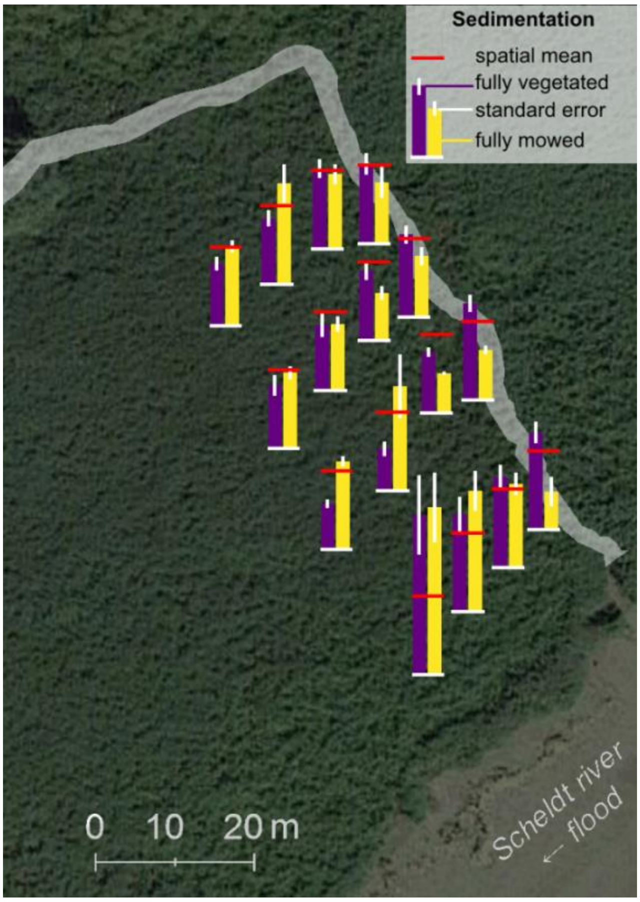

Figure 3.5: Spatial variation of short-term sedimentation, compared to the average sedimentation each tide (= red line) between the fully vegetated (pattern 1, purple) and fully mown (pattern 4, yellow) marsh. White vertical lines represent standard errors. More sediment is deposited close to the river/creek compared to the inner marsh with full vegetation, while the opposite is true for the fully mowed marsh.

Intermediate vegetation removal (i.e. inner marsh mowed, connections mowed) has inconsistent effects on spatial sedimentation patterns (Fig. SI 3.4). The situation is especially complex for pattern 3 with mowing of the inner marsh vegetation and corridors connecting to the creek and river. This is probably a result of complex flow routing patterns and is difficult to explain because we do not know for every location if the water and sediment supplied to that location was routed through the mown corridors or through the remaining vegetation. In any case, comparison of the fully vegetated versus fully mown situations, clearly demonstrates that flow and sediment routing through vegetated portions of the marsh platform results in higher sedimentation rates closer to the creek and lower sedimentation rates at farther distance from the creek, while vice versa, flow and sediment routing over non-vegetated marsh surfaces results in reduced sedimentation rates close the creek and increased sediment supply and deposition farther away from the creek.

3.4.3 Implications for marsh die-off areas

Our findings may have important implications for areas that experience large-scale marsh loss, even though one should bear in mind that these areas are usually micro-tidal and lacking sufficient suspended sediment import whereas our study site is macro-tidal with suspended sediment concentrations up to 300 mgL^{-1}(Temmerman et al., 2003b).

Our results demonstrate on the one hand vegetation-induced sedimentation close to creeks or river channels, and on the other hand an increase in sediment deposition further into the marsh platform with vegetation loss (Fig. 3.5). Tidal marsh vegetation die-off typically starts at inner marsh basins (Redfield, 1972; Kearney et al., 1988; Schepers et al., 2017), so these areas need sediment import and deposition to keep up with sea level rise. Our results suggest that complete vegetation die-off might facilitate the transport and deposition of sediments on inner marsh parts after which marsh plants could re-establish. However, complete vegetation die-off over large marsh areas is not an instantaneous process, and typically marsh vegetation is able to survive longer on the higher elevated and better drained levees bordering creeks and channels (e.g. Schepers et al., 2017). Our study suggests that these vegetated buffers alongside creeks and channels hinder the transport of sediments to the bare inner marsh parts. Once these inner marsh parts get connected to the channel network, and in areas with sufficient sediment import, die-off areas may indeed recover after sediment infilling (Redfield, 1972; Wilson et al., 2010, 2014; Elschot et al., 2017). Winter mowing of vegetation on the levees bordering creeks and channels could be a proper management tool increasing vegetation recovery potentials of inner marshes.

On the marsh platform, removal and connections in the vegetation canopy increase flow velocities significantly (Fig. 3.3B, 3.3C), but the flow velocities remain too low (<0.2 ms^{-1}) to enhance erosion from the marsh substrate. However, several researchers have suggested that the soil substrate in degraded, submerging marshes is unconsolidated, liquefied and easily eroded (Stevenson et al., 1985; Wilson et al., 2010; Day et al., 2011). This has also recently been measured by Schepers et al. (Chapter 6). Thus an increase in flow velocity might be able to export the sediment from the marsh platform, especially when the ebb velocities are higher than the flood velocities (Fig. 3.3B, 3.3C). Future research should verify these hypotheses by in-situ flow, erodibility and flux measurements in the areas that really experience large-scale marsh loss.

The ultimate recovery or degradation of the marshes depends on where and how much sediment is deposited on the marsh surface. Our experiments, with rather structured mowing patterns (Fig. 3.1), show the complexity of the resulting sediment transport and spatial sedimentation patterns. Deeper understanding of these sediment transport processes are needed to correctly predict which of the remaining marshes will be able to survive in submerging coastal areas, or to determine where to focus restoration efforts. Hence we conclude that future hydrodynamic and sediment transport modeling of marsh die-off areas could contribute to deeper insights in support of sustainable management of these stressed environments.

3.5 Conclusion

Our study reports on a large-scale field experiment where for the first time consecutive stages of coastal marsh loss are simulated by different mowing patterns. We show that initial vegetation loss in inner marshes, with vegetation still surrounding the tidal channels, resulted in limited increases of the flow velocities. However creating vegetation-less corridors between the bare inner marsh and channels lead locally to higher velocities over the unvegetated surfaces. The flow velocities in remaining vegetation patches remain unaffected. With complete vegetation removal, sheet flow over the marsh surface replaces flooding through the channels, although channel velocities are unaffected. Effects on spatial sedimentation patterns are complex, but our experiments clearly showed that complete vegetation loss does not simply lead to reduced sedimentation rates everywhere on the marsh platform. On the contrary complete vegetation loss results in redistributed sedimentation patterns, with locally reduced sedimentation rates at short distances from channels and increased sediment supply and increased sedimentation rates in inner marshes at farther distance from channels.

Acknowledgements

We would like to thank the early voluntary managers of the Kijkverdriet marsh for their efforts, the current conservator Joris Goossens and his team from the Flemish Agency for Nature and Forests for their assistance and support in mowing the marsh in different patterns. Thank you Tom de Dobbelaer for the valuable field support as part of his master's program. This project was financed by UA-BOF DOCPRO grant (to L.S. and S.T.) and the Research Foundation Flanders (FWO, PhD grants L.S., 11S9614N, 11S9616N).

3.6 References

Allen, J.R.L., 2000. Morphodynamics of Holocene salt marshes: A review sketch from the Atlantic and Southern North Sea coasts of Europe. Quat. Sci. Rev. 19, 1155–1231. doi:10.1016/S0277-3791(99)00034-7

Ashall, L.M., Mulligan, R.P., Van Proosdij, D., Poirier, E., 2016. Application and validation of a three-dimensional hydrodynamic model of a macrotidal salt marsh. Coast. Eng. 114, 35–46. doi:10.1016/j.coastaleng.2016.04.005

Baustian, J.J., Mendelssohn, I.A., Hester, M.W., 2012. Vegetation's importance in regulating surface elevation in a coastal salt marsh facing elevated rates of sea level rise. Glob. Chang. Biol. 18, 3377–3382. doi:10.1111/j.1365-2486.2012.02792.x

Bouma, T.J., De Vries, M.B., Low, E., Kusters, L., Herman, P.M.J., Tánczos, I.C., Temmerman, S., Hesselink, A., Meire, P., van Regenmortel, S., 2005a. Flow hydrodynamics on a mudflat and in salt marsh vegetation: identifying general relationships for habitat characterisations. Hydrobiologia 540, 259–274. doi:10.1007/s10750-004-7149-0

Bouma, T.J., De Vries, M.B., Low, E., Peralta, G., Tánczos, I.C., Van De Koppel, J., Herman, P.M.J., 2005b. Trade-offs related to ecosystem engineering: A case study on stiffness of emerging macrophytes. Ecology 86, 2187–2199. doi:10.1890/04-1588

Bouma, T.J., Temmerman, S., van Duren, L.A., Martini, E., Vandenbruwaene, W., Callaghan, D.P., Balke, T., Biermans, G., Klaassen, P.C., van Steeg, P., Dekker, F., van de Koppel, J., de Vries, M.B., Herman, P.M.J., 2013. Organism traits determine the strength of scale-dependent bio-geomorphic feedbacks: A flume study on three intertidal plant species. Geomorphology 180–181, 57–65. doi:10.1016/j.geomorph.2012.09.005

Bouma, T.J., Vries, M. De, Herman, P., 2010. Comparing Ecosystem Engineering Efficiency of 2 Plant Species With Contrasting Growth Strategies. Ecology 91, 100125221703024--100125221703024. doi:10.1890/09-0690

Butzeck, C., Eschenbach, A., Gröngröft, A., Hansen, K., Nolte, S., Jensen, K., 2014. Sediment Deposition and Accretion Rates in Tidal Marshes Are Highly Variable Along Estuarine Salinity and Flooding Gradients. Estuaries and Coasts 38, 434–450. doi:10.1007/s12237-014-9848-8

Christiansen, T., Wiberg, P.L., Milligan, T.G., 2000. Flow and Sediment Transport on a Tidal Salt Marsh Surface. Estuar. Coast. Shelf Sci. 50, 315–331. doi:10.1006/ecss.2000.0548

D'Alpaos, A., Lanzoni, S., Marani, M., Rinaldo, A., 2007. Landscape evolution in tidal embayments: Modeling the interplay of erosion, sedimentation, and vegetation dynamics. J. Geophys. Res. Earth Surf. 112, 1–17. doi:10.1029/2006JF000537

Day, J.W., Kemp, G.P., Reed, D.J., Cahoon, D.R., Boumans, R.M., Suhayda, J.M., Gambrell, R., 2011. Vegetation death and rapid loss of surface elevation in two contrasting Mississippi delta salt marshes: The role of sedimentation, autocompaction and sea-level rise. Ecol. Eng. 37, 229–240. doi:10.1016/j.ecoleng.2010.11.021

DeLaune, R.D., Nyman, J.A., Patrick, W.H., 1994. Peat collapse, ponding and wetland loss in a rapidly submerging coastal marsh. J. Coast. Res. 10, 1021–1030.

Duarte, C.M., Losada, I.J., Hendriks, I.E., Mazarrasa, I., Marbà, N., 2013. The role of coastal plant communities for climate change mitigation and adaptation. Nat. Clim. Chang. 3, 961–968. doi:10.1038/nclimate1970

Elschot, K., Vermeulen, A., Vandenbruwaene, W., Bakker, J.P., Bouma, T.J., Stahl, J., Castelijns, H., Temmerman, S., 2017. Top-down vs. bottom-up control on vegetation composition in a tidal marsh depends on scale. PLoS One 12, e0169960. doi:10.1371/journal.pone.0169960

Fettweis, M., Sas, M., Monbaliu, J., 1998. Seasonal, Neap-spring and Tidal Variation of Cohesive Sediment Concentration in the Scheldt Estuary, Belgium. Estuar. Coast. Shelf Sci. 47, 21–36. doi:10.1006/ecss.1998.0338

Franca, M.J., Lemmin, U., 2006. Eliminating velocity aliasing in acoustic Doppler velocity profiler data. Meas. Sci. Technol. 17, 313–322. doi:10.1088/0957-0233/17/2/012

Friedrichs, C.T., Perry, J.E., 2001. Tidal Salt Marsh Morphodynamics: A Synthesis. J. Coast. Res. SI 27, 7–37.

Gedan, K.B., Kirwan, M.L., Wolanski, E., Barbier, E.B., Silliman, B.R., 2011. The present and future role of coastal wetland vegetation in protecting shorelines: Answering recent challenges to the paradigm. Clim. Change 106, 7–29. doi:10.1007/s10584-010-0003-7

Kearney, M.S., Grace, R.E., Stevenson, J.C., 1988. Marsh Loss in Nanticoke Estuary, Chesapeake Bay. Geogr. Rev. 78, 205–220. doi:10.2307/214178

Kearney, W.S., Fagherazzi, S., 2016. Salt marsh vegetation promotes efficient tidal channel networks. Nat. Commun. 7, 12287.

doi:10.1038/ncomms12287

Kirwan, M.L., Guntenspergen, G.R., D'Alpaos, A., Morris, J.T., Mudd, S.M., Temmerman, S., 2010. Limits on the adaptability of coastal marshes to rising sea level. Geophys. Res. Lett. 37, L23401. doi:10.1029/2010GL045489

Kirwan, M.L., Langley, J.A., Guntenspergen, G.R., Megonigal, J.P., 2013. The impact of sea-level rise on organic matter decay rates in Chesapeake Bay brackish tidal marshes. Biogeosciences 10, 1869–1876.

Kirwan, M.L., Murray, A.B., 2007. A coupled geomorphic and ecological model of tidal marsh evolution. Proc. Natl. Acad. Sci. U. S. A. 104, 6118–6122. doi:10.1073/pnas.0700958104

Kirwan, M.L., Murray, A.B., Boyd, W.S., 2008. Temporary vegetation disturbance as an explanation for permanent loss of tidal wetlands. Geophys. Res. Lett. 35, L05403. doi:10.1029/2007GL032681

Kirwan, M.L., Temmerman, S., Skeehan, E.E., Guntenspergen, G.R., Fagherazzi, S., 2016. Overestimation of marsh vulnerability to sea level rise. Nat. Clim. Chang. 6, 253–260. doi:10.1038/nclimate2909

Leonard, L.A., Croft, A.L., 2006. The effect of standing biomass on flow velocity and turbulence in Spartina alterniflora canopies. Estuar. Coast. Shelf Sci. 69, 325–336. doi:10.1016/j.ecss.2006.05.004

Mariotti, G., 2016. Revisiting salt marsh resilience to sea level rise: Are ponds responsible for permanent land loss? J. Geophys. Res. Earth Surf. 121, 1391–1407. doi:10.1002/2016JF003900

McLeod, E., Chmura, G.L., Bouillon, S., Salm, R., Björk, M., Duarte, C.M., Lovelock, C.E., Schlesinger, W.H., Silliman, B.R., 2011. A blueprint for blue carbon: Toward an improved understanding of the role of vegetated coastal habitats in sequestering CO2. Front. Ecol. Environ. 9, 552–560. doi:10.1890/110004

Meire, D.W.S.A., Kondziolka, J.M., Nepf, H.M., 2014. Interaction between neighboring vegetation patches: Impact on flow and deposition. Water Resour. Res. 50, 3809–3825. doi:10.1002/2013WR015070

Millette, T.L., Argow, B.A., Marcano, E., Hayward, C., Hopkinson, C.S., Valentine, V., 2010. Integration of Multitemporal Multispectral Remote Sensing with LIDAR and GIS. J. Coast. Res. 265, 809–816. doi:10.2112/JCOASTRES-D-09-00101.1

Möller, I., 2006. Quantifying saltmarsh vegetation and its effect on wave height dissipation: Results from a UK East coast saltmarsh. Estuar. Coast. Shelf Sci. 69, 337–351. doi:10.1016/j.ecss.2006.05.003

Möller, I., Kudella, M., Rupprecht, F., Spencer, T., Paul, M., van Wesenbeeck, B.K., Wolters, G., Jensen, K., Bouma, T.J., Miranda-Lange, M., Schimmels, S., 2014. Wave attenuation over coastal salt marshes under storm surge conditions. Nat. Geosci. 7, 727–731. doi:10.1038/ngeo2251

Morton, R.A., Tiling, G., Ferina, N.F., 2003. Causes of hot-spot wetland loss in the Mississippi delta plain. Environ. Geosci. 10, 71–80. doi:10.1306/eg100202007

Mudd, S.M., D'Alpaos, A., Morris, J.T., 2010. How does vegetation affect sedimentation on tidal marshes? Investigating particle capture and hydrodynamic controls on biologically mediated sedimentation. J. Geophys. Res. 115, F03029. doi:10.1029/2009JF001566

Nardin, W., Edmonds, D.A., Fagherazzi, S., 2016. Influence of vegetation on spatial patterns of sediment deposition in deltaic islands during flood. Adv. Water Resour. 93, 236–248. doi:10.1016/j.advwatres.2016.01.001

Neumeier, U., Amos, C.L., 2006. The influence of vegetation on turbulence and flow velocities in European salt-marshes. Sedimentology 53, 259–277. doi:10.1111/j.1365-3091.2006.00772.x

Nolte, S., Koppenaal, E.C., Esselink, P., Dijkema, K.S., Schuerch, M., De Groot, a. V., Bakker, J.P., Temmerman, S., 2013. Measuring sedimentation in tidal marshes: A review on methods and their applicability in biogeomorphological studies. J. Coast. Conserv. 17, 301–325. doi:10.1007/s11852-013-0238-3

Perillo, G.M.E., Ripley, M.D., Piccolo, M.C., Dyer, K.R., 1996. The Formation of Tidal Creeks in a Salt Marsh : New Evidence from the Loyola Bay Salt Marsh, Rio Gallegos Estuary, Argentina. Mangroves Salt Marshes 1, 37–46. doi:10.1023/A:1025942111382

Plancke, Y., Ides, S., Mostaert, F., 2009. Vervolgstudie Inventarisatie en historische analyse van slikken en schorren langs de Zeeschelde: Verkennende vlottermetingen Ballooi en Notelaer. Versie 2_0. WL Rapport.

R Core Team, 2017. R: A Language and Environment for Statistical Computing, Vienna, Austria.

Redfield, A.C., 1972. Development of a New England Salt Marsh. Ecol. Monogr. 42, 201–237. doi:10.2307/1942263

Schepers, L., Kirwan, M., Guntenspergen, G., Temmerman, S., 2017. Spatio-temporal development of vegetation die-off in a submerging coastal marsh. Limnol. Oceanogr.

62, 137–150. doi:10.1002/lno.10381

Schoelynck, J., Oosterlee, L., De Groote, T., Maris, T., Struyf, E., Meire, P., Temmerman, S., 2015. Design and evaluation of a multifunctional plate sediment trap suitable for subaqueous and floodplain environments. Ecohydrology 8, 286–293. doi:10.1002/eco.1507

Sheehan, M.R., Ellison, J.C., 2015. Tidal marsh erosion and accretion trends following invasive species removal, Tamar Estuary, Tasmania. Estuar. Coast. Shelf Sci. 164, 46–55. doi:10.1016/j.ecss.2015.06.013

Silliman, B.R., van de Koppel, J., McCoy, M.W., Diller, J., Kasozi, G.N., Earl, K., Adams, P.N., Zimmerman, A.R., 2012. Degradation and resilience in Louisiana salt marshes after the BP-Deepwater Horizon oil spill. Proc. Natl. Acad. Sci. 109, 11234–11239. doi:10.1073/pnas.1204922109

Smolders, S., Plancke, Y., Ides, S., Meire, P., Temmerman, S., 2015. Role of intertidal wetlands for tidal and storm tide attenuation along a confined estuary: a model study. Nat. Hazards Earth Syst. Sci. 15, 1659–1675. doi:10.5194/nhess-15-1659-2015

Stark, J., Van Oyen, T., Meire, P., Temmerman, S., 2015. Observations of tidal and storm surge attenuation in a large tidal marsh. Limnol. Oceanogr. 60, 1371–1381. doi:10.1002/lno.10104

Stevenson, J.C., Kearney, M.S., Pendleton, E.C., 1985. Sedimentation and erosion in a Chesapeake Bay brackish marsh system. Mar. Geol. 67, 213–235. doi:10.1016/0025-3227(85)90093-3

Temmerman, S., Bouma, T.J., Govers, G., Wang, Z.B., De Vries, M.B., Herman, P.M.J., 2005. Impact of vegetation on flow routing and sedimentation patterns: Three-dimensional modeling for a tidal marsh. J. Geophys. Res. Earth Surf. 110, 1–18. doi:10.1029/2005JF000301

Temmerman, S., Bouma, T.J., van de Koppel, J., van der Wal, D., De Vries, M.B., Herman, P.M.J., 2007. Vegetation causes channel erosion in a tidal landscape. Geology 35, 631–634. doi:10.1130/G23502A.1

Temmerman, S., Govers, G., Meire, P., Wartel, S., 2003a. Modelling long-term tidal marsh growth under changing tidal conditions and suspended sediment concentrations, Scheldt estuary, Belgium. Mar. Geol. 193, 151–169. doi:10.1016/S0025-3227(02)00642-4

Temmerman, S., Govers, G., Wartel, S., Meire, P., 2003b. Spatial and temporal factors controlling short-term sedimentation in a salt and freshwater tidal marsh, Scheldt estuary, Belgium, SW Netherlands. Earth Surf. Process. Landforms 28, 739–755. doi:10.1002/esp.495

Temmerman, S., Moonen, P., Schoelynck, J., Govers, G., Bouma, T.J., 2012. Impact of vegetation die-off on spatial flow patterns over a tidal marsh. Geophys. Res. Lett. 39, 1–5. doi:10.1029/2011GL050502

Vandenbruwaene, W., Bouma, T.J., Meire, P., Temmerman, S., 2013. Bio-geomorphic effects on tidal channel evolution: Impact of vegetation establishment and tidal prism change. Earth Surf. Process. Landforms 38, 122–132. doi:10.1002/esp.3265

Vandenbruwaene, W., Schwarz, C., Bouma, T.J., Meire, P., Temmerman, S., 2015. Landscape-scale flow patterns over a vegetated tidal marsh and an unvegetated tidal flat: Implications for the landform properties of the intertidal floodplain. Geomorphology 231, 40–52. doi:10.1016/j.geomorph.2014.11.020

Vandenbruwaene, W., Temmerman, S., Bouma, T.J., Klaassen, P.C., De Vries, M.B., Callaghan, D.P., Van Steeg, P., Dekker, F., Van Duren, L.A., Martini, E., Balke, T., Biermans, G., Schoelynck, J., Meire, P., 2011. Flow interaction with dynamic vegetation patches: Implications for biogeomorphic evolution of a tidal landscape. J. Geophys. Res. Earth Surf. 116, 1–13. doi:10.1029/2010JF001788

Wilson, C.A., Hughes, Z.J., FitzGerald, D.M., Hopkinson, C.S., Valentine, V., Kolker, A.S., 2014. Saltmarsh pool and tidal creek morphodynamics: Dynamic equilibrium of northern latitude saltmarshes? Geomorphology 213, 99–115. doi:10.1016/j.geomorph.2014.01.002

Wilson, K.R., Kelley, J.T., Tanner, B.R., Belknap, D.F., 2010. Probing the Origins and Stratigraphic Signature of Salt Pools from North-Temperate Marshes in Maine, U.S.A. J. Coast. Res. 26, 1007–1026. doi:10.2112/JCOASTRES-D-10-00007.1

Wu, G., Li, H., Liang, B., Shi, F., Kirby, J.T., Mieras, R., 2017. Subgrid modeling of salt marsh hydrodynamics with effects of vegetation and vegetation zonation. Earth Surf. Process. Landforms 42, 1755–1768. doi:10.1002/esp.4121

Supplementary Information

Table SI 3.1: Overview of suitable tides for flow and sedimentation measurements

Local high water time	High water level	Vegetation Pattern	Flow	Sedimentation
10/9/2013 7:45	0.23	FullVeg		x
10/9/2013 20:09	0.25	FullVeg		x
10/10/2013 8:35	0.68	FullVeg	x	x
11/3/2013 15:56	0.58	FullVeg	x	x
11/4/2013 4:13	0.52	FullVeg	x	
11/4/2013 16:45	0.87	FullVeg		x
11/5/2013 4:57	0.77	FullVeg		x
11/5/2013 17:11	0.59	FullVeg	x	x
11/6/2013 5:29	0.83	FullVeg		x
11/6/2013 17:58	0.75	FullVeg		x
11/7/2013 6:20	0.61	FullVeg	x	
11/7/2013 18:39	0.56	FullVeg	x	
12/4/2013 17:08	0.53	InnerMowed	x	x
12/5/2013 5:36	0.35	InnerMowed		x
12/5/2013 17:58	0.37	InnerMowed		x
1/2/2014 16:48	0.59	InnerMowed		x
1/3/2014 5:14	0.43	InnerMowed	x	x
1/3/2014 17:35	0.57	InnerMowed	x	x
1/4/2014 18:22	0.59	InnerMowed	x	x
1/5/2014 6:37	0.79	InnerMowed		x
2/1/2014 17:15	0.57	ConnectionMowed	x	x
2/2/2014 18:10	0.44	ConnectionMowed	x	x
2/3/2014 6:33	0.51	ConnectionMowed	x	x
2/3/2014 19:01	0.38	ConnectionMowed		x
3/1/2014 16:27	0.58	ConnectionMowed	x	x
3/2/2014 4:43	0.52	ConnectionMowed	x	x
3/2/2014 17:14	0.39	ConnectionMowed		x
3/3/2014 17:48	0.56	ConnectionMowed	x	x
3/4/2014 6:11	0.54	ConnectionMowed	x	x
3/4/2014 18:39	0.44	ConnectionMowed	x	x
3/5/2014 6:54	0.43	ConnectionMowed	x	x
2/20/2015 17:27	0.61	FullyMowed	x	
2/21/2015 5:46	0.61	FullyMowed	x	x
2/21/2015 18:18	0.76	FullyMowed		x
2/22/2015 6:27	0.65	FullyMowed	x	x
2/22/2015 18:57	0.27	FullyMowed		x
2/23/2015 19:35	0.59	FullyMowed	x	x

*water level relative to the average marsh elevation

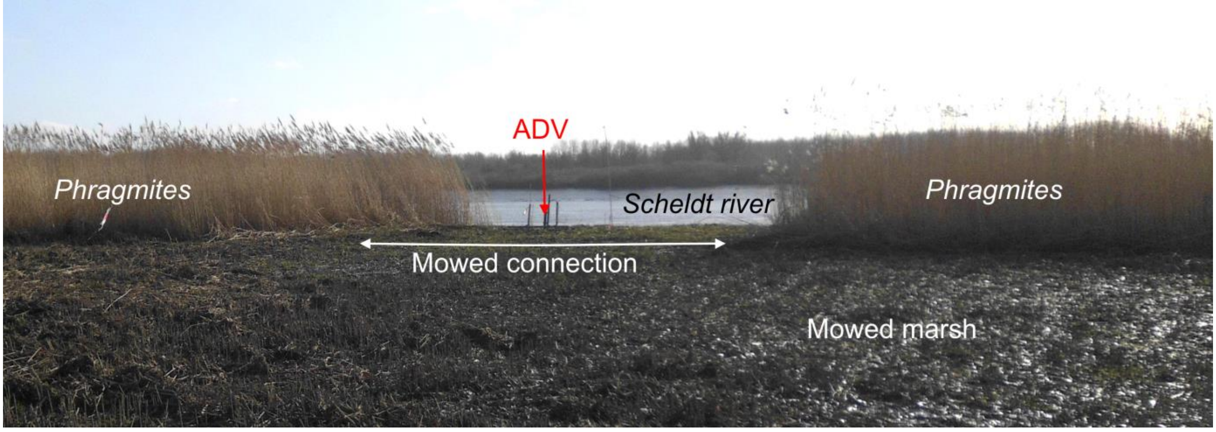

Figure SI 3.1: Field picture of the third mowing pattern with connections mowed. The approximate location of the photograph is shown in Fig. 3.1.

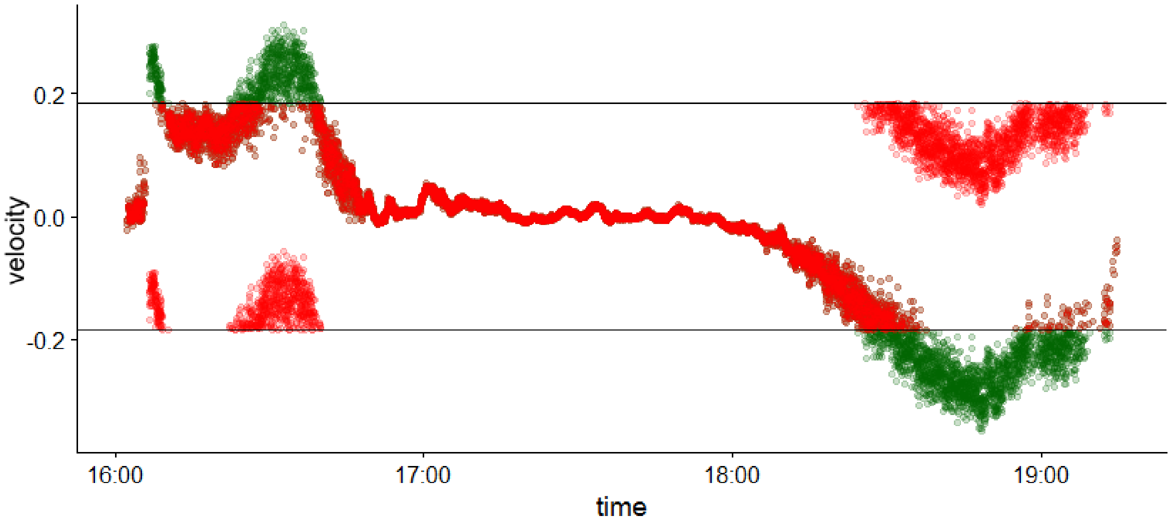

Figure SI 3.2 : Example of velocity folding (red), and the corrected measurements (green).

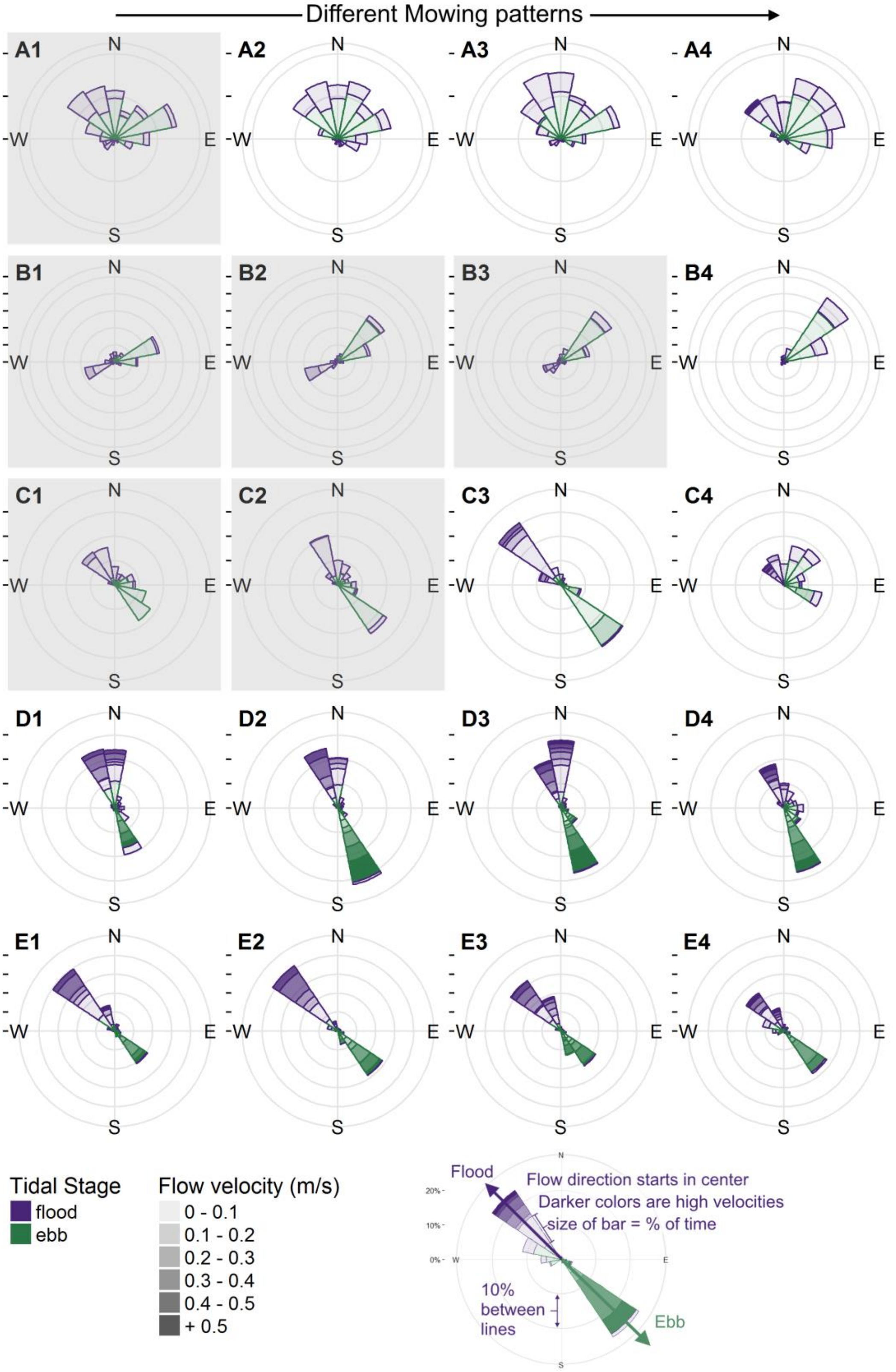

Figure SI 3.3: Flow velocities and directions of the different measurement locations. A: inner marsh platform, B: on the platform near the main creek, C: on the platform near the Scheldt River, D: in the creek most inland, E: in the creek closest to the river. Mowing patterns: 1: Fully Vegetated, 2: Inner marsh mowed, 3: Connections mowed, 4: All Mowed. Light grey background means that the measuring point is within the vegetation.

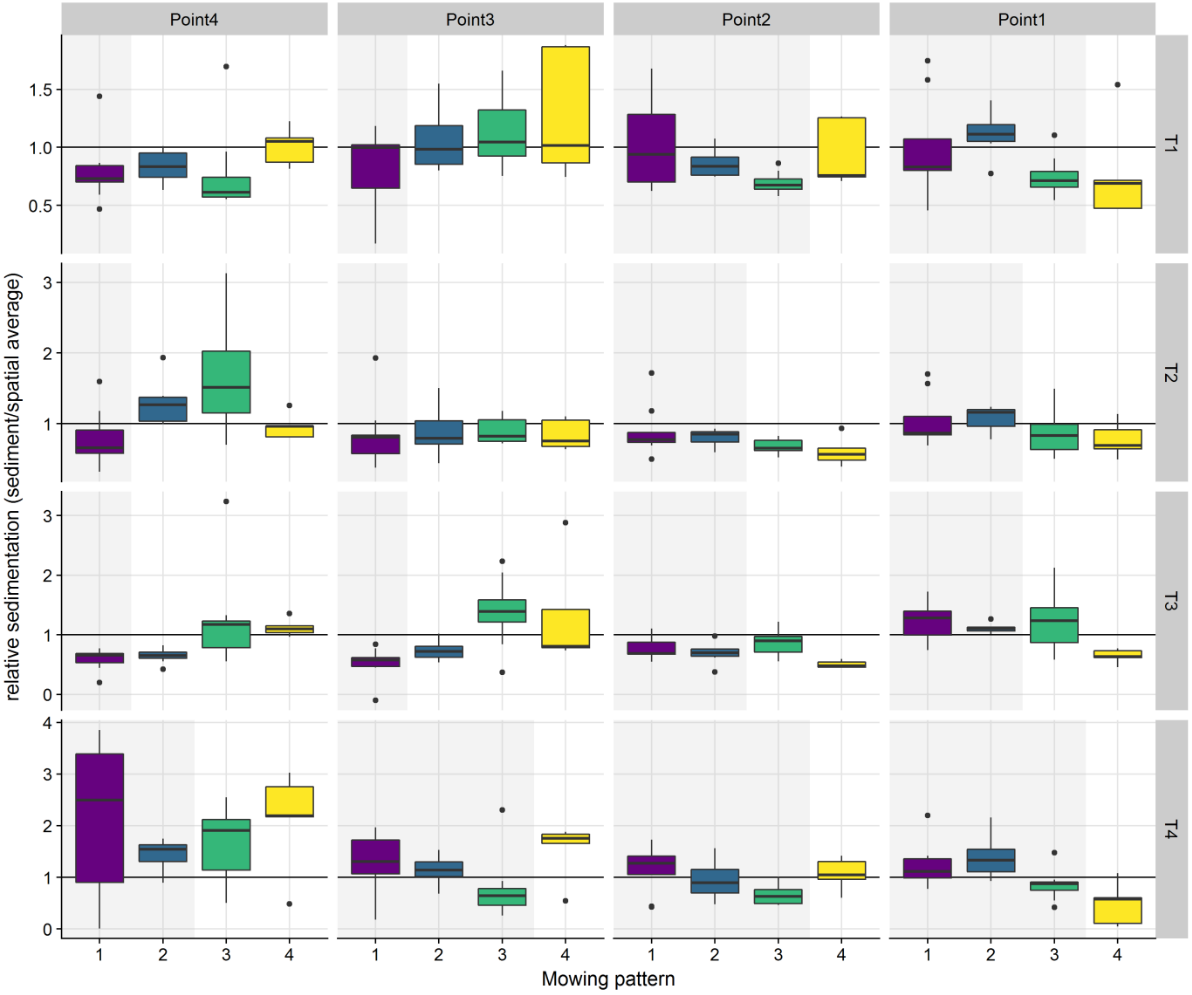

Figure SI 3.4: Spatial variation of short-term sedimentation patterns, given as deviation from the average sedimentation each tide (= 1). The lower row is positioned next to the Scheldt River, the last column is positioned next to the tidal creek. Light grey background means that this location was within the vegetation. (See Fig. 3.1 for an overview of the area).

4

Coastal marsh conversion to ponds induces irreversible elevation loss relative to sea level

Lennert Schepers, Patrick Brennand, Matthew Kirwan, Glenn Guntenspergen, Stijn Temmerman

Submitted to Nature Geoscience (under review)

4.1 Abstract

Coastal marsh conversion to ponds is a major contributor to loss of these highly valued ecosystems. Yet the mechanisms of ponding and potential recovery in the face of sea level rise are poorly understood. We studied a gradient of extensive marsh loss in an organogenic micro-tidal system (Blackwater River, Maryland, U.S.A.), and found that marsh conversion to ponds corresponds to a shift between alternative stable elevation states. Ponds deepen with increasing width of tidal channels connecting ponds to the river, pointing at a previously unknown feedback mechanism for pond deepening, where expanding channels lead to enhanced tidal export of eroded pond bottom material. Pond elevations also decrease with increasing pond size, consistent with previous work identifying a positive feedback between wind-wave erosion and pond size. These two positive feedbacks, coupled with observations of bimodal elevation distributions and sharp topographic boundaries between interior ponds and the marsh platform indicate that these two geomorphic features occupy alternative elevation states. Together, these results imply that marsh loss by pond formation is nearly irreversible once pond deepening exceeds a critical level, and hence sustainable marsh management should focus on conserving remaining habitat before it may be permanently lost.

4.2 Introduction

Although many coastal marshes have the capacity to sustain themselves in response to sea level rise, they are disappearing on large scales and converting to bare tidal flats or open water in several areas around the world (Kirwan et al., 2016). Marsh conversion to interior ponds is considered an important mechanism of coastal marsh loss, particularly where sediment supply and tidal range are very low (e.g. (Kearney et al., 1988; Penland et al., 2000; Morton et al., 2003; Mariotti and Fagherazzi, 2013; Mariotti, 2016), with large implications for the loss of highly valued ecosystem services, such as protection against storm impacts (Temmerman et al., 2013; Möller et al., 2014; Stark et al., 2015), nursery habitat for fisheries (Barbier et al., 2011), and storage of soil carbon (McLeod et al., 2011; Duarte et al., 2013).

We hypothesize that shifts from marshes to open water ponds can be considered as catastrophic shifts between alternative stable geomorphic states within the larger coastal marsh ecosystem. If true, this would have the important implication that marsh conversion to ponds is very hard to reverse, as shifts between alternative stable states are typically irreversible because each state is sustained by positive feedback mechanisms that provide long-term stability (Scheffer et al., 2001; Moffett and Gorelick, 2016). Marshes have indeed been identified as one stable state of intertidal landforms (Fagherazzi et al., 2006; Marani et al., 2010; Wang and Temmerman, 2013; van Belzen et al., 2017), as they are known to maintain their elevation relative to rising sea level by feedbacks between tidal inundation and accretion of mineral and organic sediments (Morris et al., 2002; Temmerman et al., 2004; Kirwan and Megonigal, 2013). However, it's unknown if marsh ponds are an alternative, low elevated state. Previous work suggests that positive feedbacks such as collapse and disintegration of underlying soil organic matter after initial vegetation die-off may reinforce the pond state (Delaune and Pezeshki, 1994; van Huissteden and van de Plassche, 1998; Day et al., 2011). Furthermore, modeling and aerial image analysis suggest that ponds expand by wind-wave erosion after they reach a critical size (Mariotti, 2016; Ortiz et al., 2017). However, expanding ponds may recover when they intersect a tidal channel and when drainage and sediment infilling promotes the recovery of marsh vegetation (Redfield, 1972; Perillo et al., 1996; Wilson et al., 2009, 2010, 2014; Millette et al., 2010). Hence, we do not currently understand whether ponds represent an alternative stable state, and we lack field data on elevation changes after marsh conversion to ponds, necessary to understand whether marsh collapse is irreversible.

Here, we report the results of a field study along the extensive Blackwater River marshes (Maryland, USA; 38°24' N, 76°40' W, Fig. 4.1), where relative sea level rise rates are 3-4 times the global average(Sallenger et al., 2012) and widespread marsh loss is well documented by aerial pictures for about the past century (Schepers et al. 2017, Chapter 2). We made 1121 measurements of marsh and pond bottom elevation along 15 km of transects in marshes at five stages of marsh degradation. These stages are situated along a gradient of marsh loss, i.e. a spatial gradient from intact to completely degraded marshes (Schepers et al., 2017)(Fig. 4.1 & Fig. SI 4.1). We identify erosion through connecting channels as a new mechanism for pond deepening, and show that topographic characteristics of marshes and ponds are consistent with alternative states, suggesting that reversal of pond expansion is unlikely in these rapidly deteriorating marshes.

4.3 Methods

4.3.1 Study area

The Blackwater marshes (Maryland, USA; 38°24’ N, 76°40’ W, Fig. 4.1) are organogenic, micro-tidal marshes centered around the Blackwater River that discharges into Fishing Bay, an embayment of the Chesapeake Bay. Previous research showed that the marshes are being converted to open water areas at least since the 1930s (Stevenson et al., 1985; Schepers et al., 2017). More than 2000 ha or 51 % of the 1938 marsh extent has been lost within the Blackwater National Wildlife Refuge (approximately Field sties 3-5) (Stevenson et al., 1985; Scott et al., 2009). There is a spatial gradient in marsh loss from Southeast to Northwest along the Blackwater River, from intact marshes close to Fishing Bay, to increasing pond surface area with increasing distance from Fishing Bay, up to Lake Blackwater, a vast open water area that consisted of marshes back in the 1930s (Fig. 4.1, Fig. SI 4.1). Marsh loss has been attributed to insufficient surface accretion (on average 1.7-3.6 mm yr-1 (Stevenson et al. 1985)) compared to relative sea level rise (currently 3.69 mm yr-1 nearby in Cambridge, MD, (NOAA station 8571892, http://tidesandcurrents.noaa.gov/sltrends, 10/21/2016), disturbance by invasive Nutria (*Myocastor coypus*) (Stevenson et al., 1985; Kendrot, 2011) and lateral erosion of the ponds (Stevenson et al., 1985; Ganju et al., 2013).

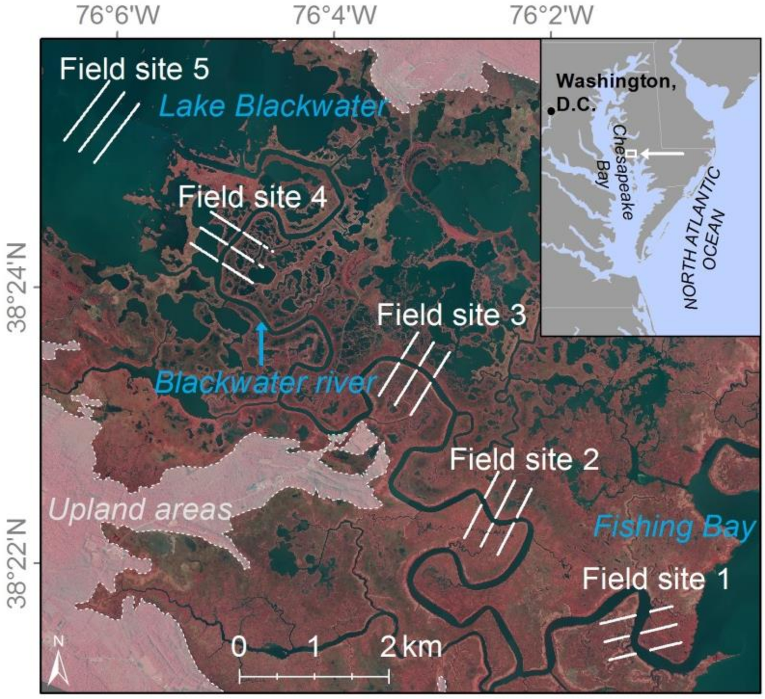

Figure 4.1: Aerial image of the Blackwater Marshes. From lower right corner to upper left corner of the image (i.e. in upstream direction along the Blackwater River) marshes are changing from high marsh vegetation cover (reddish color) close to the Fishing Bay (SE-corner) to increasing open water areas (dark color) in upstream direction, and ultimately to Lake Blackwater (NW-corner). White lines indicate GPS measurement points. White shaded areas with dashed outlines are no marshes but upland areas. Inset: Location of the Blackwater marshes along the Chesapeake Bay (white rectangle)

4.3.2 Soil elevation measurements

We selected five field sites along the marsh die-off gradient: one in the relatively intact marshes, one in the area with complete marsh degradation into open water, and three intermediate sites (Fig. 4.1). At each field site, three parallel marsh transects of 1000 m length (each 250 m apart) that straddle the Blackwater River were generated (see Fig. 4.1) and points were selected with a 10 m interval along the transects by using a GIS system (ArcGIS 10.3, ESRI). We located each point in the field and recorded the elevation relative to the North American Vertical Datum of 1988 (NAVD88) with a high-precision GPS (Trimble R8 RTK-GPS, vertical error <2 cm, at site 5 vertical error < 4.5 cm). If a point location was unvegetated and inundated, we attached a transparent plate (surface area 80 cm^2) underneath the GPS rod to prevent sinking in the soft bottom. Points located in tidal channels were not included in the analyses. At the degraded site 5, points located in the 1938 channel were also excluded. For each site, the NAVD88 elevations were recalculated to elevations relative to local mean sea level as measured by water level loggers (see next section). The non-parametric Wilcoxon rank-sum statistic (Mann-Whitney U) was used to test the elevation differences between marshes and ponds for each field site (α=0.05).

Additional topographic measurements were performed at the transitions from vegetated marshes to unvegetated pond areas while tracing the transects. At these transitions, we measured two points on the vegetated marsh platform, one as close as possible to the pond edge and still in the marsh vegetation, and one point ca. 1 m from the pond edge. Similarly, two elevation points were recorded in the unvegetated pond areas, one as close as possible to the pond edge and one ca. one meter from the pond edge in the pond. Horizontal distances between these points were calculated from the point coordinates (horizontal error <2 cm) and subsequently the slope (elevation change divided by horizontal distance) was calculated in between subsequent marsh points, pond points, and for the transition from marshes to ponds. The slope differences between these three morphological units were tested with the non-parametric pairwise Wilcoxon rank sum test with Bonferroni correction (α=0.05).

4.3.3 Water level measurements

Water levels were measured every 15 min at each field site from August 14 to October 29, 2014. Pressure transducers (Hobo U20L-02, Onset, MA, USA) were deployed in a PVC stilling tube at the river bank and the elevation of each sensor was recorded with a high-precision GPS (see previous paragraph) to refer the water level data to the NAVD88 vertical datum after local atmospheric pressure compensation. Tidal characteristics (including mean high water level, mean low water level, mean semi-diurnal tidal range, relation between elevation and inundation time (in %)) for each field site were calculated with the Tides-package in R (Cox and Schepers, 2017).

4.3.4 Environmental variables as potential controls on soil elevation

We studied the influence of several environmental variables on marsh surface elevation and pond bottom elevation. Most of the considered environmental variables were derived from an aerial image of 2010 classified into vegetated marsh areas, ponds and the Blackwater River (Chapter 2). To examine how marsh and pond elevations varied along the marsh loss gradient, we calculated the river length from the middle of each field site to the mouth of the Blackwater River. This variable accounts for several potential large-scale environmental differences between the field sites such as differences in tidal range and sediment availability, which both are known to decrease with increasing upstream distance along the Blackwater river (Ganju et al. 2013, tidal range see previous section).

To test if marsh surface elevation is related to distance from open water, we calculated the Euclidean distance of each marsh point to the Blackwater River, to secondary channels that are directly connected with the Blackwater River, and to inner marsh ponds.

To test if pond bottom elevation is related to the degree of connectivity between the pond and the Blackwater River, we measured the minimum width of the channel connecting each pond with the Blackwater River, and the distance of this connection to the Blackwater River. The minimum width for each connecting channel was calculated as the double of the minimum distance from the centerline (the middle of the connecting channel) to the channel banks. Ponds that were not connected received value zero. The connection distance was defined as the minimum travel distance from each pond point to the Blackwater River along secondary channels or water bodies. To include unconnected ponds in the analysis, the connection distance was categorized in four classes: not connected, connection <2000 m, connection 2000-4000 m, and connection > 4000 m. These connected classes coincide with three modes in the distance distribution.

To study the potential effect of waves on pond bottom elevation, we estimated wind fetch length by calculating the distance of each pond point to the nearest vegetated marsh, and by averaging marsh-to-marsh distances along the four cardinal and intercardinal directions.

Finally we tested the effect of pond age on pond bottom elevation. We defined the minimum age of the pond points based on aerial images of 1938, 1981, 1995, 2006, 2010 and 2013. Our fieldwork was carried out in 2014, so the minimum age is 2014 subtracted by the year of the earliest aerial image on which the point was located in a pond.

4.3.5 Linear regression analysis

To test which environmental variables (see previous section) significantly influence the soil elevation, we fitted a linear regression model to explain the elevation of the vegetated marsh platform using 916 marsh elevation points. We started the marsh model selection with four calculated variables ((i) downstream river length to the river mouth, (ii) the Euclidean distance to the Blackwater River, (iii) distance to secondary channels that are directly connected with the Blackwater River and (iv) distance to inner marsh ponds). A second model was fitted with 692 pond points to explain the pond bottom elevations. The mean fetch length variable was omitted to avoid collinearity with distance to the nearest marsh. We started the pond model with five variables, (i) downstream river length to the river mouth, (ii) the (log) distance to the nearest marsh, (iii) minimum width and (iv) length of connecting channel and (v) the minimum pond age. Each of the two models started with a full model including all the variables, and performed a backward model selection until only significant variables were present in the model. For more details and for the results of the regression analysis, we refer to the Supporting Information.

4.3.6 Random Forest analysis

To strengthen our analysis, we performed a Random Forest analysis (Breiman, 2001), which is a robust, non-parametric statistical method that requires no distributional or functional assumptions of variables to the response variable. The technique uses 1000 individual regression trees to quantify the relationship between the environmental variables and the pond depth/marsh elevation. The outcome is a ranking of the most important environmental variables that determine the pond depth/marsh elevation. This is measured with the variance importance and the minimal depth of the variable. The variance importance gives the difference between the prediction error when the variable is noised up by randomly permuting its values, and the prediction error under the observed values. The Minimal depth considers how soon the variable is used for the first time in each decision tree, the sooner (lower depth value) the more important this variable is. This depth is averaged over all trees in the forest.

As input variables we used all environmental variables, including the mean fetch length that we omitted in the linear regression analysis. The coordinates were also included to account for the spatial autocorrelation. The results of the Random Forest analysis, which support our linear regression analysis, are discussed in Supplementary Information.

4.4 Results

4.4.1 Alternative states hinder marsh recovery

Several indicators, such as bimodality of the elevation distribution and sharp elevation transitions between one state and the other, both in space and time, point to alternative state behaviour of marshes and ponds.

A bimodal distribution of a key environmental variable is an indicator of alternative stable states, with each mode focusing around the equilibrium values that characterizes each state (Scheffer and Carpenter, 2003; Schröder et al., 2005). From Fig. 4.2 it is clear that bimodality of the elevation distribution indeed exists between marshes and interior open water ponds: at field site 1, with almost intact marshes and very few ponds, the marsh has a clear unimodal elevation distribution around 0.25 m (Fig. 4.2, all elevations are expressed relative to local mean sea level as measured with water level loggers at each field site, see Methods). At field sites two to five, which represent a gradient of increasing marsh loss and hence an increasing proportion of pond data (Table SI 6.1) and pond area (Schepers et al., 2017), the ponds are positioned lower and lower compared to the marshes. As a consequence, a bimodal elevation distribution develops, characterized by the separation of the elevation distributions of higher elevation, vegetated marshes from low elevation, unvegetated ponds, and a low occurrence of intermediate elevations (Figure 2). At all field sites, including the most intact, the ponds and marshes occupied a significantly different elevation ($p < 0.001$). However, it seems that an equilibrium elevation in the ponds is only reached at field site 5, Lake Blackwater, which has a mode at 1.2 m below mean sea level.

Another indicator of alternative stable states is a sharp spatial boundary between contrasting sites (Scheffer and Carpenter, 2003; Schröder et al., 2005). The transitions from the marsh platform to the pond bottom are steep (Fig. 4.3), with slopes typically exceeding 0.5. In contrast, slopes within the marshes and ponds are more gradual (typically $\sim$ 0.01) and not statistically different from each other (Fig. 4.3). Steep transitions or cliffs are also observed at marsh-tidal flat borders in other areas and interpreted there as indicative of bistable states (van de Koppel et al., 2005). In our study area, the pond cliffs probably emerge from the different feedback mechanisms between marshes and ponds: it's known that marshes maintain high elevations in the tidal frame by capturing sediment or building up organic matter (Mudd et al., 2010; Baustian et al., 2012; Temmerman et al., 2012), while ponds, lacking the vegetation-induced sedimentation feedback are unable to capture sediment and deepen by the collapse of the soil and root structure (Delaune and Pezeshki, 1994; van Huissteden and van de Plassche, 1998; Day et al., 2011), thus increasing the elevation deficit between marshes and ponds.

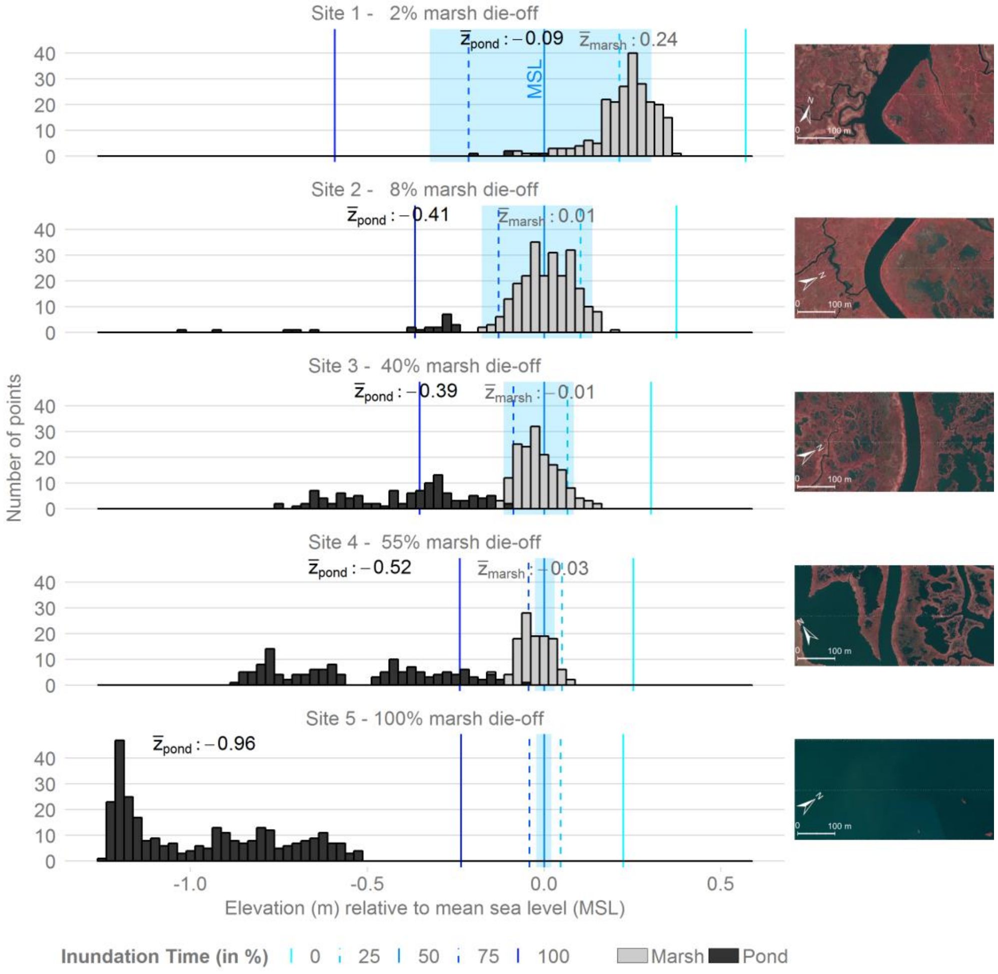

Figure 4.2: Elevation distribution of marsh (grey) and pond (black) points (marsh areas that converted to bare patches or open water without vegetation) for the five field sites (1-5) with increasing vegetation die-off in upstream direction along the Blackwater River. Histogram bin width is 0.025 m. Inundation time (in %) quartiles are visualized as blue vertical lines, the average semi-diurnal tidal range is visualized as a light blue rectangle. Aerial images of the sites are visualized on the right, with reddish colors representative for marsh vegetation and darker areas for open water

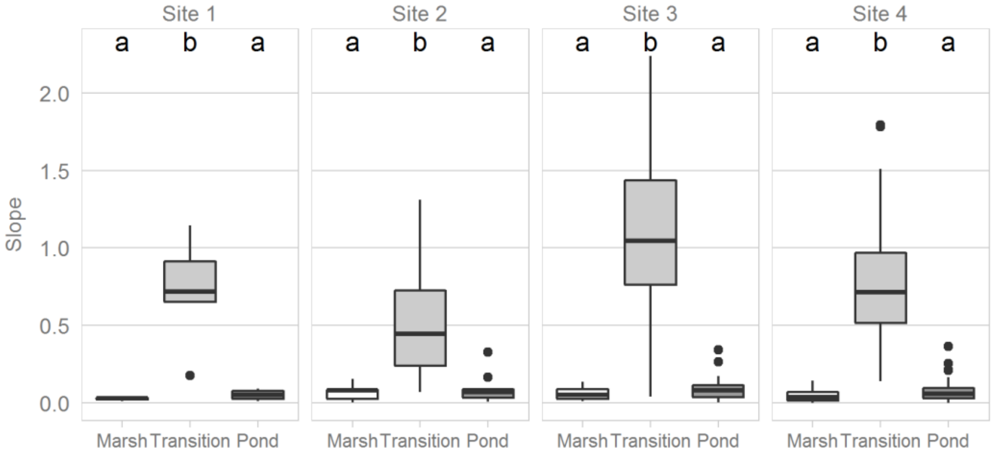

Figure 4.3: The Elevation differences in marshes or ponds are significantly more gentle than at the transition between the two states, as shown in boxplots of the slopes within marshes, the transition from marshes to ponds and within ponds for sites 1-4. Within each site, significantly different slopes are labelled with different letters (pairwise Wilcoxon rank sum test with Bonferroni correction, α= 0.05). At the transitions of site 3, two points with slope 2.8 and 6.8 are not visible on the Figure.

Our statistical model analysis, which identified significant factors explaining the pond depth, did not identify the minimum age of ponds as an explanatory variable (Fig. 4.4 right, Table SI6.3). This suggests that pond deepening is not a gradual process that continues at a steady rate, but is a process that evolves non-linearly with time. It corroborates with our above-discussed indicators of alternative stable states, as alternative states are predicted to show abrupt state transitions over time (Scheffer and Carpenter, 2003; Schröder et al., 2005; Wang and Temmerman, 2013). This implies that vegetation die-off is associated with positive feedback mechanisms leading to elevation loss and preserving an alternative, low elevation pond state (Fig. 4.2) from which recovery is unlikely.

Marsh elevation decreases along the marsh loss gradient and with increasing distance from the Blackwater River, reflecting gradients in tidal range and sediment availability (See SI for more details). Below we demonstrate the factors that control the pond elevations, which provide insights into the mechanisms involved in the elevation loss from marshes to ponds.

4.4.2 Ponds deepen by connecting to tidal system

The pond bottom elevation decreases with increasing marsh loss and hence increasing total pond surface area, from on average -0.41 to -0.52 m between field site 2 to 4, up to -0.96 m at field site 5 (Fig. 4.2), where all formerly existing marshes have converted to open water (Fig. SI4.1). Our statistical model indicates that the distance of points to the nearest marsh edge and the minimum width of channels connecting the ponds to the tidal channel network are the two statistically significant variables explaining the variations in pond bottom elevation (Fig. 4.4, Table SI 4.3).

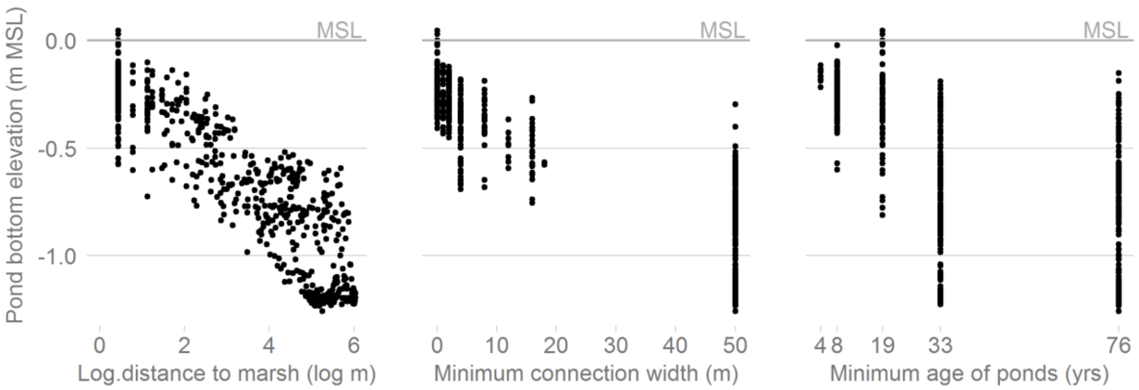

Figure 4.4: Pond bottom elevation (in m relative to mean sea level) with distance (logarithmically transformed) to the nearest marsh (left), the minimum width of the channel connecting ponds to the tidal channel network (middle), and minimum pond age (right figure). Multiple linear regression analysis (See SI for details) revealed that the distance to the marsh and the minimum width were significantly related to pond depth, minimum age was not significant.

Other factors, including downstream distance to river mouth, length of connecting channel and the minimum pond age did not have a significant effect on pond bottom elevation. The distance to the marsh edge is highly correlated with the mean fetch length (Pearson's r: 0.86), which is an important factor influencing wind wave erosion (Fagherazzi et al., 2006). Therefore our finding that the pond bottom elevations exponentially decrease with distance from the nearest marsh edge (Fig. 4.4, left) suggests increasing wave-driven erosion of the pond bottom. This finding implies that the maximum depth of a pond increases with the pond size, and hence corroborates with studies showing that as ponds expand over time, they become increasingly susceptible to pond bottom deepening by wind waves (Carniello et al., 2009; Mariotti and Fagherazzi, 2013). It seems that a stable equilibrium elevation is only reached at 1.20 m below mean sea level at Lake Blackwater. This stable pond bottom elevation might correspond to the depth of the pond at which the wind-induced wave shear stresses are too low for erosion (see e.g. Fagherazzi et al., 2006; Defina et al., 2007). However, when lateral erosion progresses, larger fetch lengths likely generate higher wave power which might continue to erode the pond bottom. Thus it seems that the pond state is in most of the areas still in transition to a (temporally) stable equilibrium depth.

Importantly, we identify the connection of ponds to the tidal channel system as a new mechanism for pond erosion, as we find that ponds get deeper with wider connecting channels (Fig. 4.4, middle). This may be explained as a wider connection would increase the tidal currents in the ponds and subsequently contribute to the erosion and export of the pond bottom sediment. One might argue that deeper ponds lead to wider channel dimensions by increasing the tidal prism (O'Brien, 1969; D'Alpaos et al., 2010; Vandenbruwaene et al., 2013). However, we note that in our study area ponds are continuously submerged (e.g. compare the tidal range with the pond elevations in Fig. 4.2), thus deeper ponds do not lead to larger tidal prisms and wider channels. Instead, we argue that the loose, liquefied pond soil material is very easily suspended and that a connection with the tidal channel system can export this suspended material out of the ponds. Measurements in these ponds show that pond soils are indeed very weak (Chapter 6). Also other studies have observed very loose pond bottom sediments that might be easily eroded by low energy currents (Stevenson et al., 1985; van

Huissteden and van de Plassche, 1998; Wilson et al., 2010; Day et al., 2011). Nyman et al. (1994) even indicate that mere exposure to pond water might be enough to suspend the highly organic, structurally weak soil below the living root zone. Hence, the connection of the pond with the tidal channels system is probably causing sediment export from the ponds, which decreases the elevation of the ponds and reinforces permanent marsh loss in the studied micro-tidal system.

The mechanism of pond deepening by tidal connections differs from previous work that focuses on wind driven erosion as the primary mechanism of pond expansion (Mariotti and Fagherazzi, 2013; Ortiz et al., 2017). Previous studies show that a connection with the tidal channel system drains ponds and thereby enables plant re-establishment, followed by fast sediment accretion (Redfield, 1972; Perillo et al., 1996; Wilson et al., 2009, 2010, 2014; Millette et al., 2010). Channel driven pond expansion and permanent marsh loss in our field sites 2-5 (Stevenson et al., 1985; Schepers et al., 2017) seems contradictory to these studies. We suggest the low tidal range of our site as a potential explanation for the different behavior, where a relatively small loss in elevation results in a large increase of tidal inundation time and hence increased stress for plant re-establishment (Kirwan and Guntenspergen, 2010; Kearney and Turner, 2016).

While our study highlights feedback mechanisms between pond bottom erosion, pond size and pond connection to the channel network, little is known on how initially small and unconnected ponds deepen and expand, i.e. before the identified feedback mechanisms start to play a role. It has been suggested that biochemical decomposition of the organic material at the bottom and edges of the ponds is the main driver of initial pond deepening and expansion (DeLaune et al., 1994; van Huissteden and van de Plassche, 1998). The fact that pond age is not a significant factor determining pond depth, also when only small (<100m), unconnected ponds are included in the regression model analysis (results not shown), suggests in any case that also the early stages of pond deepening occur non-linearly with time. Hence, identifying the drivers of initial pond deepening and expansion is an unresolved issue that merits further research.

4.4.3 Management implications

Our analyses suggest that marsh conversion to ponds is associated with a shift between alternative stable elevation states, which implies that the pond elevation loss occurs relatively rapidly up to a critically low state where reversal to the original marsh state is nearly impossible. We emphasize that this finding is specific to systems with a low tidal range, where a relatively small loss of elevation implies a high increase in tidal inundation time and hence stress to plant growth; while in systems with a high tidal range, the same magnitude of elevation loss results in a much smaller increase in tidal inundation time, and ponds may more easily recover (Redfield, 1972; Wilson et al., 2009, 2014). Nevertheless, microtidal marshes are the most vulnerable to sea level rise (Kirwan and Guntenspergen, 2010; Kearney and Turner, 2016), which make our findings especially relevant for ecosystem management. In these systems, developing indicators that foresee pending shifts between vegetated marsh and bare pond states is critical because state changes are not easily reversible. Thus, our finding that marshes and unvegetated ponds exist as alternative stable states suggest that it may be more efficient to manage towards maintaining existing habitat rather than to restore lost habitat.

Acknowledgements

This project was financed by an UA-BOF DOCPRO grant (to L.S. and S.T.), the Research Foundation Flanders (FWO, PhD grant L.S., 11S9614N, travel grants L.S. V428214N and S.T. K217414N), by the U.S. Geological Survey, Climate and Land-Use Research and Development Program (G.G.), by NSF GLD 1529245, NSF SEES 1426981, NSF LTER 1237733 (M.K.). We would like to thank the managers and biologists of the Blackwater National Wildlife Refuge for their assistance and valuable comments. We thank Erik Fransen and Joanna Horemans (UAntwerp) for their feedback and help with the statistical analysis. Any use of trade, product, or firm names is for descriptive purposes only and does not imply endorsement by the U.S. Government.

4.5 References

Barbier, E.B., Hacker, S.D., Kennedy, C., Koch, E.W., Stier, A.C., Silliman, B.R., 2011. The value of estuarine and coastal ecosystem services. Ecol. Monogr. 81, 169–193. doi:10.1890/10-1510.1

Baustian, J.J., Mendelssohn, I.A., Hester, M.W., 2012. Vegetation's importance in regulating surface elevation in a coastal salt marsh facing elevated rates of sea level rise. Glob. Chang. Biol. 18, 3377–3382. doi:10.1111/j.1365-2486.2012.02792.x

Breiman, L., 2001. Random Forests. Mach. Learn. 45, 5–32. doi:10.1017/CBO9781107415324.004

Carniello, L., Defina, A., D'Alpaos, L., 2009. Morphological evolution of the Venice lagoon: Evidence from the past and trend for the future. J. Geophys. Res. Earth Surf. 114, 1–10. doi:10.1029/2008JF001157

Cox, T., Schepers, L., 2017. Tides: Quasi-Periodic Time Series Characteristics. R package version 2.0. https://cran.r-project.org/web/packages/Tides.

D'Alpaos, A., Lanzoni, S., Marani, M., Rinaldo, A., 2010. On the tidal prism-channel area relations. J. Geophys. Res. Earth Surf. 115, 1–13. doi:10.1029/2008JF001243

Day, J.W., Kemp, G.P., Reed, D.J., Cahoon, D.R., Boumans, R.M., Suhayda, J.M., Gambrell, R., 2011. Vegetation death and rapid loss of surface elevation in two contrasting Mississippi delta salt marshes: The role of sedimentation, autocompaction and sea-level rise. Ecol. Eng. 37, 229–240. doi:10.1016/j.ecoleng.2010.11.021

Defina, A., Carniello, L., Fagherazzi, S., D'Alpaos, L., 2007. Self-organization of shallow basins in tidal flats and salt marshes. J. Geophys. Res. Earth Surf. 112, 1–11. doi:10.1029/2006JF000550

DeLaune, R.D., Nyman, J.A., Patrick, W.H., 1994. Peat collapse, ponding and wetland loss in a rapidly submerging coastal marsh. J. Coast. Res. 10, 1021–1030.

Delaune, R.D.D., Pezeshki, S.R.R., 1994. The Influence of Subsidence and Saltwater Intrusion on Coastal Marsh Stability:Louisiana Gulf Coast, U.S.A. J. Coast. Res. Sp.Issue 1, 77–89.

Duarte, C.M., Losada, I.J., Hendriks, I.E., Mazarrasa, I., Marbà, N., 2013. The role of coastal plant communities for climate change mitigation and adaptation. Nat. Clim. Chang. 3, 961–968. doi:10.1038/nclimate1970

Fagherazzi, S., Carniello, L., D'Alpaos, L., Defina, A., 2006. Critical bifurcation of shallow microtidal landforms in tidal flats and salt marshes. Proc. Natl. Acad. Sci. U. S. A. 103, 8337–8341. doi:10.1073/pnas.0508379103

Ganju, N.K., Nidzieko, N.J., Kirwan, M.L., 2013. Inferring tidal wetland stability from channel sediment fluxes: Observations and a conceptual model. J. Geophys. Res. Earth Surf. 118, 2045–2058. doi:10.1002/jgrf.20143

Kearney, M.S., Grace, R.E., Stevenson, J.C., 1988. Marsh Loss in Nanticoke Estuary, Chesapeake Bay. Geogr. Rev. 78, 205–220. doi:10.2307/214178

Kearney, M.S., Turner, R.E., 2016. Microtidal Marshes: Can These Widespread and Fragile Marshes Survive Increasing Climate–Sea Level Variability and Human Action? J. Coast. Res. 319, 686–699. doi:10.2112/JCOASTRES-D-15-00069.1

Kendrot, S.R., 2011. Restoration through eradication : protecting Chesapeake Bay marshlands from invasive nutria (Myocastor coypus), in: Veitch, C.R., Clout, M.N., Towns, D.R. (Eds.), Island Invasives: Eradication and Management. Proceedings of the International Conference on Island Invasives. Gland, Switzerland: IUCN and Auckland, New Zealand: CBB, pp. 313–319.

Kirwan, M.L., Guntenspergen, G.R., 2010. Influence of tidal range on the stability of coastal marshland. J. Geophys. Res. 115, F02009. doi:10.1029/2009JF001400

Kirwan, M.L., Megonigal, J.P., 2013. Tidal wetland stability in the face of human impacts and sea-level rise. Nature 504, 53–60. doi:10.1038/nature12856

Kirwan, M.L., Temmerman, S., Skeehan, E.E., Guntenspergen, G.R., Fagherazzi, S., 2016. Overestimation of marsh vulnerability to sea level rise. Nat. Clim. Chang. 6, 253–260. doi:10.1038/nclimate2909

Marani, M., D'Alpaos, A., Lanzoni, S., Carniello, L., Rinaldo, A., 2010. The importance of being coupled: Stable states and catastrophic shifts in tidal biomorphodynamics. J. Geophys. Res. Earth Surf. 115, 1–15. doi:10.1029/2009JF001600

Mariotti, G., 2016. Revisiting salt marsh resilience to sea level rise: Are ponds responsible for permanent land loss? J. Geophys. Res. Earth Surf. 121, 1391–1407. doi:10.1002/2016JF003900

Mariotti, G., Fagherazzi, S., 2013. Critical width of tidal flats triggers marsh collapse in the absence of sea-level rise. Proc. Natl. Acad. Sci. U. S. A. 110, 5353–5356. doi:10.1073/pnas.1219600110

McLeod, E., Chmura, G.L., Bouillon, S., Salm, R., Björk, M., Duarte, C.M., Lovelock, C.E., Schlesinger, W.H., Silliman, B.R., 2011. A blueprint for blue carbon: Toward an improved understanding of the role of vegetated coastal habitats in sequestering CO2. Front. Ecol. Environ. 9, 552–560. doi:10.1890/110004

Millette, T.L., Argow, B.A., Marcano, E., Hayward, C., Hopkinson, C.S., Valentine, V., 2010. Integration of Multitemporal Multispectral Remote Sensing with LIDAR and GIS. J. Coast. Res. 265, 809–816. doi:10.2112/JCOASTRES-D-09-00101.1

Moffett, K.B., Gorelick, S.M., 2016. Alternative stable states of tidal marsh vegetation patterns and channel complexity. Ecohydrology 9, 1639–1662. doi:10.1002/eco.1755

Möller, I., Kudella, M., Rupprecht, F., Spencer, T., Paul, M., van Wesenbeeck, B.K., Wolters, G., Jensen, K., Bouma, T.J., Miranda-Lange, M., Schimmels, S., 2014. Wave attenuation over coastal salt marshes under storm surge conditions. Nat. Geosci. 7, 727–731. doi:10.1038/ngeo2251

Morris, J.T., Sundareshwar, P. V., Nietch, C.T., Kjerfve, B., Cahoon, D.R., 2002. Responses of Coastal Wetlands to Rising Sea Level. Ecology 83, 2869–2877. doi:10.1890/0012-9658(2002)083[2869:ROCWTR]2.0.CO;2

Morton, R.A., Tiling, G., Ferina, N.F., 2003. Causes of hot-spot wetland loss in the Mississippi delta plain. Environ. Geosci. 10, 71–80. doi:10.1306/eg100202007

Mudd, S.M., D'Alpaos, A., Morris, J.T., 2010. How does vegetation affect sedimentation on tidal marshes? Investigating particle capture and hydrodynamic controls on biologically mediated sedimentation. J. Geophys. Res. 115, F03029. doi:10.1029/2009JF001566

Nyman, J.A., Carloss, M., DeLaune, R.D., Patrick, W.H., 1994. Erosion rather than plant dieback as the mechanism of marsh loss in an estuarine marsh. Earth Surf. Process. Landforms 19, 69–84. doi:10.1002/esp.3290190106

O'Brien, M.P., 1969. Equilibrium flow areas of tidal inlets on sandy coasts. J. Waterw. Harb. Div. 95, 43–52.

Ortiz, A.C., Roy, S., Edmonds, D.A., 2017. Land loss by pond expansion on the Mississippi River Delta Plain. Geophys. Res. Lett. 44, 3635–3642. doi:10.1002/2017GL073079

Penland, S., Wayne, L., Britsch, D., Williams, S.J., Beall, A.D., Butterworth, V., 2000. Geomorphic Classification of Coastal Land Loss between 1932 and 1990 in the Mississippi River Delta Plain, Southeastern Louisiana. USGS Open File Report 00-417. https://pubs.usgs.gov/of/2000/of00-417/.

Perillo, G.M.E., Ripley, M.D., Piccolo, M.C., Dyer, K.R., 1996. The Formation of Tidal Creeks in a Salt Marsh : New Evidence from the Loyola Bay Salt Marsh, Rio Gallegos Estuary, Argentina. Mangroves Salt Marshes 1, 37–46. doi:10.1023/A:1025942111382

Redfield, A.C., 1972. Development of a New England Salt Marsh. Ecol. Monogr. 42, 201–237. doi:10.2307/1942263

Sallenger, A.H., Doran, K.S., Howd, P.A., 2012. Hotspot of accelerated sea-level rise on the Atlantic coast of North America. Nat. Clim. Chang. 2, 884–888. doi:10.1038/nclimate1597

Scheffer, M., Carpenter, S., Foley, J. a, Folke, C., Walker, B., 2001. Catastrophic shifts in ecosystems. Nature 413, 591–596. doi:10.1038/35098000

Scheffer, M., Carpenter, S.R., 2003. Catastrophic regime shifts in ecosystems: Linking theory to observation. Trends Ecol. Evol. 18, 648–656. doi:10.1016/j.tree.2003.09.002

Schepers, L., Kirwan, M., Guntenspergen, G., Temmerman, S., 2017. Spatio-temporal development of vegetation die-off in a submerging coastal marsh. Limnol. Oceanogr. 62, 137–150. doi:10.1002/lno.10381

Schröder, A., Persson, L., De Roos, A.M., 2005. Direct experimental evidence for alternative stable states: a review. Oikos 110, 3–19. doi:10.1111/j.0030-1299.2005.13962.x

Scott, M., McDermott, L., Silva, E., Watson, E., 2009. Project report: Digital Spatial Data Capture of Marsh Extent in Blackwater National Wildlife Refuge, 1938 and 2006. Eastern Shore Regional GIS Cooperative, Salisbury University.

Stark, J., Van Oyen, T., Meire, P., Temmerman, S., 2015. Observations of tidal and storm surge attenuation in a large tidal marsh. Limnol. Oceanogr. 60, 1371–1381. doi:10.1002/lno.10104

Stevenson, J.C., Kearney, M.S., Pendleton, E.C., 1985. Sedimentation and erosion in a Chesapeake Bay brackish marsh system. Mar. Geol. 67, 213–235. doi:10.1016/0025-3227(85)90093-3

Temmerman, S., Govers, G., Wartel, S., Meire, P., 2004. Modelling estuarine variations in tidal marsh sedimentation: Response to changing sea level and suspended sediment concentrations. Mar. Geol. 212, 1–19. doi:10.1016/j.margeo.2004.10.021

Temmerman, S., Meire, P., Bouma, T.J., Herman, P.M.J., Ysebaert, T., De Vriend, H.J., 2013. Ecosystem-based coastal defence in the face of global change. Nature 504, 79–83. doi:10.1038/nature12859

Temmerman, S., Moonen, P., Schoelynck, J., Govers, G., Bouma, T.J., 2012. Impact of vegetation die-off on spatial flow patterns over a tidal marsh. Geophys. Res. Lett. 39, 1–5. doi:10.1029/2011GL050502

van Belzen, J., van de Koppel, J., Kirwan, M.L., van der Wal, D., Herman, P.M.J., Dakos, V., Kéfi, S., Scheffer, M., Guntenspergen, G.R., Bouma, T.J., 2017. Vegetation recovery in tidal marshes reveals critical slowing down under increased inundation. Nat. Commun. 8, 15811. doi:10.1038/ncomms15811

van de Koppel, J., van der Wal, D., Bakker, J.P., Herman, P.M.J., 2005. Self-Organization and Vegetation Collapse in Salt Marsh Ecosystems. Am. Nat. 165, E1–E12. doi:10.1086/426602

van Huissteden, J., van de Plassche, O., 1998. Sulphate reduction as a geomorphological agent in tidal marshes ("Great Marshes" at Barnstable, Cape Cod, USA). Earth Surf. Process. Landforms 23, 223–236. doi:10.1002/(SICI)1096-9837(199803)23:3<223::AID-ESP843>3.0.CO;2-I

Vandenbruwaene, W., Bouma, T.J., Meire, P., Temmerman, S., 2013. Bio-geomorphic effects on tidal channel evolution: Impact of vegetation establishment and tidal prism change. Earth Surf. Process. Landforms 38, 122–132. doi:10.1002/esp.3265

Wang, C., Temmerman, S., 2013. Does biogeomorphic feedback lead to abrupt shifts between alternative landscape states?: An empirical study on intertidal flats and marshes. J. Geophys. Res. Earth Surf. 118, 229–240. doi:10.1029/2012JF002474

Wilson, C.A., Hughes, Z.J., FitzGerald, D.M., Hopkinson, C.S., Valentine, V., Kolker, A.S., 2014. Saltmarsh pool and tidal creek morphodynamics: Dynamic equilibrium of northern latitude saltmarshes? Geomorphology 213, 99–115. doi:10.1016/j.geomorph.2014.01.002

Wilson, K.R., Kelley, J.T., Croitoru, A., Dionne, M., Belknap, D.F., Steneck, R., 2009. Stratigraphic and ecophysical characterizations of salt pools: Dynamic landforms of the Webhannet Salt Marsh, Wells, ME, USA. Estuaries and Coasts 32, 855–870. doi:10.1007/s12237-009-9203-7

Wilson, K.R., Kelley, J.T., Tanner, B.R., Belknap, D.F., 2010. Probing the Origins and Stratigraphic Signature of Salt Pools from North-Temperate Marshes in Maine, U.S.A. J. Coast. Res. 26, 1007–1026. doi:10.2112/JCOASTRES-D-10-00007.1

Supplementary Information Chapter 4

The spatial patterns of vegetation die-off in the Blackwater marshes

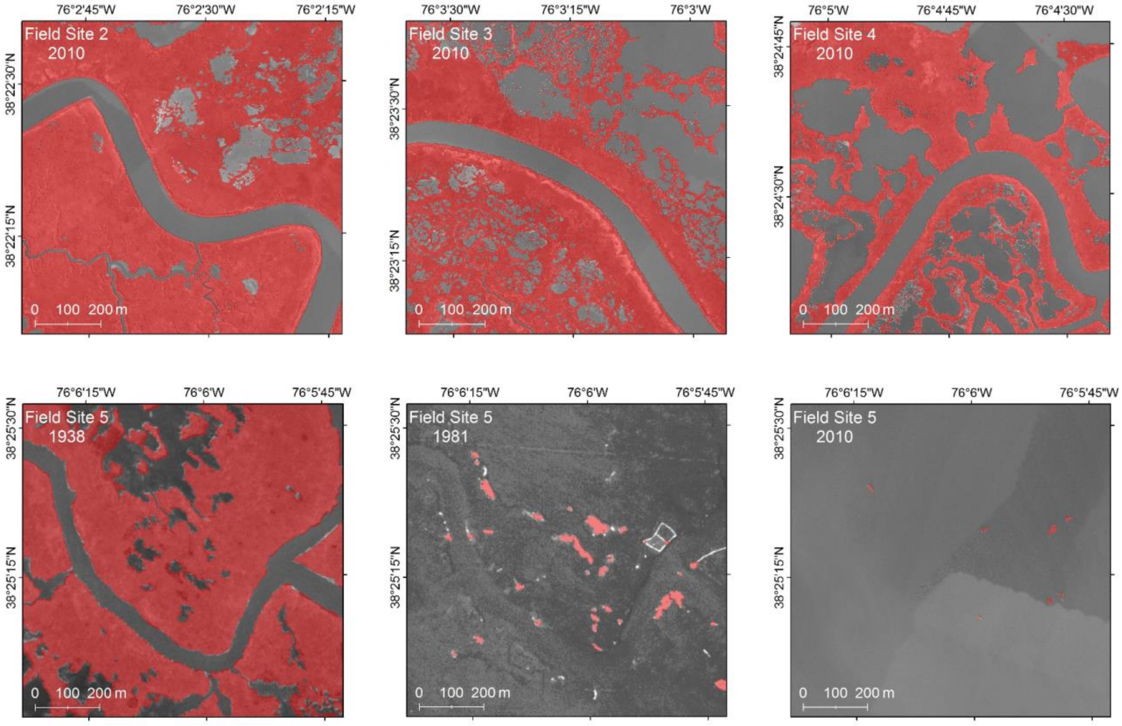

Figure SI 4.1: The spatial patterns of marsh loss. Top row: spatial pattern of marsh loss at field site 2, 3 and 4 with increasing marsh loss (see location on Fig. 4.1 in the main paper). Bottom row: also at field site 5 (Lake Blackwater), extensive marshes existed in the 1930s, but are now completely lost. Greyscale aerial images with marshes in red. For more information on the spatio-temporal patterns of marsh loss in this study area, see (Schepers et al., 2017)

Field data summary

Table SI 4.1: Number of regular transect points, mean elevation relative to local mean sea level (MSL, in m) and mean inundation time (in %) for marsh and pond points. Different letters in between brackets indicate significant differences between field sites (pairwise Wilcoxon Rank Sum Test with Bonferroni correction, α= 0.05)

	number of points (n)		**Mean Elevation (m rel. to MSL)**		**Mean Inundation Time (%)**	
	Pond	**Marsh**	**Pond**	**Marsh**	**Pond**	**Marsh**
Field site 1	5	222	-0.09 (a)	0.24 (A)	60.4 (a)	21.4 (A)
Field site 2	22	243	-0.41 (bc)	0.01 (B)	97.8 (b)	46.9 (B)
Field site 3	111	164	-0.39 (b)	-0.01 (C)	98.3 (b)	53.6 (C)
Field site 4	140	114	-0.52 (c)	-0.03 (C)	99.6 (c)	63.0 (D)
Field site 5	300	0	-0.96 (d)	/	100.0 (d)	/

Statistical analysis

All statistics were performed in R, version 3.2.2 (R Core Team, 2017). To test which environmental variables significantly influence the soil elevation, we fitted a linear regression model to explain the elevation of the vegetated marsh platform using 916 marsh elevation points (regular transects and additional measurements at the pond edges). The four calculated variables ((i) downstream river length to the river mouth, (ii) the Euclidean distance to the Blackwater River, (iii) distance to secondary channels that are directly connected with the Blackwater River and (iv) distance to inner marsh ponds) were not correlated. The Pearson's r was lower than 0.45 and the variance inflation factors (VIF, a measure for collinearity) was lower than 1.5 for all variables, hence we started the model selection with all four variables.

A second model was fitted to explain the pond bottom elevations. 692 pond points from regular transects and additional measurements at the pond edges were used, but points at Lake Blackwater that were located at the position of the former channel of the Blackwater River (as defined on old aerial images of 1938) were omitted. The nearest marsh distance data were log-transformed to obtain a linear relationship (Figure 4, left), needed in the linear regression model. The mean fetch length was highly correlated with the log-transform of distance to the nearest marsh (Pearson’s r: 0.86) and with the minimum width of the connecting channel (Pearson’s r: 0.89), so we left the mean fetch length out of the analyses to avoid collinearity. The minimum width of the connecting channel was also highly correlated to the log-transformed distance to the nearest marsh (Pearson’s r: 0.89), but the variance inflation factors (VIF, a measure for collinearity) were < 7 and the scatterplot revealed no relationship. Therefore, we started the model with five variables, (i) downstream river length to the river mouth, (ii) the (log) distance to the nearest marsh, (iii) minimum width and (iv) length of connecting channel and (v) the minimum pond age.

The spatial auto-correlation that was present in our data was modelled by an exponential correlation structure for both analyses. This correlation structure had produced the lowest Akaike Information Criterion (AIC, a measure for the goodness of fit and model complexity) values among a wide range of possible correlation structures. We started with a full model including all the variables, and performed a backward model selection by subsequently removing the least significant variable of likelihood ratio tests (a test to assess differences in model performance between including and excluding a variable), until only significant variables (α: 0.05) were present in the model. The models were fitted and validated following the procedures in (Zuur et al., 2009) with the gls (general linear model) function of the nlme-package in R (Pinheiro et al., 2016).

Decreasing marsh elevation

Marsh elevation decreases along the marsh loss gradient and with increasing distance from the Blackwater River, reflecting gradients in tidal range and sediment availability. The intact marshes (site 1) are highest and have a mean surface elevation of 0.24 m (Fig. 4.2). More degraded areas (site 2-4) have lower marsh elevations, with site 4 having a mean elevation of only -0.03 m (Fig. 4.2, Table SI 4.1). Lower marsh elevations along the marsh loss gradient might be partly explained by smaller tidal ranges (Fig. 4.2), which limit the elevation range that marshes can occupy ranges (Kirwan and Guntenspergen, 2010). Additionally, with increasing marsh loss, the elevations of remaining marshes also become lower relative to the tidal frame (Fig. 4.2), as reflected by an increase in mean inundation duration of the marshes from less than 25% at the intact marsh site (field site 1) to more than 60% at the most degraded site (field site 4, Table SI 4.1).

Decreasing marsh elevations in our system likely reflect decreasing sediment availability along the marsh loss gradient, where the most degraded marshes receive little external sediment, and experience a net export of sediment out of the system during frequent northwestern storms (Stevenson et al., 1985; Ganju et al., 2013, 2015). In contrast, the most intact marshes receive sediment from an external source (i.e. Fishing Bay) (Ganju et al., 2013), and may additionally receive sediment exported from the rapidly eroding marshes.

Our statistical model indicates that lower marsh elevations were also related to larger distances from the river (Table SI 4.2). This micro-topography is widely observed in other tidal marshes , where it originates from lower sediment deposition rates with larger distances from channels and marsh edges (Reed et al., 1999; Allen, 2000; Christiansen et al., 2000; Friedrichs and Perry, 2001; Temmerman et al., 2003; Moskalski and Sommerfield, 2012).

Table SI 4.2 : Output table of the final model explaining marsh elevation. Note that distance to (i) secondary channels and (ii) ponds were not significant variables (α: 0.05) and omitted from the regression model

Term	Value	p-value
intercept	0.40	<0.001
Downstream river length to mouth	-0.000013	<0.001
Distance to river	-0.00017	0.02

Ponds deepen by connecting to tidal system

For explanation, see main article.

Table SI 4.3 : Output table of the final model explaining pond depth. Note that (i) downstream distance to mouth, (ii) length of connecting channel and (iii) the minimum pond age were not significant variables (α: 0.05) and omitted from the regression model

Term	Value	p-value
intercept	-0.007	0.84
Log(Distance to nearest marsh)	-0.061	<0.001
Minimum width of connection	-0.010	<0.001

Random Forest analysis

The random forest analysis of the marsh elevation (1000 trees) explained 84.99 % of the variance. In decreasing order of importance, the primary predictors of the marsh elevation identified by our random forest model were the north and east coordinates. The distance to the river mouth (which represents the different field sites) was important in explaining variance (Fig. SI 4.3 left). However, this variable was usually considered late in the regression tree (Fig. SI 4.2 right). This is likely because the coordinates also can make a distinction between the different field sites. Other parameters were less important. In our linear regression analysis the distance to the river was also significant (p= 0.02), but the variance importance in our random forest model was rather low.

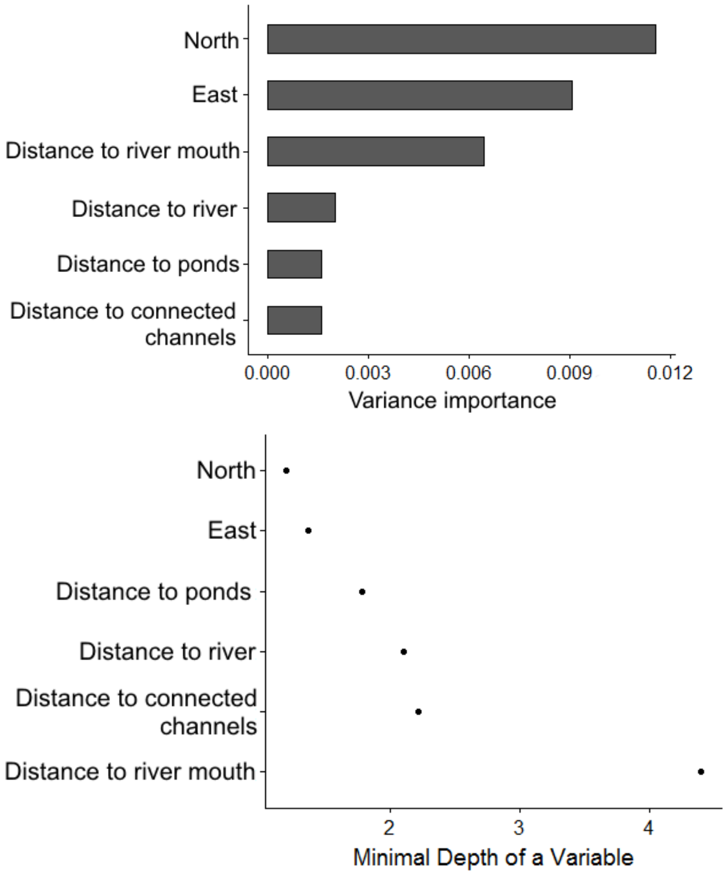

Figure SI 4.2: The variance importance (left) and Minimal depth (right) of the variables related to marsh elevation.

The random forest analysis of the pond depth (1000 trees) explained 96.66 % of the variance. The mean pond fetch length (~pond size), the minimum width as well as the distance to the nearest marsh were important predictors for the model. The minimum age was not important. This corresponds to our linear regression analysis.

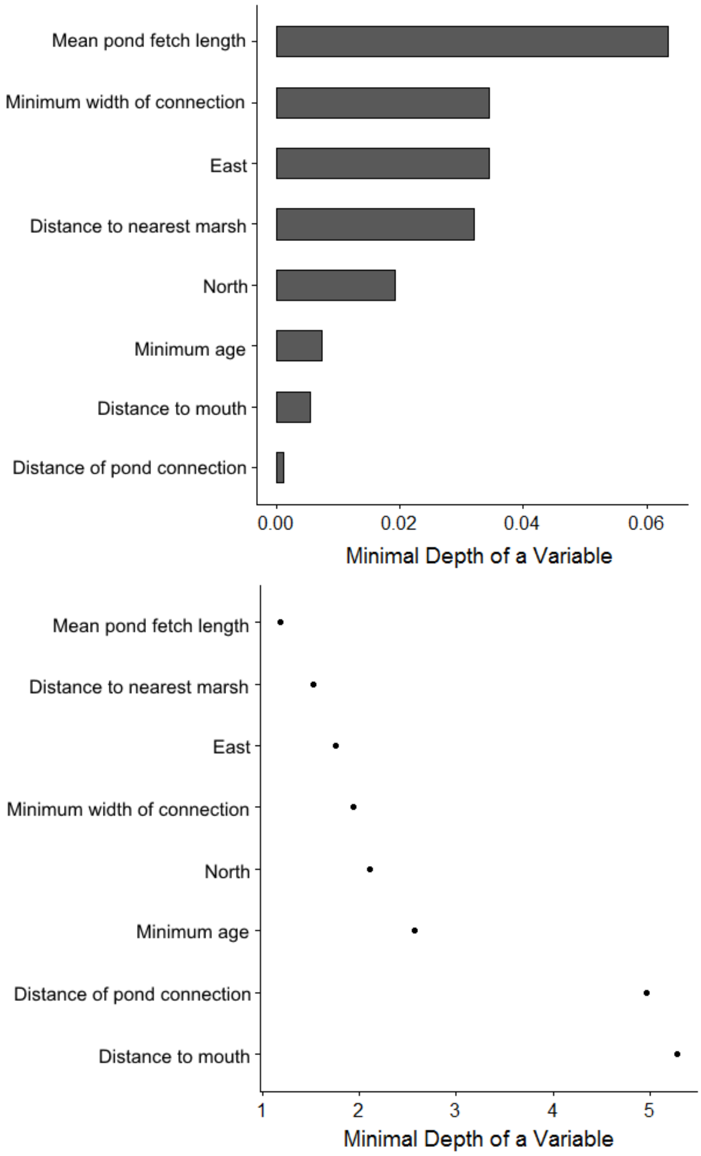

Figure SI 4.2: The variance importance (left) and Minimal depth (right) of the variables related to pond depth.

Chapter 6 Supplementary Information References

Allen, J.R.L., 2000. Morphodynamics of Holocene salt marshes: A review sketch from the Atlantic and Southern North Sea coasts of Europe. Quat. Sci. Rev. 19, 1155–1231. doi:10.1016/S0277-3791(99)00034-7

Christiansen, T., Wiberg, P.L., Milligan, T.G., 2000. Flow and Sediment Transport on a Tidal Salt Marsh Surface. Estuar. Coast. Shelf Sci. 50, 315–331. doi:10.1006/ecss.2000.0548

Friedrichs, C.T., Perry, J.E., 2001. Tidal Salt Marsh Morphodynamics: A Synthesis. J. Coast. Res. SI 27, 7–37.

Ganju, N.K., Kirwan, M.L., Dickhudt, P.J., Guntenspergen, G.R., Cahoon, D.R., Kroeger, K.D., 2015. Sediment transport-based metrics of wetland stability. Geophys. Res. Lett. 42, 7992–8000. doi:10.1002/2015GL065980

Ganju, N.K., Nidzieko, N.J., Kirwan, M.L., 2013. Inferring tidal wetland stability from channel sediment fluxes: Observations and a conceptual model. J. Geophys. Res. Earth Surf. 118, 2045–2058. doi:10.1002/jgrf.20143

Kirwan, M.L., Guntenspergen, G.R., 2010. Influence of tidal range on the stability of coastal marshland. J. Geophys. Res. 115, F02009. doi:10.1029/2009JF001400

Moskalski, S.M., Sommerfield, C.K., 2012. Suspended sediment deposition and trapping efficiency in a Delaware salt marsh. Geomorphology 139–140, 195–204. doi:10.1016/j.geomorph.2011.10.018

Pinheiro, J., Bates, D., DebRoy, S., Sarkar, D., R Core Team, 2016. nlme: Linear and Nonlinear Mixed Effects Models. R package version 3.1-128. https://cran.r-project.org/web/packages/nlme.

R Core Team, 2017. R: A Language and Environment for Statistical Computing, Vienna, Austria.

Reed, D.J., Spencer, T., Murray, A.L., French, J.R., Leonard, L., 1999. Marsh surface sediment deposition and the role of tidal creeks: Implications for created and managed coastal marshes. J. Coast. Conserv. 5, 81–90. doi:10.1007/BF02802742

Schepers, L., Kirwan, M., Guntenspergen, G., Temmerman, S., 2017. Spatio-temporal development of vegetation die-off in a submerging coastal marsh. Limnol. Oceanogr. 62, 137–150. doi:10.1002/lno.10381

Stevenson, J.C., Kearney, M.S., Pendleton, E.C., 1985. Sedimentation and erosion in a Chesapeake Bay brackish marsh system. Mar. Geol. 67, 213–235. doi:10.1016/0025-3227(85)90093-3

Temmerman, S., Govers, G., Wartel, S., Meire, P., 2003. Spatial and temporal factors controlling short-term sedimentation in a salt and freshwater tidal marsh, Scheldt estuary, Belgium, SW Netherlands. Earth Surf. Process. Landforms 28, 739–755. doi:10.1002/esp.495

Zuur, A.F., Ieno, E.N., Walker, N., Saveliev, A.A., Smith, G.M., 2009. Mixed effects models and extensions in ecology with R. Springer New York, New York, NY. doi:10.1007/978-0-387-87458-6

5

Indicators of marsh vulnerability to sea level rise neglect lateral runaway erosion

Lennert Schepers, Matthew Kirwan, Glenn Guntenspergen, Stijn Temmerman

5.1 Abstract

Sea level rise is threatening coastal marshes, leading to large-scale marsh loss in several micro-tidal systems. Early recognition of marsh vulnerability to sea level rise is critical in these systems to aid managers to take appropriate restoration or mitigation measures. However, it is not clear if current marsh vulnerability indicators correctly assess long-term stability of the marsh system. In this study, two indicators of marsh stress were studied, (i) the skewness of the marsh elevation distribution, and (ii) the abundance of codominant species in mixtures. We studied these indicators in an organogenic micro-tidal system (Blackwater River, Maryland, U.S.A.), where large-scale conversion from marshes to shallow ponds resulted in a gradient of increasing marsh loss. The two indicators reveal increasingly stressed marshes along the marsh loss gradient, but the field site with the most marsh loss seems to experience less stress, which is confirmed by prevalent indices of marsh vulnerability. We hypothesize that pond erosion generates sediment that might temporarily provide the marshes with the necessary sediment to keep up with relative sea level rise. However, lateral erosion and sediment export lead to severe marsh loss in these micro-tidal areas. These findings indicate that common marsh stress indicators might not always be accurate in determining the long-term vulnerability to marsh loss caused by lateral erosion. We argue that spatial indicators such as fetch, pond connection and the sediment budget should be included to correctly assess long-term stability of micro-tidal marshes.

5.2 Introduction

Coastal marshes provide critical ecosystem services, such as carbon sequestration (Chmura et al., 2003; McLeod et al., 2011; Ouyang and Lee, 2014), shoreline protection against storm impacts (Temmerman et al., 2013; Möller et al., 2014) and providing habitat for commercial fisheries (Boesch and Turner, 1984; Barbier et al., 2011), but the persistence of marshes over the next decades to centuries is threatened by accelerating sea level rise (SLR). When marshes cannot adapt to SLR by vertical accretion, submerging marsh vegetation dies off and is replaced by bare mudflats or open water areas, which is evident on large scales for example in the Mississippi River Delta (Day et al., 2000), the Venice Lagoon (Carniello et al., 2009) and the Chesapeake Bay (Kearney et al., 1988).

Elevated, vegetated marshes and low, unvegetated mudflats or interior open water areas have been identified as a two stable states, each with positive feedback mechanisms that provide long-term stability (Fagherazzi et al., 2006; Marani et al., 2010; Wang and Temmerman, 2013; van Belzen et al., 2017) (Chapter 4). This implies that once marsh has been converted to open water areas, it is very hard to reverse the process and to restore wetland marshes. Early recognition of marsh vulnerability to sea level rise is thus critical to foresee these pending shifts and to take early management measures to preserve marshes and their highly valued ecosystem services in face of accelerating sea level rise.

Several methods to assess marsh vulnerability to sea level rise have been developed during the last decades. Most methods assess the overall wetland condition, which is defined as the quality of the wetland as a function of physical, chemical, and biological parameters (Brooks et al., 2004). Well-known coastal assessment methods in the US are the New England Rapid Assessment Method (Carullo et al., 2007) and the Mid-Atlantic Rapid Assessment Method (Rogerson et al., 2010). These assessments do not focus specifically on how sea level rise is threating marshes, but can be used to determine and monitor the broader effects of anthropogenic disturbances.

Two indices, (i) elevation skewness and (ii) the abundance of species mixtures, have been proposed as indicators of marsh stress, but have never been tested empirically in marshes experiencing large-scale marsh loss. First, the skewness of the elevation distribution has been introduced by (Morris et al., 2005). In their study, Morris et al. (2005) argue that resilient marshes have a negative elevation skewness, i.e. with more high marsh than low marsh area, because resilient marshes have the tendency to build-up vertically until their elevation approaches mean high water level (Pethick, 1981; Allen, 1990; Temmerman et al., 2003). The highest high water level is the upper limit for marsh vegetation as sediment deposition must approach zero at elevations near that of the highest high tide (Morris et al., 2002). An increase in sea level rise rate increases flooding and provides accommodation space for marshes to grow, temporarily forming normal elevation distributions within the tidal frame. With higher rates of sea level rise, marshes will be positioned low in the tidal frame, close to their inundation tolerance limit. Marshes below this limit will die-off, which results in a positively skewed elevation distribution above this limit (Morris et al., 2005). A second indicator of marsh vulnerability to sea level rise is (ii) the co-occurrence of species in mixtures. A theoretical background for this hypothesis is the stress gradient hypothesis (Bertness and Callaway, 1994), which postulates that in harsh environments, positive interactions and facilitation between multiple species prevail, while in low stress environments competition leads to dominance by few or even one single species.

Bertness and Hacker (1994) indeed show that species interactions shift from competitive interactions at the highest marsh elevations to positive interactions when stress levels are high in the low elevated marsh areas. Examples of positive interactions are providing shading, which limits surface evaporation and salt accumulation (Callaway, 1994) and rhizosphere oxidation that can alleviate anoxic substrate conditions (Bertness, 1991a; Boaga et al., 2014). The hypothesis that marshes dominated by species mixtures are indicative for higher stress levels and higher marsh vulnerability to submergence, has however never been tested.

Recently, Raposa et al. (2016) and Ekberg et al. (2017) both have developed indicators specifically targeted to assess marsh vulnerability (or resilience) to sea level rise. The term 'resilience' is used here to indicate the ability of a system to resist and recover from perturbation (Gunderson, 2000), in this case the ability to resist sea level rise. Raposa et al. (2016) were the first to develop their MArsh Resilience to Sea-level rise (MARS) indices, specifically targeting resilience to sea level rise, and applied their method to 16 US National Estuarine Research Reserves. Ekberg et al. (2017) included in their assessment also model predictions of the impact of different sea level rise scenarios.

Although the development of such indices is highly important to assess marsh vulnerability to SLR, there is a need for validating such indices against observations of long-term (i.e. over decades) historical marsh loss, in order to increase trust in these indices to correctly assess long-term stability of marshes with sea level rise. In this study, we collected the necessary field data to test the skewness of the elevation distribution and the abundance of species mixtures as indicators of marsh vulnerability with sea level rise in the Blackwater River marshes (Blackwater Estuary, Maryland, U.S.A.), a organogenic micro-tidal marsh system where widespread historical marsh loss over the last 80 years has resulted in a spatial gradient of increasing marsh loss (Chapter 4). Based on our evaluation of the stress indicators values against observed marsh loss rates, we propose to include additional metrics to the existing indices to correctly account for long-term marsh stability with sea level rise. This will aid managers to assess the marsh condition and to take early adaptation measures.

5.3 Study area

The Blackwater marshes (Maryland, USA; 38°24' N, 76°40' W) are a brackish coastal marsh system along the Blackwater river that connects Lake Blackwater, a large (> 5 km diameter) shallow open water area, with the Fishing Bay, an interior bay of the Chesapeake Bay (Fig. 5.1.). Since 1938 more than 2000 ha or 51 % of the marshes have been converted to shallow open water, with most marsh habitat lost at or near Lake Blackwater and leaving the most downstream marshes closest to the Fishing bay relatively intact (Stevenson et al., 1985; Scott et al., 2009; Schepers et al., 2017). As a result, there is a spatial gradient of decreasing marsh area and increasing shallow open water area in upstream direction along the Blackwater River (Fig. 5.1). The marsh loss has been attributed to insufficient surface accretion relative to sea level rise (Stevenson et al., 1985), lateral marsh erosion along the pond edges (Stevenson et al., 1985; Ganju et al., 2013) and vegetation disturbance by rodents (Kendrot, 2011).

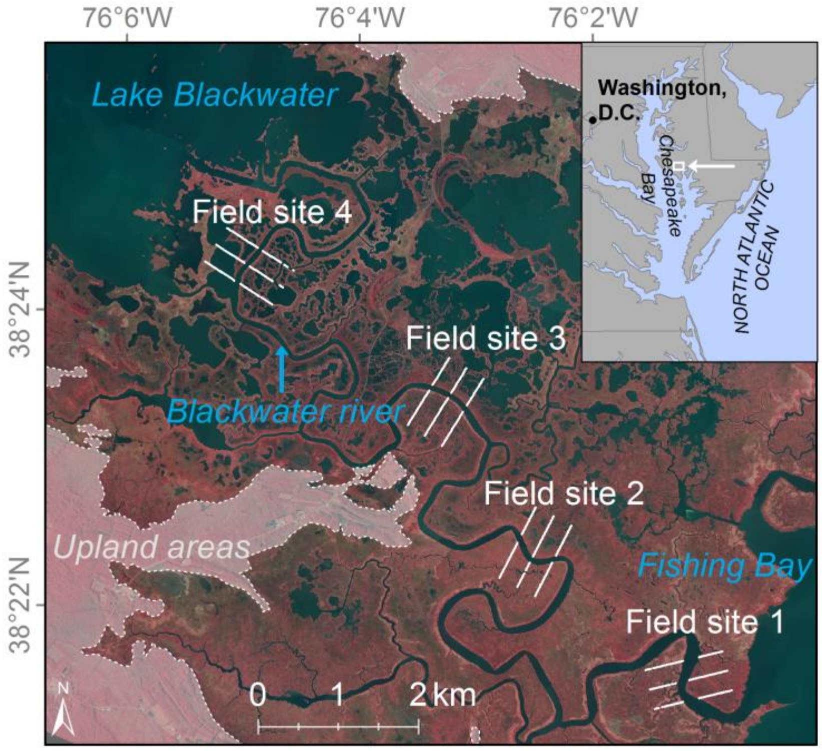

Figure 5.1: Aerial image of the Blackwater Marshes. From lower right corner to upper left corner of the image (i.e. in upstream direction along the Blackwater River) marshes are changing from high marsh vegetation cover (reddish color) close to the Fishing Bay (SE-corner) to increasing open water areas (dark color) in upstream direction, and ultimately to Lake Blackwater (NW-corner). White lines indicate GPS measurement points. White shaded areas with dashed outlines are no marshes but upland areas. Inset: Location of the Blackwater marshes along the Chesapeake Bay (white rectangle)

Short-term measurements showed that salinity varies little (<2 ppt) between the most downstream site near Fishing Bay and upstream site at Lake Blackwater, but the salinity might change significantly on seasonal timescales (Fleming et al., 2011). The tidal range (from 1 to <0.05 m) and allochthonous sediment input decreases from the Fishing Bay to Lake Blackwater(Ganju et al., 2013). At the most upstream areas, frequent northwestern storms export sediment out of the system (Stevenson et al., 1985; Ganju et al., 2013, 2015).

5.4 Methods

5.4.1 Marsh elevation and vegetation surveys

We selected four sites with an increasing proportion of open water areas as a measure of marsh loss (Fig. 5.1) along the Blackwater River, in such a way that transects of 1000 m length and perpendicular to the river would not cross other river bends or upland areas. At each site the marsh surface elevation and vegetation composition were surveyed along three transects of 1000 m (250 m apart) straddling the Blackwater River. Along each transect, data were recorded on point locations with a 10 m interval. We located each transect point in the field and recorded the elevation relative to the North American Vertical Datum of 1988 (NAVD88) with a high-precision GPS (Trimble R8 RTK-GPS, vertical error <2 cm) during a field campaign in August 2014. At the same time, we noted the dominant plant species (all species with >30% cover) within a circle with diameter of 0.5 m centered on the gps-point. Points located in tidal channels or ponds were excluded in this study.

During the same period (August 14 to October 29, 2014), water levels at each field site were recorded with pressure transducers (Hobo U20L-02, Onset, MA, USA), which were recalculated to the NAVD88 vertical datum after local atmospheric pressure compensation. Tidal characteristics, including mean tidal range and mean high water level (MHW), were calculated from this dataset with the Tides package in R (Cox and Schepers, 2017).

Additional to the GPS elevation data, we used LiDAR (Light Detection and Ranging) elevation data that were recorded in spring 2004 and downloaded from Maryland's GIS & Data portal (http://imap.maryland.gov) as a 0.91 m resolution digital terrain model. Comparison with our GPS-data (n = 737) revealed a high overall accuracy of the LiDAR data, with an average difference of 0.08 m (RMSE 0.11 m) and normally distributed residuals. Elevation changes in the area are lower than 1 cm/year (Cahoon et al., 2010), which implies that in the 10 year between the LiDAR data (2004) and the field campaign (2014), maximum elevation changes of around 10 cm are in the same order of magnitude as the vertical error on the LiDAR data. For each of the four sites, we extracted the LiDAR elevation data within an area of 125 m around the three transects. Based on an aerial image classification of 2010 (Schepers et al., 2017), only the marsh elevation was retained, resulting in >300000 elevation points at the most intact site and >150000 for the most degraded site.

5.4.2 Marsh vulnerability indices to sea level rise

Several indices of wetland vulnerability have been calculated. The skewness of the elevation distribution was calculated for each site with both the gps measurements and the LiDAR measurements. We defined the the Pearson's moment coefficient of skewness as:

$$skew = \frac{\frac{1}{n}\sum_{i=1}^{n}(x_i - \bar{x})^3}{\left[\frac{1}{n-1}\sum_{i=1}^{n}(x_i - \bar{x})^2\right]^{3/2}}$$

where n = the number of measurements, x_i = each measurement (here each elevation data point), $\bar{x}$ = the average of all measurements (all elevation data points). To verify the change of elevation skewness with increasing marsh loss, we simulated marsh conversion to open water by removing the lowest LiDAR elevation points at the most intact site (field site 1) with similar losses as the more degraded field sites (i.e. 11.4, 33.3 and 58.2 % loss). For each of these marsh loss simulations, we calculated the elevation skewness.

Species abundances along the marsh loss gradient were calculated by summing the occurences for each species in each field site. Also the number of mixtures, the points with more than one species covering 30 % of a circle with diameter of 0.5 m, were summed for each field site. All numbers were scaled to proportions for each field site, because a wider river or more marsh loss results in a different number of marsh point measurements per field site. Site 2 has most points (n=243), slightly more points than field site 1 (n=222), where the river is a little wider, and more points than field sites 3 and 4 (n= 164 and 114, respectively) with more marsh loss.

We verified the results of these two indicators (elevation skewness and vegetation composition) with the indicators of (Raposa et al., 2016; Cole Ekberg et al., 2017). We did not include all indicators because of limited data availability, and we slightly changed two species indicators of Ekberg et al. (2017). The percentage of low marsh is in Ekberg et al. (2017) defined as regularly flooded areas dominated by tall-form (>50 cm) *Spartina alterniflora*. We defined this as areas with *Spartina alterniflora* monocultures (the only species with a cover >30 %). We defined Perennial turfgrass type I as areas with *Distichlis spicata* or *Spartina patens* monocultures (or a mixture of both) but where *Spartina alterniflora* was not dominant (cover is <30 %).

To calculate the MARS average scores, we used the metric threshold table from Raposa et al. (2016, Table 2 p. 268). The average of the category scores (marsh elevation score and tidal range) produced a MARS average score for each field site. To convert the Ekberg et al. (2017) indices to field site scores, we ranked the index scores from 1-4 with increasing vulnerability and calculated an average score. Note that contrary to Ekberg et al. (2017), a higher score indicates a higher vulnerability.

5.4.3 Analyses and statistics

All data analyses, figures and maps were made in R (R Core Team, 2017). As we are interested in the skewness of a distribution, a parametric testing method cannot be applied. Therefore we applied the bootstrap technique to determine if the skewness was significantly different from zero in the measured gps-data: the elevation dataset was randomly resampled 10,000 times and on each sample the skewness was calculated. If zero is within the 2.5th and 97.5th percentile of these 10,000 skewness values, the skewness is not significantly different from zero, similarly to a statistical test with 0.05 confidence level (α). Since the LiDAR-dataset consists of a huge dataset (n>150000) and includes the whole study area rather than a selection of sample points, the bootstrap technique was deemed to be not necessary for the LiDAR data.

5.5 Results and Discussion

5.5.1 Elevation skewness

The skewness of the marsh elevation distribution shifts from significantly negative at the most intact field site 1, to non-skewed at site 2, to a positive skewness at site 3 (Fig. 5.2). This indicates that the marshes at the intact site 1 are mostly high elevated marshes close to their upper limit with a large elevation capital, and therefore highly resilient to SLR, while at field site 3 with considerable marsh loss, the positive skewness indicates that there are more low elevation marshes close to their lower limit, and hence vulnerable to SLR. The non-skewed elevation at field site 4 will be discussed later in this section.

Below we discuss two potential mechanisms that can explain the shift from negative to positive skewness with increasing marsh loss rate from site 1 to 3. First of all, an increase in the rate of sea level rise will lower the elevation of the marshes compared to the mean high water level and create accommodation space and increased flooding (Morris et al., 2005). Since marshes need time to build-up organically and mineralogenically to adjust to a new equilibrium rate, the skewness of the elevation distribution becomes more positive. The skewness of marshes with lower tidal ranges will however be more impacted by a similar sea level rise because of a proportionally bigger shift of their growth range (see also (Kirwan and Guntenspergen, 2010; Kearney and Turner, 2016). This is the case in our study area, where tidal range diminishes in upstream direction from field site 1 (0.63 m tidal range) to field site 3 (0.20 m tidal range). A second, related mechanism that might explain the change in skewness is the die-off of marshes if they become inundated more than the plant species flooding tolerance. The simulated marsh loss of the lowest elevated marshes (Fig. 5.3) indeed shows that this marsh loss is associated with a clear change from negative to positive skewness. This is not surprising since we cut off lower values, but the fact that the patterns of simulated marsh loss resemble the actual patterns (compare Fig. 5.2 with Fig. 5.3), supports the hypothesis that marsh die-off at the lowest areas are at least partly responsible for the observed shift in skewness.

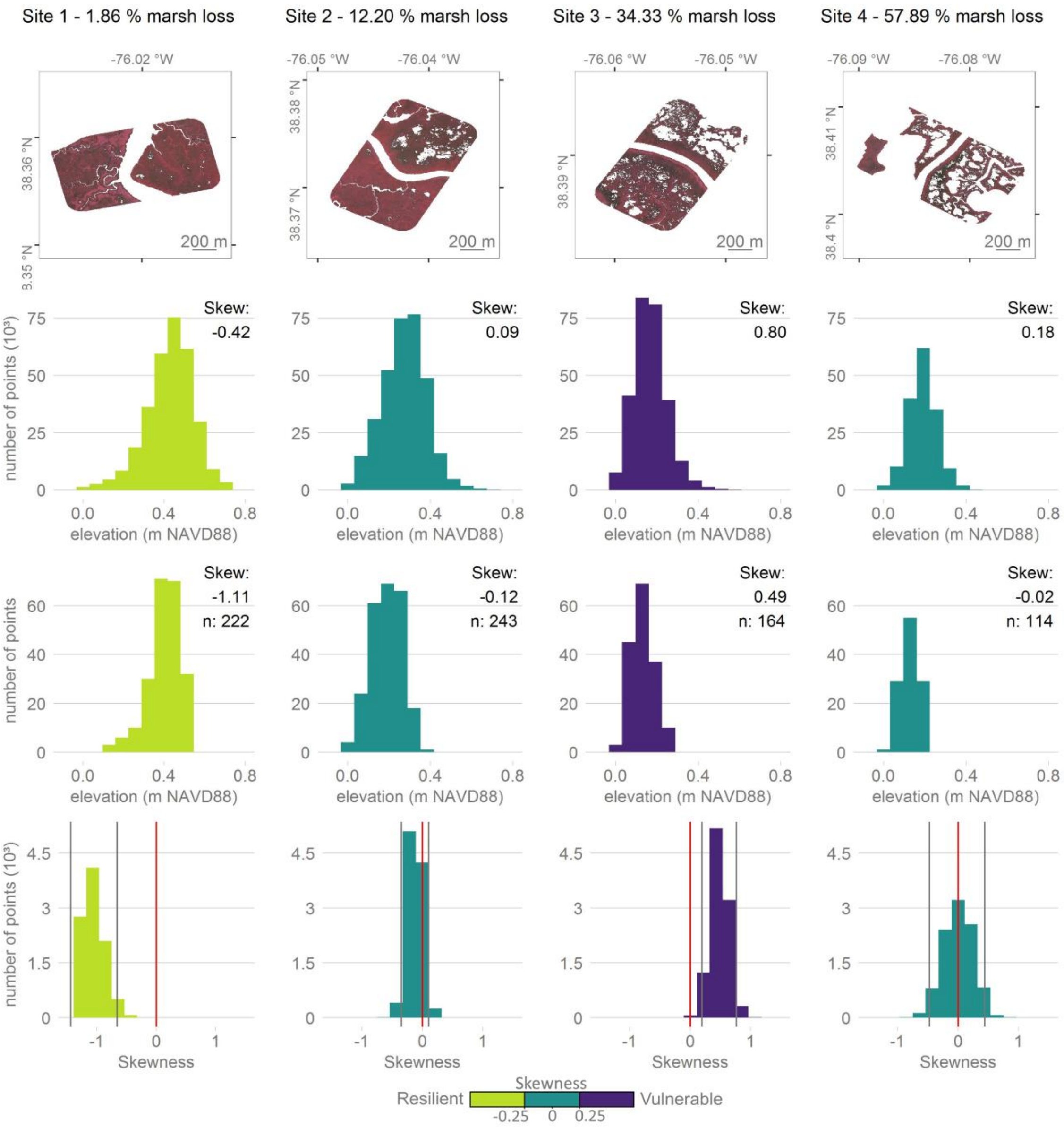

Figure 5.2: Changes in skewness of elevation distributions along the gradient of increasing marsh loss from field site 1 (left) to 4 (right). Top to bottom: aerial images of field sites with increasing marsh loss (marshes represented by reddisch color); LiDAR elevation distributions and calculated skewness; gps elevation distributions and skewness; and bootstrap analysis of the skewness of the gps elevation distributions, indicating if the skewness is significantly negative (resilient marsh), neutral or positive (vulnerable marsh) when the 0 skewness (red vertical line) is lower, in or higher than the skewness range (indicated by the grey vertical lines i.e. the 2.5th and 97.5th percentile) respectively.

At field site 4, LiDAR data shows a slightly positive skewness, while the bootstrap analysis on the GPS data reveals no significant skewness (Fig. 5.2, right column). This is remarkable, since we would expect the most vulnerable, positive skewness at the site with most marsh loss, as our marsh loss simulation clearly shows (Fig. 5.3). We hypothesize that this counterintuitive observation is due to increased sediment availability generated by eroding marsh edges or pond bottoms at the most degraded field site 4. Studies of (Ganju et al., 2013, 2015) in the same area support this hypothesis, showing appreciable suspended sediment concentrations (55 mg/L) and high accretion rates (>5 mm/yr) within marsh vegetation close to field site 4, likely originating from sediments eroding from pond bottoms and marsh edges. Furthermore, the remaining marsh portions in field site 4 are mostly located along the edges of ponds and channels (see Fig. 5.2) and therefore approximate to the local source areas of suspended sediments. These sediments build up the few remaining marsh areas, leading to non-skewed elevation distributions (Fig. 5.2). This hypothesis implies then that the lowest, most vulnerable areas have already converted to open water ponds, and that the remaining marsh portions fringing along channel and pond edges are moderately vulnerable to SLR.

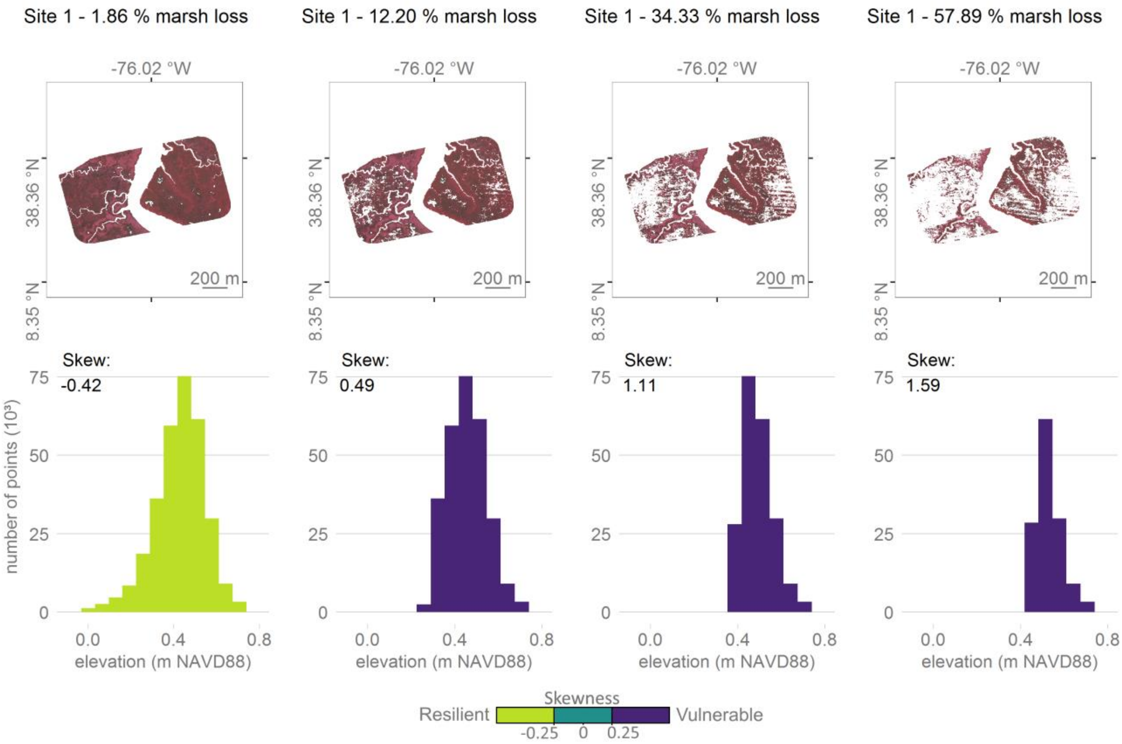

Figure 5.3: Changes in skewness of elevation distributions along a gradient of simulated increasing marsh loss (from left to right). Top row: aerial images of field site 1 with simulated progressive marsh loss of the lowest areas. Marsh areas are represented by reddish colors. Bottom row: LiDAR elevation distribution and skewness corresponding with the marsh loss simulations. Note that the simulated changes in elevation skewness with increasing marsh loss resemble the observed changes in elevation skewness with increasing marsh loss (compare with Fig. 5.2).

5.5.2 Vegetation community structure

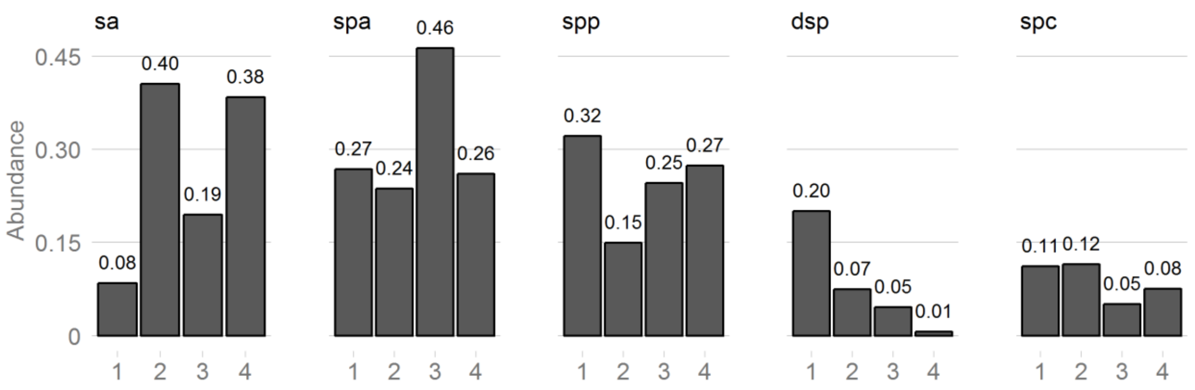

Figure 5.4: Abundances of the most abundant species (sa: Schoenoplectus americanus, spa: Spartina alterniflora, spp: Spartina patens, dsp: Distichlis spicata and spc: Spartina cynosuroides) in the four sites with increasing marsh loss (sites 1 to 4 indicated on the X-axes). The numbers do not show consistent trends with increasing marsh loss except for Distichlis spicata.

The most abundant species in the Blackwater Marshes are *Schoenoplectus americanus*, *Spartina alterniflora* and *Spartina patens* (Fig. 5.4). Although *Spartina patens* is considered as a high marsh species (Bertness, 1991b; Smith, 2009; Wigand et al., 2011; Raposa et al., 2017) and *Schoenoplectus americanus* and *Spartina alterniflora* are considered low marsh species (Bertness, 1991b; Nyman et al., 1994; Donnelly and Bertness, 2001), these species do not show a clear abundance shift with increasing marsh loss (Fig. 5.4) or with elevation (data not shown). A less abundant high marsh species is *Distichlis spicata* (dsp), which does show a clear decline along the marsh loss gradient (Fig. 5.4). *Spartina cynosuroides* (spc) occurs in more or less similar abundances throughout the study area (Fig. 5.4). *Bolboschoenus robustus*, *Juncus gerardii* and *Iva fructusea* were sparsely present (<10 points) and not included in our analysis.

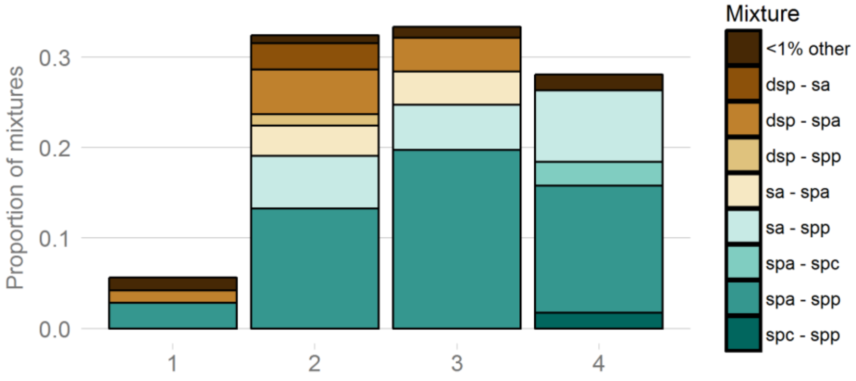

Figure 5.5: Proportion of mixtures in each field site with increasing marsh loss (sites 1 to 4 indicated on the X-axis). The total number of mixtures results in a similar trend as the skewness indicator (see Fig. 5.2). sa: Schoenoplectus americanus, spa: Spartina alterniflora, spp: Spartina patens, dsp: Distichlis spicata and spc: Spartina cynosuroides

Specific mixtures between two species show various patterns with increasing marsh loss (i.e. from field site 1 to field site 4). However, when summing all the mixture points, our results show that field site 3 has the highest proportion of mixture points (Fig. 5.5), whereas field site

4 has a lower proportion of mixtures. This might indicate that these marshes are less stressed (also likely because of local sediment import that accretes the marshes, see previous paragraph), similar as the the skewness analysis. From this we conclude that single species abundances and assemblages may show different patterns, but the total number of mixture points may be a useful indicator of marsh stress.

5.5.3 Comparison with other indices indicating marsh vulnerability to sea level rise.

When comparing the results from the two indicators with the indicators of (Raposa et al., 2016) (Table 5.1) and (Cole Ekberg et al., 2017) (Table 5.2), we see that the overall results are similar: with increasing marsh loss from field site 1 to 4, the indices indicate an increasing vulnerability to SLR fromfield site 1 to 3, but this decreases again in field site 4.

Table 5.1: vulnerability indices according to (Raposa et al., 2016)* show increasing vulnerability from field site 1 to site 3 and again a decrease in vulnerability in site 4. A lower MARS score means higher vulnerability to SLR.

Colorscale	Resilient				Vulnera-
Field site		1	2	3	4
% below MHW		79.7	96.3	93.9	86.8
% below third elevation		4.5	18.5	34.1	5.3
Skewness		-1.11	-0.12	0.49	-0.02
Average Marsh Elevation index		3.6	3	2.6	3.3
Tidal range (m)		0.63	0.31	0.20	0.06
MARS average score		2.5	2	1.5	2

*Not included: Elevation change rate, short-term and long-term accretion rate, turbidity, long-term rate of SLR, short-term inter-annual variability in water levels.

Table 5.2: vulnerability indices according to (Cole Ekberg et al., 2017)* show increasing vulnerability from field site 1 to site 3 and again a decrease in vulnerability in site 4.

Field site	1	2	3	4
Median marsh orthometric height (m NAVD88)	0.41	0.19	0.12	0.12
Median marsh elevation relative to MHW	-0.06	-0.12	-0.11	-0.06
Percentage unvegetated	1.55	11.42	33.25	58.24
Percentage *S. alterniflora* monoculture (low marsh)	23.42	9.88	34.15	15.79
Percentage turf grass type I (high marsh)	47.75	2.47	9.15	11.40
Average score (1 vulnerable – 4 resilient)	3.8	2.6	2	2.6

*Not included: average S. alterniflora height, Modelled loss with 0.3, 0.9 and 1.5 m of SLR, soil penetration depth and loading response, percent of perennial turfgrass type II.

Several indices could not be calculated because of data constraints, but it is unlikely that this will affect our results because of three reasons. (i) The factors with greatest impact on the vulnerability are related to the elevation capital (Cole Ekberg et al., 2017), which we included in our analysis. (ii) The indicators of Raposa et al. (2016) that we didn't include are related to suspended sediment deposition and accretion rates. As we discussed that in field site 4 considerable suspended sediment concentrations and accretion rates are measured, likely due to erosion of the marsh edges and pond bottoms (Ganju et al., 2013, 2015). Also the three SLAMM modelling indicators (Cole Ekberg et al., 2017) are highly dependent on elevation and sediment accretion. (iii) The species abundances (Fig. 5.4, Table 5.2) do not show a clear trend, so it is unlikely that other species indicators, also relying on species presence, will make an important difference.

5.5.4 Indices neglect erosional feedback mechanisms

Most indicators show the consistent pattern of increasing vulnerability with increasing marsh loss from the intact marshes at site 1 to the degraded marshes at field site 3. However, a major issue is that field site 4 shows a clear decrease in vulnerability in all the indices. This is especially noteworthy because field site 4 is the area with the highest proportion of marsh loss area, where more than 58% of the area consists of ponds that once were vegetated marshes (e.g. Schepers et al. 2017). However, below we highlight that all marsh vulnerability indices used so far, only account for vertical processes related to elevation and inundation, while they neglect that marsh stability is also critically dependent on lateral marsh erosional processes.

Site 4 with the highest proportion of marsh loss area also has the largest (Schepers et al., 2017) and deepest ponds (Chapter 4), providing favourable conditions for wind-generated wave erosion of the marsh edges surrounding the ponds. Furthermore, ponds in site 4 are mostly connected to the tidal channel network (Fig. 4.1), allowing the export of eroded material with tidal ebb currents (Ganju et al. 2013; Schepers under review). Also part of this eroded material can be deposited on the remaining marshes fringing along the pond and channel edges, and as such can contribute to the decreased vulnerability index values of the remaining marsh portions in site 4. However, these vulnerability indices neglect the role of lateral marsh erosion and tidal export of the eroded material. Mariotti et al (2013) and (Ortiz et al., 2017) have recently demonstrated that interior marsh ponds larger than a certain threshold width (300 m in Mississippi marshes, 200-1000 m in US Atlantic marshes) are susceptible to runaway expansion due to the positive feedback between increasing wind fetch length and wave erosion. This is also evident along the die-off gradient in our study area, where the average fetch length of the ponds increases suddenly from < 200 m at field site 4 to >1000 m just upstream at Lake Blackwater (Schepers et al., 2017) (Fig. 8 p. 144). Increasing marsh loss in these areas enhances the chance for pond merging, leading to larger ponds and higher marsh edge erosion rates, and eventually to complete runaway erosion of the marshes. Lake Blackwater, which consisted of vegetated marshes on aerial pictures of 1938 and which converted to a large (> 10 km^2) shallow open water area (Schepers et al. 2017), is a stunning preview of what field site 4 might experience.

This all indicates that the marshes at field site 4 are at the brink of irreversible marsh erosion, rather than being moderately vulnerable to sea level rise as suggested by the vulnerability indices. More generally, our analysis demonstrates that marshes can be (temporarily) stable in the vertical dimension, even though horizontal erosion may eventually erode the whole marsh

(Fagherazzi et al., 2013; Mariotti and Carr, 2014), and that existing indices for marsh vulnerability do not assess the risks of marsh loss due to horizontal erosion processes.

5.5.5 Accounting for lateral erosional processes to determine marsh loss risk

Thus we highlight a fundamental shortcoming of marsh vulnerability to sea level rise indicators. The indicators do not account for the spatial patterns of marsh die-off, which might impose erosional feedback mechanism and non-linearly lead to runaway erosion.

To overcome this problem, we recommend that the following three parameters are included to assess the risk of marsh loss: (i) fetch length of interior marsh ponds, (ii) pond connections with the tidal channel system and (iii) tidal channel sediment flux. Fetch length is a straightforward indicator for wind-generated wave erosion of marsh edges surrounding ponds, and is defined as the distance over continuous water surface, from one side of the pond to the other, over which wind can generate waves. Examples are given by (Ortiz et al., 2017; Schepers et al., 2017). Schepers et al. (2017) measure the average fetch length in 8 wind directions for all pond pixels, Ortiz et al. (2017) include the ‘simple fetch length’, the 90th percentile of the magnitude of fetch in the direction of a given wind for all edge points on the pond. Also Rohweder et al. (2012) provide an automatic method to calculate wind fetch. In the SLAMM predictions of Ekberg et al. (2017) (SLAMM version 6.1), a formulation for fetch-based erosion is included, although in this version of the model erosion only takes place when the maximum fetch is >9 km (Clough et al., 2010). This is clearly an underestimation as shown by recent work (Mariotti and Fagherazzi, 2013; Ortiz et al., 2017), which indicate that the threshold fetch length for marsh edge erosion is 200-1000 m. However, from SLAMM version 6.7 (Clough et al., 2016) onwards, also a more complicated approach based on total wave power is available, but this approach is data intensive (including average wind speeds and wind-direction data, open-water fetch and water depths at different tide stages). Here we argue that it is easier to include a simple fetch indicator to account for wind-wave vulnerability.

The pond connection with the tidal channel system might be imported for the export of sediment out of the system (Ganju et al., 2013) so we propose to look at the biggest ponds and to determine if they are connected to the tidal channels system. The connection with the tidal channel system might however have a dual effect, promoting sediment import (Redfield, 1972; Millette et al., 2010; Wilson et al., 2010, 2014) as well as sediment export (Chapter 4). The resulting effect of the connection might be measured through sediment flux measurements, since these measurements will determine if (internally generated) sediment is imported or exported from the marsh system, which will ultimately determine the final course of the marsh (French, 2006; Mariotti and Carr, 2014; Ganju et al., 2015, 2017; Mariotti, 2016). Identifying a connection is relatively easy with the good aerial imagery that is currently available, but flux measurements require intensive and long-term measuring campaigns. However, Ganju et al. (2017) suggests, based on a sediment flux study in eight micro-tidal marshes along the Atlantic and Pacific coasts, that the ratio between unvegetated-vegetated marsh area can be used as a single snapshot to infer the sediment budget.

5.5.6 Two management strategies

Our results demonstrate that there might be two management strategies, based on the extent of marsh loss. Initially, the elevation skewness and the proportion of mixtures of marshes, in combination with newly proposed indicators by Raposa et al. (2016) and Ekberg et al. (2017), can be used initially as indictors of vertical marsh vulnerability to SLR. This will aid managers to monitor existing marshes and to recognize early signs of marsh stress to SLR. If needed, the managers can take actions to alleviate the stress e.g. by ensuring that enough sediment reaches marshes to keep up with sea level rise or sediment is applied to marshes to recover optimum elevations. Aiming to keep marshes is essential, since research has indicated that recovery of lost marshes may be far more difficult to achieve due to feedback mechanisms (Chapter 4). However, if marshes are already experiencing marsh loss, our results indicate that managers should be especially cautious about lateral processes that can enhance marsh loss, such as wind waves and export of the tidal channel system. In those circumstances, managers should focus on mitigating these lateral feedbacks as these can lead to increasing marsh erosion rates that might erode the whole marsh system.

5.6 Conclusion

Along a spatial gradient of increasing marsh loss, the skewness of the marsh elevation distribution shifts from negative to positive, indicating a shift from marshes that are resilient to SLR to marshes that are highly vulnerable. The abundance of individual species was not found to be a good indicator for marsh vulnerability to SLR, but the total proportion of species mixtures increased along the marsh die-off gradient and resulted in the same vulnerability trend as the elevation skewness. These vulnerability trends were confirmed by previously proposed indices of marsh vulnerability to sea level rise.

A remarkable result was that all above-mentioned indices suggested a lower vulnerability at the site with the largest area of marsh loss. This highlights a shortcoming of the current indices, because they do not account for marsh loss by lateral erosional feedback mechanisms by wind waves and tidal currents. We recommend including three parameters, fetch length, pond connection with the tidal channel system and sediment budget to correctly assess long-term stability, which should aid managers to take the appropriate restoration or mitigation measures.

Acknowledgements

This project was financed by an UA-BOF DOCPRO grant (to L.S. and S.T.), the Research Foundation Flanders (FWO, PhD grants L.S., 11S9614N & 11S9616N, travel grants L.S. V428214N and S.T. K217414N), by the U.S. Geological Survey, Climate and Land-Use Research and Development Program (G.G.), by NSF GLD 1529245, NSF SEES 1426981, NSF LTER 1237733 (M.K.). We would like to thank the managers and biologists of the Blackwater National Wildlife Refuge for their assistance and valuable comments; and P. Brennand (USGS) for indispensable field assistance. Any use of trade, product, or firm names is for descriptive purposes only and does not imply endorsement by the U.S. Government.

5.7 References

Allen, J.R.L., 1990. Salt-marsh growth and stratification: A numerical model with special reference to the Severn Estuary, southwest Britain. Mar. Geol. 95, 77–96. doi:10.1016/0025-3227(90)90042-I

Barbier, E.B., Hacker, S.D., Kennedy, C., Koch, E.W., Stier, A.C., Silliman, B.R., 2011. The value of estuarine and coastal ecosystem services. Ecol. Monogr. 81, 169–193. doi:10.1890/10-1510.1

Bertness, M.D., 1991a. Interspecific Interactions among High Marsh Perennials in a New England Salt Marsh. Ecology 72, 125–137. doi:10.2307/1938908

Bertness, M.D., 1991b. Zonation of Spartina Patens and Spartina Alterniflora in New England Salt Marsh. Ecology 72, 138–148. doi:10.2307/1938909

Bertness, M.D., Callaway, R., 1994. Positive interactions in communities. Trends Ecol. Evol. 9, 187–191. doi:10.1016/0169-5347(94)90087-6

Bertness, M.D., Hacker, S.D., 1994. Physical Stress and Positive Associations Among Marsh Plants. Am. Nat. 144, 363. doi:10.1086/285681

Boaga, J., D'Alpaos, A., Cassiani, G., Marani, M., Putti, M., 2014. Plant-soil interactions in salt marsh environments: Experimental evidence from electrical resistivity tomography in the Venice Lagoon. Geophys. Res. Lett. 41, 6160–6166. doi:10.1002/2014GL060983

Boesch, D.F., Turner, R.E., 1984. Dependence of Fishery Species on Salt Marshes: The Role of Food and Refuge. Estuaries 7, 460–468. doi:10.2307/1351627

Brooks, R.P., Wardrop, D.H., Bishop, J.A., 2004. Assessing wetland condition on a watershed basis in the Mid-Atlantic region using synoptic land-cover maps. Environ. Monit. Assess. 94, 9–22. doi:10.1023/B:EMAS.0000016876.63062.3d

Cahoon, D.R., Guntenspergen, G.R., Baird, S., 2010. Do Annual Prescribed Fires Enhance or Slow the Loss of Coastal Marsh Habitat at Blackwater National Wildlife Refuge? Final Report to Joint Fire Science Program Project Number 06-2-1-35.

Callaway, R.M., 1994. Facilitative and Interfering Effects of Arthrocnemum Subterminale on Winter Annuals. Ecology 75, 681–686.

Carniello, L., Defina, A., D'Alpaos, L., 2009. Morphological evolution of the Venice lagoon: Evidence from the past and trend for the future. J. Geophys. Res. Earth Surf. 114, 1–10. doi:10.1029/2008JF001157

Carullo, M., Carlisle, B.K., Smith, J.P., 2007. A New England rapid assessment method for assessing condition of estuarine marshes: A Boston Harbor, Cape Cod and Islands pilot study. Massachusetts Off. Coast. Zo. Manag. Boston, USA.

Chmura, G.L., Anisfeld, S.C., Cahoon, D.R., Lynch, J.C., 2003. Global carbon sequestration in tidal, saline wetland soils. Global Biogeochem. Cycles 17. doi:10.1029/2002GB001917

Clough, J., Park, R., Propato, M., Polaczyk, A., Brennan, M., Behrens, D., Battalio, B., Fuller, R., 2016. SLAMM 6.7 Technical Documentation.

Clough, J.S., Park, R. a., Fuller, R., 2010. SLAMM 6 beta Technical Documentation SLAMM 6 Technical Documentation.

Cole Ekberg, M.L., Raposa, K.B., Ferguson, W.S., Ruddock, K., Watson, E.B., 2017. Development and Application of a Method to Identify Salt Marsh Vulnerability to Sea Level Rise. Estuaries and Coasts 40, 694–710. doi:10.1007/s12237-017-0219-0

Cox, T., Schepers, L., 2017. Tides: Quasi-Periodic Time Series Characteristics. R package version 2.0. https://cran.r-project.org/web/packages/Tides.

Day, J.W., Britsch, L.D., Hawes, S.R., Shaffer, G.P., Reed, D.J., Cahoon, D.R., 2000. Pattern and Process of Land Loss in the Mississippi Delta: A Spatial and Temporal Analysis of Wetland Habitat Change. Estuaries 23, 425–438. doi:10.2307/1353136

Donnelly, J.P., Bertness, M.D., 2001. Rapid shoreward encroachment of salt marsh cordgrass in response to accelerated sea-level rise. Proc. Natl. Acad. Sci. U. S. A. 98, 14218–14223. doi:10.1073/pnas.251209298

Fagherazzi, S., Carniello, L., D'Alpaos, L., Defina, A., 2006. Critical bifurcation of shallow microtidal landforms in tidal flats and salt marshes. Proc. Natl. Acad. Sci. U. S. A. 103, 8337–8341. doi:10.1073/pnas.0508379103

Fagherazzi, S., Mariotti, G., Wiberg, P., McGlathery, K., 2013. Marsh Collapse Does Not Require Sea Level Rise. Oceanography 26, 70–77. doi:10.5670/oceanog.2013.47

Fleming, B.J., DeJong, B.D., Phelan, D.J., 2011. Geology, hydrology, and water quality of the Little Blackwater River watershed, Dorchester County, Maryland, 2006–09: U.S. Geological

Survey Scientific Investigations Report 2011–5054. http://pubs.usgs.gov/sir/2011/5054/.

French, J., 2006. Tidal marsh sedimentation and resilience to environmental change: Exploratory modelling of tidal, sea-level and sediment supply forcing in predominantly allochthonous systems. Mar. Geol. 235, 119–136. doi:10.1016/j.margeo.2006.10.009

Ganju, N.K., Defne, Z., Kirwan, M.L., Fagherazzi, S., D'Alpaos, A., Carniello, L., 2017. Spatially integrative metrics reveal hidden vulnerability of microtidal salt marshes. Nat. Commun. 8, 14156. doi:10.1038/ncomms14156

Ganju, N.K., Kirwan, M.L., Dickhudt, P.J., Guntenspergen, G.R., Cahoon, D.R., Kroeger, K.D., 2015. Sediment transport-based metrics of wetland stability. Geophys. Res. Lett. 42, 7992–8000. doi:10.1002/2015GL065980

Ganju, N.K., Nidzieko, N.J., Kirwan, M.L., 2013. Inferring tidal wetland stability from channel sediment fluxes: Observations and a conceptual model. J. Geophys. Res. Earth Surf. 118, 2045–2058. doi:10.1002/jgrf.20143

Gunderson, L.H., 2000. Ecological Resilience—In Theory and Application. Annu. Rev. Ecol. Syst. 31, 425–439. doi:10.1146/annurev.ecolsys.31.1.425

Kearney, M.S., Grace, R.E., Stevenson, J.C., 1988. Marsh Loss in Nanticoke Estuary, Chesapeake Bay. Geogr. Rev. 78, 205–220. doi:10.2307/214178

Kearney, M.S., Turner, R.E., 2016. Microtidal Marshes: Can These Widespread and Fragile Marshes Survive Increasing Climate–Sea Level Variability and Human Action? J. Coast. Res. 319, 686–699. doi:10.2112/JCOASTRES-D-15-00069.1

Kendrot, S.R., 2011. Restoration through eradication : protecting Chesapeake Bay marshlands from invasive nutria (Myocastor coypus), in: Veitch, C.R., Clout, M.N., Towns, D.R. (Eds.), Island Invasives: Eradication and Management. Proceedings of the International Conference on Island Invasives. Gland, Switzerland: IUCN and Auckland, New Zealand: CBB, pp. 313–319.

Kirwan, M.L., Guntenspergen, G.R., 2010. Influence of tidal range on the stability of coastal marshland. J. Geophys. Res. 115, F02009. doi:10.1029/2009JF001400

Marani, M., D'Alpaos, A., Lanzoni, S., Carniello, L., Rinaldo, A., 2010. The importance of being coupled: Stable states and catastrophic shifts in tidal biomorphodynamics. J. Geophys. Res. Earth Surf. 115, 1–15. doi:10.1029/2009JF001600

Mariotti, G., 2016. Revisiting salt marsh resilience to sea level rise: Are ponds responsible for permanent land loss? J. Geophys. Res. Earth Surf. 121, 1391–1407. doi:10.1002/2016JF003900

Mariotti, G., Carr, J., 2014. Dual role of salt marsh retreat: Long-term loss and short-term resilience. Water Resour. Res. 50, 2963–2974. doi:10.1002/2013WR014676

Mariotti, G., Fagherazzi, S., 2013. Critical width of tidal flats triggers marsh collapse in the absence of sea-level rise. Proc. Natl. Acad. Sci. U. S. A. 110, 5353–5356. doi:10.1073/pnas.1219600110

McLeod, E., Chmura, G.L., Bouillon, S., Salm, R., Björk, M., Duarte, C.M., Lovelock, C.E., Schlesinger, W.H., Silliman, B.R., 2011. A blueprint for blue carbon: Toward an improved understanding of the role of vegetated coastal habitats in sequestering CO2. Front. Ecol. Environ. 9, 552–560. doi:10.1890/110004

Millette, T.L., Argow, B.A., Marcano, E., Hayward, C., Hopkinson, C.S., Valentine, V., 2010. Integration of Multitemporal Multispectral Remote Sensing with LIDAR and GIS. J. Coast. Res. 265, 809–816. doi:10.2112/JCOASTRES-D-09-00101.1

Möller, I., Kudella, M., Rupprecht, F., Spencer, T., Paul, M., van Wesenbeeck, B.K., Wolters, G., Jensen, K., Bouma, T.J., Miranda-Lange, M., Schimmels, S., 2014. Wave attenuation over coastal salt marshes under storm surge conditions. Nat. Geosci. 7, 727–731. doi:10.1038/ngeo2251

Morris, J.T., Porter, D., Neet, M., Noble, P.A., Schmidt, L., Lapine, L.A., Jensen, J.R., 2005. Integrating LIDAR elevation data, multi-spectral imagery and neural network modelling for marsh characterization. Int. J. Remote Sens. 26, 5221–5234. doi:10.1080/01431160500219018

Morris, J.T., Sundareshwar, P. V., Nietch, C.T., Kjerfve, B., Cahoon, D.R., 2002. Responses of Coastal Wetlands to Rising Sea Level. Ecology 83, 2869–2877. doi:10.1890/0012-9658(2002)083[2869:ROCWTR]2.0.CO;2

Nyman, J.A., Carloss, M., DeLaune, R.D., Patrick, W.H., 1994. Erosion rather than plant dieback as the mechanism of marsh loss in an estuarine marsh. Earth Surf. Process. Landforms 19, 69–84. doi:10.1002/esp.3290190106

Ortiz, A.C., Roy, S., Edmonds, D.A., 2017. Land loss by pond expansion on the Mississippi River Delta Plain. Geophys. Res. Lett. 44, 3635–3642. doi:10.1002/2017GL073079

Ouyang, X., Lee, S.Y., 2014. Updated estimates of carbon accumulation rates in coastal marsh sediments. Biogeosciences 11, 5057–5071. doi:10.5194/bg-11-5057-2014

Pethick, J.S., 1981. Long-term Accretion Rates on Tidal

Salt Marshes. J. Sediment. Res. 51, 571–577. doi:10.1306/212F7CDE-2B24-11D7-8648000102C1865D

R Core Team, 2017. R: A Language and Environment for Statistical Computing, Vienna, Austria.

Raposa, K.B., Wasson, K., Smith, E., Crooks, J.A., Delgado, P., Fernald, S.H., Ferner, M.C., Helms, A., Hice, L.A., Mora, J.W., Puckett, B., Sanger, D., Shull, S., Spurrier, L., Stevens, R., Lerberg, S., 2016. Assessing tidal marsh resilience to sea-level rise at broad geographic scales with multi-metric indices. Biol. Conserv. 204, 263–275. doi:10.1016/j.biocon.2016.10.015

Raposa, K.B., Weber, R.L.J., Ekberg, M.C., Ferguson, W., 2017. Vegetation Dynamics in Rhode Island Salt Marshes During a Period of Accelerating Sea Level Rise and Extreme Sea Level Events. Estuaries and Coasts 40, 640–650. doi:10.1007/s12237-015-0018-4

Redfield, A.C., 1972. Development of a New England Salt Marsh. Ecol. Monogr. 42, 201–237. doi:10.2307/1942263

Rogerson, A., Mclaughlin, E., Havens, K., 2010. Mid-Atlantic Tidal Wetland Rapid Assessment Method Version 3.0.

Rohweder, J., Rogala, J.T., Johnson, B.L., Anderson, D., Clark, S., Chamberlin, F., Potter, D., Runyon, K., 2012. Application of wind fetch and wave models for habitat rehabilitation and enhancement projects—2012 update. U.S. Army Corp. Eng. Contract Rep. doi:10.1017/CBO9781107415324.004

Schepers, L., Kirwan, M., Guntenspergen, G., Temmerman, S., 2017. Spatio-temporal development of vegetation die-off in a submerging coastal marsh. Limnol. Oceanogr. 62, 137–150. doi:10.1002/lno.10381

Scott, M., McDermott, L., Silva, E., Watson, E., 2009. Project report: Digital Spatial Data Capture of Marsh Extent in Blackwater National Wildlife Refuge, 1938 and 2006. Eastern Shore Regional GIS Cooperative, Salisbury University.

Smith, S.M., 2009. Multi-Decadal Changes in Salt Marshes of Cape Cod, MA: Photographic Analyses of Vegetation Loss, Species Shifts, and Geomorphic Change. Northeast. Nat. 16, 183–208. doi:10.1656/045.016.0203

Stevenson, J.C., Kearney, M.S., Pendleton, E.C., 1985. Sedimentation and erosion in a Chesapeake Bay brackish marsh system. Mar. Geol. 67, 213–235. doi:10.1016/0025-3227(85)90093-3

Temmerman, S., Govers, G., Meire, P., Wartel, S., 2003. Modelling long-term tidal marsh growth under changing tidal conditions and suspended sediment concentrations, Scheldt estuary, Belgium. Mar. Geol. 193, 151–169. doi:10.1016/S0025-3227(02)00642-4

Temmerman, S., Meire, P., Bouma, T.J., Herman, P.M.J., Ysebaert, T., De Vriend, H.J., 2013. Ecosystem-based coastal defence in the face of global change. Nature 504, 79–83. doi:10.1038/nature12859

van Belzen, J., van de Koppel, J., Kirwan, M.L., van der Wal, D., Herman, P.M.J., Dakos, V., Kéfi, S., Scheffer, M., Guntenspergen, G.R., Bouma, T.J., 2017. Vegetation recovery in tidal marshes reveals critical slowing down under increased inundation. Nat. Commun. 8, 15811. doi:10.1038/ncomms15811

Wang, C., Temmerman, S., 2013. Does biogeomorphic feedback lead to abrupt shifts between alternative landscape states?: An empirical study on intertidal flats and marshes. J. Geophys. Res. Earth Surf. 118, 229–240. doi:10.1029/2012JF002474

Wigand, C., Carlisle, B., Smith, J., Carullo, M., Fillis, D., Charpentier, M., McKinney, R., Johnson, R., Heltshe, J., 2011. Development and validation of rapid assessment indices of condition for coastal tidal wetlands in southern New England, USA. Environ. Monit. Assess. 182, 31–46. doi:10.1007/s10661-010-1856-y

Wilson, C.A., Hughes, Z.J., FitzGerald, D.M., Hopkinson, C.S., Valentine, V., Kolker, A.S., 2014. Saltmarsh pool and tidal creek morphodynamics: Dynamic equilibrium of northern latitude saltmarshes? Geomorphology 213, 99–115. doi:10.1016/j.geomorph.2014.01.002

Wilson, K.R., Kelley, J.T., Tanner, B.R., Belknap, D.F., 2010. Probing the Origins and Stratigraphic Signature of Salt Pools from North-Temperate Marshes in Maine, U.S.A. J. Coast. Res. 26, 1007–1026. doi:10.2112/JCOASTRES-D-10-00007.1

6

Decreasing soil strength in relation to increasing coastal marsh submergence and marsh loss by pond expansion

Lennert Schepers, Matthew Kirwan, Glenn Guntenspergen, Stijn Temmerman

6.1 Abstract

Micro-tidal marshes are prone to lateral erosion, especially when sea level rise converts inner marshes to open-water ponds that are large enough to generate significant wind driven waves. The effective erosion, however, is not only determined by the wind-induced waves, but also by the soil erodibility and soil strength, and it is currently unknown how sea level rise is affecting the soil strength. In this study we studied soil strength in an organogenic micro-tidal system (Blackwater River, Maryland, U.S.A.), where large-scale conversion from marshes to shallow ponds resulted in a gradient of increasing marsh loss. In this study we demonstrate clear relationships between increasing inundation, lower belowground biomass and decreasing soil strength. Our results show that the marsh topsoil strength is high and related to belowground biomass (r=0.91), but decreases dramatically below 30 cm or when vegetation is absent. Pond soil strengths were very low. Our study indicates that the most flooded regions, which have the largest and deepest ponds, are especially vulnerable to pond expansion. As ponds deepen below the resistant marsh topsoil, the underlying loose layers are likely easily eroded. Additionally, weak pond bottom soil strengths might suspend and transport pond bottom sediments outside the marsh complex, which can hamper the recovery of these important coastal ecosystems.

6.2 Introduction

Marshes protect coastal areas against storm waves and surges (Temmerman et al., 2013; Möller et al., 2014; Stark et al., 2015), they are an important carbon sink (McLeod et al., 2011; Duarte et al., 2013) and provide necessary nursing grounds for marine fisheries (Barbier et al., 2011). Therefore these ecosystems are highly valued for their ecosystem services (Barbier et al., 2011). However, when sea level rise exceeds the capacity of tidal marshes to build vertically and horizontally, marshes are being replaced by interior ponds (Kearney et al., 1988; Nyman et al., 1993). The formation and lateral expansion of these ponds is widely regarded as one of the main mechanisms of large-scale marsh loss (Kearney et al., 1988; Penland et al., 2000; Morton et al., 2003; Mariotti and Fagherazzi, 2013; Mariotti, 2016), which severely affects their valuable ecosystem functions.

Lateral erosion in interior ponds is determined by the wave power and the erodibility or soil strength of the marsh substrate. While we focus in this paper on the variability in marsh soil strength, we interpret and discuss our results in terms of soil erodibility by waves, and therefore first start with an overview of the key factors determining the wave power in marshes. The wave power is a function of the wind speed, fetch length and the water depth of a tidal basin (Young and Verhagen, 1996a, 1996b; Fagherazzi and Wiberg, 2009). The wind fetch length, which is the unobstructed distance over which the wind can blow over a water surface, is controlled by the pond size. Modeling studies and aerial image analysis (Mariotti and Fagherazzi, 2013; Ortiz et al., 2017) have shown that when open water areas within marshes reach a critical threshold (200-1000 m), erosion of the marsh edges surrounding the open water areas accelerates due to the positive feedback between fetch length and wave size. Water depth also controls wave power, as waves do not build up to their full size in shallow water. The water depth has an internal positive feedback on erosion, since deeper water enables the generation of larger waves, which in turn can deepen the ponds again when wave shear stresses exceed the critical erosion threshold of the pond bottom. This feedback is however limited, since the shear stresses exerted by waves also decrease deeper in the water column. This creates an equilibrium water depth at which generated waves no longer erode the underlying pond bottom (Fagherazzi et al., 2006; Defina et al., 2007; Wilson and Allison, 2008).

How much lateral wave-induced erosion actually takes place, depends on the marsh soil strength or erodibility, which is an integrated measure of sediment properties and belowground plant biomass structure (Coops et al., 1996; Feagin et al., 2009; Chen et al., 2012; Francalanci et al., 2013; Wang et al., 2017). There have been some experimental studies that show the effect of increased sea level rise on belowground biomass production and decomposition. Kirwan and Guntenspergen (2012, 2015) for example demonstrated that a small increase in the hydroperiod (% of time the marsh is inundated) initially stimulates belowground plant growth, but productivity quickly declines when the hydroperiod becomes higher than 35-45 %. The decline of belowground productivity above a hydroperiod threshold has been confirmed by other experiments (Langley et al., 2013; Voss et al., 2013; Watson et al., 2014). The decomposition of organic material, which might also be important for the soil strength, is little affected by flooding (Kirwan et al., 2013; Mueller et al., 2016). Thus it seems that excessive flooding decreases belowground productivity, which might affect marsh soil strength.

However, apart from two studies mentioning weak soil strengths in deteriorating Mississippi deltaic marshes by (Howes et al., 2010; Day et al., 2011), the effect of increased flooding on soil strength has never been studied. We hypothesize that increasing inundation decreases belowground biomass and marsh soil strength. This is especially relevant because decreasing soil strength might amplify lateral wave erosion at the edges of large ponds and this might, when a critical threshold pond width has passed, lead to irreversible marsh erosion (Mariotti and Fagherazzi, 2013; Ortiz et al., 2017).

In this study, we quantified and analyzed the changes in soil strength along a well-documented gradient of increasing marsh submergence and marsh loss (Schepers et al., 2017) in the organogenic, micro-tidal Blackwater marshes (Maryland, USA). Also bare, unvegetated areas and ponds of different ages, sizes and depths were included to cover the whole marsh loss sequence, from intact marshes, to degraded marshes and ultimately ponds. Our analysis showed clear relationships between decreasing soil strength, decreasing belowground biomass and increasing tidal hydroperiod along the marsh loss gradient, and we discuss implications for lateral marsh erosion and marsh loss by pond expansion.

6.3 Methods

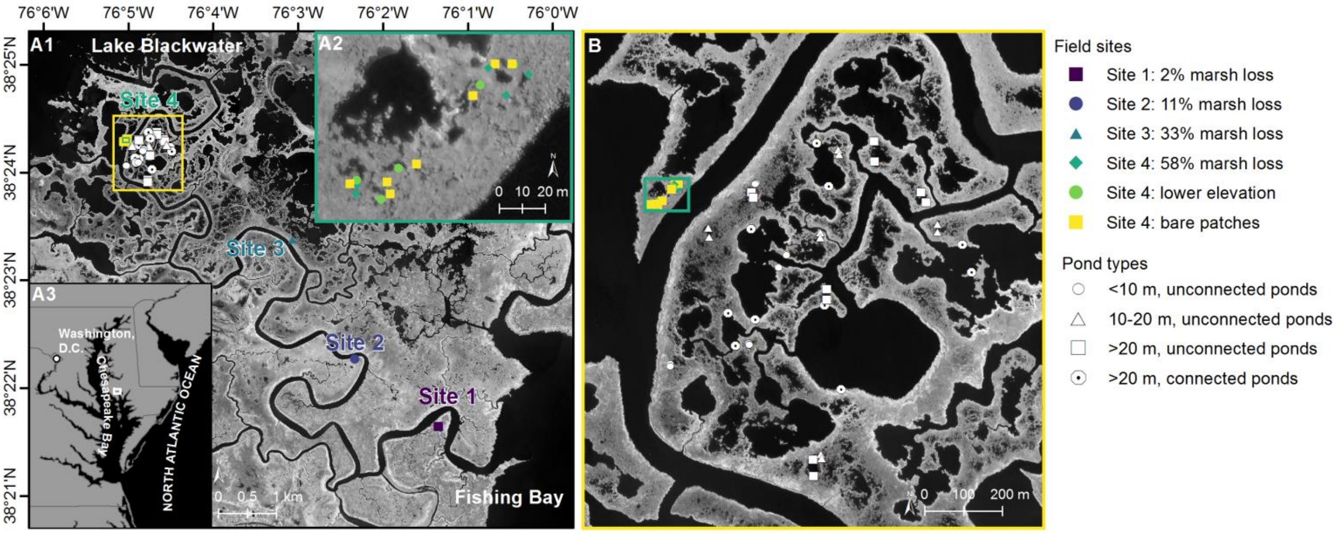

Figure 6.1: A1: Aerial images of the Blackwater marshes (black: water, grey: marsh) with indication of the field sites. The yellow box is the extent of figure B. A2: Marsh points sampled at site 4. A3: Position of the Blackwater marshes (white box) along the Chesapeake Bay, Maryland, USA. B. Pond points sampled at site 4. Green box is the extent of figure A2.

6.3.1 Study Area

The Blackwater River marshes (Maryland, USA: 38°24’ N, 76°40’ W, Fig. 6.1) are micro-tidal, brackish marshes bordered in the southeast by the Fishing Bay, a tributary of the Chesapeake Bay. Short-term measurements showed that salinity varies little (<2 ppt) between the most downstream site near Fishing Bay and upstream site at Lake Blackwater, but the salinity might change significantly on seasonal timescales (Fleming et al., 2011). The tidal range decreases from 63 cm close to field site 1 to 6 cm at Lake Blackwater, close to field site 4 (Fig 6.1 A1). The marshes are characterized by mesohaline marsh vegetation: *Spartina cynosuroides* is dominant in a small elevated band adjacent to the river and the bigger tidal channels. *Spartina alterniflora* and *Schoenoplectus americanus* are most abundant in the other areas, often in assemblages with *Spartina patens* and *Distichlis spicata* (Chapter 5).

There is a spatial gradient of increasing marsh loss in upstream direction along the Blackwater River, from intact marshes close to the bay (southeastern corner on Fig. 6.1 A1) to complete marsh loss at Lake Blackwater (northwestern corner of Fig. 6.1 A1), which is nowadays a vast open water area that historically consisted of expansive marshes as can be seen for example on aerial pictures back to 1938 (Stevenson et al. 1985; Chapter 2). Interestingly, in a previous study based on historical time series analyses of aerial pictures (Chapter 2), we showed that the spatial patterns of vegetation loss along the present-day spatial gradient of increasing vegetation loss resembles the historical, temporal development of marsh loss of the most degraded areas (Chapter 2).

The main causes of marsh loss that are considered for this area are insufficient surface accretion (on average 1.7-3.6 mm yr-1 (Stevenson et al. 1985)) compared to relative sea level rise (currently 3.7 mm yr-1 nearby in Cambridge, MD, (NOAA station 8571892, http://tidesandcurrents.noaa.gov/sltrends, 7/26/2017) leading to vegetation submergence, changes in soil conditions and ultimately die-off, as well as vegetation disturbance by Nutria (*Myocastor coypus*) (Stevenson et al., 1985; Kendrot, 2011), lateral erosion and expansion of the ponds (Stevenson et al., 1985; Ganju et al., 2013) and downstream export of the eroded material out of the marsh complex during northeasterly wind events (Ganju et al. 2013).

6.3.2 Sampling design

First we describe the selection of sampling locations, followed by an explanation of the belowground biomass properties that were measured. Along the marsh loss gradient, we selected four field sites with increasing proportion of open water areas as a measure of marsh loss rate (Fig. 6.1 A1) (Chapter 2, Chapter 4). At each field site, we selected five locations with monospecific stands of *Schoenoplectus americanus*. This species was selected since it is the most abundant in low elevation marsh zones surrounding existing ponds and hence expected to be most vulnerable to conversion to ponds (Chapter 5). Only locations located > 20 m from the river and > 1.5 m from ponds were selected to reduce any edge effect. The 5 locations at each field site had topographic elevations similar to the average elevation of the each site as measured in a previous field campaign (Chapter 4). At field site 4, we additionally selected 5 locations at a lower elevation than the average marsh elevation and 5 locations in small (ca. 0.5-5 m^2), bare patches surrounded by marsh vegetation. We also selected 20 ponds in field site 4, categorized into 4 pond classes, based on average diameter and connection to the tidal channel system: (i) <10 m (average) diameter and unconnected; (ii) 10-20 m (average) diameter and unconnected, (iii) >20 m (average) diameter and unconnected and (iv) >20 m diameter and connected to the channel network (Fig. 6.1 B). These classes correspond to different ages of the ponds, as the ponds of class 1 are visible since the aerial images of 1995-2010, class 2 ponds appear all since 1995, class 3 since 1981-1995 and class 4 since 1938-1981 (Chapter 4). At each pond, the north and south side was sampled (see Fig. 6.1).

At each of the locations described above (and see Fig. 6.1), the elevation relative to the North American Vertical Datum of 1988 (NAVD88) was recorded with a high-precision GPS (Trimble

R10 RTK-GPS, vertical error <1.5 cm). At the pond bottom locations we recorded 5 elevations within 1m along the pond edge to account for possible variability. Making use of tidal water level time series measured in each field site during a previous field campaign (using Hobo U20L-02 sensors; from August 14 to October 29, 2014, Chapter 4, Chapter 5), we calculated the duration of tidal inundation (hydroperiod) for each sampling location, as the % of time that the water level is higher than the elevation of the location.

6.3.3 Soil strength measurements

Soil strength was measured with two devices, a shear vane device and a soil penetrologger. The shear vane (H-4227 Vane Inspection Set, Humboldt Mfg. Co., USA) measures the maximum shear stress (N/m^2) to break the soil by torsion exerted by a rod fitted with four vanes that can be inserted into the soil and rotated at different depths. As such, this maximum shear stress to break the soil is further referred to as the shear vane soil strength (in N/m^2). At each marsh point, we measured the shear vane soil strength at just below the soil surface and at 30 cm below the soil surface. For ponds, we only performed measurements at the surface of the pond bottom. We also measured the cone penetration resistance (in N/m^2) with a soil penetrologger (06.15.SA, Ijkelkamp, NL). This device electronically records the force (N) needed to push a cone with a given surface area through the soil, while simultaneously registering the depth by an ultrasonic sensor. By dividing the force by the cone base area, the soil resistance in N/m^2 was calculated. Each soil strength measurement was replicated five times within 0.5 m from the gps point.

6.3.4 Belowground biomass sampling

Soil cores were collected with a 10.0 cm diameter stainless steel coring tube sampling the soil from the surface to a depth of 15 cm. A sharpened edge enabled to cut easily through the organic-rich soil, while an airtight plug enabled to take the core out of the soil without disturbance. The upper 15 cm of the pond substrate was sampled with a transparent tube with sharpened edges and vacuum cap. Half of each core was analyzed for belowground biomass fractions.

These were manually broken apart and thoroughly rinsed with a commercial kitchen spray arm above a 2mm screen to remove all the mineral particles. The rinsed belowground biomass was visually sorted into red rhizomes, white rhizomes, stems and the remaining litter fraction (macroremains) according to the descriptions in (Saunders et al., 2006). Each fraction was dried for minimum 60 h at 70°C to a constant weight. In the bare patches, we could not determine an exact volume, but we determined the relative contribution of the different types of belowground biomass.

Soil sampling and analysis

Soil cores were collected with a 10.0 cm diameter stainless steel coring tube sampling the soil from the surface to a depth of 15 cm. A sharpened edge enabled to cut easily through the organic-rich soil, while an airtight plug enabled to take the core out of the soil without disturbance. At the bare patches, the loose soil prevented us taking core samples of an exact volume, but grab samples of the upper 15 cm were taken for chemical analysis. The upper 15 cm of the pond substrate was sampled with a transparent tube with sharpened edges and vacuum cap.

At each point, two cores were sampled. One of the two cores was dried for minimum 120 h at 105°C to a constant weight to determine dry bulk density. Water content was determined by the difference in weight before and after drying. The other core was sliced in two half cores. One half was ground and homogenized with a 0.5 mm grinder (Retsch ZM2000) and ashed to 550° to determine the organic content of the soil samples (Loss On Ignition). The other half of the core was used to determine belowground biomass fractions.

The soil cores for belowground biomass analyses were manually broken apart and thoroughly rinsed with a commercial kitchen spray arm above a 2mm screen to remove all the mineral particles. The rinsed belowground biomass was visually sorted into red rhizomes, white rhizomes, stems and the remaining litter fraction (macroremains) according to the descriptions in (Saunders et al., 2006). Each fraction was dried for minimum 60 h at 70°C to a constant weight. In the bare patches, we could not determine an exact volume, but we determined the relative contribution of the different types of belowground biomass.

6.3.5 Statistical analyses

All analyses were performed and graphs were made in R (R Core Team, 2017). All soil strength measurements were combined per field site and pond type. At field site 4, we distinguished between the sampling locations at the average elevation (similar to the other field sites), the locations that were located at a lower elevation and small bare patches.

The penetrologger depths were converted to NAVD88 elevations for the marsh and pond locations of field site 4, while for the other field sites (having other NAVD88 elevations) they were referenced to the marsh surface. In this way the pond measurements can be directly compared with marsh measurements in field site 4, while the marsh measurements in the different field sites can also be compared in one graph. To visualize the data we used a moving average over depth intervals of 9 cm and visualized the standard error every 10 cm.

Correlations were tested with the Pearson's product moment correlation coefficient (referred to as Pearson’s correlation). Differences of soil strength between groups were tested by the non-parametric pairwise Wilcoxon rank sum test with Bonferroni correction (α=0.05).

6.4 Results and Discussion

6.4.1 Decreasing soil strength along marsh loss gradient

Table 6.1: Overview of the field sites with mean elevation, tidal range, hydroperiod and marsh loss percentage.

Field site	Elevation(m NAV88)	Mean tidal range (m)	Hydroperiod (%)	Marsh loss (%)
1	0.35	0.63	29.4	1.6
2	0.16	0.31	54.3	11.4
3	0.12	0.20	58.2	33.3
4	0.11	0.06	73.7	58.2
4-low	0.07	0.06	86.5	58.2
4-Bare patches	0.04	0.06	91.7	58.2

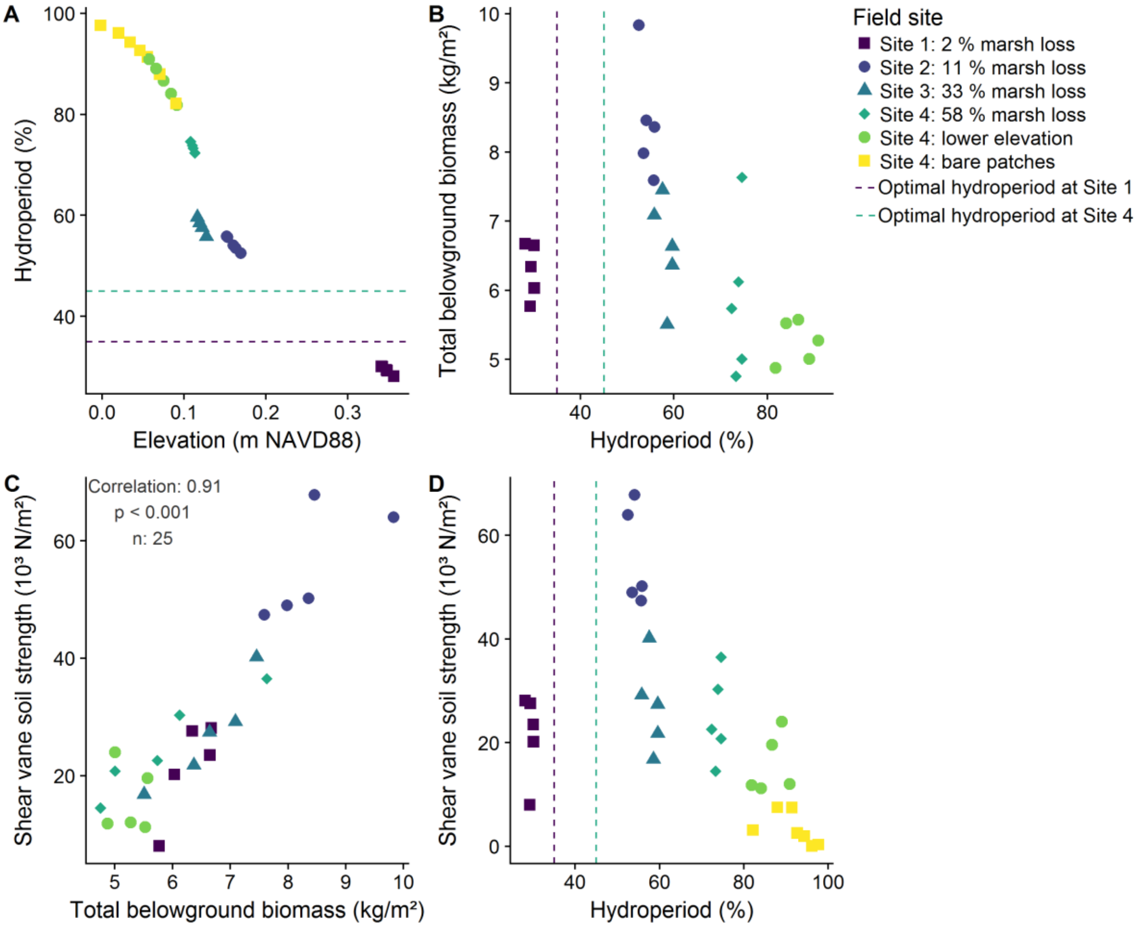

Figure 6.2: A: Relationship between site elevation (in m relative to the North American Vertical Datum of 1988) and hydroperiod (% of time inundated that the site is inundated). B: Total belowground biomass (in kg/m^2) versus hydroperiod. C: Total belowground biomass versus Shear vane soils strength. D: hydroperiod versus Shear vane soil strength. There is an increase in belowground biomass and soil strength (both are highly correlated) from field site 1 to field site 2, followed by a clear decrease from field site 2 to the lower plots of field site 4. The optimal hydroperiods for belowground biomass production as determined by an experimental setup close to field sites 1 and 4 (Kirwan & Guntenspergen, 2015) are indicated by dashed lines.

The field sites along the marsh loss gradient experience increasing hydroperiods, from 30 % (Table 6.1, Fig. 6.2A) at field site 1 to more than 90 % in the bare, unvegetated patches at field site 4. The hydroperiod has a clear effect on belowground biomass (Fig. 6.2B) and the shear vane soil strength (Fig. 6.2D), which are both highly correlated (Pearson's correlation 0.91, p <0.001, Fig. 6.2C). When field site 1 is excluded (discussion see below), the shear vane soil strength of the topsoil decreases with increasing hydroperiod (Pearson's correlation -0.83, p <0.001), this is evident from the shear vane data (Fig. 6.2D) as well as from the penetrologger data (Fig. 6.4). This corresponds to the gradient with increasing marsh loss (Fig. 6.1 A1, Table 6.1).

The shear vane soil strength just below the soil surface of the marsh is highly correlated with the total belowground biomass of the top 15 cm (Fig. 6.2C, Fig. 6.3). It seems that especially the amount of macroremains (the fraction >2mm that could not be identified) determines the soil strength (Fig. 6.3), as these show the highest correlation with the shear vane soil strength measurements (Pearson's correlation 0.82, $p < 0.001$, Fig. 6.3). Also the red rhizomes and the belowground stems show significant correlations (Fig. 6.3). These results match previous studies indicating that belowground marsh vegetation stabilizes the soil against erosion (Chen et al., 2012; Francalanci et al., 2013; Wang et al., 2017) and that belowground productivity declines above a hydroperiod threshold (Langley et al., 2013; Voss et al., 2013; Watson et al., 2014). It is likely that not only the hydroperiod but also the decreasing tidal range (Table 6.1) affects the soil drainage and the productivity of belowground biomass.

In the bare patches without aboveground vegetation there was a considerable amount of belowground biomass present, but red rhizomes were absent and the macroremains were generally composed of smaller particles, which is reflected in lower soil strength values (Fig. 6.2D).

Our results indicate that field site 1, which is the most intact marsh area with lowest hydroperiod, has a lower soil strength than field site 2, which seems to be contradictory. This can be explained by the fact that this study is focussed on *Schoenoplectus americanus* stands. *Schoenoplectus americanus* is considered a low marsh species (Nyman et al., 1994; Broome et al., 1995; Kirwan and Guntenspergen, 2015) and is only present on 11% of the typical high marsh area in field site 1 (Chapter 5). Also previous research suggests that *Schoenoplectus americanus* productivity is lower when less frequently inundated (Nyman et al., 1994; Kirwan and Guntenspergen, 2015). Kirwan and Guntenspergen (2015) concluded that the optimal hydroperiod for belowground productivity of *Schoenoplectus americanus* is between 35 and 45 % of the time as determined in an experimental setup close to field site 1 and 4, respectively (indicated by dashed lines in Fig. 6.2A,B,D) and that lower frequencies lead to lower root productivity. Field site 1 in our study floods less frequently (<30 %, Fig. 6.2A), which supports our findings that field site 2 has a higher belowground biomass and hence a higher soil strength than field site 1.

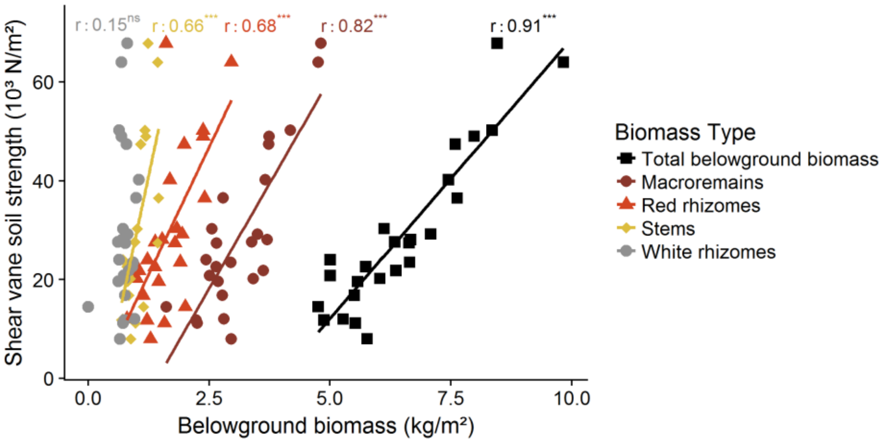

Figure 6.3: Correlation between different types of belowground biomass and the topsoil shear van soil strength (n=25). Total belowground biomass is the sum of all the components. Pearson's correlation coefficients are all highly significant (***: $p<0.001$) except for white rhizomes (ns: $p = 0.48$).

Table 6.2: Overview of the field sites with loss of ignition, water content and bulk density of the soil samples (upper 15 cm). Average values (n=5, bare patches n=7)±standard deviation.

Field site	Loss on Ignition (%)	Water content (%)	Bulk density (g/cm^3)
1	58.1±2.6	86.4±0.3	0.14±0.01
2	66.6±1.9	85.0±1.0	0.17±0.01
3	51.4±4.2	83.3±1.4	0.17±0.02
4	49.0±8.5	83.5±2.4	0.17±0.03
4-low	48.5±3.6	84.1±2.2	0.16±0.02
4-Bare patches	43.5±4.3	NA	NA

While clear differences in the belowground biomass exist between the different field sites (Fig. 6.2B, Table 6.2), the bulk density and water content changed little.

6.4.2 Decreasing soil strength with depth

Soil strength decreases dramatically when no vegetation is present or below 30 cm from the marsh surface (Fig. 6.4). The shear vane soil strengths at 30 cm depth (<3000 N/m^2) are all consistently lower than the surface measurements (>8000 N/m^2, compare Fig. 6.3 and Fig. 6.5), and there are only a very small changes in soil strength at 30 cm depth along the marsh loss gradient (Fig. 6.5). This indicates that an intact root mat provides structural stability in the upper 30 cm of the soil profile, but below this threshold depth both roots and the soil strength rapidly decrease. Although we only took soil samples of the upper 15 cm (see 6.3: Methods), several studies illustrate that the majority of the rhizomes and roots are situated in the top 15 cm of the soil profile (Valiela et al., 1976; Saunders et al., 2006).

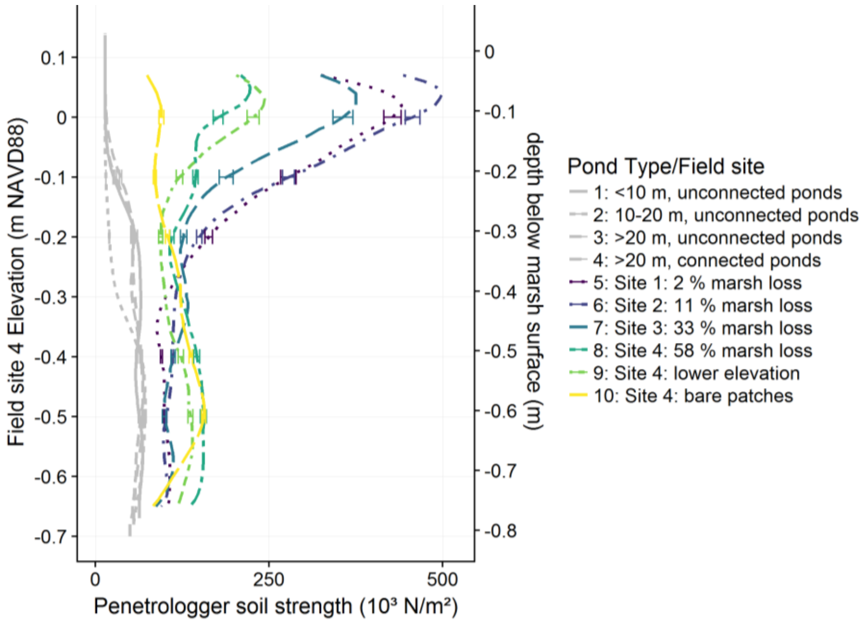

Figure 6.4: Penetrologger soil strength decreases with depth for the marsh sites. Bare patches and ponds have lower resistance than the marshes at the surface. Left y-axis is NAVD88 elevation for all sampling locations at field site 4, including bare patches and ponds. Right y-axis is elevation relative to marsh surface to compare the marsh sampling locations of the different field sites. A moving average over 9 cm depth intervals was calculated per site (n=25, ponds n=50), error bars every 10 cm depict standard errors.

6.4.3 Ponds have a low soil strength

The ponds have a much lower shear vane soil strength (generally below 3000 N/m^2, Fig. 6.5) than the vegetated marshes (8000 to 67 000 N/m^2, Fig. 6.3). All the ponds consisted of a loose ooze layer at the top of the soil profile, overlying deeper organic rich layers with varying strength. This seems to be a typical pond signature comparable to pond sediments in salt marshes in Maine (Wilson et al. 2010). No rhizomes or stems were found in the pond soil cores. There was however quite some organic material present in the top of the profile (Table 6.3), but this consisted of hard refractory material. These small rounded parts did not contribute to soil stabilization and were very different than the highly fibrous organic matrix in the marsh soils. These differences likely originate from degradation and decomposition of the organic soils after conversion of vegetated marshes into bare patches and ponds (Stevenson et al., 1985; DeLaune et al., 1994; van Huissteden and van de Plassche, 1998), resulting in a loose 'ooze' layer below the root zone and in the ponds. This weak layer might have important consequences for the stability of marshes facing lateral erosion.

Table 6.3: Overview of the Loss on ignition (%) of the different pond types. Average values (n=10)±standard deviation.

Pond type	Loss on ignition (%)
<10 m, unconnected ponds	43.9±9.7
10-20 m, unconnected ponds	44.4±9.8
>20 m, unconnected ponds	42.3±9.2
>20 m, connected ponds	39.8±8.5

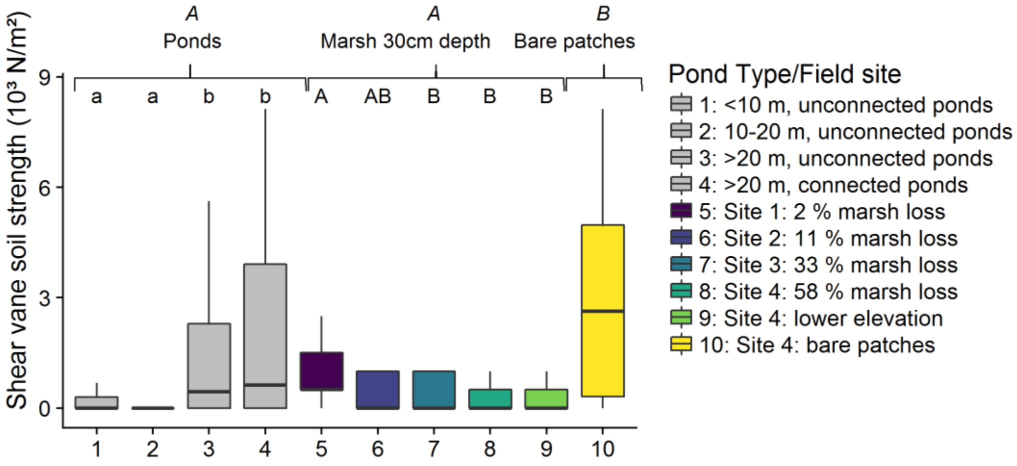

Figure 6.5: shear vane soil strength measurements of pond bottoms (n=50 for each boxplot), marsh soil at 30 cm depth (n=25 for each boxplot) and just below the soil surface of bare patches (n=35). Significant differences between pond types or marsh field sites have different letters (pairwise Wilcoxon rank sum test with Bonferroni correction, α= 0.05).

6.4.4 Vulnerability to lateral erosion

Our results indicate that the share vane soil strength values measured just below the marsh surface are high due to high amounts of belowground biomass. This corresponds with other studies demonstrating that vegetated marshes are robust in protecting the substrate against wave erosion (Möller, 2006; Gedan et al., 2011; Möller et al., 2014). In our study area, our analysis suggests that soil strengths are much lower when vegetation is absent (as measured in the bare patches)(Fig. 6.5).

The subsurface soil strength is, although significant differences exist, within the same range along the gradient (Fig. 6.5). Still, the increasing size and depth of the ponds with increasing marsh loss along the gradient makes the more degraded areas far more susceptible for lateral erosion. At the intact marsh sites, the ponds are too small (<20 m) and shallow (<0.5 m) to generate significant waves (Chapter 2, Chapter 4). With progressive marsh loss, ponds expand (Chapter 2) and deepen (Chapter 4). Once ponds deepen below the rooted zone of around 25 cm depth, the soil strength decreases dramatically (Fig. 6.5). Thus waves generated in large, deep ponds can easily erode the structurally weak marsh edge below the living root layer during low water periods, resulting in undercutting of rooted topsoil and ultimately cantilever failure and collapse of the rooted topsoil into the pond, which all together enhances lateral pond expansion. This has also been suggested by (Stevenson et al., 1985; Nyman et al., 1994), and our empirical study on soil strength confirms this hypothesis.

Three additional features might accelerate lateral marsh erosion in these systems. Firstly, pond edges are steep cliffs (Chapter 4), which makes them extremely vulnerable for wave attack. The deep ponds are also permanently submerged, which prevents pioneer plants to establish and protect the cliffs against further erosion as is observed in other marsh systems (van de Koppel et al., 2005; van der Wal et al., 2008; Wang et al., 2017). Secondly, research has shown that differential erodibility between a rooted top layer and underlying weaker soils promotes cantilever failures (Bendoni et al., 2016). These mass failures are found to increase lateral erosion (Bendoni et al., 2016). Lastly, connections of ponds with the tidal channel system might transport suspended material out of the ponds (Chapter 4) and possibly export it downstream out of the marsh system (Ganju et al., 2013, 2017). As such, the easily eroded material from the pond bottom or below the vegetated root zone is removed and enables further erosion of the pond edges instead of providing the necessary sediment to keep up with sea level rise. Thus not only the increasing wave power with increasing pond sizes, but also the topographic and soil properties enhance lateral marsh erosion in degraded marshes with ponds.

6.5 Conclusion

Our study shows that the soil strength in submerging marshes decreases with increased inundation along the marsh loss gradient, which is highly related to belowground biomass. However, even at the most degraded site, the structural root mat protects against lateral erosion as long as vegetation is present. In absence of vegetation or below the root zone, the soils are structurally weak and might be eroded by waves or currents.

How easily these weak layers are eroded, depends however on different spatial and topographic pond properties. The size and depth of ponds controls wave generation. The depth and the water level are especially relevant because they determine at which depth (and hence what soil strength) the waves are attacking the marsh edge. Hence we highlight that the pond properties are equally important as the strength measurements in determining long-term marsh stability. We conclude that the marshes with most marsh loss are more prone to lateral erosion, potentially leading to lateral runaway erosion.

Acknowledgements

This project was financed by an UA-BOF DOCPRO grant (to L.S. and S.T.), the Research Foundation Flanders (FWO, PhD grants L.S., 11S9614N & 11S9616N, travel grants L.S. K220916N), by the U.S. Geological Survey, Climate and Land-Use Research and Development Program (G.G.), by NSF GLD 1529245, NSF SEES 1426981, NSF LTER 1237733 (M.K.). We would like to thank the managers and biologists of the Blackwater National Wildlife Refuge for their assistance and valuable comments; Patrick Brennand and Liza McFarland (USGS) for indispensable field assistance. Steven Bouillon (KULeuven) assisted in analyzing soil samples. Any use of trade, product, or firm names is for descriptive purposes only and does not imply endorsement by the U.S. Government.

6.6 References

Barbier, E.B., Hacker, S.D., Kennedy, C., Koch, E.W., Stier, A.C., Silliman, B.R., 2011. The value of estuarine and coastal ecosystem services. Ecol. Monogr. 81, 169–193. doi:10.1890/10-1510.1

Bendoni, M., Mel, R., Solari, L., Lanzoni, S., Francalanci, S., Oumeraci, H., 2016. Insights into lateral marsh retreat mechanism through localized field measurements. Water Resour. Res. 52, 1446–1464. doi:10.1002/2015WR017966

Broome, S.W., Mendelssohn, I.A., McKee, K.L., 1995. Relative growth of Spartina patens (Ait.) Muhl. and Scirpus olneyi gray occurring in a mixed stand as affected by salinity and flooding depth. Wetlands 15, 20–30. doi:10.1007/BF03160676

Chen, Y., Thompson, C.E.L., Collins, M.B., 2012. Saltmarsh creek bank stability: Biostabilisation and consolidation with depth. Cont. Shelf Res. 35, 64–74. doi:10.1016/j.csr.2011.12.009

Coops, H., Geilen, N., Verheij, H.J., Boeters, R., van der Velde, G., 1996. Interactions between waves, bank erosion and emergent vegetation: an experimental study in a wave tank. Aquat. Bot. 53, 187–198. doi:10.1016/0304-3770(96)01027-3

Day, J.W., Kemp, G.P., Reed, D.J., Cahoon, D.R., Boumans, R.M., Suhayda, J.M., Gambrell, R., 2011. Vegetation death and rapid loss of surface elevation in two contrasting Mississippi delta salt marshes: The role of sedimentation, autocompaction and sea-level rise. Ecol. Eng. 37, 229–240. doi:10.1016/j.ecoleng.2010.11.021

Defina, A., Carniello, L., Fagherazzi, S., D'Alpaos, L., 2007. Self-organization of shallow basins in tidal flats and salt marshes. J. Geophys. Res. Earth Surf. 112, 1–11. doi:10.1029/2006JF000550

DeLaune, R.D., Nyman, J.A., Patrick, W.H., 1994. Peat collapse, ponding and wetland loss in a rapidly submerging coastal marsh. J. Coast. Res. 10, 1021–1030.

Duarte, C.M., Losada, I.J., Hendriks, I.E., Mazarrasa, I., Marbà, N., 2013. The role of coastal plant communities for climate change mitigation and adaptation. Nat. Clim. Chang. 3, 961–968. doi:10.1038/nclimate1970

Fagherazzi, S., Carniello, L., D'Alpaos, L., Defina, A., 2006. Critical bifurcation of shallow microtidal landforms in tidal flats and salt marshes. Proc. Natl. Acad. Sci. U. S. A. 103, 8337–8341. doi:10.1073/pnas.0508379103

Fagherazzi, S., Wiberg, P.L., 2009. Importance of wind conditions, fetch, and water levels on wave-generated shear stresses in shallow intertidal basins. J. Geophys. Res. Solid Earth 114, 1–12. doi:10.1029/2008JF001139

Feagin, R.A., Lozada-Bernard, S.M., Ravens, T.M., Möller, I., Yeager, K.M., Baird, A.H., 2009. Does vegetation prevent wave erosion of salt marsh edges? Proc. Natl. Acad. Sci. U. S. A. 106, 10109–13. doi:10.1073/pnas.0901297106

Fleming, B.J., DeJong, B.D., Phelan, D.J., 2011. Geology, hydrology, and water quality of the Little Blackwater River watershed, Dorchester County, Maryland, 2006–09: U.S. Geological Survey Scientific Investigations Report 2011–5054. http://pubs.usgs.gov/sir/2011/5054/.

Francalanci, S., Bendoni, M., Rinaldi, M., Solari, L., 2013. Ecomorphodynamic evolution of salt marshes: Experimental observations of bank retreat processes. Geomorphology 195, 53–65. doi:10.1016/j.geomorph.2013.04.026

Ganju, N.K., Defne, Z., Kirwan, M.L., Fagherazzi, S., D'Alpaos, A., Carniello, L., 2017. Spatially integrative metrics reveal hidden vulnerability of microtidal salt marshes. Nat. Commun. 8, 14156. doi:10.1038/ncomms14156

Ganju, N.K., Nidzieko, N.J., Kirwan, M.L., 2013. Inferring tidal wetland stability from channel sediment fluxes: Observations and a conceptual model. J. Geophys. Res. Earth Surf. 118, 2045–2058. doi:10.1002/jgrf.20143

Gedan, K.B., Kirwan, M.L., Wolanski, E., Barbier, E.B., Silliman, B.R., 2011. The present and future role of coastal wetland vegetation in protecting shorelines: Answering recent challenges to the paradigm. Clim. Change 106, 7–29. doi:10.1007/s10584-010-0003-7

Howes, N.C., FitzGerald, D.M., Hughes, Z.J., Georgiou, I.Y., Kulp, M.A., Miner, M.D., Smith, J.M., Barras, J.A., 2010. Hurricane-induced failure of low salinity wetlands. Proc. Natl. Acad. Sci. 107, 14014–14019. doi:10.1073/pnas.0914582107

Kearney, M.S., Grace, R.E., Stevenson, J.C., 1988. Marsh Loss in Nanticoke Estuary, Chesapeake Bay. Geogr. Rev. 78, 205–220. doi:10.2307/214178

Kendrot, S.R., 2011. Restoration through eradication : protecting Chesapeake Bay marshlands from invasive nutria (Myocastor coypus), in: Veitch, C.R., Clout, M.N., Towns, D.R. (Eds.), Island Invasives: Eradication and Management. Proceedings of the International Conference on Island Invasives. Gland, Switzerland: IUCN and Auckland, New Zealand: CBB, pp. 313–319.

Kirwan, M.L., Guntenspergen, G.R., 2015. Response of Plant Productivity to Experimental Flooding in a Stable and a Submerging Marsh. Ecosystems 18, 903–913. doi:10.1007/s10021-015-9870-0

Kirwan, M.L., Guntenspergen, G.R., 2012. Feedbacks between inundation, root production, and shoot growth in a rapidly submerging brackish marsh. J. Ecol. 100, 764–770. doi:10.1111/j.1365-2745.2012.01957.x

Kirwan, M.L., Langley, J.A., Guntenspergen, G.R., Megonigal, J.P., 2013. The impact of sea-level rise on organic matter decay rates in Chesapeake Bay brackish tidal marshes. Biogeosciences 10, 1869–1876.

Langley, J.A., Mozdzer, T.J., Shepard, K.A., Hagerty, S.B., Megonigal, J.P., 2013. Tidal marsh plant responses to elevated CO2, nitrogen fertilization, and sea level rise. Glob. Chang. Biol. 19, 1495–1503. doi:10.1111/gcb.12147

Mariotti, G., 2016. Revisiting salt marsh resilience to sea level rise: Are ponds responsible for permanent land loss? J. Geophys. Res. Earth Surf. 121, 1391–1407. doi:10.1002/2016JF003900

Mariotti, G., Fagherazzi, S., 2013. Critical width of tidal flats triggers marsh collapse in the absence of sea-level rise. Proc. Natl. Acad. Sci. U. S. A. 110, 5353–5356. doi:10.1073/pnas.1219600110

McLeod, E., Chmura, G.L., Bouillon, S., Salm, R., Björk, M., Duarte, C.M., Lovelock, C.E., Schlesinger, W.H., Silliman, B.R., 2011. A blueprint for blue carbon: Toward an improved understanding of the role of vegetated coastal habitats in sequestering CO2. Front. Ecol. Environ. 9, 552–560. doi:10.1890/110004

Möller, I., 2006. Quantifying saltmarsh vegetation and its effect on wave height dissipation: Results from a UK East coast saltmarsh. Estuar. Coast. Shelf Sci. 69, 337–351. doi:10.1016/j.ecss.2006.05.003

Möller, I., Kudella, M., Rupprecht, F., Spencer, T., Paul, M., van Wesenbeeck, B.K., Wolters, G., Jensen, K., Bouma, T.J., Miranda-Lange, M., Schimmels, S., 2014. Wave attenuation over coastal salt marshes under storm surge conditions. Nat. Geosci. 7, 727–731. doi:10.1038/ngeo2251

Morton, R.A., Tiling, G., Ferina, N.F., 2003. Causes of hot-spot wetland loss in the Mississippi delta plain. Environ. Geosci. 10, 71–80. doi:10.1306/eg100202007

Mueller, P., Jensen, K., Megonigal, J.P., 2016. Plants mediate soil organic matter decomposition in response to sea level rise. Glob. Chang. Biol. 22, 404–414. doi:10.1111/gcb.13082

Nyman, J.A., Carloss, M., DeLaune, R.D., Patrick, W.H., 1994. Erosion rather than plant dieback as the mechanism of marsh loss in an estuarine marsh. Earth Surf. Process. Landforms 19, 69–84. doi:10.1002/esp.3290190106

Nyman, J.A., DeLaune, R.D., Roberts, H.H., Patrick, W.H., 1993. Relationship between vegetation and soil formation in a rapidly submerging coastal marsh. Mar. Ecol. Prog. Ser. 96, 269–279. doi:10.3354/meps096269

Ortiz, A.C., Roy, S., Edmonds, D.A., 2017. Land loss by pond expansion on the Mississippi River Delta Plain. Geophys. Res. Lett. 44, 3635–3642. doi:10.1002/2017GL073079

Penland, S., Wayne, L., Britsch, D., Williams, S.J., Beall, A.D., Butterworth, V., 2000. Geomorphic Classification of Coastal Land Loss between 1932 and 1990 in the Mississippi River Delta Plain, Southeastern Louisiana. USGS Open File Report 00-417. https://pubs.usgs.gov/of/2000/of00-417/.

R Core Team, 2017. R: A Language and Environment for Statistical Computing, Vienna, Austria.

Saunders, C.J., Megonigal, J.P., Reynolds, J.F., 2006. Comparison of belowground biomass in C3- and C4-dominated mixed communities in a Chesapeake Bay brackish marsh. Plant Soil 280, 305–322. doi:10.1007/s11104-005-3275-3

Schepers, L., Kirwan, M., Guntenspergen, G., Temmerman, S., 2017. Spatio-temporal development of vegetation die-off in a submerging coastal marsh. Limnol. Oceanogr. 62, 137–150. doi:10.1002/lno.10381

Stark, J., Van Oyen, T., Meire, P., Temmerman, S., 2015. Observations of tidal and storm surge attenuation in a large tidal marsh. Limnol. Oceanogr. 60, 1371–1381. doi:10.1002/lno.10104

Stevenson, J.C., Kearney, M.S., Pendleton, E.C., 1985. Sedimentation and erosion in a Chesapeake Bay brackish marsh system. Mar. Geol. 67, 213–235. doi:10.1016/0025-3227(85)90093-3

Temmerman, S., Meire, P., Bouma, T.J., Herman, P.M.J., Ysebaert, T., De Vriend, H.J., 2013. Ecosystem-based coastal defence in the face of global change. Nature 504, 79–83. doi:10.1038/nature12859

Valiela, I., Teal, J.M., Persson, N.Y., 1976. Production and dynamics of experimentally enriched salt marsh vegetation: Belowground biomass. Limnol. Oceanogr. 21, 245–252. doi:10.4319/lo.1976.21.2.0245

van de Koppel, J., van der Wal, D., Bakker, J.P., Herman, P.M.J., 2005. Self-Organization and Vegetation Collapse in Salt Marsh Ecosystems. Am. Nat. 165, E1–E12. doi:10.1086/426602

van der Wal, D., Wielemaker-Van den Dool, A., Herman, P.M.J., 2008. Spatial patterns, rates and mechanisms of saltmarsh cycles (Westerschelde, The Netherlands). Estuar. Coast. Shelf Sci. 76, 357–368. doi:10.1016/j.ecss.2007.07.017

van Huissteden, J., van de Plassche, O., 1998. Sulphate reduction as a geomorphological agent in tidal marshes ("Great Marshes" at Barnstable, Cape Cod, USA). Earth Surf. Process. Landforms 23, 223–236. doi:10.1002/(SICI)1096-9837(199803)23:3<223::AID-ESP843>3.0.CO;2-I

Voss, C.M., Christian, R.R., Morris, J.T., 2013. Marsh macrophyte responses to inundation anticipate impacts of sea-level rise and indicate ongoing drowning of North Carolina marshes. Mar. Biol. 160, 181–194. doi:10.1007/s00227-012-2076-5

Wang, H., van der Wal, D., Li, X., van Belzen, J., Herman, P.M.J., Hu, Z., Ge, Z., Zhang, L., Bouma, T.J., 2017. Zooming in and out: Scale dependence of extrinsic and intrinsic factors affecting salt marsh erosion. J. Geophys. Res. Earth Surf. 122, 1455–1470. doi:10.1002/2016JF004193

Watson, E.B., Oczkowski, A.J., Wigand, C., Hanson, A.R., Davey, E.W., Crosby, S.C., Johnson, R.L., Andrews, H.M., 2014. Nutrient enrichment and precipitation changes do not enhance resiliency of salt marshes to sea level rise in the Northeastern U.S. Clim. Change 125, 501–509. doi:10.1007/s10584-014-1189-x

Wilson, C.A., Allison, M.A., 2008. An equilibrium profile model for retreating marsh shorelines in southeast Louisiana. Estuar. Coast. Shelf Sci. 80, 483–494. doi:10.1016/j.ecss.2008.09.004

Young, I.R., Verhagen, L.A., 1996a. The growth of fetch limited waves in water of finite depth. Part 1. Total energy and peak frequency. Coast. Eng. 29, 47–78. doi:10.1016/S0378-3839(96)00006-3

Young, I.R., Verhagen, L.A., 1996b. The growth of fetch limited waves in water of finite depth. Part 2. Spectral evolution. Coast. Eng. 29, 101–121. doi:10.1016/S0378-3839(96)00026-9

7

Synthesis

7.1 Objectives of this thesis

In this thesis, we focused on the loss of coastal marshes, which has been observed in several places around the world and due to which valuable ecosystem services of coastal marshes are reduced.

Throughout this thesis, we pursued the general aim of determining the spatial patterns of vegetation loss (**Chapter 2**) and to reveal their bio-geomorphological effect on flow and sedimentation dynamics. We studied short-term effects of the spatial patterns of vegetation loss on tidal flow and sedimentation patterns (**Chapter 3**), as well as long-term effects on elevation of marshes and ponds (**Chapter 4**). We tested if two marsh metrics, the skewness of the marsh elevations and the co-occurrence of species in mixtures, can be used to assess marsh vulnerability to sea level rise and thus foresee marsh loss (**Chapter 5**). Finally, we tested how belowground biomass affects soil strength and potential marsh erosion (**Chapter 6**). We particularly tried to cover the full spectrum of marsh loss, from intact marshes to large open water areas. In the next paragraph, we combine the insights from the different chapters to outline and highlight the evolution and the processes involved in marsh loss.

7.2 The evolution of marsh loss: from intact marshes to shallow lakes

By analyzing aerial images since 1938 (**Chapter 2**) we demonstrated that marsh vegetation loss is a gradual process with distinct spatial patterns. This is schematically visualized in the top panel of Figure 7.1 ‘plan view’, from intact marshes (left side) to degraded marshes (right-hand side). In the lower panel, we schematized a cross-section of a similar gradient (left intact, right degraded). Numbers between brackets refer to the numbers on these schemes.

The initial vegetation loss starts as small areas at a far distance (> 75 m) from tidal channels and these restricted bare areas are still surrounded by intact marsh vegetation **(1).** Topographic measurements showed that these initial marsh loss areas are bare patches with a similar elevation as the marsh platform **(2)** (**Chapter 4**). The results of our field experiment (**Chapter 3**) show that the effect of these small, bare patches on the flow velocities is negligible, as long as the bare patches are small (< 20 m) and a surrounding buffer of vegetation between the channels and inner marsh is still intact. The marshes experiencing little vegetation loss are typically positioned high in the tidal frame, close to the mean high water level, resulting in a left-tailed elevation distribution, indicative of resilient marshes with a high elevation capital (indicated as **(2)**, green vegetation in Fig. 7.1) (**Chapter 5**). The marshes are even positioned higher than the optimal elevation for maximum belowground biomass (**Chapter 6**).

As inundation becomes more frequent, the initial bare patches deepen and develop into continuously submerged ponds **(3)** (**Chapter 4**). Smaller ponds enlarge horizontally, leading to complex patterns of ponds and remaining marsh vegetation **(4).** In the largest ponds (> 100 m), wind-induced wave generation might start to erode the soft layers beneath the strong, vegetated root mat **(5)**(**Chapter 6**) or suspend the pond substrate, which is a loose ooze layer, probably the end product of biochemical decomposition of the root mat or deeper peat layers. These sediments are generally not exported as long as the ponds are still surrounded by marsh vegetation.

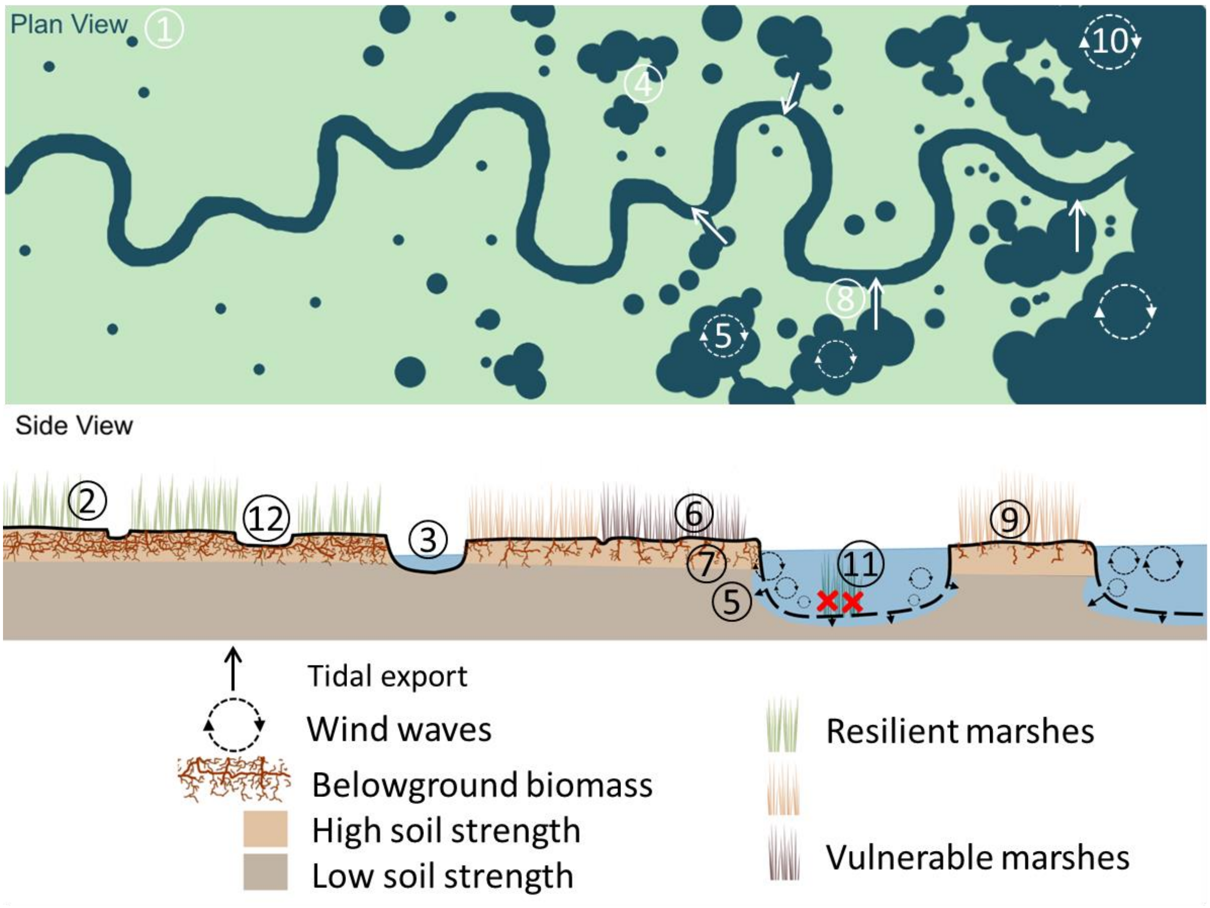

Figure 7.1: Schematic overview of marsh loss from intact marshes at the left-hand side to extensive marsh loss (right-hand side). The top panel is a plan view, the lower panel a cross-section. Numbers refer to descriptions in the text.

Within the remaining marshes, the effect of die-off in the surrounding areas on flow and sedimentation patterns is limited (**Chapter 3**). Topographic measurements demonstrated that marsh elevation decreases with increasing distance from the river (**Chapter 4**), showing the long-term effect of marsh vegetation reducing flow velocities and promoting sediment deposition along the channels (**Chapter 3**). When the lowest areas have been converted into ponds, the elevation of the remaining marsh areas approaches normal distributions (**Chapter 5**). However, at several places, marsh vegetation species are co-occurring, which we interpret as a sign of more stressed conditions **(6)** (**Chapter 5**). The effect of prolonged inundation is also visible in the soil cores as excessive flooding limits belowground biomass productivity and leads to lower soil strength **(7)** (**Chapter 6**).

When ponds continue to increase in size, they ultimately become connected to the tidal channel system **(8)**. This has important consequences for the tidal currents, as flow velocities are significantly increased in unvegetated (mowed) corridors (**Chapter 3**). In this way, eroded pond sediments might be exported out of the ponds which may explain why ponds are generally deeper when channels are wider and connecting the ponds to the broader channel network **(8)** (**Chapter 4**). Significant wave erosion during storm events along the largest ponds lead to high suspended sediment concentrations (Ganju et al 2013), which locally benefits the leftover marshes **(9)**, leading to sufficient accretion relative to sea level rise (Cahoon et al. 2010, Guntenspergen 2017, unpublished data). However, the vertical survival of the marshes will eventually be superseded by horizontal erosion due to the positive feedbacks between pond size, connection to the tidal system and erosion, which will eventually lead to a runaway process of permanent marsh loss **(10)** (Mariotti and Fagherazzi, 2013).

7.3 Feedback mechanisms make natural recovery unlikely

We showed that marshes and ponds can be regarded as two alternative elevation and vegetation states (**Chapter 4**), implying that recovery from the pond state to the vegetated marsh state might be particularly difficult due to positive feedback mechanisms stabilizing the pond state.

Indeed, the spatial transitions from ponds to marshes are steep **(5)** and pond deepening occurs non-linearly with time (**Chapter 4**), which makes it unlikely that vegetation will be able to recolonize the ponds **(11)**. The vertical soil structure, showing a resistant root mat up to 30 cm below the soil surface but very weak layers below the reach of the roots **(7 & 5)**(**Chapter 6**), explains these two observations. Initial bare ponds and shallow ponds (< 25 cm deep) only affect the resistant root mat **(12)**(**Chapter 4**). From the moment this resistant layer has been eroded **(3)**, the underlying loose layers are eroded much faster **(5)**. This results in non-linear deepening **(Chapter 4**). The steep transitions from the marsh platform into the ponds probably result from undercutting of the vegetated mat **(5)**.

Furthermore, we showed in **Chapter 6** that there is a positive feedback between marsh loss and wave erosion, due to increased pond size and wind fetch **(5)**, deeper ponds and the above-described vertical soil structure. The soil strength of the rooted mat decreases with hydroperiod and marsh loss **(7)** (**Chapter 6**). This might indirectly lead to more marsh loss, as weaker root zones probably also lead to higher root zone subsidence, an important process in the Blackwater marshes (Cahoon et al., 2010) determining the subsidence and flooding frequency of the wetland.

The connection of ponds with the channels might increase local flow velocities **(5)** (**Chapter 3**) and might lead erosion of the pond bottom (**Chapter 4**).

Thus, we conclude that natural recovery of the studied submerging marshes is rather unlikely.

7.4 Implications for restoration – lessons learned

Our results have important implications for management aiming at restoration of submerging marshes. Although several feedback mechanisms prevent natural recovery of the marshes (see previous paragraph), some guidelines to protect existing marshes against further marsh loss or to strategically restore parts of the marshes, might still be interesting in order to benefit as long as possible from the ecosystem services that these irreplaceable wetlands provide.

First, we could not detect any recovery of the coastal Blackwater Marshes since 1938. This drastic example shows that early recognition of the vulnerability for vegetation loss is needed to foresee pending shifts from the vegetated marsh state to the bare pond state. In **Chapter 5** we demonstrated empirically that two new indicators, the skewness of the marsh elevations and the co-occurrence of species in mixtures, were reliable proxies for estimating overall marsh stress. However, all indices, including newly developed indicators especially targeting the estimation of vulnerability to sea level rise, failed to correctly assess the most degraded state, probably due to internally generated sediment from eroding marshes. Thus the indices might correctly assess the initial stages of marsh stress, but in highly degraded areas the results should be interpreted with caution. Including a measure of the soil strength of the upper 30 cm of the soil (also included in the (Cole Ekberg et al., 2017) vulnerability) might improve the results of this vulnerability index (**Chapter 6**). We suggest in **Chapter 5** to include sediment flux measurements, as proposed by Ganju et al. (2013, 2015, 2017), since the sediment budget will ultimately determine the final course of the marsh (French, 2006; Mariotti and Carr, 2014; Ganju et al., 2015, 2017; Mariotti, 2016). Recently, van Belzen et al. (2017) provided empirical evidence that declining recovery rates after disturbance indicate apparent shifts. This is in line with findings of Slocum and Mendelssohn (2008), who observed faster rates of recovery with low stress (sediment-rich) compared to no recovery in highly stressed (no sediment availability) areas. This indicator can easily be applied to our study area.

When a marsh is considered vulnerable, one should counteract pending marsh loss as quickly as possible, because recovery is unlikely (see previous paragraph). However, the best option is to draft a holistic management plan of the whole marsh complex, rather than focusing on the affected sites. For example, local installation of a breakwater might prevent further wave erosion, but still be unsuccessful by not taking into account the sediment budget of the system (Ravens et al., 2009). Thus, in sediment-limited areas one could focus on retaining marshes, preferably sheltered from the most dominant winds, while enabling others to erode and generate sediments for the remaining marshes. This is what Mariotti and Carr (2014) describe as the modular management strategy, allowing certain ponds to slowly expand and thereby increasing the sediment supply to feed the marsh platform and as such prevent large-scale marsh drowning. However, determining the fate of this internally generated sediment is crucial, since our results show that a connection with the tidal channel system might export the majority of the sediment (**Chapter 4**) out of the system without locally increasing the sediment budget, which is also highlighted by large-scale sediment flux studies (Ganju et al., 2015, 2017). One could prevent such critical sediment export by installing a sluice or weirs during sediment-export conditions and removing these sediment barriers when sediment import conditions prevail.

7.5 Applicability of our findings to other areas

Our study mainly focussed on one specific marsh system with organogenic soils, low mineral suspended sediment concentrations, a low tidal range and a high rate of sea level rise. The combination of these factors lead to the marsh loss in our study area and the processes that we observed. As such, the same processes would probably also apply for other areas with similar characteristics. Kearney and Turner (2016) however indicate that most of these factors are related: a micro-tidal range (< 2 m tidal range) generates flood velocities that are too low to import appreciable mineral sediment to the marshes, and this is also the reason why they rely mostly on organic accumulation to keep up with sea level rise.

Micro-tidal marshes are widely present in the contiguous United States, where 59% of all coastal marshes have a tidal range lower than 1 m. These marshes are concentrated in the Chesapeake and Delaware Bay, and the Mississippi River deltaic plain (Kearney and Turner, 2016). Micro-tidal marshes are also present in other areas at middle lattitudes like the Venice Lagoon (e.g. Day et al., 1998; Carniello et al., 2009), the Baltic Sea (e.g. Möller et al., 2011), or the Rio de la Plata in Argentina (Cellone et al., 2016).

When sea level rise rates are high e.g. by the subsidence of the glacial forebulb at the US middle Atlantic Coast (Engelhart et al., 2009) or the subsiding Mississippi Delta (Day et al., 2007), it is likely that similar marsh loss as in our study area is happening here. Indeed, it is known that several marshes from the Chesapeake Bay and Delaware Bay (Stevenson et al., 1985; Kearney et al., 1988, 2002) and the Mississippi River deltaic plain are degrading (Turner and Cahoon, 1987; DeLaune et al., 1994; Penland et al., 2000; Morton et al., 2003; Day et al., 2007, 2011; Wilson and Allison, 2008; Ortiz et al., 2017).

In the more tropical areas, organogenic mangrove forests with low tidal ranges are mainly focussed on the Caribbean region (Balke and Friess, 2016). Interestingly, rapid peat collapse and a decrease in stability has also been observed in these systems after die-off events (Cahoon et al., 2003; Mckee et al., 2007) or disturbances (McKee and Vervaeke, 2009). However, the different morphology of mangrove trees and roots compared to tidal marshes might hamper direct comparisons between mangroves and marshes.

Even if the abovementioned micro-tidal areas are keeping up with sea level rise (and the results of this thesis would not be directly applicable), increasing rates of sea level rise or local changes in the sediment supply (e.g. by diverting rivers, constructing dams,…) might shift these systems to degrading systems. The indices in **Chapter 5** are in these scenarios useful to monitor the vulnerability of coastal marshes.

A large part of this thesis was focussed on the spatial patterns of vegetation loss and their effect on flow and sedimentation patterns. We demonstrated in **Chapter 2** that the marsh platform next to the river is most stable and experiences little marsh loss, likely due to a higher elevation (**Chapter 4**). This corresponds to typical levee-basin structures that are omnipresent in coastal marshes (e.g. Temmerman et al. (2004) and references therein). Our field experiment (**Chapter 3**) demonstrated the effect of these general vegetation patterns on flow and sedimentation patterns. However, there are a number of processes (besides marsh drowning, which we studied in this thesis), that can remove or disturb (inner) marsh vegetation, such as salt stress (Delaune and Pezeshki, 1994; Silliman et al., 2005; Baustian et al., 2012), herbivory by crabs (Perillo and Iribarne, 2003; Holdredge et al., 2009; Hughes et al., 2009), snails (Stevenson et al., 1985; Silliman et al., 2005; Kirwan et al., 2008) or geese (Esselink et al., 1997; Handa et al., 2002; Jefferies et al., 2006; Kotanen and Abraham, 2013; Elschot et al., 2017) or a physical disturbance by tidal deposition of litter or ice rafting (Pethick, 1974; Boston, 1983; Ewanchuk and Bertness, 2003). Also livestock grazing, which has a long tradition in the European Wadden Sea marshes, changes the vegetation structure by reducing the vegetation height (Elschot et al., 2013; Nolte et al., 2015), which is comparable to our mowing experiment. By focussing our field experiment (**Chapter 3**) on the effect of the general vegetation patterns rather than focussing on site-specific causes of vegetation disturbance, we think that our general conclusions can be more broadly applicable to areas where the same patterns are observed.

The magnitude of these effects, however, will depend on local factors such as tidal amplitude, marsh morphology and suspended sediment concentrations.

7.6 Limitations of this study and recommendations for further research

A PhD thesis is limited by a number of factors, especially time constraints, which affects the scope and the completeness of this work. As such, several important aspects of submerging marshes are not included in this thesis, but can be an inspiration for further research.

First of all, I approached the evolution of marsh loss given the historical extent of the marsh, thereby neglecting the capability of many organisms to migrate to locations with better conditions. Particularly, I did not include lateral marsh creation by seaward or landward expansion. Seaward expansion is unlikely in the setting of limited sediment delivery and increased sea level rise, but migration upland is an important aspect of marsh survival that is often overlooked (Kirwan et al., 2016). For example, a study within the boundaries of the Blackwater National Wildlife Refuge (a part of the Blackwater marsh complex) demonstrated that although 52 % of the 1938 marsh extent has been lost to open water areas between 1938 and 2006, marshes were able to migrate along their inland boundary and extended their area by 30%, limiting the total marsh area loss to 22% (Scott et al., 2009). Schieder et al. (2017) found even a complete replacement of the lost Chesapeake Bay marshes by upland migration, From the 311 km^2 mapped 19th century marshes, 30 percent (94 km^2), but this was more than compensated by new marshes at the upland edge (101 km^2) (Schieder et al., 2017). In another study by (Smith, 2013), the forest edge along the coastal marshes retreated on average by 141 m between 1930 and 2006, enabling brackish and freshwater wetland species to invade these places. Thus, neglecting the upland marsh migration would overestimate the marsh loss as we report it in this study that specifically focusses on the processes of marsh loss. Nevertheless, since overall marsh survival is the combination of marsh loss and marsh expansion, both processes are important and need further research to fully understand the effect of sea level rise on coastal wetlands. We highlight the importance of safeguarding natural areas for landward marsh expansion, without anthropogenic barriers. An example is given by the managers of the Blackwater National Wildlife Refuge, who are designing corridors for landward migration to ensure the persistence of tidal marshes beyond AD 2100.

Some aspects of marsh loss are still unknown and for some conclusions we still rely on assumptions. First, the initial phases of marsh loss, i.e. pond deepening and pond expansion, are thought to be caused by decomposition and disintegration of the organic soil (Delaune and Pezeshki, 1994; van Huissteden and van de Plassche, 1998; Day et al., 2011), but empirical evidence is still lacking. This is remarkable, as this is the start of the marsh loss process and prevention of early pond formation before positive feedback mechanisms start might be the key to keep marsh loss under control.

Second, we assume sediment export through channels because (i) the width of the connection of the channels significantly determines the depth of the ponds (**Chapter 4**), (ii) the flow velocities (flood and ebb) significantly increases in unvegetated corridors (**Chapter 3**) and (iii) the pond bottoms consist of very loose sediments (**Chapter 6**). However, field studies on actual export of material should confirm our hypothesis. Also, actual wave erosion should be measured in the field (e.g. such as Bendoni et al. (2016)).

Lastly, the field methods mentioned could give us an indication of the processes involved, but cannot provide any answers on the importance of currents vs waves for pond expansion. Neither do we fully understand the complex effects of intermediate marsh loss patterns (e.g. **Chapter 3**) on flow and sedimentation patterns. To solve these complex issues, a numerical hydrodynamic and sediment transport model could be developed for (part of the) Blackwater marsh complex.

7.6 References

Balke, T., Friess, D.A., 2016. Geomorphic knowledge for mangrove restoration: a pan-tropical categorization. Earth Surf. Process. Landforms 41, 231–239. doi:10.1002/esp.3841

Baustian, J.J., Mendelssohn, I.A., Hester, M.W., 2012. Vegetation's importance in regulating surface elevation in a coastal salt marsh facing elevated rates of sea level rise. Glob. Chang. Biol. 18, 3377–3382. doi:10.1111/j.1365-2486.2012.02792.x

Bendoni, M., Mel, R., Solari, L., Lanzoni, S., Francalanci, S., Oumeraci, H., 2016. Insights into lateral marsh retreat mechanism through localized field measurements. Water Resour. Res. 52, 1446–1464. doi:10.1002/2015WR017966

Boston, K.G., 1983. The development of salt pans on tidal marshes, with particular reference to south-eastern Australia. J. Biogeogr. 10, 1–10.

Cahoon, D.R., Guntenspergen, G.R., Baird, S., 2010. Do Annual Prescribed Fires Enhance or Slow the Loss of Coastal Marsh Habitat at Blackwater National Wildlife Refuge? Final Report to Joint Fire Science Program Project Number 06-2-1-35.

Cahoon, D.R., Hensel, P., Rybczyk, J., McKee, K.L., Proffitt, C.E., Perez, B.C., 2003. Mass tree mortality leads to mangrove peat collapse at Bay Islands, Honduras after Hurricane Mitch. J. Ecol. 91, 1093–1105. doi:10.1046/j.1365-2745.2003.00841.x

Carniello, L., Defina, A., D'Alpaos, L., 2009. Morphological evolution of the Venice lagoon: Evidence from the past and trend for the future. J. Geophys. Res. Earth Surf. 114, 1–10. doi:10.1029/2008JF001157

Cellone, F., Carol, E., Tosi, L., 2016. Coastal erosion and loss of wetlands in the middle Río de la Plata estuary (Argentina). Appl. Geogr. 76, 37–48. doi:10.1016/j.apgeog.2016.09.014

Cole Ekberg, M.L., Raposa, K.B., Ferguson, W.S., Ruddock, K., Watson, E.B., 2017. Development and Application of a Method to Identify Salt Marsh Vulnerability to Sea Level Rise. Estuaries and Coasts 40, 694–710. doi:10.1007/s12237-017-0219-0

Day, J.W., Boesch, D.F., Clairain, E.J., Kemp, G.P., Laska, S.B., Mitsch, W.J., Orth, K., Mashriqui, H., Reed, D.J., Shabman, L., Simenstad, C. a, Streever, B.J., Twilley, R.R., Watson, C.C., Wells, J.T., Whigham, D.F., 2007. Restoration of the Mississippi Delta: lessons from Hurricanes Katrina and Rita. Science 315, 1679–1684. doi:10.1126/science.1137030

Day, J.W., Kemp, G.P., Reed, D.J., Cahoon, D.R., Boumans, R.M., Suhayda, J.M., Gambrell, R., 2011. Vegetation death and rapid loss of surface elevation in two contrasting Mississippi delta salt marshes: The role of sedimentation, autocompaction and sea-level rise. Ecol. Eng. 37, 229–240. doi:10.1016/j.ecoleng.2010.11.021

Day, J.W., Scarton, F., Rismondo, A., Are, D., 1998. Rapid deterioration of a salt marsh in Venice Lagoon, Italy. J. Coast. Res. 14, 583–590.

DeLaune, R.D., Nyman, J.A., Patrick, W.H., 1994. Peat collapse, ponding and wetland loss in a rapidly submerging coastal marsh. J. Coast. Res. 10, 1021–1030.

Delaune, R.D.D., Pezeshki, S.R.R., 1994. The Influence of Subsidence and Saltwater Intrusion on Coastal Marsh Stability:Louisiana Gulf Coast, U.S.A. J. Coast. Res. Sp.Issue 1, 77–89.

Elschot, K., Bouma, T.J., Temmerman, S., Bakker, J.P., 2013. Effects of long-term grazing on sediment deposition and salt-marsh accretion rates. Estuar. Coast. Shelf Sci. 133, 109–115. doi:10.1016/j.ecss.2013.08.021

Elschot, K., Vermeulen, A., Vandenbruwaene, W., Bakker, J.P., Bouma, T.J., Stahl, J., Castelijns, H., Temmerman, S., 2017. Top-down vs. bottom-up control on vegetation composition in a tidal marsh depends on scale. PLoS One 12, e0169960. doi:10.1371/journal.pone.0169960

Engelhart, S.E., Horton, B.P., Douglas, B.C., Peltier, W.R., Törnqvist, T.E., 2009. Spatial variability of late Holocene and 20th century sea-level rise along the Atlantic coast of the United States. Geology 37, 1115–1118.

doi:10.1130/G30360A.1

Esselink, P., Helder, G.J.F., Aerts, B.A., Gerdes, K., 1997. The impact of grubbing by Greylag Geese (Anser anser) on the vegetation dynamics of a tidal marsh. Aquat. Bot. 55, 261–279.

Ewanchuk, P.J., Bertness, M.D., 2003. Recovery of a northern New England salt marsh plant community from winter icing. Oecologia 136, 616–626. doi:10.1007/s00442-003-1303-7

French, J., 2006. Tidal marsh sedimentation and resilience to environmental change: Exploratory modelling of tidal, sea-level and sediment supply forcing in predominantly allochthonous systems. Mar. Geol. 235, 119–136. doi:10.1016/j.margeo.2006.10.009

Ganju, N.K., Defne, Z., Kirwan, M.L., Fagherazzi, S., D'Alpaos, A., Carniello, L., 2017. Spatially integrative metrics reveal hidden vulnerability of microtidal salt marshes. Nat. Commun. 8, 14156. doi:10.1038/ncomms14156

Ganju, N.K., Kirwan, M.L., Dickhudt, P.J., Guntenspergen, G.R., Cahoon, D.R., Kroeger, K.D., 2015. Sediment transport-based metrics of wetland stability. Geophys. Res. Lett. 42, 7992–8000. doi:10.1002/2015GL065980

Ganju, N.K., Nidzieko, N.J., Kirwan, M.L., 2013. Inferring tidal wetland stability from channel sediment fluxes: Observations and a conceptual model. J. Geophys. Res. Earth Surf. 118, 2045–2058. doi:10.1002/jgrf.20143

Handa, I.T., Harmsen, R., Jefferies, R.L., 2002. Patterns of vegetation change and the recovery potential of degraded areas in a coastal marsh system of the hudson bay lowlands. J. Ecol. 90, 86–99. doi:10.1046/j.0022-0477.2001.00635.x

Holdredge, C., Bertness, M.D., Altieri, A.H., 2009. Role of Crab Herbivory in Die-Off of New England Salt Marshes. Conserv. Biol. 23, 672–679. doi:10.1111/j.1523-1739.2008.01137.x

Hughes, Z.J., FitzGerald, D.M., Wilson, C.A., Pennings, S.C., Wiçski, K., Mahadevan, A., 2009. Rapid headward erosion of marsh creeks in response to relative sea level rise. Geophys. Res. Lett. 36, 1–5. doi:10.1029/2008GL036000

Jefferies, R.L., Jano, A.P., Abraham, K.F., 2006. A biotic agent promotes large-scale catastrophic change in the coastal marshes of Hudson Bay. J. Ecol. 94, 234–242. doi:10.1111/j.1365-2745.2005.01086.x

Kearney, M.S., Grace, R.E., Stevenson, J.C., 1988. Marsh Loss in Nanticoke Estuary, Chesapeake Bay. Geogr. Rev. 78, 205–220. doi:10.2307/214178

Kearney, M.S., Rogers, A.S., Townshend, J.R.G., Rizzo, E., Stutzer, D., Stevenson, J.C., Sundborg, K., 2002. Landsat imagery shows decline of coastal marshes in Chesapeake and Delaware Bays. Eos, Trans. Am. Geophys. Union 83, 173–178. doi:10.1029/2002EO000112

Kearney, M.S., Turner, R.E., 2016. Microtidal Marshes: Can These Widespread and Fragile Marshes Survive Increasing Climate–Sea Level Variability and Human Action? J. Coast. Res. 319, 686–699. doi:10.2112/JCOASTRES-D-15-00069.1

Kirwan, M.L., Murray, A.B., Boyd, W.S., 2008. Temporary vegetation disturbance as an explanation for permanent loss of tidal wetlands. Geophys. Res. Lett. 35, L05403. doi:10.1029/2007GL032681

Kirwan, M.L., Temmerman, S., Skeehan, E.E., Guntenspergen, G.R., Fagherazzi, S., 2016. Overestimation of marsh vulnerability to sea level rise. Nat. Clim. Chang. 6, 253–260. doi:10.1038/nclimate2909

Kotanen, P.M., Abraham, K.F., 2013. Decadal changes in vegetation of a subarctic salt marsh used by lesser snow and Canada geese. Plant Ecol. 214, 409–422. doi:10.1007/s11258-013-0178-x

Mariotti, G., 2016. Revisiting salt marsh resilience to sea level rise: Are ponds responsible for permanent land loss? J. Geophys. Res. Earth Surf. 121, 1391–1407. doi:10.1002/2016JF003900

Mariotti, G., Carr, J., 2014. Dual role of salt marsh retreat: Long-term loss and short-term resilience. Water Resour. Res. 50, 2963–2974. doi:10.1002/2013WR014676

Mariotti, G., Fagherazzi, S., 2013. Critical width of tidal flats triggers marsh collapse in the absence of sea-level rise. Proc. Natl. Acad. Sci. U. S. A. 110, 5353–5356. doi:10.1073/pnas.1219600110

Mckee, K.L., Cahoon, D.R., Feller, I.C., 2007. Caribbean mangroves adjust to rising sea level through biotic controls on change in soil elevation. Glob. Ecol. Biogeogr. 16, 545–556. doi:10.1111/j.1466-8238.2007.00317.x

McKee, K.L., Vervaeke, W.C., 2009. Impacts of Human Disturbance on Soil Erosion Potential and Habitat Stability of Mangrove-Dominated Islands in the Pelican Cays and Twin Cays Ranges, Belize. Smithson. Contrib. Mar. Sci. 38, 415–427.

Möller, I., Mantilla-Contreras, J., Spencer, T., Hayes, a., 2011. Micro-tidal coastal reed beds: Hydro-morphological insights and observations on wave transformation from the southern Baltic Sea. Estuar. Coast. Shelf Sci. 92, 424–436.

doi:10.1016/j.ecss.2011.01.016

Morton, R.A., Tiling, G., Ferina, N.F., 2003. Causes of hot-spot wetland loss in the Mississippi delta plain. Environ. Geosci. 10, 71–80. doi:10.1306/eg100202007

Nolte, S., Esselink, P., Bakker, J.P., Smit, C., 2015. Effects of livestock species and stocking density on accretion rates in grazed salt marshes. Estuar. Coast. Shelf Sci. 152, 109–115. doi:10.1016/j.ecss.2014.11.012

Ortiz, A.C., Roy, S., Edmonds, D.A., 2017. Land loss by pond expansion on the Mississippi River Delta Plain. Geophys. Res. Lett. 44, 3635–3642. doi:10.1002/2017GL073079

Penland, S., Wayne, L., Britsch, D., Williams, S.J., Beall, A.D., Butterworth, V., 2000. Geomorphic Classification of Coastal Land Loss between 1932 and 1990 in the Mississippi River Delta Plain, Southeastern Louisiana. USGS Open File Report 00-417. https://pubs.usgs.gov/of/2000/of00-417/.

Perillo, G.M.E., Iribarne, O.O., 2003. New mechanisms studied for creek formation in tidal flats: From crabs to tidal channels. Eos, Trans. Am. Geophys. Union 84, 1–12. doi:10.1029/2003EO010001

Pethick, J.S., 1974. The Distribution of Salt Pans on Tidal Salt Marshes. J. Biogeogr. 1, 57–62.

Ravens, T.M., Thomas, R.C., Roberts, K.A., Santschi, P.H., 2009. Causes of Salt Marsh Erosion in Galveston Bay, Texas. J. Coast. Res. 252, 265–272. doi:10.2112/07-0942.1

Schieder, N.W., Walters, D.C., Kirwan, M.L., 2017. Massive Upland to Wetland Conversion Compensated for Historical Marsh Loss in Chesapeake Bay, USA. Estuaries and Coasts. doi:10.1007/s12237-017-0336-9

Scott, M., McDermott, L., Silva, E., Watson, E., 2009. Project report: Digital Spatial Data Capture of Marsh Extent in Blackwater National Wildlife Refuge, 1938 and 2006. Eastern Shore Regional GIS Cooperative, Salisbury University.

Silliman, B.R., van de Koppel, J., Bertness, M.D., Stanton, L.E., Mendelssohn, I.A., 2005. Drought, Snails, and Large-Scale Die-Off of Southern U.S. Salt Marshes. Science 310, 1803–1806. doi:10.1126/science.1118229

Slocum, M.G., Mendelssohn, I.A., 2008. Use of experimental disturbances to assess resilience along a known stress gradient. Ecol. Indic. 8, 181–190. doi:10.1016/j.ecolind.2007.01.011

Smith, J.A.M., 2013. The Role of Phragmites australis in Mediating Inland Salt Marsh Migration in a Mid-Atlantic Estuary. PLoS One 8. doi:10.1371/journal.pone.0065091

Stevenson, J.C., Kearney, M.S., Pendleton, E.C., 1985. Sedimentation and erosion in a Chesapeake Bay brackish marsh system. Mar. Geol. 67, 213–235. doi:10.1016/0025-3227(85)90093-3

Temmerman, S., Govers, G., Meire, P., Wartel, S., 2004. Simulating the long-term development of levee-basin topography on tidal marshes. Geomorphology 63, 39–55. doi:10.1016/j.geomorph.2004.03.004

Turner, R.E., Cahoon, D.R., 1987. Causes of wetland loss in the coastal central Gulf of Mexico. Volume II: Technical Narrative. Final Report submitted to Minerals Management Service, New Orleans, LA. Contract NO. 14-12-0001-30252. OCS Study/MMS 87-0120. 400pp.

van Belzen, J., van de Koppel, J., Kirwan, M.L., van der Wal, D., Herman, P.M.J., Dakos, V., Kéfi, S., Scheffer, M., Guntenspergen, G.R., Bouma, T.J., 2017. Vegetation recovery in tidal marshes reveals critical slowing down under increased inundation. Nat. Commun. 8, 15811. doi:10.1038/ncomms15811

van Huissteden, J., van de Plassche, O., 1998. Sulphate reduction as a geomorphological agent in tidal marshes (“Great Marshes” at Barnstable, Cape Cod, USA). Earth Surf. Process. Landforms 23, 223–236. doi:10.1002/(SICI)1096-9837(199803)23:3<223::AID-ESP843>3.0.CO;2-I

Wilson, C.A., Allison, M.A., 2008. An equilibrium profile model for retreating marsh shorelines in southeast Louisiana. Estuar. Coast. Shelf Sci. 80, 483–494. doi:10.1016/j.ecss.2008.09.004